


**Martin Jilg**

Hierarchical and Cooperative Control  
of Complex Distributed Systems

kassel  
university   
press

**Martin Jilg**

**Hierarchical and Cooperative Control  
of Complex Distributed Systems**

This work has been accepted by the Faculty of Electrical Engineering / Computer Science of the University of Kassel as a thesis for acquiring the academic degree of Doktor der Ingenieurwissenschaften (Dr.-Ing.).

Supervisor: Prof. Dr.-Ing. Olaf Stursberg, University of Kassel  
Co-Supervisor: Prof. Dr.-Ing. Jörg Raisch, TU Berlin

Defense day: 7<sup>th</sup> December 2017

Bibliographic information published by Deutsche Nationalbibliothek  
The Deutsche Nationalbibliothek lists this publication in the Deutsche Nationalbibliografie;  
detailed bibliographic data is available in the Internet at <http://dnb.dnb.de>.

Zugl.: Kassel, Univ., Diss. 2017  
ISBN 978-3-7376-0454-3 (print)  
ISBN 978-3-7376-0455-0 (e-book)  
DOI: <http://dx.medra.org/10.19211/KUP9783737604550>  
URN: <http://nbn-resolving.de/urn:nbn:de:0002-404554>

© 2018, kassel university press GmbH, Kassel  
[www.upress.uni-kassel.de](http://www.upress.uni-kassel.de)

Printed in Germany

# Contents

<b>Summary</b>	<b>vii</b>
<b>I. Introduction and Theoretical Background</b>	<b>1</b>
<b>1. Introduction and Literature Review</b>	<b>3</b>
1.1. Introduction . . . . .	3
1.2. Literature Review . . . . .	9
1.3. Contribution of this Thesis . . . . .	22
<b>2. Problem Setup and Preliminaries</b>	<b>23</b>
2.1. General Problem Setup and Notation . . . . .	23
2.2. Model of the Communication Network . . . . .	32
2.3. Stabilizability Criteria and Stability Notions . . . . .	33
2.4. The $\mathcal{H}_2$ -Norm and its Generalizations . . . . .	37
2.5. Semidefinite Programming . . . . .	40
2.6. Decompositions of Matrices and Dynamic Systems . . . . .	42
<b>II. Hierarchical Control of Time-Invariant Systems</b>	<b>47</b>
<b>3. Synchronous Hierarchical Control</b>	<b>49</b>
3.1. Dynamic Model and Problem Setup . . . . .	50
3.2. Subsystem Clustering . . . . .	52
3.3. Lower Layer Control Design . . . . .	55
3.4. Upper Layer Control Design . . . . .	60
3.4.1. Full Communication Topology . . . . .	60
3.4.2. Optimized Communication Topology . . . . .	64
3.4.3. Stability of the Original Interconnected System . . . . .	66
3.4.4. Alternative Performance Indices . . . . .	67
3.5. Implementation . . . . .	68
3.6. Numerical Example . . . . .	69
3.7. Discussion . . . . .	74

<b>4. Asynchronous Hierarchical Control</b>	<b>77</b>
4.1. Problem Setup . . . . .	78
4.2. Fundamentals of Periodic Systems . . . . .	80
4.3. Upper Layer Control Design . . . . .	84
4.3.1. Modeling as Periodic System . . . . .	84
4.3.2. Distributed Control Design . . . . .	87
4.3.3. Optimal Switching Sequence . . . . .	93
4.4. Implementation . . . . .	93
4.4.1. Optimal Controller Initialization . . . . .	95
4.4.2. Stability of the Original Interconnected System . . . . .	97
4.5. Numerical Example . . . . .	97
4.6. Discussion . . . . .	99

<b>5. Application Example</b>	<b>103</b>
5.1. Linearized Power System Model . . . . .	103
5.2. Hierarchical Control Design . . . . .	107
5.3. Simulation Results and Discussion . . . . .	111

### III. Distributed and Hierarchical Control of Uncertain Systems 119

<b>6. Distributed Control of Interconnected Jump Markov Systems</b>	<b>121</b>
6.1. Problem Setup . . . . .	122
6.2. Centralized Modeling of Interconnected JMLS . . . . .	123
6.3. Distributed Controller Design . . . . .	127
6.3.1. Synthesis Problem . . . . .	130
6.3.2. Implementation . . . . .	132
6.4. Numerical Example . . . . .	133
6.5. Discussion . . . . .	135

<b>7. Hierarchical Control of Interconnected Semi-Markov Systems</b>	<b>137</b>
7.1. Problem Setup . . . . .	138
7.2. Subsystem Clustering . . . . .	140
7.3. Lower Layer Control Design . . . . .	143
7.4. Upper Layer Control Design . . . . .	144
7.5. Reducing the Synthesis Complexity . . . . .	150
7.6. Numerical Example . . . . .	152
7.7. Discussion . . . . .	154

<b>8. Discussion and Outlook</b>	<b>157</b>
8.1. Summary and Comparison of the Presented Approaches . . . . .	157
8.2. Outlook . . . . .	160

<b>Appendix A. Equivalence of Output Variance and <math>\mathcal{H}_2</math>-Norm</b>	<b>163</b>
A.1. Proof of Lemma 2.1 . . . . .	163
A.2. Proof of Lemma 2.3 . . . . .	164
<b>Appendix B. Expected Performance for Stochastic Initial States</b>	<b>165</b>
<b>Appendix C. Comparison of Interconnection Measures</b>	<b>173</b>
<b>Appendix D. Asynchronous Hierarchical Control</b>	<b>177</b>
D.1. Proof of Lemma 4.3 . . . . .	177
D.2. Proof of Lemma 4.4 . . . . .	178
D.3. Numerical Example . . . . .	183
<b>Appendix E. Numerical Values</b>	<b>185</b>
E.1. Numerical Values of Section 4.5 . . . . .	185
E.2. Numerical Values of Section 7.6 . . . . .	189
E.2.1. Subsystem Dynamics . . . . .	189
E.2.2. Lower Layer Controllers . . . . .	193
E.2.3. Upper Layer Controllers . . . . .	194
<b>List of Symbols</b>	<b>199</b>
<b>List of Abbreviations</b>	<b>205</b>
<b>References</b>	<b>207</b>



# Summary

In this thesis, a theory of hierarchical and cooperative feedback control for spatially distributed, physically interconnected systems is developed. A particular requirement is that the resulting control laws are suitable for a distributed implementation, meaning that the subsystems are equipped with local controllers and exchange information via a communication network. Distributed control schemes steadily gain practical significance, since an ever increasing number of technical systems, like power networks or manufacturing systems, is comprised of an interconnection of subsystems. In combination with competitive, powerful embedded computers and modern communication technology, a distributed implementation of control algorithms intuitively makes sense for such types of systems.

When designing distributed control algorithms, an immediate question is how to select an appropriate communication topology for connecting the local controllers. While classical approaches typically propose schemes with fixed communication structures, some modern approaches consider the communication topology underlying the distributed controller as an additional degree of freedom for the control design. However, these approaches often suffer from the combinatorial complexity arising from the binary decisions whether to activate a link within the communication topology or not. While some approximation techniques exist in order to deal with this complexity, the hierarchical control structures have not yet been considered as a possible remedy. It is the main goal of this thesis to close this gap by combining ideas from the domains of system decomposition, hierarchical control, and simultaneous control and communication topology design.

In particular, a two-layer distributed control scheme for time-invariant interconnected dynamic systems is proposed. Prior to the control design, the system structure is analyzed. Based on the result of this analysis, the structure of the distributed controller can be adopted to the structure of the interconnected system. Common control goals are either encoded by a global quadratic cost function or by a system norm with respect to a global controlled variable, and the local controllers on both layers are designed to cooperate for optimizing the performance index.

In the above scheme, the controllers on the upper control layer synchronously operate on a coarser time-scale compared to the lower control layer. In order to improve the distribution of the exchanged data over time, an extension of the scheme considering asynchronous communication is presented. Distributed frequency control of a power network serves as an application example for the synchronous and asynchronous two-layer scheme.

In the last part of this thesis, the approach is extended to a class of uncertain



interconnected dynamic systems. More precisely, interconnected jump Markov and jump semi-Markov systems are considered, which allow to model stochastic abrupt changes of the system behavior. Starting from a monolithic partitioned model, it is shown how distributed single- and two-layer controllers can be designed for such types of interconnected systems, where a particular requirement is to respect information constraints w.r.t. the local Markov states.

## **Acknowledgments**

In the first place, I would like to thank my supervisor Prof. Dr.-Ing. Olaf Stursberg for his guidance and his enduring support during the time when preparing this thesis. He always gave me valuable advice and honest feedback about my work.

I am very grateful to Prof. Dr.-Ing. Jörg Raisch for his willingness to be on the thesis committee, and I would like to thank him for the time and efforts he spent on reading and assessing my work. I would also like to thank Prof. Dr. rer. nat. Arno Linnemann and Prof. Dr. rer. nat. Bernhard Sick for being on the defence committee and for the interesting discussions about my work.

Furthermore, I would like to thank all members of the Institute of Control and System Theory for the pleasant and productive collaboration during the time when I was working there. Special thanks go to my former colleagues Dipl.-Ing. Leonhard Asselborn, Dr.-Ing. Jens Tonne, and Dr.-Ing. Dominic Groß for sharing many inspiring thoughts and technical discussions.

I highly appreciate the financial support provided by the state of Hessen, and by the European Union through the network of excellence HYCON2.

Last but not least, I would like to thank my parents Jutta and Franz, my sister Carina, my whole family and all of my friends for their encouragement, interest, and support over the years, especially during the long time when I was writing this thesis.

Martin Jilg  
Fürstentagen, January 2018

**Part I.**

**Introduction and Theoretical  
Background**



# 1. Introduction and Literature Review

## 1.1. Introduction

In the last decades, the complexity of man-made technical systems has significantly increased. This trend is not only due to the increasing size and technical capabilities of large systems like, e.g., production plants in the steel or petrochemical industry [92], but is mainly driven by recent developments in the area of *interconnected systems*<sup>1</sup>. The term interconnected system refers to technical systems comprised of a collection of interacting dynamical subsystems  $\mathcal{P}^i$  [70]. Many interconnected systems, like electrical power systems or autonomous vehicles, are furthermore characterized by a spatial distribution of the attendant subsystems. The interactions between the subsystems are typically classified into the following three categories:

- *physical interconnections*, like the interactions between several loads and generators in an electrical power network, interactions between reservoirs and pumps in a water distribution network, or the dependencies of room temperatures in a large building.
- *information exchange*, typically occurring in networked structures like telecommunication networks or the internet.
- *common control goals*, i.e. a desired collective behavior of (possibly autonomous) subsystems, like a collection of autonomous vehicles that are to follow a lead vehicle or reference trajectory while maintaining a desired formation.

Naturally, an interconnected system may contain interconnections from all of these three categories at the same time. A major reason for the increasing number of interconnected systems is the technological progress in the fields of communication technology and *embedded systems*. In this thesis, an embedded system (or *embedded computer*) is understood as a compact computer system which is part of a larger mechanical or electrical system and is designed to accomplish a dedicated task. It is assumed to be equipped with real-time computing capabilities and with an interface

---

<sup>1</sup>In the literature, the terms *interconnected system*, *distributed system*, and *large-scale system* are often used interchangeably. While many authors generally refer to such systems as *complex systems* [13] [140], the term *interconnected system* is used in this thesis to emphasize their modular character.

to communicate with similar devices via a wired or wireless network. Products of both domains, embedded systems and communication technology, have continuously been improved regarding capability, compactness, reliability, and acquisition costs, motivating the design of interconnected systems on the one hand and providing more flexibility for the design process on the other. While communication between the subsystems may be necessary to create interconnections via information exchange, it is mostly needed to exchange information for the purpose of controlling an interconnected system, i.e. coordinating the subsystems in order to impose a desired global behavior. Combined with the broad availability of efficient embedded computers, such a hardware framework allows the implementation of distributed control algorithms. Not surprisingly, the development of such distributed algorithms has become one of the major research directions of modern control theory [12] [13] [80].

A recent and concise characterization of the role of modern control methods for interconnected systems can be found in a topical textbook on *Control Theory of Digitally Networked Dynamic Systems*:

*“Modern means of communication make it easy to connect system components whenever information links may contribute to improving the overall system performance. Actuators, sensors and controllers can now exchange information from nearly any place within a technological system, and wireless connections allow to implement advanced control technology for mobile objects. Due to this flexibility, a new challenge for control theory is to elaborate systematic ways for the selection of information structures that are suitable for a given control task.” [80]*

Regarding the implementation structure of control algorithms for interconnected systems, one distinguishes four general structures: centralized, decentralized<sup>2</sup>, distributed, and hierarchical control structures. All four of them are exemplarily shown in Figure 1.1 for the case of  $N_s = 4$  subsystems  $\mathcal{P}^i$ . The centralized control structure (top left) is the one typically employed in classical control theory. In a centralized control structure, all sensors and actuators are connected to a centralized control device  $\mathcal{C}$ , which performs all necessary computations. From the viewpoint of interconnected systems, such a control structure can be implemented by establishing full communication between the subsystems  $\mathcal{P}^i$  and the centralized controller  $\mathcal{C}$ , gathering all measurements for processing and sending the computed control inputs back to the actuators. While providing the highest control performance in general, such a control structure is unfavorable for an actual implementation in an interconnected system, especially for subsystems with a distinct spatial distribution, or for mobile subsystems. Furthermore, the scheme is prone to communication link failure, requires highly aggregated computational resources, and does not make full

---

<sup>2</sup>In some related publications, the term *decentralized control* actually refers to a control structure which is called a *distributed control* structure throughout this thesis and in most of the relevant literature.

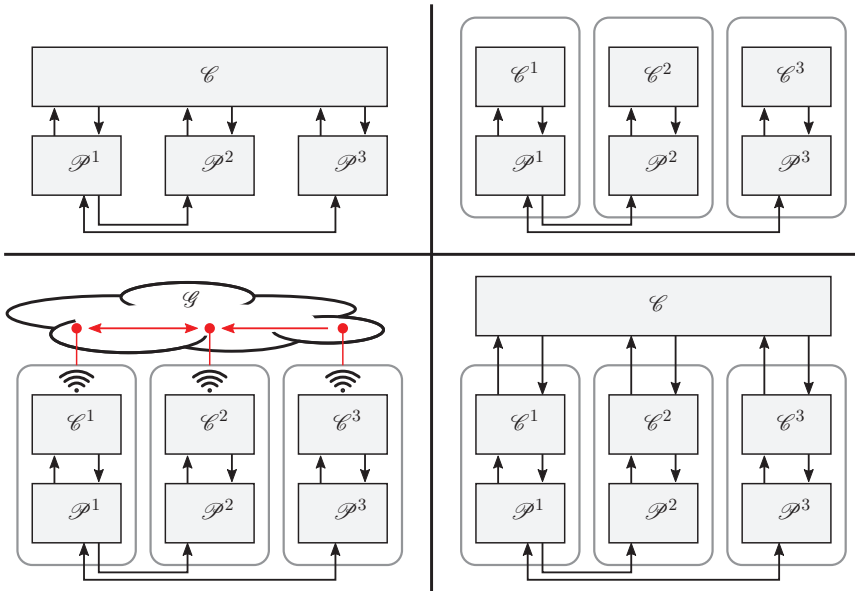


**Figure 1.1.:** Classical control structures: centralized (top left), decentralized (top right), distributed (bottom left), and hierarchical (bottom right). Solid black lines denote physical interactions or connections, and red lines indicate networked communication.

use of the potential of distributed computation and embedded hardware. In order to overcome some of these issues and ease both the implementation and maintenance of controllers, decentralized control structures (top right) have been extensively developed since the 1970s [131]. In a decentralized control structure, every subsystem  $\mathcal{P}^i$  is equipped with a local controller  $\mathcal{C}^i$ , which only has access to local measurements. Consequently, there is no explicit information exchange between the controllers, which renders the scheme inherently robust against communication failure. However, decentralized controllers generally either perform worse than their centralized counterparts, or must possess a very high order to accomplish a similar performance [69]. Furthermore, some types of interconnected systems can not be stabilized by purely decentralized feedback [10]. As an attempt to combine the advantages of centralized and decentralized control at its best, distributed and hierarchical control structures have been proposed. In a distributed control scheme (bottom left), every subsystem is equipped with a local controller  $\mathcal{C}^i$ , similar to a decentralized control scheme. However, distributed controllers have the ability to exchange information via a communication network  $\mathcal{G}$ , which leads to an improved control performance.

Relying on both, distributed computation capacity and information exchange, this type of controllers fully exploits the capabilities of embedded systems. Since the communication topology of distributed controllers is often sparse, the scheme is less prone to communication failures compared to a centralized control scheme. Hierarchical control schemes (bottom right) can be regarded as a combination of the former three schemes. A hierarchical control scheme is comprised of two or more vertically interconnected *control layers*, where each layer is designed to accomplish a specific task. In general, when considering the hierarchy from the topmost layer to the lowest layer<sup>3</sup>, the layers possess an increasing degree of decentralization, and the tasks vary from a global planning and coordination perspective to a local, rather subsystem-specific, perspective. Depending on the design, hierarchical control schemes often provide a good trade-off between communication effort and control performance.

Besides the need for control algorithms which can be implemented in a distributed manner, the complexity of analysis and synthesis tasks arising in the context of interconnected systems requires special attention. In many cases, classical tools from control and system theory, which have been developed for the scope of centralized control systems, can not directly deal with the arising complexity and novel requirements like distributed implementation. A famous example is the Riccati equation, which is involved in solving classical, centralized linear quadratic regulator (LQR) problems, but becomes inapplicable when structural constraints are to be considered [107]. In the literature, the complexity of a problem from the domain of system analysis or control design is often associated with the dimensionality of the underlying mathematical model. This point of view can be found in many approaches, especially from the 1970s to the late 1990s, and researchers at that time coined the term *large-scale system* [108] [131] [132]. More recent insights show that structural constraints on control laws or on state observers, model uncertainties, and stochastic communication delays likewise render analysis and synthesis problems complex, even for models with moderate dimension [13] [107]. Hence, the development of tractable mathematical and numerical analysis and control design tools for interconnected systems is another demanding challenge.

Recently, research in the domain of interconnected systems has laid emphasis on a more comprehensive treatment of the communication network used to exchange information between local control algorithms. An increasing number of approaches aims to incorporate more realistic models of the communication network into the system model. The resulting models are often referred to as *networked control systems (NCS)* [12] [80]. By doing so, the impacts of network-induced effects like variable transmission-delay, jitter, packet dropout, and communication link failure on the performance of a given control algorithm can either be analyzed, or these

---

<sup>3</sup>Throughout this thesis, the lowest control layer (or lower control layer, depending on the number and corresponding terminology of the layers) is always associated to the control layer that actually connects to the physical subsystems  $\mathcal{P}^i$

effects can already be taken into account for control synthesis. Another class of approaches is concerned with the structure of a communication network underlying a distributed control algorithm. The main line of thought pursued in these studies is to consider the topology of the underlying communication network as an additional degree of freedom for the control design, thus performing a co-design of the distributed control algorithm and the network topology [103] [50]. Throughout this thesis, these approaches will be referred to as *simultaneous control and topology (SCT) design*.

It is needless to say that the incorporation of network-induced effects as well as SCT design further increases the complexity of the design of distributed controllers. By summarizing the challenges identified so far, the general problem tackled in this thesis can be characterized as follows: Given a collection of  $N_s$  heterogeneous interconnected subsystems  $\mathcal{P}^i$  and a global control objective, develop an offline control design procedure which:

- yields feedback controllers that are suitable for a distributed implementation on networked embedded computers,
- seeks for a controller structure that yields a good (preferably parametrizable) trade-off between control performance and communication effort,
- is numerically tractable for system dimensions (in total) of up to  $n_x \approx 100$  continuous states.

The usage of feedback controllers is mainly motivated with regard to an easy and reliable implementation of the distributed control algorithm. Since the amount of required online computations is reduced to a minimum, the hardware requirements on the embedded systems can be kept low. Furthermore, a quick processing of the control laws renders feedback controllers particularly suited for the control of fast dynamics. In particular, no additional software like, e.g., optimization algorithms, has to be implemented in the embedded control devices, which is typically required by online control methods like *model predictive control* (MPC) [51].

It can be observed that most approaches considering similar objectives tackle the problem either by a decomposition of the overall synthesis problem, or by employing different kinds of approximations. However, a proper decomposition of a distributed control design problem into coupled or decoupled subproblems generally requires rigorous assumptions on the structure of the interconnected system. Furthermore, there is currently no approach which performs SCT design within a decomposition scheme. Approximations, on the other hand, are a popular means to decrease the complexity arising from large system dimensions. However, in the case that the control objectives are encoded by a (quadratic) cost function, the relation to the original cost function can only be partially preserved under specific assumptions [86]. A more thorough discussion on related work is provided in the subsequent section. Altogether, it can be noticed that the majority of approaches consider



single-layer control structures. Only few results in this direction are available which propose hierarchical, multi-layer control structures. Such structures are mainly used in distributed optimization schemes or for the control of *discrete-event systems* (DES).

This thesis aims to develop a distributed two-layer control scheme for interconnected dynamic systems. Referring to Figure 1.1, this structure can be interpreted as a hierarchy (bottom right) which is implemented in a distributed manner (bottom left). The idea behind this structure is as follows: At first, the interconnection strength and structure of the interconnected system is analyzed. Based on this information, the communication topology of the local controllers on the lower control layer is chosen according to the strong interconnections between the subsystems. The second, upper control layer accounts for common control goals and provides global stability and performance guarantees. Here, additional information is weighted against increased overall performance, such that a trade-off between performance and communication effort is reached. The control structure will be explained in more detail in Section 2.1.

The goal of this approach is to break down the complexity of SCT design by employing ideas from the domains of system decomposition, distributed, and hierarchical control. Regardless of reducing the complexity of the control design, it is demanded that the resulting control law guarantees global performance and stability properties. Focusing on linear time-invariant dynamics, a particular aim is to make as few assumptions on the subsystem interconnection structure as possible, rendering the approach amenable to a preferably broad class of applications.

Furthermore, this thesis aims to extend the aforementioned concepts to a class of uncertain dynamic systems. The considered systems are comprised of a finite set of time-invariant dynamics and a stochastic, set-valued switching function which selects the currently active dynamics. This kind of dynamic models is well suited to model abrupt changes in the system behavior, like failures of sensors, actuators, or communication links. In the frequent case that the evolution of the switching function over time is modeled by a Markov chain, such systems are referred to as *jump Markov systems* (JMS) [31]. Most approaches to distributed control can not be directly extended to this system class. Hence, only few results exist on decentralized or distributed control of jump Markov systems, most of them considering single-layer control structures.

### Outline of this Thesis

This thesis is organized in three parts. In the first part, consisting of Chapters 1 and 2, the contents of this thesis are classified with respect to relevant research. The general problem setup and theoretical background are presented. In the remainder of this chapter, a comprehensive review on relevant literature from the field of decentralized, distributed, and hierarchical control is given. Since a vast number of publications related to this field have appeared in the last 40 years, the review

focuses on distributed and hierarchical feedback control for linear time-invariant systems and for jump Markov linear systems. Chapter 2 introduces the notation and the general problem setup. Furthermore, some theoretical background on the considered system classes and on the used mathematical tools is provided.

In the second part of this thesis, comprised of Chapter 3 to Chapter 5, two distributed hierarchical control schemes for interconnected systems modeled by linear time-invariant dynamic subsystems are presented. The basic principle of these schemes, which build on an analysis of the interconnection structure of the overall system, is presented in Chapter 3. The underlying assumption in this chapter is that all local controllers associated with the upper control layer perform synchronous, time-triggered updates. In Chapter 4, this assumption is relaxed in the interest of an equably distributed communication load. In particular, it is shown how the upper layer controllers can be designed for asynchronous, time-triggered operation within a periodic sequence. Chapter 5 considers frequency control of an electrical power network as an application example for the control schemes presented in the preceding two chapters. After stating the modeling assumptions and principles, the two-layer schemes are compared with well-established single-layer controllers with respect to performance and implementation effort.

The third part of this thesis, beginning with Chapter 6, is concerned with extending the ideas presented in the second part to a class of interconnected systems with stochastic uncertainty. In particular, a collection of jump Markov linear subsystems is considered, where the subsystems are interconnected via physical interactions and a common cost function. Chapter 6 presents the new problem setup and a modeling procedure which allows to consider the overall system as a partitioned jump Markov system similar to the Chapters 3 and 4. In Chapter 7, the hierarchical two-layer scheme is extended to a class of jump semi-Markov linear systems, where the continuous dynamics and the underlying Markov chain are defined on different time-scales. Finally, the thesis is concluded in Chapter 8, and an outlook on further developments in the field of hierarchical distributed feedback control is given.

## 1.2. Literature Review

The aim of this section is to provide an overview over relevant literature from the fields of decentralized, distributed, and hierarchical<sup>4</sup> feedback control of interconnected systems. For the sake of completeness, a rough insight is also provided in the fields of distributed and hierarchical optimization, model predictive control (MPC) as well as hierarchical control of discrete-event systems (DES). Most work on non-centralized control schemes focuses on interconnected systems modeled by linear time-invariant (LTI) differential or difference equations, while rather few results are available for nonlinear, uncertain, or hybrid dynamics.

---

<sup>4</sup>For the sake of brevity, decentralized, distributed, and hierarchical control schemes are often jointly referred to as *non-centralized* control schemes.

In general, approaches to non-centralized control can be classified according to the following categories:

- *modeling domain*: typical choices are state-space models (time-domain) or transfer functions (frequency domain).
- *model class*: the assumed type of system model, e.g. linear or nonlinear, time-invariant or time-varying, continuous-time or discrete-time, continuous- or discrete-valued, possibly uncertain or hybrid.
- *model adjustment*: the way the original system model is treated, e.g. exact, or being decomposed, approximated<sup>5</sup>, or abstracted.
- *subsystem interconnections*: subsystems can be interconnected, e.g. via inputs, states, outputs, shared information sets, or a cost function. Furthermore, specific interconnection structures may be assumed.
- *task and specifications*: which task should be performed, e.g. stability or performance analysis, stabilizing control design,  $\mathcal{H}_2$ -,  $\mathcal{H}_\infty$ - or multi-objective control design with guaranteed or optimized performance.
- *controller structure*: the implementation structure of the controller: centralized, decentralized, distributed, hierarchical, where the latter two structures may be either fixed a-priori or are co-designed with the controller (SCT design)
- *control layers*: the number of control layers in the case of a hierarchical structure.
- *controller type*: the assumed type of controller, e.g. static state-feedback, static output-feedback, dynamic output-feedback, MPC, or switching control.
- *network model*: the network effects incorporated in the overall system model, which is often assumed to be ideal, but may include constant or time-varying transmission delays, random packet dropouts, quantization effects, jitter, etc.
- *network usage*: the usage of the communication network, e.g. once or multiple times per time-step, time- or event-triggered.

The beginning of non-centralized control can be traced back until the late 1960s, where new control structures were sought for high-dimensional systems, often referred to as *large-scale systems*. The work on this emerging line of research was mainly motivated by the requirement of new concepts for the control of power systems and digital communication networks [108]. In 1970, first hierarchical and

---

<sup>5</sup>Although model reduction and system approximation methods are common tools for the analysis, simulation and control design of complex systems, they are not within the scope of this thesis. The interested reader is referred to [8] [19] [93].

multi-layer concepts were formalized and utilized to decompose constrained optimization problems [92]. A milestone in the field of decentralized control is the textbook of Šiljak [131] published in 1978, which presents graph-theoretic approaches to the analysis of emerging notions like *decentralized reachability* and *connective stability*, and first approaches to decentralized feedback stabilization. Furthermore, first approaches to the analysis and classification of the interconnection structure of interconnected systems are presented. Another early work with large impact is the survey paper of Sandell et al. [108], in which first state-aggregation techniques are shown. In addition, a hierarchical filtering approach for systems with separable slow and fast dynamics is presented. Methods for decentralized stability analysis are shown which are based on the construction of vector Lyapunov functions or small gain concepts, both using worst-case bounds of the interconnection signals. Concerning decentralized control, it is demonstrated that the separation principle does not hold for non-centralized  $\mathcal{H}_2$  control design, and that decentralized pole-placement can be performed by designing auxiliary controllers which render the system fully reachable from the last decentralized control loop to be closed.

In the sequel, the most relevant recent approaches to non-centralized control of interconnected systems are grouped according to the proposed controller structure or the model treatment.

### **Decentralized Control**

The graph-theoretic framework for decentralized control introduced in [131] is further developed in [132]. The relations between structural controllability and observability and structurally fixed modes and the underlying interconnection graph of a dynamic system are investigated in more detail. Most notably, first approaches combining system decomposition and control design are presented. These decomposition approaches will be described later in more detail. From the viewpoint of decentralized control, one of the major contributions in [132] is an algorithm for the sequential design of  $\mathcal{H}_2$ -optimized decentralized state-feedback controllers.

Besides sequential design, another popular approach to the design of decentralized controllers is to design the local subsystem controllers robustly with respect to the incoming interconnection signals. This is done in [66] for linear systems interconnected via states and inputs. First, the system is rewritten in input-decentralized form by using a descriptor system with extended state vector. Then, the local robust controllers are designed using eigenstructure assignment. A similar approach is pursued in [116] for interconnected homogeneous subsystems, where it is assumed that magnitude bounds are known for all incoming interconnection signals. The local controllers are then designed robust w.r.t. these bounds, while imposing magnitude bounds on the outgoing interconnections themselves. While treating interconnections as unknown disturbances is a common means to decompose a decentralized control design problem into local robust control problems, this approach is usually conservative, especially under the consideration of common control goals.

In order to reduce the conservativeness of decentralized control schemes, the local controllers require knowledge about the incoming interactions. In [69], a method is proposed which derives a decentralized controller from a given centralized one. Therefore, every subsystem is equipped with a copy of the global system dynamics in order to estimate the full system state. The approach is extended in [70] to consider steady-state accuracy and suboptimal  $\mathcal{H}_2$ -performance. While being able to provide the same performance as the centralized controller in the ideal case, the main drawback of this approach is the high dimensionality of the resulting controllers.

Decentralized control for nonlinear systems is considered in [93, Chap. 6], where high feedback gains are used to render the local control inputs dominant w.r.t. the incoming interconnections, and gain-scheduling is employed to handle the nonlinearity of the dynamics. In general, high feedback gains often occur when designing decentralized controllers for strongly coupled subsystems, which has led to the notion of (block-) *diagonal dominance* in terms of the system-matrix of linear dynamic state-space models [131].

Modern approaches to decentralized control increasingly investigate the impacts of network-induced effects or already incorporate these effects in the control design problem [14]. A frequently considered setup is a decentralized control structure where sensors, controllers, and actuators communicate via a shared network. Thus, besides the design of the actual control algorithm, the scheduling of the shared network is a typical problem occurring in such setups. An approach based on periodic scheduling protocols is presented in [18].

In summary, decentralized control is an active line of research for about 50 years, being an attractive option due to its uncomplicated implementation. However, especially for a large number of subsystems, it is well known that the performance of decentralized controllers is limited. This is mainly due to the lack of information exchange between the controllers, rendering the scheme ineffective for models with strong interconnections [140]. The work in [15] presents a study of decentralized distance control of a string of vehicles under the influence of local disturbances. The simulation results reveal that the coherence of the formation significantly decreases with an increasing number of vehicles. The lack of coherence manifests itself in the form of oscillations of the vehicle string, which can only be reduced by increasing the information set of the local controllers, naturally leading to distributed control schemes.

In [140], communication links are iteratively added to a decentralized control law based on a heuristic method. These so called *low-rank centralized corrections* increase the performance of the closed-loop system, or may even be required to render the closed-loop system stable [10].

## Distributed Control

The majority of recent approaches to distributed control assumes the interconnected system to be modeled by interconnected linear time-invariant differential or difference equations. In addition, many approaches impose assumptions on the subsystem structure, like (groups of) homogeneous subsystems which are either decoupled [24] or possess particular (e.g., symmetric) interconnection patterns [55] [90] [91] [97], scalar interconnection signals [35], local control inputs [74] [105], or hierarchical interconnection structures [114] [125]. In many cases, these assumptions allow to significantly simplify the distributed control design.

One method to synthesize distributed control laws is *spatial truncation*. This approach was first introduced in [16] for spatially invariant systems, i.e. subsystem dynamics which do not depend on a spatial variable, typically resulting from the discretization of *partial differential equations* (PDE). It is shown that for such systems, both  $\mathcal{H}_2$ - and  $\mathcal{H}_\infty$ -optimal (centralized) controllers are spatially invariant, and that the magnitudes of the control gains decay with an increasing distance of the corresponding subsystems. Thus, the concept of spatial truncation is to neglect all control gains corresponding to subsystems outside a desired radius, leading to a suboptimal distributed control law accessing the information of neighboring subsystems. In [96], this approach is extended to systems which possess spatially decaying interconnection strengths. The controllers resulting from these truncation methods are not guaranteed to be stabilizing, and no general information structures can be taken into account.

Most approaches to distributed control assume the underlying communication topology of the subsystem controllers to be given a-priori. A frequent practice is to search for a distributed controller which has the same information structure as the given interconnected system. This is done in [67] for the case of heterogeneous subsystems interconnected via states and inputs over a graph with arbitrary structure. A common control goal is given by a desired  $\mathcal{H}_\infty$ -performance of the overall system. It is shown that the synthesis conditions result in a set of coupled linear matrix inequalities (LMI). The authors propose to solve these inequalities in a distributed manner within a two-layer optimization scheme. The approach is extended in [36] to the case of time-varying linear systems interconnected via an infinite graph with periodic time and space structure.

A more general problem setup is to assume an arbitrary (but a-priori given) information structure which may differ from the interconnection structure of the plant. These approaches are often referred to as *structured control design* or control design w.r.t. arbitrary information constraints. A great challenge for solving these problems is that the feasible set of controllers with respect to an arbitrary information constraint is generally non-convex [107]. Within the framework of linear matrix inequalities, this drawback can be circumvented by establishing convex under-approximations of the feasible set [50]: Structured dynamic output feedback for LTI systems with local inputs and optimized global  $\mathcal{H}_2$ -performance is consid-

ered in [74] based on LMI-relaxations of Riccati equations. In [140], an approach to impose structural constraints on a state-feedback gain matrix by constraining the structure of the Lyapunov matrix in an LMI-constrained optimization problem is shown.

LMI formulations are widespread in the domain of non-centralized control design, and only few alternatives exist. One of them is *dual decomposition*, which decomposes a global optimization problem into local subproblems, which are coupled and coordinated via a super-ordinated pricing mechanism. In [105], dynamic dual decomposition is employed to optimize structured state-feedback controllers for LTI systems with local inputs and local costs, interconnected via states. A second alternative are *distributed gradient methods*, which require similar assumptions on the system structure in order to enable a distributed optimization of the distributed state-feedback control laws [83]. While both methods enable a decomposition of the global synthesis problem into coupled subproblems, such distributed optimization schemes often suffer from slow convergence properties. Finally, a third alternative is the *alternating direction method of multipliers* (ADMM), where the augmented Lagrangian of the structured control problem is decomposed into two coupled summands by introducing a copy of the feedback gain. Similar to dual decomposition, those two cost terms are coupled by a price mechanism, and the optimization is performed by minimizing the first cost function, the second cost function, and the prices sequentially in an iterative manner. This algorithm is applied to structured control problems for LTI subsystems interconnected via inputs, states, and a global cost function in [77]. In order to achieve a result in acceptable time, the algorithm is stopped when the difference between the copies of the control gain is sufficiently small.

In [107], the convexity of structured optimal control problems is investigated in a frequency domain setting. A notion of quadratic invariance of the constraint set w.r.t. the plant is defined, and it is shown that the structured optimal control problem is convex for all structures belonging to this class. Subsequent results extend this work by parametrizing all stabilizing controllers subject to any structural constraint, using a Youla parametrization [106]. However, these results are not directly applicable to state-space representations of both system and controller, since the interpretation of structure differs in both domains. More precisely, a state-space representation of a dynamic system is considered to carry more structural information than the corresponding transfer function [104]. Indeed, it can be easily verified that a sparse state-space model may possess a dense (or even full) transfer function matrix. Vice versa, it is not guaranteed that a sparse transfer function matrix has a sparse state-space realization. In [104], the *dynamical structure function* (DSF) is defined as a stronger notion of structure in the frequency domain. Here, the plant is represented as an interconnection of two MIMO transfer functions, carrying more structural information than a classical transfer function, but still less than a state-space representation. Moreover, an algorithm is presented which constructs a stabilizing distributed controller (in the sense of the DSF) by adding randomly

picked scalar controller links in a sequential manner.

As mentioned earlier, many approaches to distributed control impose assumptions on the structure of the interconnected system model. A particular class of interconnected systems are *multi-agent systems* (MAS). MAS are formed by a collection of autonomous subsystems (agents) like mobile robots, unmanned air vehicles, or satellites. In general, they are required to show collective or swarm behavior like flocking, formation keeping, area coverage, or distributed task assignment [7] [115]. Therefore, MAS are typically modelled by dynamically decoupled, often similar or identical, subsystems, which are interconnected via a global cost function to encode the common control goals [80, Chap. 6]. Approaches to MAS often make use of this particular structure to simplify the distributed controller synthesis. A well-established work is [24], where distributed LQR design for identical dynamically decoupled systems with a specific structure of the global quadratic cost function is considered. In this particular case, the global LQR problem can be boiled down to one subproblem, involving only one subsystem and its neighboring subsystems. From the result of this subproblem, a distributed controller can be constructed which relies on information transmitted from neighboring subsystems.

The concept of decomposing a control problem can also be applied for certain classes of dynamically coupled subsystems. A subset of these classes is described in [97], where optimal state-feedback design w.r.t. a quadratic cost function is considered for linear subsystems. In this work, classes of matrices are characterized which preserve their structural properties under matrix operations like addition, multiplication, and inversion. Hence, if all matrices of the state-space model belong to such a particular class, this will also hold true for the optimal state-feedback gain, such that the distributed controller can be found by solving a Riccati equation. In the case of hierarchically interconnected subsystems and costs, the global LQR problem is additionally inherently decomposable into LQR subproblems, as shown in [114] and [125]. The  $\mathcal{H}_\infty$ -case is studied in [109]. A more general class of *decomposable systems* are systems where *all* matrices of the state-space representation are of the form:

$$M = I_n \otimes M_a + P_n \otimes M_b, \quad (1.1)$$

with the same diagonalizable interconnection structure matrix  $P_n$  and some matrices  $M_a$  and  $M_b$  [91]. Here, the first summand corresponds to equal entries on the block diagonal, and the second one is an interconnection matrix  $M_b$  which occurs with a pattern encoded by  $P_n$ . If this strong assumption holds, the plant can be block-diagonalized, and the control synthesis problem can be expressed in terms of decoupled LMI constraints. However, the resulting controller structure can not be influenced in this case. In order to design a structured controller with the same structure as the plant, the independent LMIs have to be coupled by local control variables again, which also induces additional conservatism. Accepting further conservatism, this approach can be extended to *linear parameter-varying* (LPV)



decomposable systems [54], or to heterogeneous groups of identical subsystems interconnected via time-varying interconnection topologies. In the latter case, the controllers can either be designed robust against [90] or depending on the current interconnection topology [55]. Notably, all the approaches to distributed control mentioned so far have in common that a single control layer with an a-priori given communication topology is considered. The potentials of additional control layers and SCT design are not taken into account.

## System Decomposition and Interaction Measures

Besides the procedure to break down a control design problem into subproblems, system decomposition can also be understood as the problem of finding a *partitioning* of a holistic dynamic system<sup>6</sup> with respect to a given criterion. Suitable decomposition criteria are often based on interaction measures, quantifying the interconnection strength between separable elements of a dynamic system, e.g. between system states or input-output channels.

The history of this field reaches back to the *relative gain array* (RGA) introduced by Bristol in 1966. The RGA is a measure of the input-output channel interaction, based on the steady-state gain of a dynamic MIMO process. Dynamic extensions of the RGA exist, which are based on the Gramians of a stable system [30] or on the Hankel-Norm [138], and also take the transient behavior into account. An energy-based approach to quantify the interconnection strength between subsystems is taken in [5], where a supply rate to the energy stored by each subsystem is defined as a function of the incoming and outgoing interconnection signals. However, this measure strongly depends on the choice of the supply functions.

Approaches to system partitioning which are based on the system matrix of a state-space representation are proposed in [132] and [140]. The so called  *$\epsilon$ -decomposition* neglects off-diagonal elements of the system matrix which are small in magnitude, trying to identify which states are weakly coupled. The *hierarchical UBT decomposition* seeks for a hierarchical interconnection structure of the system matrix by permuting the state vector. For hierarchically interconnected subsystems, the overall system is stable if and only if every subsystem is stable [132]. Further partitioning variants are the *nested  $\epsilon$ -decomposition* and the *balanced border block-diagonal decomposition*. The main purpose of these algorithms is to find a suitable partitioning and distributed controller structure for a holistic dynamic system.

## Simultaneous Controller and Communication Topology Design

In contrast to conventional distributed control design, SCT design considers the underlying communication topology of the distributed control law as an additional

---

<sup>6</sup>A holistic dynamic system is understood as a centralized dynamic mathematical model without any information regarding the partitioning of the overall system into subsystems or input-output pairs.

degree of freedom. In order to achieve a trade-off between closed-loop performance and communication effort, costs depending on the topology or usage of the communication network are introduced. Based on this idea, the communication topology of a consensus algorithm for multi-agent systems is optimized in [103] via *mixed-integer programming* (MIP). In [111],  $\mathcal{H}_\infty$ -optimized decentralized dynamic output feedback controllers with distributed feed-through are designed, where the  $\ell_0$ -norm of the feed-through matrix is penalized to promote its sparsity. The synthesis problem is formulated subject to non-convex *bilinear matrix inequalities* (BMI), where a weighted  $\ell_1$ -norm is used as a relaxation of the  $\ell_0$ -norm to avoid a mixed-integer formulation. Hence, an approximate solution is obtained. A re-weighted  $\ell_1$ -norm formulation for semidefinite programming is also proposed in [45], which is used to optimize sparse interconnection graphs for the synchronization of oscillator networks.

The aforementioned ADMM is used in [78] to design  $\mathcal{H}_2$ -optimized sparse feedback gains, where sparsity is promoted by penalizing the number of non-zero entries in the feedback gain matrix. A holistic system model is assumed, i.e. no structural information is contained in the model. Due to the separation of the cost function by using the ADMM, the subproblem minimizing the communication cost can be solved analytically. A more general variant of SCT design is proposed in [50], where individual costs can be assigned to each communication link necessary to implement the distributed controller. The control synthesis is formulated as a mixed-integer semidefinite program (MISDP), where the sum of a quadratic performance index and the communication cost is minimized.

The guiding thoughts of SCT design have also influenced *coalitional control schemes*. In these non-centralized control schemes, subsystems form time-varying coalitions during runtime, which can be interpreted as an online adaption of the communication structure. This idea is pursued in [84] for linear time-invariant subsystems interconnected via states and inputs, and with local quadratic cost functions. It is assumed that the network topology changes every  $D$  time-steps, where the topology is decentralized w.r.t. the coalitions. The scheme requires to pre-compute a controller for every admissible set of coalitions. For choosing the optimal topology online, the effect of each link on the overall performance is approximated by employing concepts of game theory. However, the performance loss due to switching the control law is not taken into account.

## Hierarchical Feedback Control

Although first schemes were already developed in the 1970s, surprisingly few approaches to hierarchical feedback control exist. The initial motivation to introduce a super-ordinated feedback layer was to compensate subsystem interconnections in order to facilitate ‘decentralized’ control [120] [131]. The disadvantages of these approaches are that they also compensate supportive interconnections and generally require full communication between the subsystems. Addressing the first drawback,

subsequent approaches propose an upper feedback layer with a coordinating, instead of a compensating function, advancing the idea of cooperative control layers [86]. However, the approach is limited to local cost functions, and the upper control layer is still considered as a centralized entity, having full information about all subsystems.

A particular two-layer feedback structure is proposed in [64] for a collection of actuator subsystems which are connected to a central mechanical or electrical subsystem, but are decoupled otherwise. Local lower-layer controllers are designed for these actuator subsystems, which reduce their dynamic order by steering them onto a sub-manifold of the state-space. Then, an upper-layer controller is designed for the global system. While using local controllers to reduce the dynamic order of subsystems is a suitable means to reduce the complexity of the overall control problem, the restricting action of the lower control layer generally contradicts common control goals. Furthermore, the concept is limited to particular subsystem interconnection topologies.

An application domain where hierarchical feedback control is being employed successfully since many years is control of power systems. Close to steady-state operation, power systems seem to be particularly amenable to hierarchical control structures, since the separate consideration of single control layers, typically defined by the different occurring time-scales, has led to a desired global behavior in practice. A distributed hierarchical control architecture for transient dynamics improvement in power systems is proposed in [88]. Local controllers for power generators are designed robust w.r.t. incoming connections, which are modeled as quadratically bounded signals. The local controllers are designed as a part of the classical control hierarchy for power systems, where the superordinate *area generation control* (AGC) layer adjusts the set-points of the generators.

It is important to note that, to the best of the author's knowledge, no connection between the fields of SCT design and hierarchical feedback control has been made so far. However, it is believed that many ideas and benefits from both fields can be combined within an interdisciplinary approach, which allows to perform SCT design for a considerably larger number of interconnected subsystems. For this reason, it is the main goal of this thesis to close this gap by providing algorithms for designing two-layer feedback structures with a parametrizable trade-off between closed-loop performance and communication effort.

### **Hierarchical Optimization and Model Predictive Control**

In contrast to hierarchical feedback control, hierarchical optimization and hierarchical MPC schemes have already been investigated to a considerable extent. While not directly related to this thesis, some relations and analogies to this field exist, such that the main advances are presented hereafter for the sake of completeness.

Hierarchical optimization schemes can be used to calculate optimal input trajectories or optimal centralized feedback controllers [86] [119]. Recent approaches also

consider the calculation of optimized distributed feedback controllers [105], which may be adjusted to a time-varying interconnection structure of the subsystems by running the optimization online [80, Chap. 3.3]. In general, hierarchical optimization is based on the separation of either the Lagrangian or the Lagrangian dual function, which mostly requires subsystems with local costs and local control inputs, and naturally results in a two-layer scheme. Schemes consisting of multiple layers, like the three-layer scheme presented in [73], are rather seldom.

Likewise, the majority of hierarchical MPC schemes consists of two layers. The upper layer is typically a centralized, distributed, or decentralized MPC, and the lower layer may consist of local MPC or local feedback controllers. The lower layer is typically fed with setpoints or reference trajectories by the upper layer. These reference values are sometimes calculated on a coarser time-scale, which is often referred to as *multi-rate* schemes [17]. Few approaches also consider the idea of grouping subsystems in order to structure the overall problem. A nested primal decomposition scheme for model predictive control of linear systems with input constraints and local costs is presented in [122]. The groups are assumed to be a-priori given. A coalitional hierarchical MPC scheme is presented in [47], where the coalitions are chosen on-line, requiring to solve the underlying combinatorial problem repeatedly during runtime.

### Hybrid Hierarchical Control and Hierarchical Discrete Event Control

A popular form of hierarchical controllers are *hybrid hierarchical controllers*, which are a combination of a set of continuous control laws and finite state machines [81]. More precisely, the finite state machine, constituting the upper layer of the hierarchical scheme, switches between different continuous lower layer control laws in order to impose a desired overall behavior. In general, the lower layer controllers are designed to implement *elementary maneuvers*, which are pre-defined time sequences of the continuous state. Then, the task of the upper control layer is to plan and implement a sequence of these elementary maneuvers such that the system is steered into the desired region of the state-space [94]. Since the choice of the elementary maneuvers is not unique and often non-trivial, hybrid hierarchical control requires intense knowledge about the system characteristics, and is mostly implemented in a centralized manner. Furthermore, the possibly adverse effects of switching between different strategies are often neglected.

Similar switching schemes selecting control laws on a lower control layer exist for the control of interconnected systems with unknown uncertainty. For instance, decentralized switching control is proposed in [1], where it is assumed that there exists a known finite set of decentralized controllers containing at least one controller which is able to stabilize the overall system at any time. The objective is then to design a decentralized switching strategy for the upper control layer such that the overall system is stabilized.

Another model class where hierarchical schemes are frequently used for control are

discrete-event systems. Discrete-event systems are often used to model automated manufacturing processes by considering the manufacturing process as a collection of modular production units, which are again described by a discrete set of sub-processes or events. Due to the discrete state-space and the inherent modularity of the resulting models, these are particularly amenable to model abstraction and refinement by accumulating or decomposing possible sequences of discrete events [124]. Hence, in a first step, lower layer discrete event controllers are typically designed for the modular units of the overall manufacturing process. In a second step, a coordinating upper layer discrete event controller is designed based on an abstracted model [29]. Theoretical research on this field often focuses on the formal connection and implementation of the single control layers, e.g. by defining standard interfaces [71].

### **Non-Centralized Control of Jump Markov and Jump Semi-Markov Systems**

In the third part of this thesis, the hierarchical distributed control schemes originally developed for time-invariant dynamic systems are extended to a class of uncertain dynamic systems. In particular, interconnected discrete-time jump Markov systems (JMS) are considered, which have been investigated to a considerable extent in the context of centralized control schemes [31] [37] [117]. Non-centralized control schemes for jump Markov systems, however, do barely exist. Most approaches to non-centralized control of JMS consider decentralized schemes, e.g. [85]. Robust approaches using only the local continuous state and the global Markov state [75], the local Markov state [139] [93, Chap. 7], or the Markov states of neighboring subsystems [82] exist. These robust approaches require to specify infinite horizon integral quadratic constraints (ICQ) on all disturbance and interconnection signals. Furthermore, even though [139], [93, Chap. 7], and [82] require communication to exchange the local Markov states, they do not make use of the ability to exchange the local measurements of the continuous states.

Distributed control of jump Markov multi-agent systems with identical subsystem dynamics is considered in [36] and [133]. In [133], distributed output feedback controllers are designed for the case that all agents possess the same Markov chain, while the system class is used in [36] to model communication uncertainties in a string of vehicles. Distributed team-decision strategies for identical, decoupled JMS are designed in [134]. Distributed model predictive control for JMS with polytopic uncertainty is considered in [121]. However, the scheme is computationally involving, since a series of LMI-constrained optimization problems has to be solved at each time-step.

Jump Semi-Markov Systems (JSMS) are a natural extension of JMS. They are obtained from JMS by dropping the assumption of time-invariant transition probabilities, leading to more modeling flexibility regarding the discrete-valued part of the dynamics. So far, JSMS have mainly been studied in the context of centralized settings. An overview of several special cases regarding the time-dependency of the

transition probabilities is provided in [141]. Furthermore, the article presents an approach to the stabilization of discrete-time JSMS in the case that the probability density function depends on the current and on the next system mode. In [56], an approach to the robust stabilization of continuous-time JSMS with polytopic uncertainty in the system matrices is presented, and [112] considers the stabilization of continuous-time JSMS in the sense of mean-square stability and w.r.t. a quadratic loss function.

### **Control of Cyber-Physical Systems and Systems-of-Systems**

Cyber-physical systems and systems of systems are relatively new notions of complex systems which emerged in the past decade. While both of them contain many parallels to other notions of complex systems, they focus on incorporating new technical aspects and requirements into the system analysis and control design process. In the sequel, both notions will be described in more detail.

A system of systems (SoS) is a class of complex systems comprised of subsystems which are complex systems themselves. It can be thought of as a collection of individual, possibly heterogeneous, but functional systems which collaborate for enhancing the overall robustness, lowering the cost of operation, and increasing the reliability of the overall complex system [57]. An SoS is often characterized by operational and managerial independence of the single systems, by their geographic distribution, and by their evolutionary development. From an engineering perspective, one is typically interested in the emergent behavior of the overall system. A major goal of SoS research is to design these systems to deliver higher capabilities and performance than traditional systems. This design process is termed system of systems engineering, and requires new approaches for a suitable modeling, architecture, and simulation frameworks, as well as system identification and control synthesis algorithms [57]. The system of systems perspective recently has been applied to system theoretic problems from various application domains, including networked microgrids [99], infrastructure planning [98], military defense systems, or aerospace systems [57], to name a few.

Research on cyber-physical systems (CPS), on the other hand, focuses on integrations of computation and physical processes. The main observation is that the physical components of these systems introduce safety and reliability requirements which go far beyond those of general purpose computing. Existing abstractions and semantics used in computing and networking environments do not take these requirements into account, since there is a general lack of temporal semantics and adequate concurrency models [72]. For instance, a perfectly working code written in C may still practically fail when executed in a CPS if timing deadlines are missed. CPS are assumed to be incorporated in networked environments, meaning that their internal behavior can be influenced by external information. This makes it hard to verify the correct operation of a CPS, and leaves the system vulnerable to malicious attacks. Consequently, CPS research has a strong focus on robustness,

fault-diagnosis, and cyber-security, see for instance [126], [127].

### 1.3. Contribution of this Thesis

As can also be deduced from the previous section, hierarchical distributed feedback control schemes are so far not considered as an alternative for non-centralized control of interconnected systems. It is the aim of this dissertation to close this gap by developing computationally tractable synthesis procedures for **distributed two-layer feedback control schemes** for both time-invariant and uncertain dynamic systems. In particular, algorithms for a **structural analysis** of the interconnection structure are provided, which group strongly coupled subsystems into clusters. It is shown that this clustering procedure is a productive means to significantly reduce the computational complexity of solving SCT design problems.

In this thesis, global control goals will be encoded either by a global quadratic infinite horizon cost function, or by a norm of the system w.r.t. a global controlled variable. A particular problem that will be addressed in the sequel is to design the hierarchical distributed controller such that both control layers and all local controllers **cooperate** for minimizing this cost function or system norm, respectively.

Due to the usage of feedback control laws, the implementation of the proposed distributed two-layer control scheme is simple compared to, e.g., distributed MPC schemes, which usually require additional optimization software and hence more powerful embedded hardware. By adopting the ideas of SCT design for this scheme, the implementation is furthermore simplified by using only those communication channels which significantly contribute to the global system performance. In Chapter 4, it is shown how the communication load of the distributed two-layer feedback scheme can be equably distributed over time by switching from synchronous to **asynchronous operation** on the upper control layer.

The control synthesis procedures presented in this thesis are based on the **versatile framework** of Linear Matrix Inequalities. Such inequalities have a very natural connection to control synthesis, and allow to incorporate various requirements and aspects during control design, such as  $\mathcal{H}_2$ - and  $\mathcal{H}_\infty$ -performance, passivity, time-domain constraints (e.g., peak values of the control input, or of the impulse- or step-response), minimum decay rate, or pole-placement constraints [25] [110]. Therefore, the author believes that the results presented in this thesis can be extended towards many of these features.

## 2. Problem Setup and Preliminaries

This chapter introduces the problem setup, the basic notation, and the mathematical and methodical preliminaries required for the subsequent chapters. The first section introduces the considered classes of dynamic systems and two different notions of closed-loop performance that will be used throughout this thesis. The problem setup is completed by formalizing the controller structure as well as the time scales of the hierarchical control scheme. In the second section, a mathematical model of the available communication network is introduced, and common stability notions for the considered types of dynamic systems are reviewed in the third section. Section 2.4 reviews the definition and several interpretations of the  $\mathcal{H}_2$ -norm of linear time-invariant dynamic systems and the generalization of these concepts to jump Markov linear systems. In Section 2.5, some basics of semidefinite programming and linear matrix inequalities are presented, which serve as framework for the control design process. Finally, Section 2.6 presents some decomposition concepts that are part of the structural analysis performed prior to the control design.

### 2.1. General Problem Setup and Notation

The general problem setup is shown in Figure 2.1: Given an interconnection of  $N_s$  dynamic subsystems  $\mathcal{P}^i$ , determine distributed hierarchical two-layer controllers  $\mathcal{C}^{\downarrow i}$  and  $\mathcal{C}^{\uparrow i}$  such that the closed-loop system is stable and an a-priori given global performance index is optimized. Here,  $\mathcal{C}^{\downarrow i}$  denotes the  $i$ -th lower-layer controller, and  $\mathcal{C}^{\uparrow i}$  denotes the  $i$ -th upper-layer controller. These controllers are distributed in the sense that they can be locally implemented, i.e. spatially associated to the subsystems  $\mathcal{P}^i$ , while exchanging necessary information from other subsystems via a communication network  $\mathcal{G}$ . The particular challenge is to design all controllers on both control layers such that they cooperate for optimizing the global performance index. Furthermore, a parametrizable trade-off between closed-loop performance and communication cost is sought.

#### System Dynamics

In the second part of this thesis, the overall dynamic system is given by the discrete-time linear time-invariant (LTI) system:

$$\mathcal{P} : x_{k+1} = Ax_k + Bu_k + Ew_k, \quad (2.1)$$



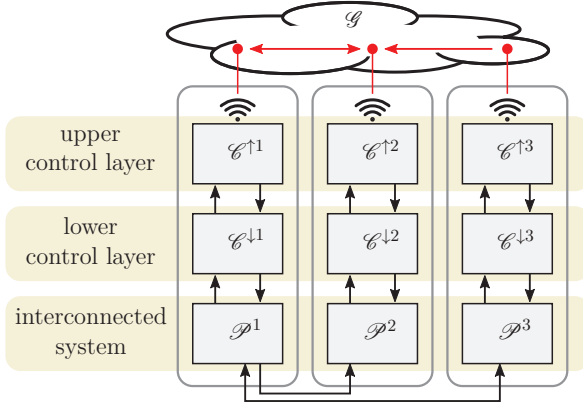


**Figure 2.1.:** General setup of a two-layer hierarchical distributed control structure.

where  $k$  denotes the discrete time,  $x_k \in \mathbb{X} \subseteq \mathbb{R}^{n_x}$  and  $u_k \in \mathbb{U} \subseteq \mathbb{R}^{n_u}$  are the global state and the input vector of  $\mathcal{P}$ , respectively, and  $w_k \in \mathbb{W} \subseteq \mathbb{R}^{n_w}$  is a global disturbance input. The system matrix  $A \in \mathbb{R}^{n_x \times n_x}$ , the input matrix  $B \in \mathbb{R}^{n_x \times n_u}$ , and the disturbance input matrix  $E \in \mathbb{R}^{n_x \times n_w}$  parametrize the dynamic behavior of  $\mathcal{P}$ . The signals  $u_k$  and  $w_k$  are assumed to be piecewise constant and updated at time  $t = k\Delta t$ , i.e.:

$$u(t) = u(k\Delta t) =: u_k \quad \text{for } k\Delta t \leq t < k\Delta t + \Delta t, \quad (2.2)$$

using the example of the input vector  $u_k$ . Likewise,  $x_k$  is sampled at time  $k\Delta t$ , i.e.:

$$x(k\Delta t) =: x_k. \quad (2.3)$$

Suppose that the vectors  $x_k = (x_k^1; \dots; x_k^{N_s})$ ,  $u_k = (u_k^1; \dots; u_k^{N_s})$ , and  $w_k = (w_k^1; \dots; w_k^{N_s})$  are partitioned according to the subsystems. Here,  $(y^1; \dots; y^N) := [(y^1)^\top, \dots, (y^N)^\top]^\top$  with  $y^i \in \mathbb{R}^{n^i \times 1}$  denotes a stacked column vector. Then, the global system  $\mathcal{P}$  can be interpreted as an interconnection of  $N_s \in \mathbb{N}$  subsystems:

$$\mathcal{P}^i : x_{k+1}^i = A_{i,i}x_k^i + B_{i,i}u_k^i + E_{i,i}w_k^i + r_{x,k}^i, \quad (2.4)$$

with  $i \in \mathcal{N}_s := \mathbb{I}_{N_s} = \{1, 2, \dots, N_s\}$ , and  $x_k^i \in \mathbb{X}^i \subseteq \mathbb{R}^{n_x^i}$ ,  $u_k^i \in \mathbb{U}^i \subseteq \mathbb{R}^{n_u^i}$ , and  $w_k^i \in \mathbb{W}^i \subseteq \mathbb{R}^{n_w^i}$  being the local state, input, and disturbance input, respectively. The local matrices  $A_{i,i} \in \mathbb{R}^{n_x^i \times n_x^i}$ ,  $B_{i,i} \in \mathbb{R}^{n_x^i \times n_u^i}$ , and  $E_{i,i} \in \mathbb{R}^{n_x^i \times n_w^i}$  denote the corresponding block entries of the matrices  $A$ ,  $B$ , and  $E$ . Furthermore,  $r_{x,k}^i \in \mathbb{R}^{n_x^i}$

is the interconnection input, which is given by:

$$r_{x,k}^i = \sum_{j \in \mathcal{N}_s^i} (A_{i,j} x_k^j + B_{i,j} u_k^j + E_{i,j} w_k^j), \quad (2.5)$$

with  $\mathcal{N}_s^i := \mathcal{N}_s \setminus \{i\}$ .

In the third part of this thesis, a class of discrete-time uncertain dynamic systems  $\mathcal{P}_\theta$ , called jump Markov systems (JMS) [31], is considered. In particular, interconnected jump Markov linear systems are considered, where the  $i$ -th subsystem  $\mathcal{P}_\theta^i$  takes the form:

$$\mathcal{P}_\theta^i : x_{k+1}^i = A_{i,i}[\theta_k^i] x_k^i + B_{i,i}[\theta_k^i] u_k^i + E_{i,i}[\theta_k^i] w_k^i + r_{x,k}^i[\theta_k^i]. \quad (2.6)$$

In contrast to the LTI subsystems given in (2.4), the local matrices  $A_{i,i}[\theta_k^i] \in \mathbb{R}^{n_x^i \times n_x^i}$ ,  $B_{i,i}[\theta_k^i] \in \mathbb{R}^{n_x^i \times n_u^i}$ , and  $E_{i,i}[\theta_k^i] \in \mathbb{R}^{n_x^i \times n_w^i}$  depend on the discrete state  $\theta_k^i \in \Theta^i$  of a local Markov chain:

$$\mathcal{M}^i = (\Theta^i, P^i, \mu_0^i), \quad (2.7)$$

with the discrete state space  $\Theta^i := \mathbb{I}_{N_\theta^i}$  and a right-stochastic transition probability matrix  $P^i = [p_{m,n}^i] \in [0, 1]^{N_\theta^i \times N_\theta^i}$ , with entries given by:

$$p_{m,n}^i := \Pr(\theta_{k+1}^i = n \mid \theta_k^i = m). \quad (2.8)$$

Furthermore,  $\mu_0^i \in [0, 1]^{N_\theta^i}$  is the initial distribution of the Markov state, i.e.:

$$\mu_{0,m}^i := \Pr(\theta_0^i = m), \quad (2.9)$$

where  $\mu_{0,m}^i$  denotes the  $m$ -th component of the vector  $\mu_0^i$ . In (2.6), the interconnection signal  $r_{x,k}^i[\theta_k^i]$  takes the general form:

$$r_{x,k}^i[\theta_k^i] = \sum_{j \in \mathcal{N}_s^i} (A_{i,j}[\theta_k^i] x_k^j + B_{i,j}[\theta_k^i] u_k^j + E_{i,j}[\theta_k^i] w_k^j). \quad (2.10)$$

For the case of interconnected jump Markov linear systems, the global uncertain interconnected system is denoted by  $\{\mathcal{P}_\theta^i\}_{i \in \mathcal{N}_s}$ . Furthermore, the tuple  $\zeta_k^i := (x_k^i, \theta_k^i)$  is referred to as the *hybrid state* of subsystem  $\mathcal{P}_\theta^i$ .

## Quadratic Performance Indices

In order to prepare specifying the performance of the global system  $\mathcal{P}$  governed by a given control law, the controlled variable:

$$z_k = Cx_k + Du_k + Fw_k \quad (2.11)$$

is introduced, where  $z_k = (z_k^1, \dots, z_k^{N_s}) \in \mathbb{R}^{n_z}$ , and  $C = [C_{i,j}] \in \mathbb{R}^{n_z \times n_x}$ ,  $D = [D_{i,j}] \in \mathbb{R}^{n_z \times n_u}$ , and  $F = [F_{i,j}] \in \mathbb{R}^{n_z \times n_w}$  are parameters to be chosen by the designer. Depending on their non-zero pattern, the matrices  $C$  and  $D$  may induce further coupling between the subsystems  $\mathcal{P}^i$ .

For the uncertain subsystems  $\mathcal{P}_\theta^i$ , the matrices  $C$  and  $D$  may additionally depend on the local Markov state  $\theta_k^i$ . Consequently, local controlled variables:

$$z_k^i = C_{i,i}[\theta_k^i]x_k^i + D_{i,i}[\theta_k^i]u_k^i + \sum_{j \in \mathcal{N}_s^i} (C_{i,j}[\theta_k^i]x_k^j + D_{i,j}[\theta_k^i]u_k^j) \quad (2.12)$$

are defined, with  $z_k^i \in \mathbb{R}^{n_z^i}$ .

In the sequel, the controlled variables  $z_k^i$  will be used to specify quadratic performance criteria of the closed-loop system with respect to the operating point of interest. These performance indices can be used to evaluate the transient behavior or the effect of disturbances on the controlled system. The operating point is assumed to be an equilibrium point of the dynamic system according to:

**Definition 2.1.** *The constant tuple  $(x_{\text{eq}}, u_{\text{eq}}, w_{\text{eq}})$  determines an equilibrium point for the dynamic system  $\mathcal{P}$ , if the following relations hold:*

$$x_{\text{eq}} = Ax_{\text{eq}} + Bu_{\text{eq}} + Ew_{\text{eq}}, \quad (2.13a)$$

$$z_{\text{eq}} = Cx_{\text{eq}} + Du_{\text{eq}} + Fw_{\text{eq}}. \quad (2.13b)$$

△

For the interconnected jump Markov linear system  $\{\mathcal{P}_\theta^i\}_{i \in \mathcal{N}_s}$ , the equilibria  $x_{\text{eq}}$  and  $z_{\text{eq}}$  of the global state and controlled variable are required to be independent of the local Markov states  $\theta_k^i$ . Hence, an equilibrium point for  $\{\mathcal{P}_\theta^i\}_{i \in \mathcal{N}_s}$  can be defined as follows:

**Definition 2.2.** *The set  $\{(x_{\text{eq}}^i, u_{\text{eq}}^i[\theta], w_{\text{eq}}^i[\theta])\}_{i \in \mathcal{N}_s}$  with  $\theta := (\theta^1, \dots, \theta^{N_s}) \in \Theta^1 \times \dots \times \Theta^{N_s}$  determines an equilibrium point for the uncertain interconnected system  $\{\mathcal{P}_\theta^i\}_{i \in \mathcal{N}_s}$  if the following relations hold for all  $\theta^i \in \Theta^i$  and all  $i \in \mathcal{N}_s$ :*

$$x_{\text{eq}}^i = \sum_{j \in \mathcal{N}_s^i} (A_{i,j}[\theta^i]x_{\text{eq}}^j + B_{i,j}[\theta^i]u_{\text{eq}}^j[\theta] + E_{i,j}[\theta^i]w_{\text{eq}}^j[\theta]), \quad (2.14a)$$

$$z_{\text{eq}}^i = \sum_{j \in \mathcal{N}_s^i} (C_{i,j}[\theta^i]x_{\text{eq}}^j + D_{i,j}[\theta^i]u_{\text{eq}}^j[\theta]). \quad (2.14b)$$

△

Here, the input signals  $u_{\text{eq}}^j[\theta]$  and  $w_{\text{eq}}^j[\theta]$  may additionally depend on the aggregate Markov state  $\theta$  for  $x_{\text{eq}}^i$  to be an equilibrium for all  $\theta^i \in \Theta$ . In order to simplify the presentation in the sequel, it is assumed from now on that the origin of the state space  $\mathbb{X}$  is the equilibrium of interest. Note that generality is not lost by imposing this assumption, since for both,  $\mathcal{P}$  and  $\{\mathcal{P}_\theta^i\}_{i \in \mathcal{N}_s}$ , any equilibrium point can be shifted to the origin by introducing affine transformations for  $x_k^i$ ,  $u_k^i$ ,  $w_k^i$ , and  $z_k^i$  (cf. [87, p.161] or [9, p.490]).

**Assumption 2.1.** *Without loss of generality, it is assumed that:*

$$x_{\text{eq}} = 0_{n_x \times 1}, \quad u_{\text{eq}} = 0_{n_u \times 1}, \quad w_{\text{eq}} = 0_{n_w \times 1}, \quad z_{\text{eq}} = 0_{n_z \times 1}, \quad (2.15a)$$

for the system  $\mathcal{P}$ , as well as:

$$x_{\text{eq}}^i = 0_{n_x^i \times 1}, \quad u_{\text{eq}}^i[\theta] = 0_{n_u^i \times 1}, \quad w_{\text{eq}}^i[\theta] = 0_{n_w^i \times 1}, \quad z_{\text{eq}}^i[\theta] = 0_{n_z^i \times 1}, \quad (2.15b)$$

for all uncertain subsystems  $\mathcal{P}_\theta^i$  with  $i \in \mathcal{N}_s$  and all  $\theta \in \Theta^1 \times \dots \times \Theta^{N_s}$ .  $\Delta$

Next, an admissible control law for  $\mathcal{P}$  and for  $\{\mathcal{P}_\theta^i\}_{i \in \mathcal{N}_s}$  is defined as follows:

**Definition 2.3.** *For the system  $\mathcal{P}$ , a control law  $\kappa : \mathbb{X} \rightarrow \mathbb{U}$  is called admissible if:*

$$\lim_{k \rightarrow \infty} \|x_k\|_2 = 0 \quad (2.16)$$

whenever  $w_k = 0$  for all  $k \in \mathbb{N}_0$ .

**Definition 2.4.** *For the uncertain interconnected system  $\{\mathcal{P}_\theta^i\}_{i \in \mathcal{N}_s}$ , a control law  $\kappa : \mathbb{X} \times \Theta^1 \times \dots \times \Theta^{N_s} \rightarrow \mathbb{U}$  is called admissible if:*

$$\lim_{k \rightarrow \infty} \mathbb{E}(\|x_k^i\|_2) = 0 \quad \forall i \in \mathcal{N}_s \quad (2.17)$$

whenever  $w_k^i = 0$  for all  $i \in \mathcal{N}_s$  and all  $k \in \mathbb{N}_0$ .

For the definition of the quadratic performance index, the following two cases are distinguished throughout this thesis:

**Case 2.1.** *The dynamic system  $\mathcal{P}$  is initialized in the equilibrium point, i.e.:*

$$x_0 = x_{\text{eq}} = 0_{n_x \times 1}. \quad (2.18)$$

For all times  $k \in \mathbb{N}_0$ , the disturbance inputs  $w_k^i$  are driven by independent Gaussian discrete-time white noise processes<sup>1</sup>, i.e.:

$$\mathbb{E}(w_k^i) = 0_{n_w^i \times 1}, \quad \mathbb{E}((w_k^i (w_k^i)^\top)) = I_{n_w^i}, \quad \mathbb{E}(w_k^i (w_l^j)^\top) = 0_{n_w^i \times n_w^j}, \quad (2.19)$$

for all  $(i, j) \in \mathcal{N}_s \times \mathcal{N}_s$ ,  $(k, l) \in \mathbb{N}_0 \times \mathbb{N}_0$  which satisfy either  $i \neq j$  or  $k \neq l$ . Furthermore, assume that all  $w_k^i$  are independent of  $x_0$  for all  $i \in \mathcal{N}_s$  and all  $k \in \mathbb{N}_0$ . Given an admissible control law  $u_k = \kappa(x_k)$ , the performance of the closed-loop system is measured by:

$$J := \lim_{k_e \rightarrow \infty} \mathbb{E} \left( \frac{1}{k_e} \sum_{k=0}^{k_e-1} z_k^\top z_k \right) = z_{\text{RMS}}^2. \quad (2.20)$$

<sup>1</sup>For details on these noise processes, see e.g. [65, Chap. 6] or [31, Chap. 4].

For the case of uncertain interconnected systems  $\{\mathcal{P}_\theta^i\}_{i \in \mathcal{N}_s}$ , let:

$$x_0^i = x_{\text{eq}}^i = 0_{n_i^x \times 1} \quad \forall i \in \mathcal{N}_s, \quad (2.21)$$

and  $\theta_0^i \in \Theta^i$  random according to the initial distribution  $\mu_0^i$ . Furthermore, assume that (2.19) holds and that all  $w_k^i$  are independent of  $\theta_0^j$  and  $x_0^j$  for all  $(i, j) \in \mathcal{N}_s \times \mathcal{N}_s$  and all  $k \in \mathbb{N}_0$ . Given an admissible control law  $u_k = \kappa(x_k, \theta_k)$ , the performance of the closed-loop system is measured by:

$$J := \limsup_{k_e \rightarrow \infty} \mathbb{E} \left( \frac{1}{k_e} \sum_{k=0}^{k_e-1} z_k^\top z_k \right). \quad (2.22)$$

△

**Case 2.2.** The dynamic system  $\mathcal{P}$  has an arbitrary initialization  $x_0 \in \mathbb{R}^{n_x}$ , and the disturbance inputs  $w_k^i = 0$  for all  $i \in \mathcal{N}_s$  and all  $k \in \mathbb{N}_0$ . Given an admissible control law  $u_k = \kappa(x_k)$ , the performance of the closed-loop system is measured by:

$$J := \sum_{k=0}^{\infty} z_k^\top z_k = \|z\|_{\ell_2}^2. \quad (2.23)$$

For the case of uncertain interconnected systems  $\{\mathcal{P}_\theta^i\}_{i \in \mathcal{N}_s}$ , let  $x_0^i \in \mathbb{X}^i$  be arbitrary,  $w_k^i = 0$  for all  $i \in \mathcal{N}_s$  and all  $k \in \mathbb{N}_0$ , and  $\theta_0^i \in \Theta^i$  random according to the initial distribution  $\mu_0^i$ . Given an admissible control law  $u_k = \kappa(x_k, \theta_k)$ , the performance of the closed-loop system is measured by:

$$J := \sum_{k=0}^{\infty} \mathbb{E}(z_k^\top z_k) = \mathbb{E}(\|z\|_{\ell_2}^2). \quad (2.24)$$

△

## Time Synchronization and Time Scales

Before explaining the intended controller structure, the aspect of time synchronization shall be discussed. Time synchronization is an important aspect in both distributed control and networked communication. As stated, e.g., in [51, Chap. 2.2], a deterministic transmission of communicated values using protocols with pre-determined schedules can only be ensured if a time-slot for the transmission is reserved by a network scheduler. In order to avoid overlaps of these time-slots, which would result in collisions and packet loss, all terminal points of the communication network must have knowledge about a common reference time as precise as possible. Protocols which use arbitration to determine which terminal point gets access to the communication network, on the other hand, also crucially rely on clock synchronization [51, Chap. 2.2].

Similarly, the bigger part of distributed and hierarchical control algorithms, be it from the domain of model predictive control or feedback control, relies on time

synchronization. A synchronized clock is required for a controller to be able to interpret a measured state or calculated input received from another controller correctly, and for all controllers to act synchronously. Furthermore, measurements may be equipped with absolute time-stamps, which may be used by the receivers to compensate for transmission delays. Therefore, regarding time synchronization of the local controllers  $\mathcal{C}^{\downarrow i}$  and  $\mathcal{C}^{\uparrow i}$ , the following assumption is imposed:

**Assumption 2.2.** *The clocks of the distributed controllers  $\mathcal{C}^{\downarrow i}$  and  $\mathcal{C}^{\uparrow i}$  are synchronized, and sampling and actuation is performed synchronously by all controllers.  $\Delta$*

Multiple control layers also give reason to consider multiple time scales. If those time scales are different, the corresponding control schemes are sometimes referred to as *multi-rate* control schemes [17]. For the hierarchical two-layer control scheme presented in this thesis, it is assumed that the upper control layer operates on a coarser time scale than the lower control layer. The motivation for this choice will become clear when introducing the controller structure in the next subsection.

Figure 2.2 shows the relation between those two time scales. The lower control layer operates with the sampling frequency  $1/\Delta t$  already introduced in Eq. (2.2), and performs zero-order hold in between. Hence, the corresponding signals  $(\cdot)_k$  are piecewise constant on the lower layer time-domain:

$$\mathbb{T}^\downarrow := \{t_k \mid t_k = k\Delta t + t_0, k \in \mathbb{N}_0, \Delta t \in \mathbb{R}_{>0}\}, \quad (2.25)$$

such that the controllers  $\mathcal{C}^{\downarrow i}$  sample  $x_k^i$  and update  $u_k^i$  at time  $t_k$ .

The upper control layer is designed to only act every  $\Delta k$ -th time of the lower layer. Here,  $\Delta k \in \mathbb{N}_{>1}$  is a parameter to be chosen by the designer. Given  $\Delta k$ , the upper layer time-domain can be defined as:

$$\mathbb{T}^\uparrow := \{\hat{t}_s \mid \hat{t}_s = s\Delta k\Delta t + t_0, s \in \mathbb{N}_0, \Delta t \in \mathbb{R}_{>0}, \Delta k \in \mathbb{N}_{>1}\}. \quad (2.26)$$

The corresponding signals, denoted by  $(\hat{\cdot})_s$ , are assumed to be piecewise constant on  $\mathbb{T}^\uparrow$ , and are related to the lower layer time domain by [58]:

$$(\hat{\cdot})_s = (\cdot)_{s\Delta k}, \quad s\Delta k = k - k \bmod \Delta k. \quad (2.27)$$

In subsequent figures and block diagrams, the sampling time of single components will be indicated, e.g., by  $@\mathbb{T}^\uparrow$ , if not clear from the context.

### Subsystem Clustering and Hierarchical Controller Structure

For the hierarchical two-layer control approach presented in this thesis, the subsystem structure is analyzed prior to the control design. Figure 2.3, which is an extension of Fig. 2.1, illustrates the effect of this structural analysis. According to the interconnection strength and structure, strongly coupled subsystems  $\mathcal{P}^i$  are

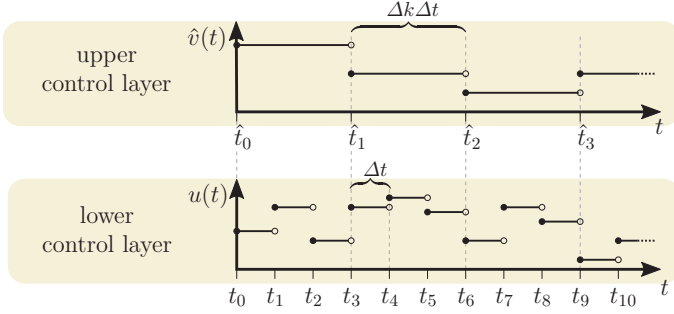


**Figure 2.2.:** Relation between the lower layer and upper layer time scales for the exemplary case  $\Delta k = 3$ .

grouped into *clusters*. These clusters are described by  $N_c \in \mathbb{N}$  disjoint index sets  $\mathcal{C}^p \subseteq \mathcal{N}_s$ , with  $p \in \mathcal{N}_c := \mathbb{I}_{N_c}$  and:

$$\bigcup_{p \in \mathcal{N}_c} \mathcal{C}^p = \mathcal{N}_s, \quad \mathcal{C}^p \cap \mathcal{C}^q = \emptyset \quad \forall p \neq q. \quad (2.28)$$

Each cluster can be thought of as a ‘virtual aggregate subsystem’  $\bar{\mathcal{P}}^p$ , where the bar indicates the new partitioning of the interconnected system. In Figure 2.3,

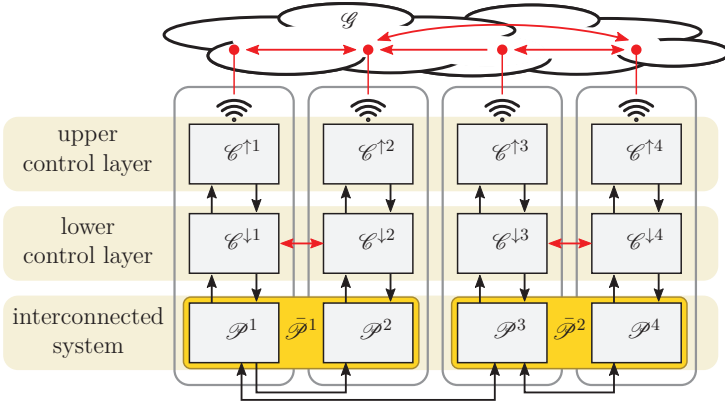


**Figure 2.3.:** Two-layer hierarchical distributed control structure with clustered subsystems  $\bar{\mathcal{P}}^p$  (enframed in yellow).

subsystems  $\mathcal{P}^1$  and  $\mathcal{P}^2$  form the cluster  $\bar{\mathcal{P}}^1$ , and subsystems  $\mathcal{P}^3$  and  $\mathcal{P}^4$  form the cluster  $\bar{\mathcal{P}}^2$ , indicated by the yellow boxes. The distributed lower control layer

accounts for the strong interconnections of the subsystems within the clusters, and is therefore allowed to exchange information within each cluster only. Hence, from the viewpoint of the clusters, the lower control layer has a decentralized structure. Consequently, by the help of the mapping:

$$p : \mathcal{N}_s \rightarrow \mathcal{N}_c, \quad i \mapsto p(i) = p \in \mathcal{N}_c \mid i \in \mathcal{C}^p, \quad (2.29)$$

the lower layer control law takes the general form:

$$\mathcal{E}^{\downarrow i} : u_k^i = \kappa^{\downarrow i}(\bar{x}_k^{p(i)}) + v_k^i, \quad (2.30)$$

with  $i \in \mathcal{N}_s$ . Here,  $\bar{x}_k^p := [x_k^i]_{i \in \mathcal{C}^p} \in \mathbb{R}^{\bar{n}^p}$  denotes the aggregated state of subsystem  $\mathcal{P}^p$ . The vectors  $v_k^i \in \mathbb{R}^{n_i}$  are external inputs to be chosen by the upper control layer later. The lower control layer is distributed in the sense that a local input  $u_k^i$  is calculated as a function of the local state  $x_k^i$  and of the states  $x_k^j$  transmitted from all subsystems within the same cluster, i.e. all  $x_k^j$  with  $j \in \mathcal{C}^p$ . These states are transmitted to the  $i$ -th subsystem via the communication network  $\mathcal{G}$ .

On the upper control layer, distributed controllers  $\mathcal{E}^{\uparrow i}$  are designed which have the task to coordinate the clusters. A coordination of the clusters is necessary to account for the global character of the performance index  $J$ , and to ensure the stability of the overall system. The coordination is accomplished by exchanging information between controllers  $\mathcal{E}^{\uparrow i}$  in different clusters. Since the fast and strongly coupled dynamics are already handled by the lower control layer, the upper control layer is implemented on a coarser time-scale. The positive side-effect of this decision is a reduced communication and computation load when implementing the distributed two-layer control scheme. Denote the set of states available to controller  $\mathcal{E}^{\uparrow i}$  at time  $s\Delta k$  by:

$$\hat{\mathcal{X}}_s^p := \{\hat{x}_s^q \in \bar{\mathbb{X}}^q \mid q \in \bar{\mathcal{R}}^{\uparrow p} \subseteq \mathcal{N}_c\}, \quad (2.31)$$

where  $\bar{\mathcal{R}}^{\uparrow p} \subseteq \mathcal{N}_c \setminus \{p\}$  is the index set of clusters transmitting their local information sets to cluster  $\mathcal{C}^p$ . Then, the general form of the upper layer controllers is given by:

$$\mathcal{E}^{\uparrow i} : \hat{v}_s^i = \kappa^{\uparrow i}(\hat{x}_s^{p(i)}, \hat{\mathcal{X}}_s^{p(i)}). \quad (2.32)$$

### Considered Optimal Control Problem

With the notions and notation introduced so far, the general problem of optimized hierarchical two-layer control design can be summarized as follows: Given  $\Delta k > 1$ , find admissible distributed control laws  $\kappa^{\downarrow}(\cdot)$  and  $\kappa^{\uparrow}(\cdot)$  for the lower and upper control layer such that the performance index  $J + J^{\text{com}}$  is minimized. Here,  $J$  is chosen according to Case 2.1 or Case 2.2, and  $J^{\text{com}} \in \mathbb{R}_{\geq 0}$  is a cost term describing the “quality” of the topology of the communication network  $\mathcal{G}$  that will be defined in the next section. By minimizing the sum of the performance index and a communication cost, a trade-off between control performance and communication load is attained.



## 2.2. Model of the Communication Network

If not specified otherwise, it is generally assumed in this thesis that the communication network  $\mathcal{G}$  is ideal in the following sense:

**Assumption 2.3.** *The communication network  $\mathcal{G}$  is neither subject to failure nor to time-delay.*  $\triangle$

For a practical implementation, this assumption requires the usage of reliable network protocols like TCP, and a transmission delay which is sufficiently small compared to the sampling interval  $\Delta t$  of the control system. In fact, similar assumptions are imposed in many current approaches to distributed control, either in implicit or in explicit form (see, e.g., [50] [75] [76] [111], among many others).

Since the main interest concerning the communication network is the underlying network topology, it is convenient to model the communication network by a directed graph  $\mathcal{G} = (\mathcal{N}, \mathcal{E})$ . Here, the set of nodes  $\mathcal{N}$  corresponds to the local controllers, and  $\mathcal{E} \subseteq \mathcal{N} \times \mathcal{N}$  denotes the set of directed edges. Hence,  $(i, j) \in \mathcal{E}$  if and only if there exists a communication link from controller  $\mathcal{C}^j$  to controller  $\mathcal{C}^i$ . From the perspective of a practical implementation of distributed control laws, it is reasonable to assume that  $(i, i) \in \mathcal{E}$  for all  $i \in \mathcal{N}$ , i.e. each controller can access its local information.

In accordance with the hierarchical two-layer control scheme, this graph can be associated either with the lower or with the upper control layer, giving rise to the following definitions:

$$\mathcal{G}^\downarrow := (\mathcal{N}_s, \mathcal{E}^\downarrow), \quad \mathcal{G}^\uparrow := (\mathcal{N}_c, \mathcal{E}^\uparrow), \quad (2.33)$$

with  $\mathcal{E}^\downarrow \subseteq \mathcal{N}_s \times \mathcal{N}_s$  and  $\mathcal{E}^\uparrow \subseteq \mathcal{N}_c \times \mathcal{N}_c$ . Given  $\mathcal{G}^\downarrow$  and  $\mathcal{G}^\uparrow$ , the set of directed edges  $\mathcal{E}$  of  $\mathcal{G}$  can be constructed as follows:

$$(i, j) \in \mathcal{E}^\downarrow \Rightarrow (i, j) \in \mathcal{E}, \quad (2.34a)$$

$$(p, q) \in \mathcal{E}^\uparrow \Rightarrow \mathcal{C}_p \times \mathcal{C}_q \subset \mathcal{E}. \quad (2.34b)$$

In the remainder of this thesis, directed graphs will be frequently represented by their adjacency matrix  $\Sigma = [\sigma_{i,j}] \in \mathbb{B}^{\mathcal{N}_s \times \mathcal{N}_s}$ , with  $\mathbb{B} := \{0, 1\}$ . The binary entries  $\sigma_{i,j} \in \mathbb{B}$  are defined as:

$$\sigma_{i,j} := \begin{cases} 1 & \text{if } (i, j) \in \mathcal{E}, \\ 0 & \text{otherwise.} \end{cases} \quad (2.35)$$

With a network topology specified by  $\Sigma$ , a communication cost function:

$$J^{\text{com}}(\Sigma) := \sum_{(i,j) \in \mathcal{E}} \sigma_{i,j} c_{i,j}^{\text{com}} \quad (2.36)$$

is associated, where the weights  $c_{i,j}^{\text{com}} \in \mathbb{R}_{\geq 0}$ ,  $c_{i,i}^{\text{com}} = 0$  encode the costs for (setting up) the communication link from  $\mathcal{C}^j$  to  $\mathcal{C}^i$ . For instance, the choice of these weights may be based on hardware cost, or on the spatial distance of the corresponding subsystems, see [50].

In Chapter 6, Assumption 2.3 is partially relaxed, and a subset of the available communication links  $(i, j) \in \mathcal{E}$  is assumed to be prone to stochastic link failures and packet dropouts. Both cases can be modeled by regarding the respective link to be temporarily unavailable, i.e. by setting  $\sigma_{i,j} = 0$  temporarily [128]. By doing so, the adjacency matrix  $\Sigma$  becomes a time-varying variable  $\Sigma[\theta_{\Sigma,k}] \in \mathbf{\Sigma}$ , where  $\mathbf{\Sigma} \subset \mathbb{B}^{N_s \times N_s}$  denotes the set of possible network topologies. Furthermore,  $\theta_{\Sigma,k}$  is the state of a Markov chain:

$$\mathcal{M}_{\Sigma} := (\Theta_{\Sigma}, P_{\Sigma}, \mu_{\Sigma,0}), \quad (2.37)$$

modeling the temporal availability of the communication links. Here,  $\Theta_{\Sigma} = \mathbb{I}_{N_{\Sigma}}$  is the discrete state-space,  $P_{\Sigma} \in [0, 1]^{N_{\Sigma} \times N_{\Sigma}}$  is the transition probability matrix, and  $\mu_{\Sigma,0} \in [0, 1]^{N_{\Sigma}}$  is the initial distribution of the Markov chain  $\mathcal{M}_{\Sigma}$ . Modeling probabilistic link failures and packet dropouts in communication networks by a Markov chain is a common means, see e.g. [62] and the references therein.

## 2.3. Stabilizability Criteria and Stability Notions

One of the major properties required for controlled dynamic systems is stability. This chapter briefly reviews the notions and conditions for stabilizability and stability for both linear time-invariant and jump Markov linear systems, which will be used in the subsequent chapters of this thesis.

### Stabilizability and Stability of LTI Systems

The stability of an LTI system  $\mathcal{P}$  as defined in (2.1) is first defined for the autonomous system, i.e. for  $u_k = 0$  and  $w_k = 0$  for all  $k \in \mathbb{N}_0$ . Recall the definition of an equilibrium point in Def. 2.1, as well as Assumption 2.1, and consider the following established definitions:

**Definition 2.5** (Lyapunov stability, cf. [31]). *The equilibrium point  $x_{\text{eq}} = 0$  is said to be stable in the sense of Lyapunov if for each  $\epsilon > 0$  there exists  $\delta = \delta(\epsilon) > 0$  such that  $\|x_k\| \leq \epsilon$  for all  $k \in \mathbb{N}_0$  whenever  $\|x_0\| \leq \delta$ .*  $\triangle$

**Definition 2.6** (Asymptotic stability, cf. [31]). *The equilibrium point  $x_{\text{eq}} = 0$  is said to be asymptotically stable if it is stable in the sense of Lyapunov and there exists  $\delta > 0$  such that whenever  $\|x_0\| \leq \delta$ , it follows that  $\lim_{k \rightarrow \infty} x_k = 0$ . It is globally asymptotically stable if it is asymptotically stable and  $\lim_{k \rightarrow \infty} x_k = 0$  for any  $x_0 \in \mathbb{X}$ .*  $\triangle$

The stability of discrete-time dynamic systems is closely related to the eigenvalues of the system matrix  $A$ . The following definition characterizes a subset of square matrices referred to as *Schur matrices* based on the corresponding eigenvalues:

**Definition 2.7.** *A matrix  $A \in \mathbb{R}^{n_x \times n_x}$  is called a Schur matrix if all of its eigenvalues lie in the open unit disc of the complex plane, i.e. if it holds that:*

$$\text{spec}(A) < 1, \quad (2.38)$$

where  $\text{spec}(A) := \max\{|\lambda_1(A)|, \dots, |\lambda_{n_x}(A)|\}$  denotes the spectral radius of  $A$ , with  $\lambda_i \in \mathbb{C}$  being the  $i$ -th eigenvalue.  $\triangle$

In the light of the above definition, the following holds for the stability of autonomous discrete-time LTI systems:

**Theorem 2.1** (cf. [31] [142]). *For the dynamic system  $\mathcal{P}$ , the following statements are equivalent:*

- (a) *The point  $x_{\text{eq}} = 0$  is the only globally asymptotically stable equilibrium point for the dynamic system  $\mathcal{P}$  with  $u_k = 0$  and  $w_k = 0$  for all  $k \in \mathbb{N}_0$ .*
- (b)  *$A$  is a Schur matrix, i.e.  $\text{spec}(A) < 1$ .*
- (c) *For some  $V \in \mathbb{S}_{>0}^{n_x} := \{M \in \mathbb{R}^{n_x \times n_x} \mid M = M^T, M \succ 0\}$ , it holds that<sup>2</sup>:*

$$V - A^T V A \succ 0. \quad (2.39)$$

- (d) *There exist constants  $\alpha \in \mathbb{R}_{>1}$  and  $\beta \in (0, 1)$  such that:*

$$\|x_k\|_2^2 \leq \alpha \beta^k \|x_0\|_2^2 \quad \forall k \in \mathbb{N}_0, x_0 \in \mathbb{X}. \quad (2.40)$$

$\square$

A proof for statements (a) to (c) can be found in Chapter 2.4 of [31]. Equivalence of statements (c) and (d) can be deduced from Theorem 3.9 in Chapter 3.3 of the same reference, considering the special case  $\text{card}(\Theta_0) = 1$ .

In the case that the disturbance input  $w_k$  takes arbitrary values, the following notion of input-output stability is considered:

**Definition 2.8** (BIBO stability [9]). *The dynamic system  $\mathcal{P}$  with input  $w_k$  and  $u_k = 0$  for all  $k \in \mathbb{N}_0$  is said to be bounded-input/bounded-output (BIBO) stable if there exists a constant  $c \in \mathbb{R}_{>0}$  such that  $x_0 = 0$  and  $\|w_k\| \leq 1$  imply that  $\|x_k\| \leq c$  for all  $k \in \mathbb{N}_0$ .  $\triangle$*

---

<sup>2</sup>The symbol  $\succ$  is used to denote inequality of symmetric matrices, e.g.  $\mathcal{A} \succ \mathcal{B}$  is equivalent to  $y^T \mathcal{A} y > y^T \mathcal{B} y$  for all  $y \in \mathbb{R}^n$ .

**Theorem 2.2** ([9]). *The dynamic system  $\mathcal{P}$  with input  $w_k$  and  $u_k = 0$  for all  $k \in \mathbb{N}_0$  is BIBO stable if  $x_{\text{eq}} = 0$  is an asymptotically stable equilibrium for  $w_k = 0$ . If, in addition,  $\mathcal{P}$  is controllable from the origin via the input  $w_k$ , then the converse holds.  $\square$*

A proof for Theorem 2.2 can be found on page 508 in [9]. For more information about controllability of dynamic systems, the reader is referred to [9] or [142].

Another important notion to be introduced here is *stabilizability* of a dynamic system  $\mathcal{P}$ , which is related to the question if it is possible to stabilize a dynamic system by a proper choice of the control input  $u_k$ .

**Definition 2.9** (Stabilizability, cf. [9] or [142]). *The pair  $(A, B)$  and the corresponding dynamic system  $\mathcal{P}$  are called stabilizable if there exists a matrix  $K \in \mathbb{R}^{n_u \times n_x}$  such that  $(A + BK)$  is a Schur matrix.  $\triangle$*

### Stabilizability and Stability of Jump Markov Linear Systems

For generalizing the notions of stability and stabilizability introduced for LTI systems to jump Markov linear systems, the stochasticity induced by the Markov chain  $\mathcal{M}$  has to be taken into account. For presenting the following results, consider the centralized JMLS:

$$\mathcal{P}_\theta : \begin{cases} x_{k+1} = A[\theta_k]x_k + B[\theta_k]u_k + E[\theta_k]w_k, \\ \mathcal{M} = (\Theta, P, \mu_0). \end{cases} \quad (2.41)$$

As for LTI systems, the autonomous system  $\mathcal{P}_\theta$  with  $w_k = 0$  and  $u_k = 0$  for all  $k \in \mathbb{N}_0$  is considered first, such that  $x_{\text{eq}} = 0$  is the corresponding equilibrium point. A common notion of stability of jump Markov linear systems is then given as follows:

**Definition 2.10** (Mean-square stability, cf. [31]). *The jump Markov linear system  $\mathcal{P}_\theta$  with  $w_k = 0$  and  $u_k = 0$  for all  $k \in \mathbb{N}_0$  is said to be mean-square stable (MSS) if for any initial condition  $x_0 \in \mathbb{X}$ ,  $\theta_0 \in \Theta$  it holds that:*

$$\|E(x_k)\| \rightarrow 0 \text{ as } k \rightarrow \infty, \quad (2.42a)$$

$$\|E(x_k x_k^\top)\| \rightarrow 0 \text{ as } k \rightarrow \infty. \quad (2.42b)$$

$\triangle$

For presenting results related to the mean-square stability of jump Markov linear systems, it is convenient to define the set  $\mathbb{H}^N(\mathbb{R}^{m \times n})$  of all  $N$ -sequences of  $\mathbb{R}^{m \times n}$  matrices as:

$$\mathbb{H}^N(\mathbb{R}^{m \times n}) := \{\mathbf{V} = (V[1], \dots, V[N]) \mid V[h] \in \mathbb{R}^{m \times n}, h \in \mathbb{I}_N\}. \quad (2.43)$$

Furthermore, with  $\mathbf{V} \in \mathbb{H}^N(\mathbb{R}^{m \times n})$ ,  $\mathbf{W} \in \mathbb{H}^N(\mathbb{R}^{m \times n})$ , and  $\mathbf{X} \in \mathbb{H}^N(\mathbb{R}^{n \times p})$ , the sum and product of two  $N$ -sequences of matrices are defined as:

$$\mathbf{V} + \mathbf{W} := (V[1] + W[1], \dots, V[N] + W[N]) \in \mathbb{H}^N(\mathbb{R}^{m \times n}), \quad (2.44)$$

$$\mathbf{V}\mathbf{X} := (V[1]X[1], \dots, V[N]X[N]) \in \mathbb{H}^N(\mathbb{R}^{m \times p}). \quad (2.45)$$

A generalized notion of Schur matrices<sup>3</sup> can be obtained for a sequence of system matrices  $\mathbf{A} = (A[1], \dots, A[N_\theta]) \in \mathbb{H}^{N_\theta}(\mathbb{R}^{n_x \times n_x})$  by defining the spectral radius of  $\mathbf{A}$  as follows:

**Definition 2.11** (cf. [31]). *The spectral radius of a set of matrices  $\mathbf{A} \in \mathbb{H}^{N_\theta}(\mathbb{R}^{n_x \times n_x})$  associated with the Markov chain  $\mathcal{M}$  is defined as:*

$$\text{spec}(\mathbf{A}) := \text{spec}\left((P^\top \otimes I_{(n_x)^2}) \text{blkdiag}(A[\theta] \otimes A[\theta])\right), \theta \in \Theta. \quad (2.46)$$

△

Furthermore, in accordance with [31] and [37], the following operators are introduced, which are related to the stability analysis of a JMLS  $\mathcal{P}_\theta$ . Each of these operators takes as argument a sequence of matrices  $\mathbf{V} \in \mathbb{H}^{N_\theta}(\mathbb{R}^{n_x \times n_x})$ :

$$\mathcal{D}(\cdot) := (\mathcal{D}_1(\cdot), \dots, \mathcal{D}_{N_\theta}(\cdot)) : \mathbb{H}^{N_\theta}(\mathbb{R}^{n_x \times n_x}) \rightarrow \mathbb{H}^{N_\theta}(\mathbb{R}^{n_x \times n_x}), \quad (2.47a)$$

$$\mathcal{E}(\cdot) := (\mathcal{E}_1(\cdot), \dots, \mathcal{E}_{N_\theta}(\cdot)) : \mathbb{H}^{N_\theta}(\mathbb{R}^{n_x \times n_x}) \rightarrow \mathbb{H}^{N_\theta}(\mathbb{R}^{n_x \times n_x}), \quad (2.47b)$$

$$\mathcal{T}(\cdot) := (\mathcal{T}_1(\cdot), \dots, \mathcal{T}_{N_\theta}(\cdot)) : \mathbb{H}^{N_\theta}(\mathbb{R}^{n_x \times n_x}) \rightarrow \mathbb{H}^{N_\theta}(\mathbb{R}^{n_x \times n_x}), \quad (2.47c)$$

where:

$$\mathcal{D}_n(\mathbf{V}) := \sum_{m=1}^{N_\theta} p_{m,n} V[m], \quad (2.47d)$$

$$\mathcal{E}_m(\mathbf{V}) := \sum_{n=1}^{N_\theta} p_{m,n} V[n], \quad (2.47e)$$

$$\mathcal{T}_n(\mathbf{V}) := \sum_{m=1}^{N_\theta} p_{m,n} A[m]V[m](A[m])^\top. \quad (2.47f)$$

With the above definitions, the following result holds for the mean-square stability of an autonomous jump Markov linear system:

**Theorem 2.3** (cf. [31]). *The following statements are equivalent:*

(a) *The system  $\mathcal{P}_\theta$  with  $u_k = 0$  and  $w_k = 0$  for all  $k \in \mathbb{N}_0$  is MSS.*

(b)  $\text{spec}(\mathbf{A}) < 1$ .

---

<sup>3</sup>Although the interpretation is similar w.r.t. the spectral radius, a sequence of matrices with  $\text{spec}(\mathbf{A}) < 1$  is generally not referred to by a distinctive name.

(c) For some  $\mathbf{V}, \mathbf{W} \in \mathbb{H}^{N_\theta}(\mathbb{S}_{>0}^{n_x})$ , either or both of the following inequalities hold:

$$V[\theta] - \mathcal{T}_\theta(\mathbf{V}) \succ 0 \quad \forall \theta \in \Theta, \quad (2.48)$$

$$W[\theta] - (A[\theta])^\top \mathcal{E}_\theta(\mathbf{W}) A[\theta] \succ 0 \quad \forall \theta \in \Theta. \quad (2.49)$$

(d) There exist constants  $\alpha \in \mathbb{R}_{>1}$  and  $\beta \in (0, 1)$  such that:

$$\mathbb{E}(\|x_k\|_2^2) \leq \alpha \beta^k \|x_0\|_2^2 \quad \forall k \in \mathbb{N}_0, x_0 \in \mathbb{X}, \theta_0 \in \Theta. \quad (2.50)$$

□

A proof for Theorem 2.3 can be found in Chapter 3.3 of [31].

In the case that the disturbance input  $w_k$  takes arbitrary values, the notion of BIBO stability can be extended to JMLS as follows:

**Definition 2.12** (BIBO stability in the mean-square sense). *The jump Markov linear system  $\mathcal{P}_\theta$  with input  $w_k$  and  $u_k = 0$  for all  $k \in \mathbb{N}_0$  is said to be bounded-input/bounded-output (BIBO) stable in the mean-square sense if  $x_0 = 0$  and  $\sum_{k \in \mathbb{N}_0} \|w_k\|^2 < \infty$  imply that  $\sum_{k \in \mathbb{N}_0} \mathbb{E}(\|x_k\|^2) < \infty$  for all  $\theta_0 \in \Theta$ .* △

**Theorem 2.4** (cf. [31]). *The jump Markov linear system  $\mathcal{P}_\theta$  with input  $w_k$  and  $u_k = 0$  for all  $k \in \mathbb{N}_0$  is BIBO stable in the mean-square sense if and only if  $\text{spec}(\mathbf{A}) < 1$ .* □

The result follows from Thm. 3.34 and Remark 3.5 in [31].

Finally, mean-square stabilizability of JMLS is defined as follows:

**Definition 2.13** (Mean-square stabilizability [31]). *The jump Markov linear system  $\mathcal{P}_\theta$  is called mean-square stabilizable if there exists an  $N_\theta$ -sequence of matrices  $\mathbf{K} \in \mathbb{H}^{N_\theta}(\mathbb{R}^{n_u \times n_x})$  such that  $\text{spec}(\mathbf{A} + \mathbf{BK}) < 1$ .* △

## 2.4. The $\mathcal{H}_2$ -Norm and its Generalizations

The  $\mathcal{H}_2$ -norm is one of the most popular norms for dynamic systems. It is frequently used in the fields of optimal control [3] [37] [38], optimal filtering [4], non-centralized control [24] [77], model reduction [8] [19], and system decomposition [5]. Originally defined for LTI systems, the  $\mathcal{H}_2$ -norm has afterwards been generalized to various classes of dynamic systems, including the jump Markov linear systems considered in the third part of this thesis [31]. This chapter first presents the basic definition of the  $\mathcal{H}_2$ -norm for the system classes introduced in Section 2.1. Afterwards, well-established relations between the norm and the different variants of the performance index  $J$  are presented, which are frequently used in the subsequent chapters. Since these results are only valid for linear and linear parameter-dependent systems, linear control laws  $\kappa(\cdot)$  are considered here.

Consider the system  $\mathcal{P}$  with controlled variable  $z_k$  as defined in Equations (2.1) and (2.11). Additionally, let  $u_k = Kx_k$  with  $K \in \mathbb{R}^{n_u \times n_x}$  be an admissible control law, i.e.  $K$  is chosen such that  $(A + BK)$  is a Schur matrix. Denote the resulting closed-loop system by:

$$\mathcal{P}_{\text{cl}} : \begin{cases} x_{k+1} = (A + BK)x_k + Ew_k, \\ z_k = (C + DK)x_k + Fw_k. \end{cases} \quad (2.51)$$

The  $\mathcal{H}_2$ -norm of the system  $\mathcal{P}_{\text{cl}}$  with input  $w_k$  and output  $z_k$  is defined as the  $\ell_2$ -norm of its impulse response:

**Definition 2.14** (see e.g. [8]). *The  $\mathcal{H}_2$ -norm of an asymptotically stable discrete-time LTI system  $\mathcal{P}_{\text{cl}}$  is defined as:*

$$\|\mathcal{P}_{\text{cl}}\|_{\mathcal{H}_2} := \|\mathbf{z}\|_{\ell_2} = \sqrt{\sum_{k=0}^{\infty} \text{tr}(\mathbf{z}_k^{\top} \mathbf{z}_k)} = \sqrt{\sum_{k=0}^{\infty} \text{tr}(\mathbf{z}_k \mathbf{z}_k^{\top})}. \quad (2.52\text{a})$$

Here,  $\mathbf{z}_k$  denotes the impulse response matrix of  $\mathcal{P}_{\text{cl}}$  at time  $k$ , given by:

$$\mathbf{z}_k = \begin{cases} F & \text{for } k = 0, \\ C(A + BK)^{k-1}E & \text{for } k > 0. \end{cases} \quad (2.52\text{b})$$

△

For an uncertain system  $\mathcal{P}_{\theta}$ , let  $u_k = K[\theta_k]x_k$  with  $\mathbf{K} \in \mathbb{H}^{N_{\theta}}(\mathbb{R}^{n_u \times n_x})$  be an admissible control law such that  $\text{spec}(\mathbf{A} + \mathbf{BK}) < 1$ , and denote the resulting closed-loop system by:

$$\mathcal{P}_{\theta, \text{cl}} : \begin{cases} x_{k+1} = (A[\theta_k] + B[\theta_k]K[\theta_k])x_k + E[\theta_k]w_k, \\ z_k = (C[\theta_k] + B[\theta_k]K[\theta_k])x_k, \\ \mathcal{M} = (\Theta, P, \mu_0). \end{cases} \quad (2.53)$$

The  $\mathcal{H}_2$ -norm is generalized to  $\mathcal{P}_{\theta, \text{cl}}$  by taking the expected value of the impulse response with respect to the Markov state  $\theta_k$ :

**Definition 2.15** (e.g. [31]). *The  $\mathcal{H}_2$ -norm of a mean-square stable discrete-time jump Markov linear system  $\mathcal{P}_{\theta, \text{cl}}$  is defined as:*

$$\|\mathcal{P}_{\theta, \text{cl}}\|_{\mathcal{H}_2} := \sqrt{\sum_{m=1}^{N_{\theta}} \sum_{k=0}^{\infty} \mu_{0,m} \mathbb{E}(\text{tr}(\mathbf{z}_k^{\top} \mathbf{z}_k) \mid \theta_0 = m)}. \quad (2.54\text{a})$$

Here,  $\mu_{0,m}$  denotes the  $m$ -th component of the vector  $\mu_0$ , and  $\mathbf{z}_k \in \mathbb{R}^{n_z \times n_w}$  denotes the impulse response matrix at time  $k$ . The  $(i, j)$ -th entry of  $\mathbf{z}_k$  is given by the  $i$ -th component of  $z_k$  for  $w_0 = e_j$ ,  $w_k = 0$  for all  $k \in \mathbb{N}$ ,  $x_0 = 0$ , and  $\theta_0 \in \Theta$ . △

A property of the  $\mathcal{H}_2$ -norm that is in great demand is that it has significant interpretations in the time-domain, in the frequency-domain, and for the case of stochastic disturbances and initial states. In particular, the  $\mathcal{H}_2$ -norm and the performance indices  $J$  defined in Section 2.1 are related as follows:

**Lemma 2.1.** *Consider an asymptotically stable dynamic system  $\mathcal{P}_{\text{cl}}$  under the conditions described in Case 2.1. Then, the squared  $\mathcal{H}_2$ -norm and the performance index  $J$  as defined in Eq. (2.20) are equal, i.e. it holds that:*

$$\|\mathcal{P}_{\text{cl}}\|_{\mathcal{H}_2}^2 = \lim_{k_e \rightarrow \infty} \mathbb{E} \left( \frac{1}{k_e} \sum_{k=0}^{k_e-1} z_k^T z_k \right). \quad (2.55)$$

□

A proof of Lemma 2.1 can be found in Appendix A.1.

Under some moderate conditions, a similar result holds for the case of jump Markov linear systems. More precisely, the Markov chain  $\mathcal{M}$  must possess a *limit probability distribution*:

**Definition 2.16.** (cf. [31, p.48]) *The vector  $\mu_\infty \in [0, 1]^{N_\theta}$  is called limit probability distribution of a Markov chain  $\mathcal{M}$  if there exists a unique solution of the linear system of equations:*

$$\begin{bmatrix} P^T - I \\ 1_{1 \times N_\theta} \end{bmatrix} \mu_\infty = \begin{bmatrix} 0_{N_\theta \times 1} \\ 1 \end{bmatrix}, \quad (2.56)$$

and if:

$$\|\mu_{k,m} - \mu_{\infty,m}\| \leq \alpha \beta^k \quad (2.57)$$

for some  $\alpha \in \mathbb{R}_{>0}$  and  $\beta \in (0, 1)$  for all  $k \in \mathbb{N}_0$ . △

**Lemma 2.2** ([31]). *Consider a mean-square stable discrete-time jump Markov linear system  $\mathcal{P}_{\theta, \text{cl}}$  under the conditions described in Case 2.1. Assume that the limit probability distribution exists, and set  $\mu_0 := \mu_\infty$ . Then, the squared  $\mathcal{H}_2$ -norm and the performance index  $J$  as defined in Eq. (2.22) are equal:*

$$\|\mathcal{P}_{\theta, \text{cl}}\|_{\mathcal{H}_2}^2 = \limsup_{k_e \rightarrow \infty} \mathbb{E} \left( \frac{1}{k_e} \sum_{k=0}^{k_e-1} z_k^T z_k \right). \quad (2.58)$$

□

This relation follows from Theorems 4.6 and 4.10 and Prop. 4.8 of [31]. In cases where no limit probability distribution exists, an alternative definition of the performance index can be used instead. For details, the reader is referred to Chapter 4.3 of [31].

As for Case 2.1, similar relations between the  $\mathcal{H}_2$ -norm and the performance index specified in Case 2.2 exist:



**Lemma 2.3.** Consider an asymptotically stable dynamic system  $\mathcal{P}_{\text{cl}}$  under the conditions described in Case 2.2, and set  $E := x_0$  and  $F := 0_{n_z \times n_w}$ . Then, the squared  $\mathcal{H}_2$ -norm and the performance index  $J$  as defined in Eq. (2.23) are equal:

$$\|\mathcal{P}_{\text{cl}}\|_{\mathcal{H}_2}^2 = \sum_{k=0}^{\infty} z_k^T z_k. \quad (2.59)$$

□

A proof of Lemma 2.3 can be found in Appendix A.2. Again, a similar result holds for jump Markov linear systems:

**Lemma 2.4.** Consider a mean-square stable discrete-time jump Markov linear system  $\mathcal{P}_{\theta, \text{cl}}$  under the conditions described in Case 2.2, and set  $E[\theta] := x_0$  for all  $\theta \in \Theta$ . Then, the squared  $\mathcal{H}_2$ -norm and the performance index  $J$  as defined in Eq. (2.24) are equal:

$$\|\mathcal{P}_{\theta, \text{cl}}\|_{\mathcal{H}_2}^2 = \sum_{k=0}^{\infty} \mathbb{E}(z_k^T z_k). \quad (2.60)$$

□

Lemma 2.4 follows with Thm. 4.5 and Prop. 4.8 of [31], and with their respective proofs.

In the remaining chapters, the above results are used to relate the optimization of the performance index  $J$  to the optimization of the  $\mathcal{H}_2$ -norm of the dynamic system under consideration.

## 2.5. Semidefinite Programming

The hierarchical distributed controllers proposed in this thesis are synthesized by the help of *semidefinite programs* (SDP). SDP are a class of constrained continuous optimization problems, which are widespread in system and control theory (see, e.g. [25] or [39]). They can be considered as a generalization of *linear programs* (LP) to matrix-valued optimization variables and semidefiniteness constraints. Similar to LP, SDP include a linear objective function, and may additionally be constrained by linear equality and inequality constraints. An important property of SDP is that they belong to the class of *convex* optimization problems [26]. Consequently, any point that is locally optimal is also globally optimal, and therefore many SDP can be efficiently and reliably solved, even when their sizes become very large [39].

**Definition 2.17** (cf. [26]). *The general form of a semidefinite program is:*

$$\min_{\mathfrak{X}} \text{tr}(W\mathfrak{X}) \quad (2.61a)$$

$$\text{subject to: } \mathcal{L}_h(\mathfrak{X}) \preceq 0, \quad h \in \{1, \dots, N_{\text{se}}\}, \quad (2.61b)$$

$$\text{tr}(G_{\text{in}}[i]\mathfrak{X}) \leq h_{\text{in}}[i], \quad i \in \{1, \dots, N_{\text{in}}\}, \quad (2.61c)$$

$$\text{tr}(G_{\text{eq}}[j]\mathfrak{X}) = h_{\text{eq}}[j], \quad j \in \{1, \dots, N_{\text{eq}}\}. \quad (2.61d)$$

Here,  $\mathfrak{X} \in \mathbb{R}^{m \times n}$  is a continuous matrix-valued optimization variable,  $W \in \mathbb{R}^{n \times m}$  is a weighting matrix,  $\mathcal{L}_h(\mathfrak{X}) : \mathbb{R}^{m \times n} \rightarrow \mathbb{S}^n$  are linear symmetric matrix functions of  $\mathfrak{X}$ , and  $\mathbf{G}_{\text{in}} \in \mathbb{H}^{N_{\text{in}}}(\mathbb{R}^{n \times m})$ ,  $\mathbf{G}_{\text{eq}} \in \mathbb{H}^{N_{\text{eq}}}(\mathbb{R}^{n \times m})$ ,  $\mathbf{h}_{\text{in}} \in \mathbb{H}^{N_{\text{in}}}(\mathbb{R})$ , and  $\mathbf{h}_{\text{eq}} \in \mathbb{H}^{N_{\text{eq}}}(\mathbb{R})$  are sequences of constant matrices and scalars.  $\triangle$

### Linear Matrix Inequalities

A constraint of the form (2.61b) is called a *linear matrix inequality*. LMI may be written in different forms, depending, among other things, on the number and partitioning of the optimization variables. Two particular forms of LMI are the *general form* and the *standard form*. By the help of the operator:

$$\text{He}(M) := \frac{1}{2}(M + M^\top), \quad (2.62)$$

they are defined as follows:

**Definition 2.18** ([39]). *The general form of an LMI is given by:*

$$\mathcal{L}(\mathfrak{X}) = M_0 + \text{He}(M_1^\top \mathfrak{X}) + \sum_{i=1}^{N_g} \text{He}(M_2[i]^\top \mathfrak{X} M_3[i]) \preceq 0, \quad (2.63)$$

with a matrix variable  $\mathfrak{X} \in \mathbb{R}^{m \times n}$ , constant matrices  $M_0 \in \mathbb{S}^n$  and  $M_1 \in \mathbb{R}^{m \times n}$ , and  $N_g$ -sequences of constant matrices  $M_2 \in \mathbb{H}^{N_g}(\mathbb{R}^{m \times n})$  and  $M_3 \in \mathbb{H}^{N_g}(\mathbb{R}^{n \times n})$ .  $\triangle$

**Definition 2.19** ([39], [25]). *The standard form for an LMI is given by:*

$$\mathcal{L}(\mathfrak{X}) = N_0 + \sum_{i=1}^m \sum_{j=1}^n \mathfrak{r}_{i,j} N_1[i, j] \preceq 0, \quad (2.64)$$

where  $\mathfrak{X} = [\mathfrak{r}_{i,j}] \in \mathbb{R}^{m \times n}$  is a matrix variable, and  $N_0 \in \mathbb{S}^p$ ,  $N_1[i, j] \in \mathbb{S}^p$  are constant matrices.  $\triangle$

In control theory, LMI are mostly presented as  $\mathcal{L}(\mathfrak{X}_1, \mathfrak{X}_2, \dots, \mathfrak{X}_N) \succ 0$ , where  $\mathcal{L}(\cdot)$  is an affine function of the matrix variables  $\mathfrak{X}_i$ ,  $i \in \mathbb{I}_N$  [31]. LMI provide a versatile framework to encode specifications like asymptotic or mean-square stability and  $\mathcal{H}_2$ - or  $\mathcal{H}_\infty$ -performance bounds for a large class of quasi-linear continuous-time and discrete-time dynamic systems [39]. To this end, LMI are used to establish convex inner approximations or convex transformations of the original feasible set of controllers. Many of the mentioned control design problems initially lead to bilinear matrix inequalities (BMI), which are not jointly convex in all matrix variables  $\mathfrak{X}_i$ . A very popular result that can be applied to linearize such BMI is the so-called *Schur-complement*, which will be frequently used in the remainder of this thesis:

**Lemma 2.5** (cf. [25] or [39]). *Let  $M \in \mathbb{S}_{>0}^n$  be a symmetric positive definite matrix partitioned into two-by-two block-matrices  $M_{i,j}$ . Then, the following statements are equivalent:*

$$(a) \quad M = \begin{bmatrix} M_{1,1} & M_{1,2} \\ M_{1,2}^\top & M_{2,2} \end{bmatrix} \succ 0, \quad (2.65a)$$

$$(b) \quad M_{2,2} \succ 0, \quad M_{1,1} - M_{1,2}M_{2,2}^{-1}M_{1,2}^\top \succ 0, \quad (2.65b)$$

$$(c) \quad M_{1,1} \succ 0, \quad M_{2,2} - M_{1,2}^\top M_{1,1}^{-1}M_{1,2} \succ 0. \quad (2.65c)$$

□

A proof of Lemma 2.5 can be found, for instance, in Chapter 2.2 of [39].

Numerically, SDP are solved by employing either ellipsoid algorithms or interior-point algorithms [39]. In this thesis, the optimization solvers SeDuMi [123] and Mosek [95], which belong to the class of interior-point algorithms, are used together with the Yalmip interface [79] to solve the proposed SDP problems.

### Mixed-Integer Semidefinite Programming

In addition to real-valued variables, semidefinite programs may include variables which are restricted to the set of integers  $\mathbb{Z}$ . For instance, the general problem of SCT design includes binary decisions whether to include a communication link  $(i, j) \in \mathcal{N}_s \times \mathcal{N}_s$  into the communication graph  $\mathcal{G}$  or not. This can be encoded by introducing decision variables  $\sigma_{i,j}$  which are restricted to the set of binaries  $\mathbb{B} = \{0, 1\}$ . If Problem (2.61) contains additional integer variables, then it is referred to as *mixed-integer semidefinite program* (MISDP). In general, an MISDP is a non-convex problem which may have multiple global solutions. However, if the integer variables are either fixed or if they are relaxed to real-valued variables, the resulting problem becomes convex again. This property is exploited by branch-and-bound (BnB) and cutting plane methods, which can be employed in combination with conventional SDP solvers to iteratively solve relaxations of an MISDP. This way, most MISDP can be solved very efficiently, and the global optimum is guaranteed to be found [51]. However, in worst-case situations, the computation time for obtaining the global optimum grows combinatorially with the number of integer variables.

## 2.6. Decompositions of Matrices and Dynamic Systems

For the structural analysis and clustering procedure applied prior to the control design, the interconnection structure and interconnection strength of the subsystems has to be identified. As already discussed in Section 1.2, various approaches to the evaluation of interconnection strengths and to system decomposition exist. In the

remainder of this section, a selection of these approaches is presented, which serves as basis for the clustering algorithm to be presented in the subsequent chapter.

The  $\epsilon$ -decomposition developed by Šiljak [132] aims to decompose a monolithic LTI system into weakly coupled subsystems. More precisely, it identifies partitions of the state vector  $x_k$  that may be considered as decoupled if some weak interconnections between them are neglected. Assuming that the input matrix  $B$  of a dynamic system  $\mathcal{P}$  is diagonal, the off-diagonal entries of the system matrix  $A$  encode the interconnections between the components of the state vector  $x_k$ . In order to perform an  $\epsilon$ -decomposition of such a system, a small positive number  $\epsilon \in \mathbb{R}_{>0}$  is chosen by the designer, and the system matrix  $A$  encoding the interdependencies of the states is decomposed as:

$$T_x^T A T_x = A_D + \epsilon A_E. \quad (2.66)$$

Here,  $T_x \in \mathbb{B}^{n_x \times n_x}$  is a permutation matrix,  $A_D \in \mathbb{R}^{n_x \times n_x}$  is a block-diagonal matrix, and  $A_E \in [-1, 1]^{n_x \times n_x}$  is selected such that none of its elements is larger than one in absolute value. Hence, the groups of states defined by the diagonal blocks of the matrix  $A_D$  can be considered as decoupled if the weak interconnections  $\epsilon A_E$  with magnitude less than or equal to  $\epsilon$  are neglected. Consequently, each of these weakly coupled groups of states is considered as a subsystem.

The original purpose of the  $\epsilon$ -decomposition is to identify weakly-coupled groups of subsystems for which decentralized control laws can be designed independently. However, stability of the resulting closed-loop system is not guaranteed, since the neglected interconnections may render the overall system unstable. Furthermore, an optimal control law that is designed by the help of the  $\epsilon$ -decomposition will not be optimal when implemented in the actual system (cf. [58]). In particular, there are numerical examples where weak interconnections may have a quite large influence on the optimal control law when not considered for the control design [63].

The concept of  $\epsilon$ -decomposition can be extended to consider input and output interconnections by forming an extended system matrix, see [132, Chap. 7] for details. Despite the simple measure of the interconnection strength, the  $\epsilon$ -decomposition has proven to be useful and has received much attention. Indeed, it can still be found in recent publications, see for instance [140].

Another fundamental decomposition scheme is the *hierarchical lower block-triangular (LBT) decomposition* of holistic LTI systems [132]. This decomposition takes advantage of the sparsity that can typically be observed in the state space matrices of large interconnected systems. Often, this sparsity provides significant numerical advantage for the control design process, but cannot be exploited as long as it is not recognized by the designer or by the design algorithm. The hierarchical LBT decomposition aims to identify sparse structures by partitioning a system  $\mathcal{P}$  into LBT-form, which corresponds to identifying the strongly-coupled components of the underlying interconnection graph. In terms of the state-space matrices, this corresponds to permuting the rows and columns of the matrices  $A$  and  $B$  into LBT

form, i.e. finding permutation matrices  $T_x \in \mathbb{B}^{n_x \times n_x}$  and  $T_u \in \mathbb{B}^{n_u \times n_u}$  such that:

$$T_x^\top A T_x = \begin{bmatrix} A_{1,1} & 0 & \dots & 0 \\ A_{2,1} & A_{2,2} & \ddots & \vdots \\ \vdots & \ddots & \ddots & 0 \\ A_{N_s,1} & \dots & \dots & A_{N_s,N_s} \end{bmatrix}, \quad T_x^\top B T_u = \begin{bmatrix} B_{1,1} & 0 & \dots & 0 \\ B_{2,1} & B_{2,2} & \ddots & \vdots \\ \vdots & \ddots & \ddots & 0 \\ B_{N_s,1} & \dots & \dots & B_{N_s,N_s} \end{bmatrix}. \quad (2.67)$$

Similar to the  $\epsilon$ -decomposition, the states and inputs corresponding to the diagonal blocks of  $T_x^\top A T_x$  and  $T_x^\top B T_u$  are interpreted as the subsystems identified by the decomposition. The particularity of the subsystems identified by the hierarchical

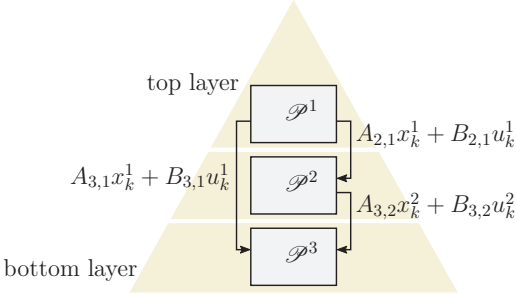


**Figure 2.4.:** Three hierarchically interconnected subsystems  $\mathcal{P}^i$ .

LBT decomposition is that they possess a hierarchical interconnection structure, as shown in Figure 2.4 for the exemplary case of three subsystems. The first subsystem  $\mathcal{P}^1$  only has outgoing interconnection signals and thus constitutes the top layer of the hierarchy. On the other hand, the third subsystem  $\mathcal{P}^3$  only has incoming interconnection signals and constitutes the bottom layer of the hierarchy. Due to the hierarchical interconnection structure, subsystems identified by the hierarchical LBT decomposition possess particular technical properties, which are summarized in the following lemma.

**Lemma 2.6** (following [132]). *Let  $\mathcal{P}$  be a dynamic system consisting of  $N_s = 2$  interconnected subsystems  $\mathcal{P}^1$  and  $\mathcal{P}^2$ , and let the feedback matrix  $K \in \mathbb{R}^{n_u \times n_x}$  be structured accordingly, i.e.:*

$$A = \begin{bmatrix} A_{1,1} & A_{1,2} \\ A_{2,1} & A_{2,2} \end{bmatrix}, \quad B = \begin{bmatrix} B_{1,1} & B_{1,2} \\ B_{2,1} & B_{2,2} \end{bmatrix}, \quad K = \begin{bmatrix} K_{1,1} & K_{1,2} \\ K_{2,1} & K_{2,2} \end{bmatrix}. \quad (2.68)$$

Furthermore, assume that the closed-loop system has a hierarchical interconnection structure, i.e. either  $A_{1,2} = 0$ ,  $B_{1,2} = 0$ , and  $K_{1,2} = 0$ , or  $A_{2,1} = 0$ ,  $B_{2,1} = 0$ , and  $K_{2,1} = 0$  holds. Then, the following statements hold:

(a) The eigenvalues of the closed-loop systems are related according to:

$$\Lambda(A + BK) = \Lambda(A_{1,1} + B_{1,1}K_{1,1}) \cup \Lambda(A_{2,2} + B_{2,2}K_{2,2}). \quad (2.69)$$

Here,  $\Lambda(M) \subset \mathbb{C}$  denotes the set of eigenvalues of a square matrix  $M \in \mathbb{R}^{n \times n}$ .

(b)  $(A + BK)$  is a Schur matrix if and only if  $(A_{1,1} + B_{1,1}K_{1,1})$  and  $(A_{2,2} + B_{2,2}K_{2,2})$  are Schur matrices.

(c) The pair  $(A, B)$  is stabilizable by decentralized state-feedback if and only if the pairs  $(A_{1,1}, B_{1,1})$  and  $(A_{2,2}, B_{2,2})$  are stabilizable.

(d) The pair  $(A, B)$  is stabilizable if the pairs  $(A_{1,1}, B_{1,1})$  and  $(A_{2,2}, B_{2,2})$  are stabilizable.

*Proof.* Due to the hierarchical interconnection structure of the closed-loop system, the matrix  $A + BK$  is either in upper or in lower block-triangular form:

$$A + BK = \begin{bmatrix} A_{1,1} + B_{1,1}K_{1,1} & 0 \\ A_{2,1} + B_{2,1}K_{1,1} + B_{2,2}K_{2,1} & A_{2,2} + B_{2,2}K_{2,2} \end{bmatrix}, \quad (2.70)$$

or rather, for  $A_{2,1} = 0$ ,  $B_{2,1} = 0$ , and  $K_{2,1} = 0$ :

$$A + BK = \begin{bmatrix} A_{1,1} + B_{1,1}K_{1,1} & A_{1,2} + B_{1,1}K_{1,2} + B_{1,2}K_{2,2} \\ 0 & A_{2,2} + B_{2,2}K_{2,2} \end{bmatrix}. \quad (2.71)$$

Considering the properties of block-triangular matrices, statement (a) follows immediately, which directly implies (b). For the pair  $(A, B)$  to be stabilizable by decentralized state-feedback, there must exist  $K$  with  $K_{2,1} = 0$  and  $K_{1,2} = 0$  such that  $(A + BK)$  is a Schur matrix. Assume that  $(A_{1,1}, B_{1,1})$  and  $(A_{2,2}, B_{2,2})$  are stabilizable. Then, there exist  $K_{1,1}$  and  $K_{2,2}$  such that  $A_{1,1} + B_{1,1}K_{1,1}$  and  $A_{2,2} + B_{2,2}K_{2,2}$  are Schur matrices. Using (b), this proves sufficiency of (c). On the other hand, assume that  $\text{spec}(A_{1,1} + B_{1,1}K_{1,1}) > 1$  for all matrices  $K_{1,1}$ , i.e.  $(A_{1,1}, B_{1,1})$  is not stabilizable. Then, using (a), it follows that  $A + BK$  can not be stabilized by decentralized state-feedback. Following a similar argumentation for the second subsystem proves necessity of (c). By Definition 2.9, the pair  $(A, B)$  is stabilizable if there exists some matrix  $K$  such that  $A + BK$  is a Schur matrix. Considering a block-diagonal matrix  $K$  as a special case, it follows from (c) that (d) holds.  $\square$

By the help of Lemma 2.6, it can be deduced that for an arbitrary number of hierarchically interconnected subsystems  $\mathcal{P}^i$ , the controllability (stability) of all subsystems implies the controllability (stability) of the global system  $\mathcal{P}$ .

Permutation matrices which transform a sparse matrix  $\Gamma = [\gamma_{i,j}] \in \mathbb{R}^{m \times n}$  with  $m \geq n$  into block-triangular form can be found by applying the *Dulmage-Mendelsohn decomposition* [102]. Dulmage and Mendelsohn discovered that the process of block-triangularization is equivalent to computing a canonical decomposition of bipartite

graphs associated with the matrix under consideration. The  $m + n$  nodes of this graph correspond to the rows and columns of the matrix  $\Gamma$ , and the  $i$ -th row node is connected to the  $j$ -th column node if and only if  $\gamma_{i,j} \neq 0$ . This graph is bipartite since no connections between any two row nodes or any two column nodes exist. In the first step of the Dulmage-Mendelsohn decomposition, referred to as *coarse decomposition*, a *maximum matching* of this bipartite graph has to be determined. A *matching* is a subset of edges with no common endpoints. A maximum matching is a matching of maximum cardinality, which, in terms of the matrix  $\Gamma$ , corresponds to a diagonal with the maximum number of nonzeros in it [102].

In the remainder of this thesis, the special case  $m = n$  with  $\gamma_{i,i} \neq 0$  for all  $i \in \mathbb{I}_n$  will be considered. In this case, a trivial maximum matching is a-priori given by the set  $\{(1, 1), (2, 2), \dots, (n, n)\}$ . Hence, the first step of the Dulmage-Mendelsohn decomposition can be omitted. Then, the second and final step of the Dulmage-Mendelsohn decomposition, the so-called *fine decomposition*, can be solved in an amount of time which grows linear with the number of nonzero entries of  $\Gamma$ . Furthermore, the resulting row and column permutation will be equal, i.e. there exists a permutation matrix  $T \in \mathbb{B}^{n \times n}$  with  $T^T T = I$  such that:

$$\Gamma' = T^T \Gamma T, \tag{2.72}$$

where  $\Gamma' \in \mathbb{R}^{n \times n}$  denotes the permuted matrix. For details on the Dulmage-Mendelsohn decomposition, the reader is referred to [102] and the references therein.

**Part II.**

**Hierarchical Control of  
Time-Invariant Systems**





# 3. Synchronous Hierarchical Control

This chapter presents a distributed hierarchical two-layer feedback control scheme for LTI subsystems interconnected via inputs and states and via a common performance index. Such control problems occur, for instance, in the control of infrastructure systems like water [44] or power distribution networks [53], or in the control of civil structures, e.g. temperature control in large buildings [14]. Furthermore, many special cases of the problem concerning the interconnection structure of the inputs, states, and the performance index exist. A frequently occurring case is the class of formation control problems, which typically considers decoupled systems that are only interconnected via a common performance index. Formation control problems occur, for instance, in the context of platooning vehicles or satellite formations [51]. As already stated in Chapter 1, the majority of approaches to distributed control of such setups considers fixed communication topologies and a single control layer, or imposes particular assumptions on the interconnection structure of the dynamics and the performance index. Approaches considering single-layer SCT design can be found, e.g., in [50] [78] [103] [111]. However, approaches based on Mixed-Integer Programming suffer from the combinatorial complexity in the number of subsystems [50] [103]. On the other hand, approximations to the SCT design problem, which are usually based on weighted  $\ell_1$ -norm minimization, have to put an additional cost on the magnitude of the feedback gain matrix to promote its sparsity [111], and often can not deal with constraints on the communication topology. Even in re-weighted  $\ell_1$ -norm formulations, this cost is similar to a penalty on the magnitude of the control inputs, and thus alters the original cost. Existing approaches to multi-layer feedback control do not consider network topologies at all [86] [131].

This chapter presents an approximate solution to conventional single-layer SCT design by employing a structural analysis and a two-layer control structure. In large parts, this chapter is based on the results presented in [58] and [59]. However, while local control inputs, no bilinear cost terms and undisturbed dynamics are assumed in [58], a more general formulation is presented here.

### 3.1. Dynamic Model and Problem Setup

In this chapter, an interconnection of  $N_s$  discrete-time linear time-invariant systems  $\mathcal{P}^i$  of the form:

$$\mathcal{P}^i : \begin{cases} x_{k+1}^i = A_{i,i}x_k^i + B_{i,i}u_k^i + E_{i,i}w_k^i + \sum_{j \in \mathcal{N}_s^i} A_{i,j}x_k^j + B_{i,j}u_k^j + E_{i,j}w_k^j, \\ z_k^i = C_{i,i}x_k^i + D_{i,i}u_k^i + \sum_{j \in \mathcal{N}_s^i} C_{i,j}x_k^j + D_{i,j}u_k^j, \end{cases} \quad (3.1)$$

is assumed to be given. Each subsystem contains a local state vector  $x_k^i \in \mathbb{X}^i \subseteq \mathbb{R}^{n_x^i}$ , a local input vector  $u_k^i \in \mathbb{U}^i \subseteq \mathbb{R}^{n_u^i}$ , and a local disturbance input vector  $w_k^i \in \mathbb{W}^i \subseteq \mathbb{R}^{n_w^i}$ . Furthermore,  $z_k^i \in \mathbb{R}^{n_z^i}$  defines a vector of local controlled variables, where  $C_{i,j} \in \mathbb{R}^{n_z^i \times n_x^j}$  and  $D_{i,j} \in \mathbb{R}^{n_z^i \times n_u^j}$  are matrices to be chosen by the designer.

#### Global SCT Design Problem

In accordance with Case 2.1 and Case 2.2, the performance of the corresponding global system  $\mathcal{P}$  is measured by a global quadratic performance index  $J$  depending on the controlled variables  $z_k^i$ . Hence, the following optimal control problem can be associated with the global system  $\mathcal{P}$ :

$$\min_{\kappa(\cdot)} J \quad (3.2a)$$

$$\text{subject to: } x_{k+1} = Ax_k + Bu_k + Ew_k, \quad (3.2b)$$

$$z_k = Cx_k + Du_k, \quad (3.2c)$$

$$u_k = \kappa(x_k). \quad (3.2d)$$

For problem (3.2) to possess a unique centralized solution, the following assumptions are imposed for the global system  $\mathcal{P}$ :

**Assumption 3.1.** *The global system  $\mathcal{P}$  described by the matrices  $A = [A_{i,j}]$ ,  $B = [B_{i,j}]$ ,  $C = [C_{i,j}]$ ,  $D = [D_{i,j}]$ , and  $E = [E_{i,j}]$  has the following properties:*

(a) *The pair  $(A, B)$  is stabilizable.*

(b) *The matrix  $\begin{bmatrix} C & D \end{bmatrix}$  has full column rank.  $\Delta$*

Note that the second assumption implies that the system  $\mathcal{P}$  has no invariant zeros on the unit circle in the complex plane, or respectively:

$$\text{rank} \begin{bmatrix} A - \lambda I_{n_x} & B \\ C & D \end{bmatrix} = n_x + n_u \quad \forall \lambda \in \mathbb{C}_1. \quad (3.3)$$

Hence, the standard assumptions for the existence of an optimal solution of (3.2) are satisfied (cf. [142, Sec. 21.7] with  $y = x$ ).

It is well-known that under the above assumptions, the optimal control problem (3.2) has a globally optimal centralized solution of the form  $u_k = K^*x_k$ . Distributed optimal control design, however, requires to introduce structural constraints on the control law, rendering the problem far more complex. In general, under the influence of structural constraints, the globally optimal control law is no longer linear. This additionally increases the difficulty to synthesize such a control law [97]. As a partial remedy, linear distributed control laws are considered in the remainder of this thesis, which is a common assumption in approaches to structured control and to SCT design (see, e.g. [50] [96] [103] [105] [111], among many others). In particular, assuming the control law to be linear allows to formulate sufficient convex synthesis conditions, as will be shown later. Hence, the global SCT design problem can be stated as follows:

$$\min_{K, \Sigma} J + J^{\text{com}}(\Sigma) \quad (3.4a)$$

$$\text{subject to: } x_{k+1} = Ax_k + Bu_k + Ew_k, \quad (3.4b)$$

$$z_k = Cx_k + Du_k, \quad (3.4c)$$

$$u_k = Kx_k, \quad (3.4d)$$

$$K \in \mathcal{S}(\Sigma). \quad (3.4e)$$

Here, the adjacency matrix  $\Sigma \in \mathbb{B}^{N_s \times N_s}$  encodes the topology of the communication network,  $J^{\text{com}}(\Sigma) \in \mathbb{R}_{\geq 0}$  is the associated communication cost, and  $\mathcal{S}(\Sigma)$  is the set of admissible control gains that is structurally compatible with the communication topology  $\Sigma$ .

### Hierarchical Approach

The goal of this chapter is to develop a linear hierarchical distributed control structure as sketched in Section 2.1, where the distributed lower and upper layer controllers take the form:

$$\mathcal{C}^{\downarrow i} : u_k^i = K_{i,i}^{\downarrow} x_k^i + \sum_{j \in \mathcal{C}^{\nu(i)}} K_{i,j}^{\downarrow} x_k^j + v_k^i, \quad (3.5a)$$

$$\mathcal{C}^{\uparrow i} : \hat{v}_s^i = \sum_{j \in \mathcal{C}^{\nu(i)}} K_{i,j}^{\uparrow} \hat{x}_s^j + \sum_{q \in \bar{\mathcal{R}}^{\uparrow \nu(i)}} \sum_{j \in \mathcal{C}^q} K_{i,j}^{\uparrow} \hat{x}_s^j, \quad (3.5b)$$

with  $s = s(k) = (k - k \bmod \Delta k) / \Delta k$  and  $i \in \mathcal{N}_s$ . The approach taken here is to design the control layers sequentially in three steps: In a first step prior to the design of the lower control layer, the interconnection strength and interconnection structure of the interconnected system is analyzed. While neglecting some weak interactions, strongly connected subsystems are grouped into clusters. In a second step, a control law which is decentralized with respect to these clusters is synthesized. Establishing full communication between all subsystems within each cluster, this control law can be implemented in a distributed manner, and constitutes the lower layer of the hierarchical control scheme. Finally, in a third step, a model and performance index

for the design of the upper control layer are established. The task of this upper control layer is to compensate for the neglected interconnections, and to implement communication between the clusters on a coarser time-scale.

## 3.2. Subsystem Clustering

The first step of the hierarchical control design is an analysis of the interconnection structure between the subsystems  $\mathcal{P}^i$ . After neglecting those interconnections that are considered to be weak according to an adjustable threshold, the subsystems are grouped into hierarchically interconnected clusters by the help of the Dulmage-Mendelsohn decomposition (see Sec. 2.6). These clusters can be interpreted as an aggregation of subsystems. After the clustering process, those neglected interactions which do not affect the hierarchical interconnection structure of the aggregate subsystems are restored. The resulting models of the aggregate subsystems  $\widehat{\mathcal{P}}^p$  serve as interconnected system model for the design of the distributed lower layer controllers  $\mathcal{C}^{\downarrow i}$ , which is presented in the subsequent section. The clustering procedure consists of the following steps:

- (a) The interconnection structure and interconnection strength between the subsystems  $\mathcal{P}^i$  is mapped into a matrix  $\Gamma = [\gamma_{i,j}] \in \mathbb{R}_{\geq 0}^{N_s \times N_s}$ . Since the interconnection signals between the subsystems are, in general, vectors, the scalar entries  $\gamma_{i,j}$  of  $\Gamma$  are chosen according to:

$$\gamma_{i,j} := \|A_{i,j}\|_2 + \|B_{i,j}\|_2 \quad (3.6)$$

for all  $(i, j) \in \mathcal{N}_s \times \mathcal{N}_s$ .

- (b) Define small non-negative numbers  $\epsilon_w, \epsilon_n \in \mathbb{R}_{\geq 0}$  such that  $\epsilon_w \geq \epsilon_n$ . These design parameters determine if an interconnection between two subsystems  $\mathcal{P}^i$  and  $\mathcal{P}^j$  is considered to be weak during the structural analysis ( $\epsilon_n < \gamma_{i,j} \leq \epsilon_w$ ), or is even neglected completely for the design of the lower control layer ( $\gamma_{i,j} \leq \epsilon_n$ ).
- (c) The interconnection structure resulting from the strong interconnections is stored in the matrix  $\Gamma' = [\gamma'_{i,j}] \in \mathbb{R}_{\geq 0}^{N_s \times N_s}$ , which is defined as:

$$\gamma'_{i,j} := \begin{cases} \gamma_{i,j} & \text{if } \gamma_{i,j} > \epsilon_w, \\ 2\epsilon_w & \text{if } i = j \wedge \gamma_{i,j} = 0, \\ 0 & \text{otherwise.} \end{cases} \quad (3.7)$$

In the case  $\gamma_{i,i} = 0$ , the assignment of  $\gamma'_{i,i}$  to an (arbitrary) positive value will be important for the subsequent step.

- (d) The Dulmage-Mendelsohn decomposition is applied to the matrix  $\Gamma'$ . This decomposition permutes the rows and columns of  $\Gamma'$  such that the permuted

matrix  $\Gamma''$  is upper block-triangular (UBT). Since  $\gamma'_{i,i} > 0 \forall i \in \mathcal{N}_s$ , the column permutation and the row permutation are always equal (see Sec. 2.6). Hence, the permutation may be either described by a permutation matrix  $T \in \mathbb{B}^{N_s \times N_s}$  with  $\Gamma'' = T^\top \Gamma' T$ , or by a vector  $\tau \in \mathbb{N}^{N_s}$  containing the permuted subsystem indices such that  $\gamma''_{i,j} = \gamma'_{\tau_i, \tau_j}$ .

- (e) Let the number of blocks on the diagonal of  $\Gamma''$  be denoted by  $N_c \in \mathbb{N}$ , which corresponds to the number of identified clusters. For all  $p \in \mathcal{N}_c := \mathbb{I}_{N_c}$ , the indices  $i \in \mathcal{N}_s$  of the subsystems that belong to the  $p$ -th block are stored in an index set  $\mathcal{C}^p \subseteq \mathcal{N}_s$ .
- (f) As an optional step, clusters may be joined, while respecting a user-defined minimum and maximum cluster size. Denote this design parameters by  $c_{\min} \in \mathbb{N}$  and  $c_{\max} \in \mathbb{N}$ , with  $c_{\min} \leq \max_p \text{card}(\mathcal{C}^p)$ , and  $c_{\max} \geq \max\{c_{\min}, \max_p \text{card}(\mathcal{C}^p)\}$ . In many cases,  $c_{\min} = 2$  and  $c_{\max} = N_s/3$  are reasonable initial values for the minimum and maximum cluster size. In general, clusters may be joined according to different criteria as long as their hierarchical interconnection structure is preserved. A reasonable criterion to join two clusters  $\mathcal{C}^p$  and  $\mathcal{C}^q$  is to maximize the strength of weak and neglected interconnections between the joined clusters, which can then be reset to their original values. This thought gives rise to the following optimization problem:

$$(r^*, q^*) = \arg \max_{r \in \mathbb{I}_h, q \in \mathcal{I}_f} \sum_{p \in \mathcal{I}_r^*} \sum_{i \in \mathcal{C}^p} \sum_{j \in \mathcal{C}^q} (\gamma_{i,j} - \gamma'_{i,j}) + (\gamma_{j,i} - \gamma'_{j,i}) \quad (3.8a)$$

$$\text{subject to: } \mathcal{I}_j^r \cap \{q - 1, q + 1\} \neq \emptyset, \quad (3.8b)$$

$$\sum_{p \in \mathcal{I}_r^*} \text{card}(\mathcal{C}^p) + \text{card}(\mathcal{C}^q) \leq c_{\max}. \quad (3.8c)$$

Here, the index set  $\mathcal{I}_f \subset \mathcal{N}_c$  contains the indices of free clusters to be joined,  $\mathcal{I}_j^r \subseteq \mathcal{N}_c$  denotes the  $r$ -th group of joined clusters, and  $h$  is an auxiliary variable denoting the number of these groups. The solution  $(r^*, q^*)$  corresponds to a free cluster  $\mathcal{C}^{q^*}$  and to a group of clusters  $\{\mathcal{C}^p\}$  with  $p \in \mathcal{I}_j^{r^*}$  which possess the largest sum of weak and neglected interconnections. Constraint (3.8b) ensures that the hierarchical interconnection structure is preserved, while (3.8c) limits the number of subsystems contained in the joined clusters to  $c_{\max}$ . This optimization problem can now be embedded into an algorithm for joining the clusters as follows:

- 1: **Given**  $c_{\min}, c_{\max}, \mathcal{N}_c, \{\mathcal{C}^p\}, \Gamma, \Gamma'$
- 2: define  $\mathcal{I}_f := \{p \in \mathcal{N}_c \mid \text{card}(\mathcal{C}^p) < c_{\min}\}$
- 3: define  $h := \text{card}(\mathcal{N}_c \setminus \mathcal{I}_f)$
- 4: define  $\mathcal{I}_j^r := \{\text{vec}_r(\mathcal{N}_c \setminus \mathcal{I}_f)\} \forall r \in \mathbb{I}_h$
- 5: **while**  $\mathcal{I}_f \neq \emptyset$  **do**
- 6:   solve optimization problem (3.8) for  $(r^*, q^*)$
- 7:   **if**  $(r^*, q^*) \neq \emptyset$  **then**

```

8:   set  $\mathcal{I}_j^{r*} := \mathcal{I}_j^{r*} \cup \{q^*\}$ 
9:   set  $\mathcal{I}_f := \mathcal{I}_f \setminus \{q^*\}$ 
10:  else
11:    determine  $q^* := \arg \max_{q \in \mathcal{I}_f} \text{card}(\mathcal{C}^q)$ 
12:    set  $\mathcal{I}_j^{h+1} := \{q^*\}$ 
13:    set  $\mathcal{I}_f := \mathcal{I}_f \setminus \{q^*\}$ 
14:    set  $h := h + 1$ 
15:  end if
16: end while
17: set  $\mathcal{C}^r := \bigcup_{p \in \mathcal{I}_j^r} \mathcal{C}^p$ 
18: set  $\mathcal{N}_c := \mathbb{1}_h$ 
19: set  $N_c := h$ 
20: return  $N_c, \mathcal{N}_c, \{\mathcal{C}^p\}$ 
    
```

(g) All entries of  $\Gamma'$  that are smaller than or equal to  $\epsilon_w$  but larger than  $\epsilon_n$  are restored to their original values. Likewise, those entries of  $\Gamma'$  that are smaller than  $\epsilon_n$  and do not affect the hierarchical interconnection structure of the clusters are restored, too (cf. [61]):

```

1: Given  $\Gamma, \Gamma', N_s, \{\mathcal{C}^p\}$ 
2: set  $h := 1, p := 1$ 
3: for  $i = 1$  to  $N_s$  do
4:   if  $i \geq h + \text{card}(\mathcal{C}^p)$  then
5:     set  $h := i, p := p + 1$ 
6:   end if
7:   for  $j = 1$  to  $N_s$  do
8:     if  $\gamma_{\tau_i, \tau_j} - \gamma'_{\tau_i, \tau_j} > 0$  then
9:       if  $j \geq h$  or  $\gamma_{\tau_i, \tau_j} > \epsilon_n$  then
10:        set  $\gamma'_{\tau_i, \tau_j} := \gamma_{\tau_i, \tau_j}$ 
11:      end if
12:    end if
13:  end for
14: end for
15: return  $\Gamma'$ 
    
```

The outcome of the above clustering procedure is the matrix  $\Gamma' \in \mathbb{R}_{\geq 0}^{N_s \times N_s}$  characterizing the interconnection strength and interconnection structure of the subsystems. The permuted subsystem order is contained in the vector  $\tau \in \mathbb{N}^{N_s}$ . This vector can be used to construct the permutation matrices  $T_x = [T_{x,i,j}] \in \mathbb{B}^{n_x \times n_x}$ ,  $T_u = [T_{u,i,j}] \in \mathbb{B}^{n_u \times n_u}$ ,  $T_w = [T_{w,i,j}] \in \mathbb{B}^{n_w \times n_w}$ , and  $T_z = [T_{z,i,j}] \in \mathbb{B}^{n_z \times n_z}$  for the state, input, disturbance input, and controlled variable, respectively, as follows:

$$T_{\bullet i,j} = \begin{cases} I_{n_{\bullet}^{\tau_j}} & \text{if } \tau_j = i, \\ 0_{n_{\bullet}^i \times n_{\bullet}^{\tau_j}} & \text{otherwise.} \end{cases} \quad (3.9)$$

A further outcome of the clustering procedure are the index sets  $\mathcal{C}^p$  with  $p \in \mathcal{N}_c$ , which are constructed such that:

$$\mathcal{C}^p \cap \mathcal{C}^q = \emptyset \quad \forall (p, q) \in \mathcal{N}_c \times \mathcal{N}_c, p \neq q, \quad (3.10a)$$

$$\bigcup_{p \in \mathcal{N}_c} \mathcal{C}^p = \mathcal{N}_s. \quad (3.10b)$$

The index sets  $\mathcal{C}^p$  can be used to define the aggregate subsystems:

$$\bar{\mathcal{P}}^p : \begin{cases} \bar{x}_{k+1}^p = \bar{A}_{p,p} \bar{x}_k^p + \bar{B}_{p,p} \bar{u}_k^p + \bar{E}_{p,p} \bar{w}_k^p + \sum_{q \in \mathcal{N}_c^e} \bar{A}_{p,q} \bar{x}_k^q + \bar{B}_{p,q} \bar{u}_k^q + \bar{E}_{p,q} \bar{w}_k^q, \\ \bar{z}_k^p = \bar{C}_{p,p} \bar{x}_k^p + \bar{D}_{p,p} \bar{u}_k^p + \sum_{q \in \mathcal{N}_c^e} \bar{C}_{p,q} \bar{x}_k^q + \bar{D}_{p,q} \bar{u}_k^q, \end{cases} \quad (3.11)$$

where  $\mathcal{N}_c^p := \mathcal{N}_c \setminus \{p\}$ . Furthermore,  $\bar{x}_k^p \in \mathbb{R}^{\bar{n}_x^p}$ ,  $\bar{u}_k^p \in \mathbb{R}^{\bar{n}_u^p}$ ,  $\bar{w}_k^p \in \mathbb{R}^{\bar{n}_w^p}$ , and  $\bar{z}_k^p \in \mathbb{R}^{\bar{n}_z^p}$  denote the aggregate state, input, disturbance input, and controlled output vector, respectively. The matrices  $\bar{A}_{p,q}$ ,  $\bar{B}_{p,q}$ ,  $\bar{C}_{p,q}$ ,  $\bar{D}_{p,q}$ , and  $\bar{E}_{p,q}$  of suitable dimensions are the respective block-entries of the matrices:

$$\bar{A} := T_x^\top A T_x, \quad \bar{B} := T_x^\top B T_u, \quad \bar{C} := T_z^\top C T_x, \quad \bar{D} := T_z^\top D T_u, \quad \bar{E} := T_x^\top A T_w. \quad (3.12)$$

**Remark 3.1.** *The design parameters  $\epsilon_w$  and  $\epsilon_n$  allow to tune the outcome of the clustering procedure. A reasonable initial choice for these parameters is given by:*

$$\epsilon_w = \epsilon_n = \min_{i,j} \gamma_{i,j}. \quad (3.13)$$

Afterwards,  $\epsilon_w$  should be increased until a satisfying set of clusters is identified. Finally,  $\epsilon_n$  may be increased to facilitate the synthesis of the lower layer controller, since more interconnections will be neglected during control design. This will be explained in more detail in the upcoming section.

### 3.3. Lower Layer Control Design

For the design of the lower control layer, the model that has been identified in the clustering procedure is used. That is, the system matrices of the global system  $\mathcal{P}$  are permuted according to the new subsystem order, and neglected interconnections with  $\gamma_{i,j} < \epsilon_n$  are deleted from the matrices  $\bar{A}$  and  $\bar{B}$ . Hence, the corresponding aggregate subsystems for the design of the lower control layer can be defined as follows:

$$\bar{\mathcal{P}}^p : \begin{cases} \bar{x}_{k+1}^p = \bar{A}'_{p,p} \bar{x}_k^p + \bar{B}'_{p,p} \bar{u}_k^p + \bar{E}'_{p,p} \bar{w}_k^p + \sum_{q \in \mathcal{N}_c^e} \bar{A}'_{p,q} \bar{x}_k^q + \bar{B}'_{p,q} \bar{u}_k^q + \bar{E}'_{p,q} \bar{w}_k^q, \\ \bar{z}_k^p = \bar{C}'_{p,p} \bar{x}_k^p + \bar{D}'_{p,p} \bar{u}_k^p + \sum_{q \in \mathcal{N}_c^e} \bar{C}'_{p,q} \bar{x}_k^q + \bar{D}'_{p,q} \bar{u}_k^q. \end{cases} \quad (3.14)$$



The matrices  $\bar{A}'_{p,q}$ ,  $\bar{B}'_{p,q}$ ,  $\bar{C}'_{p,q}$ ,  $\bar{D}'_{p,q}$ , and  $\bar{E}'_{p,q}$  are given by:

$$\bar{A}'_{p,q} = [A'_{i,j}]_{i \in \mathcal{C}^p, j \in \mathcal{C}^q}, \quad A'_{i,j} := \begin{cases} A_{i,j} & \text{if } \gamma'_{i,j} > 0, \\ 0_{n_x^i \times n_x^j} & \text{otherwise,} \end{cases} \quad (3.15a)$$

$$\bar{B}'_{p,q} = [B'_{i,j}]_{i \in \mathcal{C}^p, j \in \mathcal{C}^q}, \quad B'_{i,j} := \begin{cases} B_{i,j} & \text{if } \gamma'_{i,j} > 0, \\ 0_{n_x^i \times n_u^j} & \text{otherwise,} \end{cases} \quad (3.15b)$$

$$\bar{C}'_{p,q} := \bar{C}_{p,q}, \quad \bar{D}'_{p,q} := \bar{D}_{p,q}, \quad \bar{E}'_{p,q} := \bar{E}_{p,q}. \quad (3.15c)$$

Regarding the underlying communication topology of the lower control layer, a decentralized structure w.r.t. the clusters is assumed. Consequently, the lower layer communication graph  $\mathcal{G}^\downarrow$  is fixed to the following structure:

$$\bar{\Sigma}^\downarrow = [\bar{\sigma}_{p,q}^\downarrow], \quad (3.16a)$$

$$\bar{\sigma}_{p,q}^\downarrow = [\sigma_{i,j}^\downarrow]_{i \in \mathcal{C}^p, j \in \mathcal{C}^q} = \begin{cases} 1_{N_s^p} & \text{if } p = q, \\ 0_{N_s^p \times N_s^q} & \text{otherwise,} \end{cases} \quad (3.16b)$$

where  $N_s^p := \text{card}(\mathcal{C}^p)$  denotes the number of subsystems contained in cluster  $\mathcal{C}^p$ . The structure of the graph  $\mathcal{G}^\downarrow$  corresponds to the structure of the lower layer control law as defined in Eq. (3.5a).

The interconnected system  $\bar{\mathcal{P}}' = \{\bar{\mathcal{P}}'^p\}_{p \in \mathcal{N}_c}$  with  $\bar{\Sigma}^\downarrow$  is now used to design the distributed lower control layer. To this end, the upper layer input  $\bar{v}_k$  is temporarily set to zero. The resulting control problem is a structured optimal control problem which can be solved by the help of a semidefinite program:

**Theorem 3.1.** *Suppose that the matrices  $\mathfrak{G} \in \mathbb{R}^{n_x \times n_x}$ ,  $\mathfrak{L} \in \mathbb{R}^{n_u \times n_x}$ ,  $\mathfrak{X} \in \mathbb{S}_{>0}^{n_x}$ , and  $\mathfrak{Z} \in \mathbb{S}_{>0}^{n_w}$  are a solution of the semidefinite program:*

$$\min_{\mathfrak{G}, \mathfrak{L}, \mathfrak{X}, \mathfrak{Z}} \text{tr}(\mathfrak{Z}) \quad (3.17a)$$

$$\text{subject to: } \begin{bmatrix} \mathfrak{G} + \mathfrak{G}^\top - \mathfrak{X} & \star & \star \\ \bar{A}'\mathfrak{G} + \bar{B}'\mathfrak{L} & \mathfrak{X} & \star \\ \bar{C}'\mathfrak{G} + \bar{D}'\mathfrak{L} & 0 & I_{n_z} \end{bmatrix} \succ 0, \quad (3.17b)$$

$$\begin{bmatrix} \mathfrak{Z} & \star \\ \bar{E}' & \mathfrak{X} \end{bmatrix} \succ 0, \quad (3.17c)$$

$$\mathfrak{X} = \mathfrak{X}^\top \succ 0, \quad (3.17d)$$

$$\mathfrak{Z} = \mathfrak{Z}^\top \succ 0, \quad (3.17e)$$

$$\mathfrak{G} = \text{blkdiag}(\mathfrak{G}_{p,p}), \quad \mathfrak{G}_{p,p} \in \mathbb{R}^{\bar{n}_x^p \times \bar{n}_x^p}, \quad (3.17f)$$

$$\mathfrak{L} = \text{blkdiag}(\mathfrak{L}_{p,p}), \quad \mathfrak{L}_{p,p} \in \mathbb{R}^{\bar{n}_u^p \times \bar{n}_x^p}, \quad (3.17g)$$

where  $\star$  is used as an abbreviation for representing symmetric matrices (see p. 203). Set  $\bar{K}^\downarrow := \mathfrak{L}\mathfrak{G}^{-1}$ , and denote the closed-loop system consisting of  $\bar{\mathcal{P}}'$  with  $\bar{u}_k = \bar{K}^\downarrow \bar{x}_k$  by  $\bar{\mathcal{P}}'_{\text{cl}}^\downarrow$ . Accordingly, denote the corresponding performance index by  $J'$ . Then, the following assertions hold:

- (a) The point  $\bar{x}_{\text{eq}} = 0$  is the only globally asymptotically stable equilibrium point for the dynamic system  $\bar{\mathcal{P}}'_{\text{cl}}$  with  $\bar{w}_k = 0$  for all  $k \in \mathbb{N}_0$ .
- (b) The dynamic system  $\bar{\mathcal{P}}'_{\text{cl}}$  with input  $\bar{w}_k$  is bounded-input/bounded-output stable.
- (c) For  $J'$  according to Case 2.1, the value of  $J'$  is upper-bounded by the objective function (3.17a).
- (d) For  $J'$  according to Case 2.2, and by setting  $\bar{E}' := \bar{x}_0 = T_{\bar{x}}^{\top} x_0$ , the value of  $J'$  is upper-bounded by the objective function (3.17a).
- (e) The control law  $\bar{u}_k = \bar{K}^{\downarrow} \bar{x}_k$  respects the communication topology given by  $\bar{\Sigma}^{\downarrow}$ .  $\square$

*Proof.* Assume that the LMI (3.17b) and (3.17d) are feasible. Then, the upper left entry of LMI (3.17b) implies that:

$$\mathfrak{G} + \mathfrak{G}^{\top} \succ \mathfrak{X} \succ 0. \quad (3.18)$$

Hence, any feasible matrix  $\mathfrak{G}$  must be non-singular. Using:

$$\mathfrak{G} + \mathfrak{G}^{\top} - \mathfrak{X} \preceq \mathfrak{G}^{\top} \mathfrak{X}^{-1} \mathfrak{G} \quad (3.19)$$

(e.g. [33]), and substituting  $\mathfrak{L} = \bar{K}^{\downarrow} \mathfrak{G}$ , Eq. (3.17b) implies that:

$$\begin{bmatrix} \mathfrak{G}^{\top} \mathfrak{X}^{-1} \mathfrak{G} & \star & \star \\ \bar{A}' \mathfrak{G} + \bar{B}' \bar{K}^{\downarrow} \mathfrak{G} & \mathfrak{X} & \star \\ \bar{C}' \mathfrak{G} + \bar{D}' \bar{K}^{\downarrow} \mathfrak{G} & 0 & I_{n_z} \end{bmatrix} \succ 0. \quad (3.20)$$

Factoring out the non-singular matrix  $T = \text{blkdiag}(\mathfrak{G}, I_{n_x}, I_{n_z})$  on the right-hand side and its transpose  $T^{\top}$  on the left-hand side, the above inequality is equivalent to:

$$\begin{bmatrix} \mathfrak{X}^{-1} & \star & \star \\ \bar{A}' + \bar{B}' \bar{K}^{\downarrow} & \mathfrak{X} & \star \\ \bar{C}' + \bar{D}' \bar{K}^{\downarrow} & 0 & I_{n_z} \end{bmatrix} \succ 0. \quad (3.21)$$

Let  $\bar{A}'_{\text{cl}} := \bar{A}' + \bar{B}' \bar{K}^{\downarrow}$  and  $\bar{C}'_{\text{cl}} := \bar{C}' + \bar{D}' \bar{K}^{\downarrow}$ . Applying the Schur-complement (see Lemma 2.5 on page 41) leads to:

$$\mathfrak{X}^{-1} - (\bar{A}'_{\text{cl}})^{\top} \mathfrak{X}^{-1} \bar{A}'_{\text{cl}} - (\bar{C}'_{\text{cl}})^{\top} (\bar{C}'_{\text{cl}}) \succ 0. \quad (3.22)$$

With  $(\bar{C}'_{\text{cl}})^{\top} (\bar{C}'_{\text{cl}}) \succeq 0$ , it follows that:

$$\mathfrak{X}^{-1} - (\bar{A}'_{\text{cl}})^{\top} \mathfrak{X}^{-1} \bar{A}'_{\text{cl}} \succ (\bar{C}'_{\text{cl}})^{\top} \bar{C}'_{\text{cl}} \succeq 0, \quad (3.23)$$

implying that the matrix  $\bar{A}'_{\text{cl}}$  is a Schur matrix (see Def. 2.7 and Thm. 2.1). Hence, assertions (a) and (b) follow from Theorem 2.1 and from Theorem 2.2. Multiplying inequality (3.22) with  $(\bar{A}'_{\text{cl}})^\top$  from the left-hand side and with the transpose  $\bar{A}'_{\text{cl}}$  from the right-hand side, and using (3.22) leads to:

$$\mathfrak{X}^{-1} \succ ((\bar{A}'_{\text{cl}})^2)^\top \mathfrak{X}^{-1} (\bar{A}'_{\text{cl}})^2 + \sum_{k=0}^1 ((\bar{A}'_{\text{cl}})^k)^\top (\bar{C}'_{\text{cl}})^\top \bar{C}'_{\text{cl}} (\bar{A}'_{\text{cl}})^k. \quad (3.24)$$

Repeating this procedure  $(n - 2)$  times leads to:

$$\mathfrak{X}^{-1} \succ ((\bar{A}'_{\text{cl}})^n)^\top \mathfrak{X}^{-1} (\bar{A}'_{\text{cl}})^n + \sum_{k=0}^{n-1} ((\bar{A}'_{\text{cl}})^k)^\top (\bar{C}'_{\text{cl}})^\top \bar{C}'_{\text{cl}} (\bar{A}'_{\text{cl}})^k. \quad (3.25)$$

For  $n \rightarrow \infty$ , the first summand on the right-hand side tends to zero, since  $\bar{A}'_{\text{cl}}$  is a Schur matrix (cf. [50]). Hence, it holds that:

$$\mathfrak{X}^{-1} \succ \sum_{k=0}^{\infty} ((\bar{A}'_{\text{cl}})^k)^\top (\bar{C}'_{\text{cl}})^\top \bar{C}'_{\text{cl}} (\bar{A}'_{\text{cl}})^k. \quad (3.26)$$

Multiplying the above inequality by  $(\bar{E}')^\top$  from the left-hand side and by  $\bar{E}'$  from the right-hand side and taking the trace leads to:

$$\text{tr}((\bar{E}')^\top \mathfrak{X}^{-1} \bar{E}') > \sum_{k=0}^{\infty} \text{tr}((\bar{E}')^\top ((\bar{A}'_{\text{cl}})^k)^\top (\bar{C}'_{\text{cl}})^\top \bar{C}'_{\text{cl}} (\bar{A}'_{\text{cl}})^k \bar{E}') = \|\bar{\mathcal{P}}'_{\text{cl}}\|_{\mathcal{H}_2}^2. \quad (3.27)$$

Taking the Schur-complement of the second LMI (3.17c) reveals that:

$$\mathfrak{Z} - (\bar{E}')^\top \mathfrak{X}^{-1} \bar{E}' \succ 0 \quad \Leftrightarrow \quad \mathfrak{Z} \succ (\bar{E}')^\top \mathfrak{X}^{-1} \bar{E}'. \quad (3.28)$$

Assertions (c) and (d) now follow with Lemma 2.1 and with Lemma 2.3, respectively. Finally, with  $\bar{K}^\downarrow := \mathfrak{L}\mathfrak{G}^{-1}$ , it follows that constraints (3.17f) and (3.17g) are sufficient to enforce that  $\bar{K}^\downarrow = \text{blkdiag}(\bar{K}^\downarrow_{p,p})$  with  $\bar{K}^\downarrow_{p,p} \in \mathbb{R}^{\bar{n}_w^p \times \bar{n}_w^p}$ . Hence,  $\bar{K}^\downarrow$  respects the communication topology encoded by  $\bar{\Sigma}^\downarrow$ , such that assertion (e) holds.  $\square$

It is well-known that some dynamic systems can not be stabilized by decentralized state-feedback, even though the overall system is stabilizable [32] [135]. This is due to so-called *structurally fixed modes*<sup>1</sup>, i.e. eigenvalues of the dynamic system which are invariant under structured state-feedback. In principal, such a case may occur for the design of the lower layer control law. In some cases, it can be circumvented by altering the design parameters of the clustering procedure such that the pairs  $(\bar{A}_{p,p}, \bar{B}_{p,p})$  are controllable for all  $p \in \mathcal{N}_c$ . Indeed, one can show that for a particular choice of the clustering parameters  $\epsilon_w$  and  $\epsilon_n$ , this controllability condition is sufficient for a stabilizing lower layer control law to exist.

---

<sup>1</sup>In the context of decentralized control, structurally fixed modes are also referred to as *decentralized fixed modes (DFM)*.

**Lemma 3.1.** *Let the parameters  $\epsilon_w$  and  $\epsilon_n$  of the clustering procedure be chosen such that  $\epsilon_w = \epsilon_n$ , and assume that the set of clusters  $\{\mathcal{C}^p\}$  is formed such that the pair  $(\bar{A}_{p,p}, \bar{B}_{p,p})$  is controllable for all  $p \in \mathcal{N}_c$ . Then, there exists a lower layer control law of the form (3.5a) such that the matrix  $\bar{A}' + \bar{B}'\bar{K}^\downarrow$  is a Schur matrix.  $\square$*

*Proof.* For the particular choice  $\epsilon_w = \epsilon_n$ , the matrices  $\bar{A}'$  and  $\bar{B}'$  are upper block-triangular, since all weak interconnections are also neglected. Furthermore, only those interconnections which do not alter the hierarchical interconnection structure of the clusters are restored in clustering step (g). Hence, applying Lemma 2.6 to the system  $\bar{\mathcal{P}}'$ , there must exist a linear stabilizing control law which is decentralized from the viewpoint of the clusters, such that the claim holds.  $\square$

In contrast to classical SCT design, the design of the lower layer control law has the advantage that no binary decisions regarding the activation of communication links have to be made. Nonetheless, the communication topology is fitted to the interconnection structure of the interconnected system based on the results of the clustering procedure. A further advantage of the subsystem clustering is that in particular cases, the lower layer controllers can be designed separately. In particular, when the clusters possess an exact hierarchical interconnection structure, i.e.  $\epsilon_w = \epsilon_n$ , the sequential design procedure presented in [132] can be applied. In this case, it is furthermore possible to optimize the communication topology within each cluster, as proposed in [59] and [60]. In [59], the key idea for optimizing the topology within each cluster is to start with a reference controller which considers full communication within each cluster. Then, for each cluster, an SCT design problem is formulated and solved for each cluster independently, while assuming that the controllers of the remaining clusters are fixed to their reference values. The performance indices of these local SCT problems are determined by using methods of inverse optimal control. Due to the hierarchical interconnection structure of the clusters, the stability of the overall system is preserved by preserving the stability of the single clusters. In [60], the inverse optimal control problems formulated in [59] are investigated more thoroughly. In particular, it is shown that the local performance indices are not quadratic in the local state and input variables, even though the global performance index is quadratic and the controllers of the remaining clusters are fixed. In order to circumvent this, an approach for constructing local quadratic approximations of the true performance indices is presented.

In the frequent case that  $\epsilon_n > 0$ , i.e. some weak interconnections are neglected for the design of the lower layer control law, no guarantees can be given, neither for the performance nor for the stability of the original interconnected system under the control of the lower control layer. Formally, implementing the controllers  $\mathcal{C}^{\downarrow i}$  in the original interconnected system  $\mathcal{P}$ , the following lower layer closed-loop system is obtained:

$$\bar{\mathcal{P}}_{\text{cl}}^\downarrow : \begin{cases} \bar{x}_{k+1} = (\bar{A} + \bar{B}\bar{K}^\downarrow)\bar{x}_k + \bar{B}\bar{v}_k + \bar{E}\bar{w}_k = \bar{A}_{\text{cl}}^\downarrow \bar{x}_k + \bar{B}\bar{v}_k + \bar{E}\bar{w}_k, \\ \bar{z}_k = (\bar{C} + \bar{D}\bar{K}^\downarrow)\bar{x}_k + \bar{D}\bar{v}_k = \bar{C}_{\text{cl}}^\downarrow \bar{x}_k + \bar{D}\bar{v}_k. \end{cases} \quad (3.29)$$

Following the original thought of the  $\epsilon$ -decomposition, the adverse effects of the neglected interconnections regarding global system stability and performance should be small in most cases. Nevertheless, there exist documented special cases where neglected interconnections of small magnitude may have a significant influence [63]. While this is not taken into account in the classical concept of the  $\epsilon$ -decomposition, the hierarchical two-layer control scheme compensates for the adverse effects of the neglected interconnections by adding a superordinate control layer to be introduced in the next section.

### 3.4. Upper Layer Control Design

For the design of the upper layer controllers  $\mathcal{C}^{\uparrow i}$ , two cases are distinguished. At first, a full communication graph  $\mathcal{G}^{\uparrow}$  is considered, such that any two controllers  $\mathcal{C}^{\uparrow i}$  and  $\mathcal{C}^{\uparrow j}$  can communicate bidirectionally. For this case, it is shown how the controllers  $\mathcal{C}^{\uparrow i}$  can be designed such that the global performance index  $J$  is minimized for a given lower layer control law and given  $\Delta k$ . An improvement of  $J$  by the upper control layer is possible, since the weak interconnections which were neglected in designing the lower control layer are now taken into account. In addition, the exchange of state information between the clusters may further improve the performance.

#### 3.4.1. Full Communication Topology

For a given value of  $\Delta k \in \mathbb{N}_{>1}$ , the global interconnected system  $\mathcal{P}_{\text{cl}}^{\downarrow}$  under control of the lower control layer can be expressed on the upper layer time-domain  $\mathbb{T}^{\uparrow}$  as:

$$\mathcal{P}^{\uparrow} : \begin{cases} \hat{x}_{s+1} = \bar{A}^{\uparrow} \hat{x}_s + \bar{B}^{\uparrow} \hat{v}_s + \bar{E}^{\uparrow} \hat{w}_s, \\ \hat{z}_s = \bar{C}^{\uparrow} \hat{x}_s + \bar{D}^{\uparrow} \hat{v}_s + \bar{F}^{\uparrow} \hat{w}_s, \end{cases} \quad (3.30a)$$

with matrices:

$$\begin{aligned} \bar{A}^{\uparrow} &= (\bar{A} + \bar{B}\bar{K}^{\downarrow})^{\Delta k} = (\bar{A}_{\text{cl}}^{\downarrow})^{\Delta k}, & \bar{B}^{\uparrow} &= \sum_{h=0}^{\Delta k-1} (\bar{A}_{\text{cl}}^{\downarrow})^h \bar{B}, \\ \bar{C}^{\uparrow} &= \begin{bmatrix} \bar{C}_{\text{cl}}^{\downarrow} \\ \bar{C}_{\text{cl}}^{\downarrow} \bar{A}_{\text{cl}}^{\downarrow} \\ \vdots \\ \bar{C}_{\text{cl}}^{\downarrow} (\bar{A}_{\text{cl}}^{\downarrow})^{\Delta k-1} \end{bmatrix}, & \bar{D}^{\uparrow} &= \begin{bmatrix} \bar{D} \\ \bar{D} + \bar{C}_{\text{cl}}^{\downarrow} \bar{B} \\ \vdots \\ \bar{D} + \bar{C}_{\text{cl}}^{\downarrow} (\sum_{h=0}^{\Delta k-1} (\bar{A}_{\text{cl}}^{\downarrow})^h) \bar{B} \end{bmatrix}, \\ \bar{E}^{\uparrow} &= [(\bar{A}_{\text{cl}}^{\downarrow})^{\Delta k-1} \bar{E} \quad \dots \quad \bar{A}_{\text{cl}}^{\downarrow} \bar{E} \quad \bar{E}], & \bar{F}^{\uparrow} &= \begin{bmatrix} 0 & 0 & \dots & 0 \\ \bar{C}_{\text{cl}}^{\downarrow} \bar{E} & \ddots & \ddots & \vdots \\ \vdots & \ddots & \ddots & 0 \\ \bar{C}_{\text{cl}}^{\downarrow} (\bar{A}_{\text{cl}}^{\downarrow})^{\Delta k-2} \bar{E} & \dots & \bar{C}_{\text{cl}}^{\downarrow} \bar{E} & 0 \end{bmatrix}. \end{aligned} \quad (3.30b)$$

The corresponding extended disturbance vector is obtained as:

$$\hat{w}_s = \begin{bmatrix} \bar{w}_s \Delta k \\ \vdots \\ \bar{w}_{(s+1)\Delta k-1} \end{bmatrix} \in \mathbb{R}^{\bar{n}_w^\uparrow}, \quad (3.31)$$

with  $\bar{n}_w^\uparrow := \Delta k n_w$ . Since the local stochastic processes  $w_k^i$  satisfy  $\mathbb{E}(w_k^i (w_l^j)^\top) = 0$  for either  $k \neq l$ ,  $i \neq j$ , or both (cf. Case 2.1), the stochastic process  $\hat{w}_s$  also satisfies the assumptions of Case 2.1, i.e.:

$$\mathbb{E}(\hat{w}_s) = 0_{\bar{n}_w^\uparrow \times 1}, \quad \mathbb{E}(\hat{w}_s \hat{w}_s^\top) = I_{\bar{n}_w^\uparrow \times \bar{n}_w^\uparrow}, \quad \mathbb{E}(\hat{w}_s \hat{w}_r^\top) = 0_{\bar{n}_w^\uparrow}. \quad (3.32)$$

Partitioning the vectors  $\hat{x}_s$ ,  $\hat{v}_s$ , and  $\hat{w}_s$ , as well as the matrices  $\bar{A}^\uparrow$  to  $\bar{F}^\uparrow$  according to the clusters, the interconnected aggregate upper layer systems  $\bar{\mathcal{P}}^{\uparrow p}$  with  $p \in \mathcal{N}_c$  can be obtained. When considering a full communication graph  $\mathcal{G}^\uparrow$  on the upper control layer, a linear quadratic control problem can be associated with  $\bar{\mathcal{P}}^\uparrow$ . In accordance with Case 2.1, this problem can be stated as follows:

$$\min_{\kappa^\uparrow(\cdot)} J^\uparrow = \min_{\kappa^\uparrow(\cdot)} \lim_{s_e \rightarrow \infty} \mathbb{E} \left( \frac{1}{s_e} \sum_{s=0}^{s_e-1} \hat{z}_s^\top \hat{z}_s \right) \quad (3.33a)$$

$$\text{subject to: } \hat{x}_{s+1} = \bar{A}^\uparrow \hat{x}_s + \bar{B}^\uparrow \hat{v}_s + \bar{E}^\uparrow \hat{w}_s, \quad (3.33b)$$

$$\hat{z}_s = \bar{C}^\uparrow \hat{x}_s + \bar{D}^\uparrow \hat{v}_s + \bar{F}^\uparrow \hat{w}_s, \quad (3.33c)$$

$$\hat{v}_s = \kappa^\uparrow(\hat{x}_s), \quad (3.33d)$$

where  $\bar{x}_0 = \bar{x}_{\text{eq}} = 0_{n_x \times 1}$  is independent of  $\hat{w}_s$  for all  $s \in \mathbb{N}_0$ . For the undisturbed case  $\hat{w}_s = 0$  for all  $s \in \mathbb{N}_0$  and with  $\hat{x}_0 \neq \hat{x}_{\text{eq}}$ , it follows similar to Case 2.2:

$$\min_{\kappa^\uparrow(\cdot)} J^\uparrow = \min_{\kappa^\uparrow(\cdot)} \sum_{s=0}^{\infty} \hat{z}_s^\top \hat{z}_s \quad (3.34a)$$

$$\text{subject to: } \hat{x}_{s+1} = \bar{A}^\uparrow \hat{x}_s + \bar{B}^\uparrow \hat{v}_s, \quad (3.34b)$$

$$\hat{z}_s = \bar{C}^\uparrow \hat{x}_s + \bar{D}^\uparrow \hat{v}_s, \quad (3.34c)$$

$$\hat{v}_s = \kappa^\uparrow(\hat{x}_s). \quad (3.34d)$$

The following theorem states that in both cases, the performance index  $J^\uparrow$  maps the original performance index  $J$  considered in Problem (3.33) to the upper layer. Furthermore, the Theorem addresses the existence conditions for an optimal solution.

**Theorem 3.2.** *Suppose that a global representation  $\bar{\mathcal{P}}_{\text{cl}}^\downarrow$  of interconnected systems  $\mathcal{P}^i$  with lower layer control law (3.5a) is given. Let  $\Delta k \in \mathbb{N}_{>1}$  be such that the pair  $(\bar{A}^\uparrow, \bar{B}^\uparrow)$  as defined in (3.30b) is stabilizable. Then, the control  $\hat{v}_s = \bar{K}^\uparrow \hat{x}_s$  minimizes the performance index  $J$  if it is a stabilizing solution of the optimal control problem (3.33) / (3.34). Furthermore, provided that Assumption 3.1 holds, a unique optimal solution is guaranteed to exist in both cases.*

*Proof.* Consider the performance index  $J$  on the lower layer under the conditions described in Case 2.2:

$$J = \sum_{k=0}^{\infty} \bar{z}_k^T \bar{z}_k = \sum_{k=0}^{\infty} \|\bar{C}\bar{x}_k + \bar{D}\bar{u}_k\|_2^2 =: \sum_{k=0}^{\infty} l(\bar{x}_k, \bar{u}_k). \quad (3.35)$$

Substituting the lower layer control law  $\bar{u}_k = \bar{K}^\downarrow \bar{x}_k + \bar{v}_k$  leads to:

$$J = \sum_{k=0}^{\infty} \|(\bar{C} + \bar{D}\bar{K}^\downarrow)\bar{x}_k + \bar{D}\bar{v}_k\|_2^2 =: \sum_{k=0}^{\infty} l_{\text{cl}}^\downarrow(\bar{x}_k, \bar{v}_k). \quad (3.36)$$

On the upper control layer, the task is to determine  $\bar{v}_k$  such that  $J$  is minimized. Ignoring the restriction  $\bar{v}_k = \hat{v}_s$  for all  $k \in \mathbb{N}_0$  in the first instance, applying Bellman's principle of optimality yields the well known expression [38]:

$$V(\bar{x}_k) = \min_{\bar{v}_k} l_{\text{cl}}^\downarrow(\bar{x}_k, \bar{v}_k) + V(\bar{x}_{k+1}). \quad (3.37)$$

Reapplying Eq. (3.37)  $(\Delta k - 1)$ -times yields:

$$V(\bar{x}_k) = \min_{\bar{v}_k} l_{\text{cl}}^\downarrow(\bar{x}_k, \bar{v}_k) + \dots + \min_{\bar{v}_{k+\Delta k-1}} l_{\text{cl}}^\downarrow(\bar{x}_{k+\Delta k-1}, \bar{v}_{k+\Delta k-1}) + V(\bar{x}_{k+\Delta k}). \quad (3.38)$$

Without loss of generality, assume that  $k$  is chosen such that  $(k \bmod \Delta k) = 0$ , i.e.  $s = s(k) = k/\Delta k$ . Setting  $\bar{v}_k = \hat{v}_{s(k)}$  leads to:

$$\begin{aligned} V(\bar{x}_k) &= \min_{\bar{v}_k} l_{\text{cl}}^\downarrow(\bar{x}_k, \bar{v}_k) + \dots + \min_{\bar{v}_k} l_{\text{cl}}^\downarrow(\bar{x}_{k+\Delta k-1}, \bar{v}_k) + V(\bar{x}_{k+\Delta k}) \\ &= \min_{\hat{v}_{s(k)}} \sum_{h=0}^{\Delta k-1} l_{\text{cl}}^\downarrow(\bar{x}_{k+h}, \hat{v}_{s(k)}) + V(\bar{x}_{k+\Delta k}). \end{aligned} \quad (3.39)$$

Replacing the summed up step cost  $l_{\text{cl}}^\downarrow(\cdot)$  by means of augmented matrices yields:

$$V(\bar{x}_k) = \min_{\hat{v}_{s(k)}} \left\| \begin{bmatrix} (\bar{C} + \bar{D}\bar{K}^\downarrow)\bar{x}_k \\ \vdots \\ (\bar{C} + \bar{D}\bar{K}^\downarrow)\bar{x}_{k+\Delta k-1} \end{bmatrix} + \begin{bmatrix} \bar{D}\hat{v}_{s(k)} \\ \vdots \\ \bar{D}\hat{v}_{s(k)} \end{bmatrix} \right\|_2^2 + V(\bar{x}_{k+\Delta k}). \quad (3.40)$$

Substituting the dynamics  $\bar{x}_{k+h} = (\bar{A}_{\text{cl}}^\downarrow)^h \bar{x}_k + \sum_{l=1}^h (\bar{A}_{\text{cl}}^\downarrow)^{l-1} \bar{B} \hat{v}_{s(k)}$ , and rearranging the terms by their dependence on states and inputs leads to:

$$V(\bar{x}_k) = \min_{\hat{v}_{s(k)}} \|\bar{C}^\uparrow \bar{x}_k + \bar{D}^\uparrow \hat{v}_{s(k)}\|_2^2 + V(\bar{x}_{k+\Delta k}). \quad (3.41)$$

Finally, (3.41) may be expressed for the upper layer time domain  $\mathbb{T}^\uparrow$ , which results in the standard one-step formulation of Bellman's principle of optimality:

$$V(\hat{x}_s) = \min_{\hat{v}_s} \|\bar{C}^\uparrow \hat{x}_s + \bar{D}^\uparrow \hat{v}_s\|_2^2 + V(\hat{x}_{s+1}) = \min_{\hat{v}_s} l^\uparrow(\hat{x}_s, \hat{v}_s) + V(\hat{x}_{s+1}). \quad (3.42)$$

Hence, the step cost in terms of the upper layer is given by the squared 2-norm of the controlled variable  $\hat{z}_s$ , such that  $J^\dagger$  is equivalent to  $J$ . Under the conditions described in Case 2.1 and with  $k_e = s_e \Delta k$ , the performance index  $J$  can be rewritten as follows:

$$J = \lim_{k_e \rightarrow \infty} \mathbb{E} \left( \frac{1}{k_e} \sum_{k=0}^{k_e-1} \bar{z}_k^\top \bar{z}_k \right) = \lim_{s_e \rightarrow \infty} \mathbb{E} \left( \frac{1}{s_e \Delta k} \sum_{s=0}^{s_e-1} \sum_{k=s \Delta k}^{(s+1) \Delta k - 1} \|\bar{C} \bar{x}_k + \bar{D} \bar{u}_k\|_2^2 \right). \quad (3.43)$$

Substituting the lower layer control law  $\bar{u}_k = \bar{K}^\downarrow \bar{x}_k + \bar{v}_k$  yields:

$$J = \lim_{s_e \rightarrow \infty} \mathbb{E} \left( \frac{1}{s_e \Delta k} \sum_{s=0}^{s_e-1} \sum_{k=s \Delta k}^{(s+1) \Delta k - 1} \|(\bar{C} + \bar{D} \bar{K}^\downarrow) \bar{x}_k + \bar{D} \bar{v}_k\|_2^2 \right). \quad (3.44)$$

Replacing the inner sum in a similar manner as in (3.40) and in (3.41) leads to:

$$J = \lim_{s_e \rightarrow \infty} \mathbb{E} \left( \frac{1}{s_e \Delta k} \sum_{s=0}^{s_e-1} \|\bar{C}^\dagger \hat{x}_s + \bar{D}^\dagger \hat{v}_s + \bar{F}^\dagger \hat{w}_s\|_2^2 \right). \quad (3.45)$$

Factoring out the constant factor  $1/\Delta k$  yields:

$$J = \frac{1}{\Delta k} \lim_{s_e \rightarrow \infty} \mathbb{E} \left( \frac{1}{s_e} \sum_{s=0}^{s_e-1} \hat{z}_s^\top \hat{z}_s \right) = \frac{J^\dagger}{\Delta k}. \quad (3.46)$$

Hence, minimizing  $J^\dagger$  is equivalent to minimizing  $J$  for Case 2.1.

From the structure of  $\bar{D}^\dagger$ , it can be deduced that it has full column rank: Due to Assumption 3.1, the matrix  $D$  must have full column rank. Furthermore, the matrix  $\bar{D}$  is obtained from  $D$  by row and column permutations, which do not affect the rank. Considering the first block-row of the matrix  $[\bar{C}^\dagger \ \bar{D}^\dagger]$ , it can be seen that it can be obtained from the matrix  $[C \ D]$  via row and column permutations and elementary column operations. Hence, it holds that:

$$\text{rank} [\bar{C} + \bar{D} \bar{K}^\downarrow \ \bar{D}] = \text{rank} [C \ D], \quad (3.47)$$

such that the matrix  $[\bar{C}^\dagger \ \bar{D}^\dagger]$  must have full column rank. Since  $\Delta k \in \mathbb{N}_0$  is to be chosen such that the pair  $(\bar{A}^\dagger, \bar{B}^\dagger)$  is stabilizable, the existence conditions for a unique centralized optimal control law are satisfied (see [142, Sec. 21.7]). Furthermore, since all involved matrices are time-invariant, the optimal centralized upper layer control law is of the form  $\hat{v}_s = \bar{K}^\uparrow \hat{x}_s$  [38].  $\square$

Assuming full communication on the upper control layer, the optimal upper layer control gain  $\bar{K}^\uparrow$  can be efficiently calculated by the help of an algebraic Riccati equation (ARE) [38]:

$$\bar{P}^\dagger := (\bar{A}^\dagger)^\top \bar{P}^\dagger \bar{A}^\dagger - (\bar{B}^\dagger \bar{P}^\dagger \bar{A}^\dagger + \bar{S}^\dagger)^\top (\bar{R}^\dagger + (\bar{B}^\dagger)^\top \bar{P}^\dagger \bar{B}^\dagger)^{-1} (\bar{B}^\dagger \bar{P}^\dagger \bar{A}^\dagger + \bar{S}^\dagger) + \bar{Q}^\dagger, \quad (3.48a)$$

$$\bar{K}^\uparrow := (\bar{R}^\dagger + (\bar{B}^\dagger)^\top \bar{P}^\dagger \bar{B}^\dagger)^{-1} (\bar{B}^\dagger \bar{P}^\dagger \bar{A}^\dagger + \bar{S}^\dagger), \quad (3.48b)$$



where  $\bar{Q}^\dagger := (\bar{C}^\dagger)^\top \bar{C}^\dagger$ ,  $\bar{S}^\dagger := (\bar{D}^\dagger)^\top \bar{C}^\dagger$ , and  $\bar{R}^\dagger := (\bar{D}^\dagger)^\top \bar{D}^\dagger$ . Note that the stability and implementation of the resulting two-layer control scheme will be discussed after considering an optimized communication topology on the upper control layer first.

### 3.4.2. Optimized Communication Topology

As mentioned earlier, the original goal is to perform SCT design on the upper control layer. Setting up the SCT optimization requires to define additional variables associated with the topology of the communication network. In particular, a binary adjacency matrix  $\bar{\Sigma}^\dagger = [\bar{\sigma}_{p,q}^\dagger] \in \mathbb{B}^{N_c \times N_c}$  encoding the topology of the communication graph  $\mathcal{G}^\dagger$ , and a set  $\bar{\Sigma}^\dagger \subseteq \mathbb{B}^{N_c \times N_c}$  of admissible communication topologies are required. Furthermore, a matrix  $\bar{C}^{\dagger \text{com}} = [\bar{c}_{p,q}^{\dagger \text{com}}] \in \mathbb{R}_{\geq 0}^{N_c \times N_c}$  of costs associated with the upper layer communication links has to be chosen, such that  $\bar{c}_{p,p}^{\dagger \text{com}} = 0$  for all  $p \in \mathcal{N}_c$ . The communication cost can then be defined as:

$$J^{\dagger \text{com}} := \sum_{p=1}^{N_c} \sum_{q=1}^{N_c} \bar{\sigma}_{p,q}^\dagger \bar{c}_{p,q}^{\dagger \text{com}}. \quad (3.49)$$

The SCT optimization problem for the design of a linear upper layer control law  $\hat{v}_s = \bar{K}^\dagger \hat{x}_s$  that complies with the communication topology encoded by  $\bar{\Sigma}^\dagger$  can now be stated as (exemplarily assuming the conditions of Case 2.2):

$$\min_{\bar{K}^\dagger, \bar{\Sigma}^\dagger} J^\dagger + J^{\dagger \text{com}} \quad (3.50a)$$

$$\text{subject to: } \hat{x}_{s+1} = \bar{A}^\dagger \hat{x}_s + \bar{B}^\dagger \hat{v}_s, \quad (3.50b)$$

$$\hat{z}_s = \bar{C}^\dagger \hat{x}_s + \bar{D}^\dagger \hat{v}_s, \quad (3.50c)$$

$$\hat{v}_s = \bar{K}^\dagger \hat{x}_s, \quad (3.50d)$$

$$\bar{\Sigma}^\dagger \in \bar{\Sigma}^\dagger, \quad (3.50e)$$

$$(\bar{\sigma}_{p,q}^\dagger = 0) \Rightarrow (\bar{K}_{p,q}^\dagger = 0). \quad (3.50f)$$

The following Theorem shows how the above problem can be solved by employing mixed-integer semidefinite programming.

**Theorem 3.3.** *Suppose that the matrices  $\bar{\Sigma}^\dagger \in \mathbb{B}^{N_c \times N_c}$ ,  $\mathfrak{G} \in \mathbb{R}^{n_x \times n_x}$ ,  $\mathfrak{L} \in \mathbb{R}^{n_u \times n_x}$ ,  $\mathfrak{X} \in \mathbb{S}_{>0}^{n_x}$ , and  $\mathfrak{Z} \in \mathbb{S}_{>0}^{n_w}$  are a solution of the mixed-integer semidefinite program:*

$$\min_{\bar{\Sigma}^\dagger, \mathfrak{G}, \mathfrak{L}, \mathfrak{X}, \mathfrak{Z}} \text{tr}(\mathfrak{Z}) + J^{\text{com}} \quad \text{subject to:} \quad (3.51a)$$

$$\begin{bmatrix} \mathfrak{G} + \mathfrak{G}^\top - \mathfrak{X} & \star & \star \\ \bar{A}^\dagger \mathfrak{G} + \bar{B}^\dagger \mathfrak{L} & \mathfrak{X} & \star \\ \bar{C}^\dagger \mathfrak{G} + \bar{D}^\dagger \mathfrak{L} & 0 & I_{n_z} \end{bmatrix} \succ 0, \quad (3.51b)$$

$$\begin{bmatrix} \mathfrak{Z} & \star & \star \\ \bar{E}^\dagger & \mathfrak{X} & \star \\ \bar{F}^\dagger & 0 & I \end{bmatrix} \succ 0, \quad (3.51c)$$

$$\mathfrak{X} = \mathfrak{X}^\top \succ 0, \quad (3.51d)$$

$$\mathfrak{Z} = \mathfrak{Z}^\top \succ 0, \quad (3.51e)$$

$$\bar{\Sigma}^\dagger \in \bar{\Sigma}^\dagger, \quad (3.51f)$$

$$-M\bar{\sigma}_{p,q}^\dagger 1_{\bar{n}_u^p \times \bar{n}_x^q} \leq \mathfrak{L}_{p,q} \leq M\bar{\sigma}_{p,q}^\dagger 1_{\bar{n}_u^p \times \bar{n}_x^q} \quad \forall p, q, \quad (3.51g)$$

$$-M\bar{\sigma}_{p,q}^\dagger 1_{\bar{n}_x^p \times \bar{n}_x^q} \leq \mathfrak{G}_{p,q} \leq M\bar{\sigma}_{p,q}^\dagger 1_{\bar{n}_x^p \times \bar{n}_x^q} \quad \forall p, q, \quad (3.51h)$$

$$-M(\bar{\sigma}_{p,q}^\dagger - \bar{\sigma}_{p,r}^\dagger + 1)1_{\bar{n}_x^r \times \bar{n}_x^q} \leq \mathfrak{G}_{r,q} \leq M(\bar{\sigma}_{p,q}^\dagger - \bar{\sigma}_{p,r}^\dagger + 1)1_{\bar{n}_x^r \times \bar{n}_x^q} \quad \forall p, q, r, \quad (3.51i)$$

where  $p, q, r \in \mathcal{N}_c$ , and  $M \in \mathbb{R}_{>0}$  is a number satisfying  $M > \max\{\|\mathfrak{G}\|_{1,\infty}, \|\mathfrak{L}\|_{1,\infty}\}$ . Here,  $\|\cdot\|_{1,\infty}$  denotes the  $1, \infty$ -induced norm of a matrix, corresponding to its largest entry in magnitude. Set  $\bar{K}^\dagger := \mathfrak{L}\mathfrak{G}^{-1}$ , and denote the closed-loop system consisting of  $\bar{\mathcal{P}}^\dagger$  with  $\hat{v}_s = \bar{K}^\dagger \hat{x}_s$  by  $\bar{\mathcal{P}}_{\text{cl}}^\dagger$ . Then, the following assertions hold:

- The point  $\bar{x}_{\text{eq}} = 0$  is the only globally asymptotically stable equilibrium point for the dynamic system  $\bar{\mathcal{P}}_{\text{cl}}^\dagger$  with  $\hat{w}_s = 0$  for all  $s \in \mathbb{N}_0$ .
- The dynamic system  $\bar{\mathcal{P}}_{\text{cl}}^\dagger$  with input  $\hat{w}_s$  is bounded-input/bounded-output stable.
- For  $J$  according to Case 2.1, the value of  $J + J^{\text{com}}$  is upper-bounded by the objective function (3.51a).
- For  $J$  according to Case 2.2, and by setting  $\bar{E}^\dagger := \bar{x}_0$ ,  $\bar{F}^\dagger := 0_{\bar{n}_z \times \bar{n}_w}$ , the value of  $J + J^{\text{com}}$  is upper-bounded by the objective function (3.51a).
- The control law  $\hat{v}_s = \bar{K}^\dagger \hat{x}_s$  respects the communication topology given by  $\bar{\Sigma}^\dagger$ .  $\square$

*Proof.* Similar to the proof of Theorem 3.1, it can be shown that feasibility of the LMIs (3.51b) to (3.51e) implies that  $\bar{A}_{\text{cl}}^\dagger := \bar{A}^\dagger + \bar{B}^\dagger \bar{K}^\dagger$  is a Schur matrix, and that  $\text{tr}(\mathfrak{Z}) > J$  for Case 2.1 and Case 2.2. Hence, with Theorem 2.1 and 2.2, assertions (a) to (d) follow. The constraints (3.51g) to (3.51i), which have been adopted from [50], enforce that:

$$\bar{\sigma}_{p,q}^\dagger = 0 \quad \Rightarrow \quad \bar{K}_{p,q}^\dagger = 0_{\bar{n}_u^p \times \bar{n}_x^q}. \quad (3.52)$$

Hence, the state vector  $\hat{x}_s^q$  of the aggregate subsystem  $\bar{\mathcal{P}}^q$  is not required by the aggregate subsystem  $\bar{\mathcal{P}}^p$  to calculate  $\hat{v}_s$ . Consequently, the control law  $\hat{v}_s = \bar{K}^\uparrow \hat{x}_s$  respects the communication topology given by  $\bar{\Sigma}^\uparrow$ , which proves assertion (e).  $\square$

The MISDP (3.51) for the design of the upper layer controller in the hierarchical approach creates  $N_c^2 - N_c$  binary variables. Furthermore, one additional SDP has to be solved in order to obtain the lower layer controller. In contrast, approaches that assume a single layer controller structure, e.g. [50], create  $N_s^2 - N_s$  binary variables. Since  $N_c < N_s$ , the computational time is typically significantly reduced by the hierarchical approach.

### 3.4.3. Stability of the Original Interconnected System

If the upper layer control gain  $\bar{K}^\uparrow$  is designed such that the upper layer closed-loop system:

$$\bar{\mathcal{P}}_{\text{cl}}^\uparrow : \begin{cases} \hat{x}_{s+1} = (\bar{A}^\uparrow + \bar{B}^\uparrow \bar{K}^\uparrow) \hat{x}_s + \bar{E}^\uparrow \hat{w}_s, \\ \hat{z}_s = (\bar{C}^\uparrow + \bar{D}^\uparrow \bar{K}^\uparrow) \hat{x}_s + \bar{F}^\uparrow \hat{w}_s, \end{cases} \quad (3.53)$$

is asymptotically stable, then the following result holds regarding the stability of the interconnected system  $\mathcal{P}$  under the hierarchical control:

$$\bar{u}_k = \bar{K}^\downarrow \bar{x}_k + \bar{K}^\uparrow \bar{x}_{s\Delta k}, \quad (3.54)$$

with  $s\Delta k = k - (k \bmod \Delta k)$ :

**Theorem 3.4.** *Suppose that  $\|\bar{A}_{\text{cl}}^\downarrow\|_2^2$  is finite, that the closed-loop system  $\bar{\mathcal{P}}_{\text{cl}}^\uparrow$  is asymptotically stable, and that the distributed hierarchical control (3.54) is applied to the interconnected system  $\mathcal{P}$ . Then, the following assertions hold:*

(a) *The system  $\mathcal{P}$  with  $w_k = 0$  for all  $k \in \mathbb{N}_0$  is asymptotically stable.*

(b) *The system  $\mathcal{P}$  with input  $w_k$  is bounded-input/bounded-output stable.*  $\square$

*Proof.* In order to proof assertion (a), assume that  $\bar{w}_k = 0$  for all  $k \in \mathbb{N}_0$ , and note that for every fixed  $k \in \mathbb{N}_0$  and  $\Delta k \in \mathbb{N}_{>1}$ , there exists a unique combination of  $s \in \mathbb{N}_0$  and  $l \in \{0, 1, \dots, \Delta k - 1\}$  such that:

$$\bar{x}_k = \bar{x}_{s\Delta k + l}. \quad (3.55)$$

From the definition of the induced 2-norm and the submultiplicativity property of matrix norms [8, p.31], it follows that:

$$\begin{aligned} \|\bar{x}_k\|_2^2 &= \|\bar{x}_{s\Delta k + l}\|_2^2 \\ &= \|((\bar{A}_{\text{cl}}^\downarrow)^l + \sum_{h=0}^{l-1} (\bar{A}_{\text{cl}}^\downarrow)^h \bar{B} \bar{K}^\uparrow) \bar{x}_{s\Delta k}\|_2^2 \\ &\leq \|(\bar{A}_{\text{cl}}^\downarrow)^l + \sum_{h=0}^{l-1} (\bar{A}_{\text{cl}}^\downarrow)^h \bar{B} \bar{K}^\uparrow\|_2^2 \|\bar{x}_{s\Delta k}\|_2^2. \end{aligned} \quad (3.56)$$

Since the upper layer closed-loop system  $\mathcal{P}^\dagger$  is asymptotically stable, there exist constants  $\alpha^\dagger \in \mathbb{R}_{>1}$  and  $\beta^\dagger \in (0, 1)$  such that (see Thm. 2.1 on page 34):

$$\|\bar{x}_{s\Delta k}\|_2^2 = \|\hat{x}_s\|_2^2 \leq \alpha^\dagger (\beta^\dagger)^s \|\hat{x}_0\|_2^2 = \alpha^\dagger (\beta^\dagger)^s \|\bar{x}_0\|_2^2 \quad \forall s \in \mathbb{N}_0. \quad (3.57)$$

Hence, for finite  $\|\bar{A}_{\text{cl}}^\downarrow\|_2^2$ , one can always find constants  $\alpha' \in \mathbb{R}_{\geq 1}$  and  $\beta' \in (\beta^\dagger, 1)$  such that for all  $l \in \{0, 1, \dots, \Delta k - 1\}$ :

$$\|(\bar{A}_{\text{cl}}^\downarrow)^l + \sum_{h=0}^{l-1} (\bar{A}_{\text{cl}}^\downarrow)^h \bar{B} \bar{K}^\uparrow\|_2^2 \leq \alpha' (\beta')^l, \quad (\beta')^{\Delta k} = \beta^\dagger. \quad (3.58)$$

Substituting Eq. (3.58) into Eq. (3.56) and using Eq. (3.57), it follows that:

$$\|\bar{x}_k\|_2^2 \leq \alpha' (\beta')^l \|\bar{x}_{s\Delta k}\|_2^2 \leq \alpha' \alpha^\dagger (\beta^\dagger)^s (\beta')^l \|\bar{x}_0\|_2^2 = \alpha' \alpha^\dagger (\beta')^{s\Delta k + l} \|\bar{x}_0\|_2^2. \quad (3.59)$$

Define:

$$\alpha := \alpha' \alpha^\dagger \in \mathbb{R}_{>1}, \quad \beta := \beta' \in (\beta^\dagger, 1), \quad (3.60)$$

and recall that  $\bar{x}_k$  is a permutation of  $x_k$ . Then, with Eq. (3.59), it is apparent that:

$$\|x_k\|_2^2 = \|\bar{x}_k\|_2^2 \leq \alpha \beta^k \|\bar{x}_0\|_2^2 \quad \forall k \in \mathbb{N}_0, \quad (3.61)$$

meaning that the interconnected system  $\mathcal{P}$  under the hierarchical control of (3.54) is asymptotically stable according to Theorem 2.1. Assertion (b) immediately follows from Theorem 2.2.  $\square$

### 3.4.4. Alternative Performance Indices

Under the conditions of Case 2.2, due to setting  $\bar{E}^\dagger = \bar{x}_0$ , the LMI (3.51c) depends on this particular initialization of the interconnected system. While the optimal upper layer control gain  $\bar{K}^\uparrow$  is independent of  $\bar{x}_0$  in the case of full communication on the upper layer, it becomes a function of  $\bar{x}_0$  as soon as structural constraints are imposed. In order to avoid this dependency, it may be convenient to consider a random initial state and the corresponding expectancy of the performance index instead. This can be done with minor modifications of the constraint (3.51c) and the objective function.

Assume that  $\bar{x}_0$  is normally distributed with mean  $\bar{\mu}_x \in \mathbb{R}^{n_x}$  and covariance  $\bar{\Sigma}_x \in \mathbb{S}_{>0}^{n_x}$ , i.e.  $\bar{x}_0 \sim \mathcal{N}(\bar{\mu}_x, \bar{\Sigma}_x)$ . Using the following relation from [113, p.9]:

$$\mathbb{E}(\text{tr}(\bar{x}_0^\top P \bar{x}_0)) = \text{tr}(\bar{\Sigma}_x P) + \bar{\mu}_x^\top P \bar{\mu}_x, \quad (3.62)$$

the MISDP (3.51) can be readily modified in order to minimize an upper bound on the expected performance. First, set  $\bar{E}^\dagger = I_{n_x}$  and adjust the dimension of  $\mathfrak{Z}$  accordingly to obtain from (3.51c) that:

$$\mathfrak{Z} \succ \mathfrak{X}^{-1}. \quad (3.63)$$

On the other hand, inequality (3.51b) ensures that:

$$\mathfrak{X}^{-1} \succ \sum_{s=0}^{\infty} ((\bar{A}_{\text{cl}}^\dagger)^s)^\top (\bar{C}_{\text{cl}}^\dagger)^\top \bar{C}_{\text{cl}}^\dagger (\bar{A}_{\text{cl}}^\dagger)^s =: \bar{P}^\dagger. \quad (3.64)$$

Using  $\bar{P}^\dagger$ , the performance index can be written as:

$$J^\dagger = \text{tr}(\bar{x}_0^\top \bar{P}^\dagger \bar{x}_0). \quad (3.65)$$

Using the above relations, it is easy to see that:

$$\text{tr}(\bar{\Sigma}_x \mathfrak{Z}) + \bar{\mu}_x^\top \mathfrak{Z} \bar{\mu}_x > \text{tr}(\bar{\Sigma}_x \bar{P}) + \bar{\mu}_x^\top \bar{P} \bar{\mu}_x = \text{E}(J^\dagger). \quad (3.66)$$

Consequently, the function:

$$\text{tr}(\bar{\Sigma}_x \mathfrak{Z}) + \bar{\mu}_x^\top \mathfrak{Z} \bar{\mu}_x + J^{\text{com}} \quad (3.67)$$

can be used as an objective function in (3.51) to minimize an upper bound on the sum of the expected performance index and the communication cost. Since (3.67) is linear in the matrix variable  $\mathfrak{Z}$ , the optimization problem stays convex when the integer variables are either all fixed or relaxed to the closed interval  $[0, 1]$ .

Another possible variant is to assume that the initial state  $\bar{x}_0$  is uniformly distributed over the ellipsoid:

$$\mathcal{E}_x := \{\bar{x}_0 \in \mathbb{R}^{n_x} \mid (\bar{x}_0 - \bar{\mu}_x)^\top \bar{\Sigma}_x^{-1} (\bar{x}_0 - \bar{\mu}_x) \leq 1\} \subseteq \bar{\mathbb{X}}, \quad (3.68)$$

which is denoted by  $\bar{x}_0 \sim \mathcal{U}(\mathcal{E}_x)$ . Then, the following relation can be exploited, which is derived in Appendix B:

$$\text{E}(\text{tr}(\bar{x}_0^\top P \bar{x}_0)) = \frac{1}{n_x + 2} \text{tr}(\bar{\Sigma}_x P) + \bar{\mu}_x^\top P \bar{\mu}_x. \quad (3.69)$$

Using a similar argumentation as before, the function:

$$\frac{1}{n_x + 2} \text{tr}(\bar{\Sigma}_x \mathfrak{Z}) + \bar{\mu}_x^\top \mathfrak{Z} \bar{\mu}_x + J^{\text{com}} \quad (3.70)$$

can be used as an objective function in (3.51) to minimize an upper bound on the sum of the expected performance index and the communication cost. Again, the above function is linear in the matrix variable  $\mathfrak{Z}$ . For both variants, analogous changes have to be made in the SDP for designing the lower layer controller, too.

### 3.5. Implementation

From the viewpoint of implementation, the hierarchical two-layer control scheme can be considered as a time-varying distributed control law. Since the upper control

layer only exchanges information every  $\Delta k$ -th time-step of the lower layer time-domain  $\mathbb{T}^\downarrow$ , the two-layer control scheme can actually be implemented as a single distributed control layer with periodically time-varying communication topology. The time-varying distributed control units  $\mathcal{C}_k^i$  consist of both,  $\mathcal{C}^{\downarrow i}$  and  $\mathcal{C}^{\uparrow i}$ . In the context of the original subsystem order, the corresponding local control laws are obtained by first permuting the upper and lower layer control gain matrices and partitioning them according to the subsystems:

$$K^\downarrow = [K_{i,j}^\downarrow] := T_u \bar{K}^\downarrow T_x^\top, \quad K^\uparrow = [K_{i,j}^\uparrow] := T_u \bar{K}^\uparrow T_x^\top. \quad (3.71)$$

Then, the local control inputs are obtained as:

$$u_k^i = \sum_{j=1}^{N_s} K_{i,j}^\downarrow x_k^j + K_{i,j}^\uparrow x_{s\Delta k}^j, \quad (3.72)$$

with  $s\Delta k = k - (k \bmod \Delta k)$ . The time-varying communication graph  $\mathcal{G}_k$  can be constructed from  $\mathcal{G}^\downarrow$  and  $\mathcal{G}^\uparrow$  as follows: First, define the logical variables  $l_{i,j}^\downarrow \in \mathbb{B}$  and  $l_{i,j}^\uparrow \in \mathbb{B}$  as:

$$l_{i,j}^\downarrow := (\exists p \in \mathcal{N}_c \mid (i, j) \in \mathcal{C}^p \times \mathcal{C}^p), \quad (3.73a)$$

$$l_{i,j}^\uparrow := (\exists p, q \in \mathcal{N}_c \mid (\bar{\sigma}_{p,q}^\uparrow = 1) \wedge (i \in \mathcal{C}^p) \wedge (j \in \mathcal{C}^q)). \quad (3.73b)$$

Assuming that all three graphs are represented by their adjacency matrices, the time-varying adjacency matrix  $\Sigma_k = [\sigma_{k,i,j}] \in \mathbb{B}^{N_s \times N_s}$  is given by:

$$\sigma_{k,i,j} = \begin{cases} 1 & \text{if } (l_{i,j}^\downarrow) \vee ((k \bmod \Delta k = 0) \wedge l_{i,j}^\uparrow), \\ 0 & \text{otherwise.} \end{cases} \quad (3.74)$$

In each discrete time step  $t_k \in \mathbb{T}^\downarrow$ , the controllers  $\mathcal{C}_k^i$  must first measure their local state vectors  $x_k^i$ , and transmit this information to all controllers  $\mathcal{C}_k^j$  with  $j \in \mathcal{T}_k^i := \{j \in \mathcal{N}_s \mid \sigma_{k,j,i} = 1\}$ . On the other hand, each local controller  $\mathcal{C}_k^i$  receives the state measurements of all controllers  $\mathcal{C}_k^j$  with  $j \in \mathcal{R}_k^i := \{j \in \mathcal{N}_s \mid \sigma_{k,i,j} = 1\}$ . With this information, the local control inputs  $u_k^i$  are updated according to Eq. (3.72) and held constant until the next discrete time step  $t_{k+1}$ . Introducing the set:

$$\mathcal{X}_k^i := \{x_k^j \in \mathbb{X}^j \mid j \in \mathcal{R}_k^i\} \quad (3.75)$$

of subsystem states available to controller  $\mathcal{C}_k^i$  at time  $k$ , the implementation structure of the two-layer control scheme is visualized in Fig. 3.1. Note that the physical interconnection signals are intentionally not tagged by any variables for simplicity.

## 3.6. Numerical Example

As numerical example, consider the following academic system, which is an interconnected system comprising of  $N_s = 6$  subsystems of order 1 or 2, as taken from

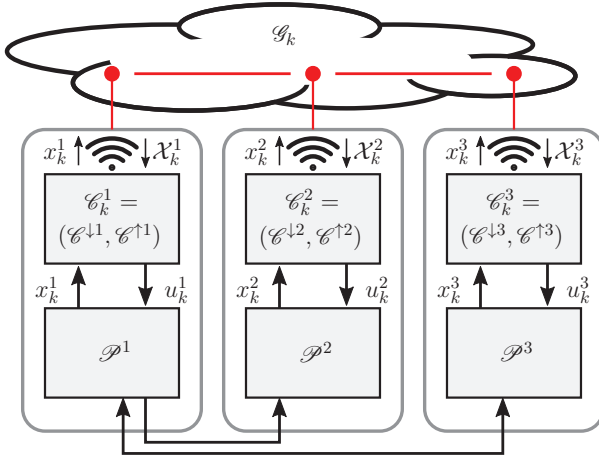


**Figure 3.1.:** Distributed implementation of the hierarchical two-layer control scheme, exemplarily shown for  $N_s = 3$  subsystems.

[58]. The partitioned matrices  $A$  to  $E$  comprising the overall system  $\mathcal{P}$  are given by:

$$A = \begin{bmatrix} 1.4 & 0.7 & 0 & 0 & -0.4 & -0.6 & 0.6 & 0.2 & 0 \\ 0 & -0.2 & 0 & 0 & 0.1 & 0 & 0 & 0 & 0 \\ 0.1 & 0 & -0.7 & 0.2 & 0 & 0 & 0.2 & 1.1 & 0.7 \\ -0.1 & 0 & 1.2 & 0.4 & 0 & 0.1 & -0.1 & 0 & 0 \\ 0 & -0.2 & 0 & 0 & 0.6 & 0 & 0 & 0 & 0 \\ 0.4 & 0 & 0.1 & 0 & 0.9 & 1.1 & -1.3 & 0 & 0 \\ 0 & 0 & 0 & 0.2 & 0.9 & 0.2 & -0.4 & 0 & 0 \\ 0.1 & 0 & 2.0 & 0.3 & 0 & 0 & 0.2 & 0.3 & 0.1 \\ -0.1 & 0 & 0 & -0.2 & 0 & 0.1 & -0.1 & 0 & 0.3 \end{bmatrix}, \quad (3.76a)$$

$$B = \text{blkdiag} \left( 0.4, -1.5, \begin{bmatrix} 0.3 & 0.7 \\ -0.2 & 0 \end{bmatrix}, 1.2, \begin{bmatrix} 0 \\ 0.6 \end{bmatrix}, \begin{bmatrix} -0.9 \\ 0.3 \end{bmatrix} \right), \quad (3.76b)$$

$$C = \text{blkdiag} \left( \begin{bmatrix} 0 \\ 1 \end{bmatrix}, \begin{bmatrix} 0 \\ 2 \end{bmatrix}, \begin{bmatrix} 0 & 0 \\ 0 & 0 \\ \sqrt{7} & 0 \\ 0 & \sqrt{10} \end{bmatrix}, \begin{bmatrix} 0 \\ \sqrt{13} \end{bmatrix}, \begin{bmatrix} 0 & 0 \\ 4 & 0 \\ 0 & \sqrt{19} \end{bmatrix}, \begin{bmatrix} 0 & 0 \\ \sqrt{22} & 0 \\ 0 & 5 \end{bmatrix} \right), \quad (3.76c)$$

$$D = \text{blkdiag} \left( \begin{bmatrix} 1 \\ 0 \end{bmatrix}, \begin{bmatrix} 1 \\ 0 \end{bmatrix}, \begin{bmatrix} 1 & 0 \\ 0 & 1 \\ 0 & 0 \\ 0 & 0 \end{bmatrix}, \begin{bmatrix} 1 \\ 0 \end{bmatrix}, \begin{bmatrix} 1 \\ 0 \end{bmatrix}, \begin{bmatrix} 1 \\ 0 \\ 0 \end{bmatrix} \right), \quad (3.76d)$$

$$E = I_9. \quad (3.76e)$$

With the above parameters,  $\mathcal{P}$  contains unstable eigenvalues and is fully reachable.

The different stages of the clustering procedure are illustrated in Figure 3.2. Initially, the sparse interconnection structure of the subsystems does not possess any particular structure (left). Neglecting the three weakest interconnections by choosing  $\epsilon_w = \epsilon_n = 0.21$  and applying the Dulmage-Mendelsohn decomposition, it becomes apparent that the overall system can be interpreted as an interconnection of  $N_c = 4$  hierarchically interconnected clusters, each of them enframed in red (middle). Finally, the third and fourth cluster may be combined to obtain three clusters, each containing two subsystems (right). Hence, the final clusters are given by:

$$\mathcal{C}^1 = \{3, 6\}, \quad \mathcal{C}^2 = \{1, 5\}, \quad \mathcal{C}^3 = \{2, 4\}. \quad (3.77)$$

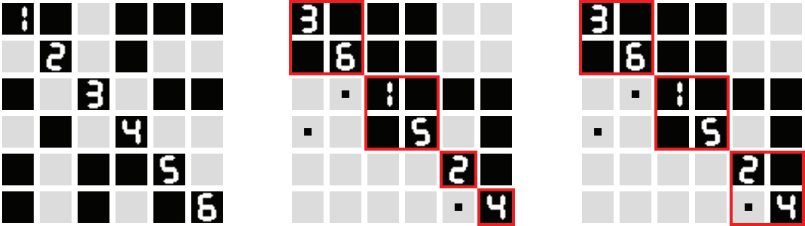


**Figure 3.2.:** Initial interconnection structure of the plant (left), after DM decomposition (middle), and after combining clusters  $\mathcal{C}^3$  and  $\mathcal{C}^4$  (right). Black boxes denote strong interconnections, black dots denote neglected interconnections, and the red squares indicate the clusters.

From the lower layer control design using the system  $\mathcal{P}'$  without the weak interconnections, the following local control laws are obtained:

$$\mathcal{C}^{\downarrow 1} : u_k^1 = -2.867x_k^1 + [0.714 \quad -0.658] x_k^5 + v_k^1, \quad (3.78a)$$

$$\mathcal{C}^{\downarrow 2} : u_k^2 = 0.002x_k^2 - 0.078x_k^4 + v_k^2, \quad (3.78b)$$



$$\mathcal{E}^{\downarrow 3} : u_k^3 = \begin{bmatrix} 1.902 & 0.542 \\ -0.121 & -0.502 \end{bmatrix} x_k^3 + \begin{bmatrix} -0.391 & -0.231 \\ -1.359 & -0.980 \end{bmatrix} x_k^6 + v_k^3, \quad (3.78c)$$

$$\mathcal{E}^{\downarrow 4} : u_k^4 = -0.533x_k^4 + 0.080x_k^2 + v_k^4, \quad (3.78d)$$

$$\mathcal{E}^{\downarrow 5} : u_k^5 = [0.484 \quad -0.293] x_k^5 + 0.438x_k^1 + v_k^5, \quad (3.78e)$$

$$\mathcal{E}^{\downarrow 6} : u_k^6 = [0.296 \quad -0.001] x_k^6 + [1.930 \quad 0.346] x_k^3 + v_k^6, \quad (3.78f)$$

where  $v_k^i$  are the inputs for the upper layer control laws. In this case, applying the lower layer controllers  $\mathcal{E}^{\downarrow i}$  to the original interconnected system yields a stable closed-loop system  $\mathcal{P}_{cl}^1$ . Hence, the hierarchical control scheme would be robust against failures of communication links related to the upper control layer.

For performing SCT design on the upper control layer, the communication cost function is parametrized by:

$$\bar{c}^{\uparrow \text{com}} = \begin{bmatrix} 0 & 1 & 5 \\ 1 & 0 & 5 \\ 5 & 5 & 0 \end{bmatrix}. \quad (3.79)$$

Solving the SDP (3.51) with  $\Delta k = 3$  then leads to the optimized upper layer communication topology:

$$\bar{\Sigma}^{\uparrow} = \begin{bmatrix} 1 & 1 & 1 & 1 & 1 & 1 \\ 1 & 1 & 0 & 1 & 1 & 0 \\ 0 & 0 & 1 & 0 & 0 & 1 \\ 1 & 1 & 0 & 1 & 1 & 0 \\ 1 & 1 & 1 & 1 & 1 & 1 \\ 0 & 0 & 1 & 0 & 0 & 1 \end{bmatrix}. \quad (3.80)$$

The upper layer control laws are given by:

$$\mathcal{E}^{\uparrow 1} : v_{s\Delta k}^1 = 0.382x_{s\Delta k}^1 - 0.442x_{s\Delta k}^2 + [-0.068 \quad 0.033] x_{s\Delta k}^3 - 0.013x_{s\Delta k}^4 \dots \\ + [-0.239 \quad 0.266] x_{s\Delta k}^5 - [0.106 \quad 0.021] x_{s\Delta k}^6, \quad (3.81a)$$

$$\mathcal{E}^{\uparrow 2} : v_{s\Delta k}^2 = -0.079x_{s\Delta k}^2 + 0.102x_{s\Delta k}^1 + 0.036x_{s\Delta k}^4 + [-0.110 \quad 0.133] x_{s\Delta k}^5, \quad (3.81b)$$

$$\mathcal{E}^{\uparrow 3} : v_{s\Delta k}^3 = \begin{bmatrix} 0.065 & -0.096 \\ -0.030 & 0.036 \end{bmatrix} x_{s\Delta k}^3 + \begin{bmatrix} 0.004 & -0.006 \\ -0.012 & 0.024 \end{bmatrix} x_{s\Delta k}^6, \quad (3.81c)$$

$$\mathcal{E}^{\uparrow 4} : v_{s\Delta k}^4 = 0.072x_{s\Delta k}^4 - 0.096x_{s\Delta k}^1 - 0.018x_{s\Delta k}^2 + [-0.116 \quad 0.124] x_{s\Delta k}^5, \quad (3.81d)$$

$$\mathcal{E}^{\uparrow 5} : v_{s\Delta k}^5 = [-0.023 \quad 0.005] x_{s\Delta k}^5 + 0.025x_{s\Delta k}^1 + 0.004x_{s\Delta k}^2 \dots \\ - [0.085 \quad 0.149] x_{s\Delta k}^3 - 0.178x_{s\Delta k}^4 - [0.004 \quad 0.007] x_{s\Delta k}^6, \quad (3.81e)$$

$$\mathcal{E}^{\uparrow 6} : v_{s\Delta k}^6 = [0.017 \quad -0.004] x_{s\Delta k}^6 + [-0.018 \quad 0.014] x_{s\Delta k}^3. \quad (3.81f)$$

Notably, many coefficients of the upper layer control laws are considerably smaller in magnitude than the coefficients of the lower layer control laws. Hence, as expected, this indicates that the influence of the neglected interconnections is small, such that only slight corrective actions are required on the upper layer.

**Table 3.1.:** Performance comparison for different controller structures with  $J$  according to Case 2.1 and  $\Delta k = 3$ .

Topology $\bar{\Sigma}^\uparrow$	n/a	n/a	$\begin{bmatrix} 1 & 0 & 0 \\ 1 & 1 & 1 \\ 0 & 1 & 1 \end{bmatrix}$	$\begin{bmatrix} 1 & 1 & 1 \\ 1 & 1 & 1 \\ 1 & 1 & 1 \end{bmatrix}$
Input $v_k$	n/a	n/a	$K^\uparrow x_{s\Delta k}$	$K^\uparrow_{\text{LQ}} x_{s\Delta k}$
Topology $\bar{\Sigma}^\downarrow$	$\begin{bmatrix} 1 & 1 & 1 \\ 1 & 1 & 1 \\ 1 & 1 & 1 \end{bmatrix}$	$\begin{bmatrix} 1 & 0 & 0 \\ 0 & 1 & 0 \\ 0 & 0 & 1 \end{bmatrix}$	$\begin{bmatrix} 1 & 0 & 0 \\ 0 & 1 & 0 \\ 0 & 0 & 1 \end{bmatrix}$	n/a
Input $u_k$	$K^\downarrow_{\text{LQ}} x_k$	$K^\downarrow x_k$	$K^\downarrow x_k + v_k$	$v_k$
$J$	251.72	296.62	280.53	475.06
$J^\uparrow_{\text{com}}$	n/a	n/a	11	22

Table 3.1 compares the performance of the closed-loop system resulting from  $\mathcal{P}$  with different types of controllers. The reference values  $J = 251.72$  and  $J = 475.06$  are obtained with the (centralized) linear quadratic regulators  $u_k = K^\downarrow_{\text{LQ}} x_k$  and  $v_k = K^\uparrow_{\text{LQ}} x_{s\Delta k}$  for the lower and for the upper control layer, respectively. Implementing just the lower layer controller  $u_k = K^\downarrow x_k$  of the hierarchical two-layer control scheme yields a performance of  $J = 296.62$ . By adding the upper control layer, the performance is improved to  $J = 280.53$ . Considering the additional communication cost  $J^\uparrow_{\text{com}} = 11$ , the combined performance  $J + J^\uparrow_{\text{com}}$  is thus improved from 296.62 to 291.53 by the upper control layer. Regarding the reference values, it can be seen that the performance  $J$  is close to the performance of the centralized linear quadratic regulator  $u_k = K^\downarrow_{\text{LQ}} x_k$ , while clearly outperforming an LQR designed for the upper layer system.

Since  $E = I$ , it follows from Eq. (3.62) that the values of  $J$  stated in Table 3.1 can be alternatively interpreted in the sense of Case 2.2 as follows: Assuming that  $x_0$  follows a standard normal distribution, i.e.  $x_0 \sim \mathcal{N}(0, I)$ , the mentioned performance values correspond to  $E(J)$  for  $J$  according to Case 2.2. For details, the reader is referred to Sec. 3.4.4.

Performing the hierarchical control design lasts about 19 seconds on an Intel Core-i5 3320m with 16 GB of RAM. In contrast, using the design procedure presented in [50] without hierarchies and clustering takes more than 5.5 hours on the same machine, showing the significant savings in computational effort.

### 3.7. Discussion

In this chapter, a hierarchical two-layer feedback control scheme for interconnected linear time-invariant systems was presented. The two-layer control scheme can be implemented in a distributed manner and provides a tradeoff between performance and communication effort. This tradeoff depends on the outcome of an initial structural analysis which is performed prior to the control design, and can additionally be parametrized by the weights of the upper layer communication cost function.

The main advantage of the proposed scheme regarding existing approaches to simultaneous communication topology and control design is that the computational complexity is significantly reduced. This is accomplished by reducing the number of binary decisions which links to incorporate into the communication topology by grouping the subsystems into clusters according to their interconnection strength and structure. A hierarchical two-layer multi-rate control scheme is then employed to deal with strong interconnections on a lower control layer, and to coordinate the hierarchically interconnected groups of controlled subsystems on an upper control layer with lower sampling frequency.

Classical hierarchical feedback control schemes either use the upper control layer to compensate for subsystem interconnections [132], or result from the decomposition of optimal control problems into subproblems and therefore correspond to the centralized linear quadratic regulator [86]. In both cases, full communication is required between all controllers in every time step. In contrast, in the hierarchical control scheme presented in this chapter, both layers are designed to cooperate for minimizing a global performance index, and the upper control layer operates with lower sampling frequency. In particular, due to the multi-rate scheme and the underlying network topology optimization on the upper control layer, full communication between the controllers in any time-step is not required. However, numerical results show that the overall performance is close to the performance of the linear quadratic regulator.

The proposed clustering procedure is an effective means for decomposing the interconnected system into strongly coupled groups of subsystems. However, there are some aspects which may require further investigation. The first aspect is the influence of the parameters  $\epsilon_n$  and  $\epsilon_w$  on the outcome of the hierarchical control design procedure. Since no analytic solution of the overall control design problem is available, the influence can only be characterized in a qualitative manner. In general, increasing  $\epsilon_w$  will lead to a finer decomposition, i.e. more clusters are obtained since an increasing number of interconnections is neglected for finding the strongly connected components. In combination with a small value for  $\epsilon_n$ , it gets harder to synthesize the lower control layer, since many interconnections that have been neglected for the clustering are contained in the lower layer model  $\bar{\mathcal{P}}'$ . On the other hand, a large value of  $\epsilon_n$  typically leads to large deviations of  $\bar{\mathcal{P}}_{cl}^\downarrow$  and  $\bar{\mathcal{P}}_{cl}^\downarrow$  regarding performance and stability, requiring more intense corrective actions from the upper control layer. In summary, the best overall performance can be

expected for small values of  $\epsilon_n$  and  $\epsilon_w$ . A second aspect of the clustering procedure is robustness with respect to parameter uncertainties in the matrices  $A$  and  $B$ . This can be handled by determining worst case interconnection measures, as proposed in the third part of this thesis. Thirdly, one may scrutinize the suitability of the proposed interconnection measure. As argued in the detailed discussion presented in Appendix C, the advantages of the proposed measure are its quick calculation, its applicability to unstable systems, and its superior performance compared to, e.g., system norms based interconnection measures.

From a control theoretic point of view, a further open question is whether the assumption that  $\begin{bmatrix} C & D \end{bmatrix}$  has full column rank can be relaxed. Although the assumption can always be satisfied by perturbing a given pair of matrices  $C$  and  $D$ , the assumptions imposed for the classical LQR Problem are undoubtedly less restrictive. However, relaxing the assumption is likely to result in additional constraints on the lower layer control gain  $\bar{K}^\downarrow$ , which may be necessary to ensure that the optimal control problem associated with the upper control layer has a solution in the case of full communication.



## 4. Asynchronous Hierarchical Control

In the previous chapter, it was shown that the combination of a decentralized lower control layer and a distributed upper control layer acting on a coarser time-scale yields a good and parametrizable balance between control performance versus required communication effort. Additionally, the time required to compute the optimized control law has been drastically reduced compared to related single-layer approaches by grouping the subsystems on the lower layer into clusters.

In the synchronous two-layer control scheme, the distributed upper layer controllers update their control inputs simultaneously at time instants  $k \in \mathbb{N}_0$  with  $k \bmod \Delta k = 0$ . From the point of view of the global communication network  $\mathcal{G}_k$ , this concept leads to periodic peaks in the network load. Clearly, such a load profile is advantageous to keep the frequency of data exchange between the clusters small. However, one can think of situations where it is desirable to avoid high peaks in the number of exchanged messages per time step, and rather distribute the communication load equably over time. It is the aim of this chapter to address this problem by establishing asynchronously operating upper layer controllers  $\mathcal{C}_k^i$ .

The main idea pursued in the sequel is to design distributed upper layer controllers which are updated sequentially in a periodic fashion. This way, the information exchange between the upper layer controllers is equably distributed over time, and the periodic peaks in the network traffic are reduced. It is shown that the synthesis problem for the distributed upper layer controller can be formulated and solved in the framework of periodic systems. As in the previous chapter, the performance of the controlled system is measured by a global performance index  $J$ , and both control layers are designed to cooperate for minimizing this performance measure. Furthermore, a tradeoff between overall performance and communication cost is sought for the upper control layer by employing tools from SCT design.

This chapter is organized as follows. First, the problem setup and the underlying assumptions are stated in Section 4.1. Subsequently, Section 4.2 provides a brief review of the framework of periodic systems, and summarizes some relevant results. Section 4.3 first shows the construction of a periodic model for designing the asynchronous controllers, and then presents a tractable algorithm for the actual control design. Details regarding the implementation of the control algorithm are discussed in Section 4.4. Finally, a numerical example is presented in Section 4.5, and the chapter is concluded in Section 4.6.

## 4.1. Problem Setup

The approach presented in this chapter directly builds on the results of Chapter 3, and presents an alternative approach for the design of an upper control layer. That is, an interconnection of  $N_s$  discrete-time linear time-invariant systems:

$$\mathcal{P}^i : \begin{cases} x_{k+1}^i = A_{i,i}x_k^i + B_{i,i}u_k^i + E_{i,i}w_k^i + \sum_{j \in \mathcal{N}_s^i} A_{i,j}x_k^j + B_{i,j}u_k^j + E_{i,j}w_k^j, \\ z_k^i = C_{i,i}x_k^i + D_{i,i}u_k^i + \sum_{j \in \mathcal{N}_s^i} C_{i,j}x_k^j + D_{i,j}u_k^j, \end{cases} \quad (4.1)$$

is taken as starting point for the asynchronous hierarchical control design. As before,  $x_k^i \in \mathbb{X}^i \subseteq \mathbb{R}^{n_x^i}$  denotes the local state vector,  $u_k^i \in \mathbb{U}^i \subseteq \mathbb{R}^{n_u^i}$  is the local input vector,  $w_k^i \in \mathbb{W}^i \subseteq \mathbb{R}^{n_w^i}$  is a local disturbance vector, and  $z_k^i \in \mathbb{R}^{n_z^i}$  defines a local controlled variable. In contrast to Chapter 3, the assumptions imposed for the global interconnected system  $\mathcal{P}$  are relaxed:

**Assumption 4.1.** *The global interconnected system  $\mathcal{P}$  described by the matrices  $A = [A_{i,j}]$ ,  $B = [B_{i,j}]$ ,  $C = [C_{i,j}]$ , and  $D = [D_{i,j}]$  has the following properties:*

- (a) *The pair  $(A, B)$  is stabilizable.*
- (b) *The matrix  $D$  has full column rank.*
- (c) *The system  $\mathcal{P}$  has no invariant zeros on the unit circle, or equivalently:*

$$\text{rank} \begin{bmatrix} A - \lambda I_{n_x} & B \\ C & D \end{bmatrix} = n_x + n_u \quad \forall \lambda \in \mathbb{C}_1. \quad (4.2)$$

△

For what follows, it is assumed that the clustering procedure of Sec. 3.2 has already been applied to the interconnected system  $\mathcal{P}$ , and that a lower control layer  $\bar{u}_k = \bar{K}^\downarrow \bar{x}_k$  has been designed according to Section 3.3. That is, the overall system is given by the lower layer closed-loop system:

$$\bar{\mathcal{P}}_{\text{cl}}^\downarrow : \begin{cases} \bar{x}_{k+1} = (\bar{A} + \bar{B}\bar{K}^\downarrow)\bar{x}_k + \bar{B}\bar{v}_k + \bar{E}\bar{w}_k = \bar{A}_{\text{cl}}^\downarrow \bar{x}_k + \bar{B}\bar{v}_k + \bar{E}\bar{w}_k, \\ \bar{z}_k = (\bar{C} + \bar{D}\bar{K}^\downarrow)\bar{x}_k + \bar{D}\bar{v}_k = \bar{C}_{\text{cl}}^\downarrow \bar{x}_k + \bar{D}\bar{v}_k, \end{cases} \quad (4.3)$$

where  $\bar{v}_k$  is the external input to be chosen by the upper control layer. Similar to Section 3.4, the goal is to design an upper control layer which takes into account the adverse effects of the interconnections which were neglected for designing the lower control layer. As before, the upper control layer is supposed to operate on a coarser time-scale, such that the upper layer controllers  $\mathcal{C}^{\uparrow i}$  are updated every  $\Delta k$ -th time-step of the lower-layer time-domain  $\mathbb{T}^\downarrow$ . However, the upper control layer

should now operate asynchronously, meaning that the controllers  $\bar{\mathcal{C}}^{\uparrow p}$  are updated periodically in a sequential manner.

Fig. 4.1 shows the difference of synchronous and asynchronous updates of the upper layer controllers from the viewpoint of the lower layer time-domain  $\mathbb{T}^\downarrow$ . For simplicity, it is assumed here that  $\Delta k = 2$ , and that the system consists of two clusters  $\mathcal{C}^1 = \{1\}$  and  $\mathcal{C}^2 = \{2\}$ . Consequently,  $\bar{\mathcal{C}}^{\uparrow 1} = \mathcal{C}^{\uparrow 1}$  and  $\bar{\mathcal{C}}^{\uparrow 2} = \mathcal{C}^{\uparrow 2}$ , i.e. each cluster controller consists of a single subsystem controller on the upper layer. Furthermore, the lower control layer and the physical subsystems are intentionally omitted. In the synchronous scheme shown at the top, both upper layer controllers  $\mathcal{C}^{\uparrow i}$  are updated synchronously at time instants  $k = s\Delta k$ ,  $s \in \mathbb{N}_0$ . Hence, two messages must be transmitted via the communication network at times  $k = s\Delta k$ , while no messages are transmitted at times  $k = s\Delta k + 1$ . In the asynchronous scheme, shown at the bottom, the first controller  $\mathcal{C}^{\uparrow 1}$  is updated at time instants  $k = s\Delta k$ , while the second controller  $\mathcal{C}^{\uparrow 2}$  is updated at time instants  $k = s\Delta k + 1$ . Hence, only one message per time step must be exchanged. In both schemes, the control input is held constant if no update occurs.

Regarding the sequential update of the upper layer controllers  $\bar{\mathcal{C}}^{\uparrow p}$ , the following assumptions are imposed:

**Assumption 4.2.** *For the updates of the upper control layer, the following holds:*

- (a) *Each cluster controller  $\bar{\mathcal{C}}^{\uparrow p}$  is updated separately and exactly once per period.*
- (b) *The length  $N_\varphi$  of a period equals the number of clusters, i.e.  $N_\varphi = N_c$ .  $\Delta$*

As a consequence, each cluster controller  $\bar{\mathcal{C}}^{\uparrow p}$  is updated every  $\Delta k = N_c$  time-steps. Note that the above assumptions are introduced to ease the presentation of the asynchronous hierarchical control scheme, and to enable a reasonable comparison with the synchronous scheme. More general asynchronous timing schemes, like multiple updates of several cluster controllers per period, the update of multiple cluster controllers per time-step, or different period lengths  $N_\varphi \neq N_c$ , can easily be considered in the presented framework.

In the light of Assumption 4.2, the update sequence of the cluster controllers can be encoded by assigning an offset time  $\bar{k}_0^p \in \mathbb{N}_0$  to each cluster such that:

$$\bigcup_{p \in \mathcal{N}_c} \bar{k}_0^p = \{0, 1, \dots, N_c - 1\}. \quad (4.4)$$

The upper layer controllers then take the following general form:

$$\mathcal{C}^{\uparrow i} : v_k^j = \begin{cases} \sum_{j \in \mathcal{C}^{p(i)}} K_{i,j}^{\uparrow} x_k^j + \sum_{q \in \bar{\mathcal{R}}^{\uparrow p(i)}} \sum_{j \in \mathcal{C}^q} K_{i,j}^{\uparrow} x_k^j & \text{if } \exists s \in \mathbb{N}_0 \mid k = \bar{k}_0^p + s\Delta k, \\ v_{k-1}^j & \text{otherwise.} \end{cases} \quad (4.5)$$

Compared with the synchronous scheme, the asynchronous scheme has two main advantages: Firstly, the periodic peak load of the communication network is distributed over time, resulting in lower requirements for the communication network. Secondly, the upper layer can now immediately react to possible disturbances.



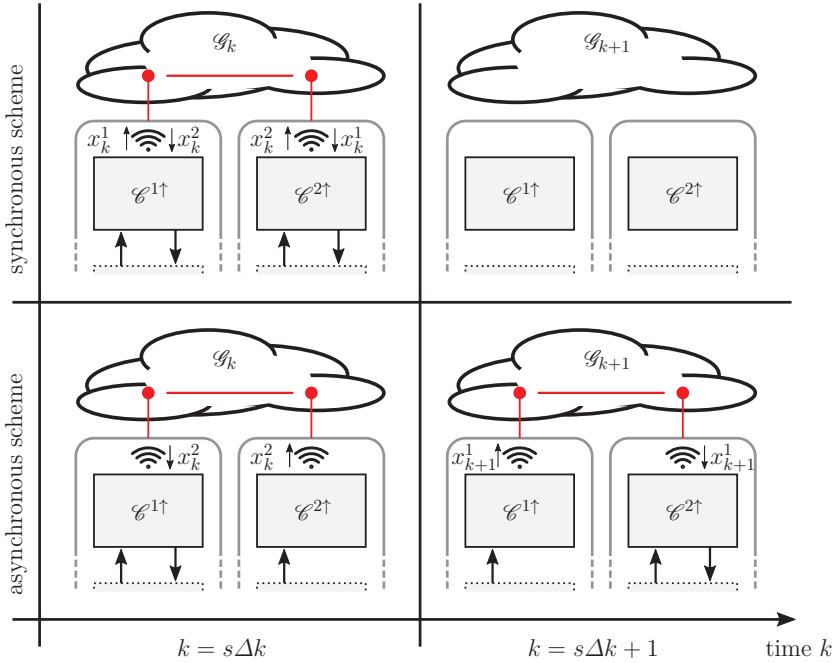


**Figure 4.1.:** Spatio-temporal information flow on the upper control layer in the synchronous scheme (top), and in the asynchronous scheme (bottom) for the exemplary case of  $N_c = \Delta k = 2$  clusters. The lower control layer and the physical subsystems are intentionally omitted.

In the sequel, it will be shown that the framework of periodic systems is well suited for modeling and designing the asynchronous upper layer controllers. Similar to the synchronous scheme, a particular goal is that both control layers should cooperate for minimizing the global performance index  $J$ . Additionally, the concepts of SCT design should be employed for designing the upper control layer.

## 4.2. Fundamentals of Periodic Systems

The purpose of this chapter is twofold: One aim is to introduce the basic notation used in the context of periodic systems. Additionally, a brief overview over the basic properties of this system class is provided. In particular, common stability notions and a generalization of the  $\mathcal{H}_2$ -norm are addressed.

In discrete-time, a periodic system is equivalent to a discrete-time LTI system with periodically time-varying system matrices<sup>1</sup>. The particular time-dependency of the system matrices is typically modeled by an  $N_\varphi$ -periodic switching function:

$$\varphi : \mathbb{N}_0 \rightarrow \mathbb{I}_{N_\varphi}, \quad (4.6)$$

which selects the valid system dynamics at each time-instant  $k \in \mathbb{N}_0$ . Accordingly, the state-space parameters of a periodic system are given by the  $N_\varphi$ -sequences of matrices  $\mathbf{A} \in \mathbb{H}^{N_\varphi}(\mathbb{R}^{n_x \times n_x})$ ,  $\mathbf{B} \in \mathbb{H}^{N_\varphi}(\mathbb{R}^{n_x \times n_u})$ ,  $\mathbf{C} \in \mathbb{H}^{N_\varphi}(\mathbb{R}^{n_z \times n_x})$ ,  $\mathbf{D} \in \mathbb{H}^{N_\varphi}(\mathbb{R}^{n_z \times n_u})$ , and  $\mathbf{E} \in \mathbb{H}^{N_\varphi}(\mathbb{R}^{n_x \times n_w})$ . Recalling that  $\mathbf{A} = (A[1], \dots, A[N_\varphi])$ , a periodic system can now be defined as:

$$\mathcal{P}_\varphi : \begin{cases} x_{k+1} = A[\varphi_k]x_k + B[\varphi_k]u_k + E[\varphi_k]w_k, \\ z_k = C[\varphi_k]x_k + D[\varphi_k]u_k, \end{cases} \quad (4.7)$$

with the established interpretations of the signals  $x_k \in \mathbb{X} \subseteq \mathbb{R}^{n_x}$ ,  $u_k \in \mathbb{U} \subseteq \mathbb{R}^{n_u}$ ,  $w_k \in \mathbb{W} \subseteq \mathbb{R}^{n_w}$ , and  $z_k \in \mathbb{R}^{n_z}$ .

The fundamental properties of periodic systems are well understood, see for instance [20], [21], and [130], among many others. Approaches for controller synthesis consider, e.g., the pure stabilization problem [34], robust analysis and control of linear periodic systems with polytopic uncertainty [11], as well as  $\mathcal{H}_2$ -control [137] and robust variants hereof for periodic systems with polytopic uncertainty [46]. A popular class of controllers used for periodic systems are so-called memory state-feedback controllers. These controllers compute the current control input based on a linear combination of the current state and a fixed number of past states. Approaches to the design of memory controllers for periodic systems consider, e.g., linear dynamics with polytopic uncertainty [41], where an a-priori bound on the  $\mathcal{H}_2$ -norm can be additionally guaranteed [129]. In the domain of networked control systems, periodic systems are used, for instance, for designing decentralized observer-based controllers which communicate via a shared communication network [18].

The *state-transition matrix*  $\Phi_A[\varphi_{k_1}, \varphi_{k_0}] \in \mathbb{R}^{n_x \times n_x}$  and the *monodromy matrix*  $\Psi_A[\varphi_k] \in \mathbb{R}^{n_x \times n_x}$  associated with a periodic system  $\mathcal{P}_\varphi$  are frequently used for the analysis of the inherent properties of these systems. These matrices are defined as follows:

$$\Phi_A[\varphi_{k_1}, \varphi_{k_0}] := \begin{cases} A[\varphi_{k_1-1}] \cdots A[\varphi_{k_0}] & \text{if } k_1 > k_0, \\ I_{n_x} & \text{if } k_1 = k_0, \\ 0_{n_x \times n_x} & \text{if } k_1 < k_0, \end{cases} \quad (4.8)$$

$$\Psi_A[\varphi_k] := A[\varphi_{k+N_\varphi-1}] \cdots A[\varphi_{k+1}]A[\varphi_k] = \Phi_A[\varphi_{k+N_\varphi}, \varphi_k]. \quad (4.9)$$

It is immediate that  $\Psi_A[\varphi_k]$  is an  $N_\varphi$ -periodic matrix. However, the characteristic polynomial of  $\Psi_A[\varphi_k]$ , and therefore its eigenvalues and spectral radius, do not

<sup>1</sup>Since only discrete-time periodic systems are considered in this thesis, these are from now on generally referred to as periodic systems.

depend on the value of the switching function  $\varphi_k$ , and are therefore time-invariant [21, p.82]. This property is of particular importance when it comes to the stability analysis of periodic systems, as will be seen later.

For a more general definition of periodic systems, the dimensions of the vectors  $x_k$ ,  $u_k$ ,  $w_k$ , and  $z_k$  may be considered as periodically time-varying, e.g.  $n_x = n_x[\varphi_k]$ . In this context, the *core spectrum* of the monodromy matrix  $\Psi_A[\varphi_k] \in \mathbb{R}^{n_x[\varphi_k] \times n_x[\varphi_k]}$  is defined as follows:

**Definition 4.1** (cf. [21, Chap. 3]). *Consider the monodromy matrix  $\Psi_A[\varphi_k]$  as defined in Eq. (4.9), and suppose that the dimension of the state vector  $n_x[\varphi_k]$  is periodically time-varying. Denote the minimal dimension of the state vector and the corresponding minimizer by:*

$$n_{x,\min} := \min_{\varphi \in \mathbb{I}_{N_\varphi}} n_x[\varphi], \quad \varphi_{\min} := \arg \min_{\varphi \in \mathbb{I}_{N_\varphi}} n_x[\varphi], \quad (4.10)$$

respectively. Then, the core spectrum of  $\Psi_A[\varphi_k]$  is defined as:

$$\Lambda_{\text{cs}}(\Psi_A) := \Lambda(\Psi_A[\varphi_{\min}]). \quad (4.11)$$

△

For the core spectrum of  $\Psi_A[\varphi_k]$ , the following result holds:

**Lemma 4.1** (cf. [21, Chap. 3]). *For all  $\varphi \in \mathbb{I}_{N_\varphi}$ , the core spectrum  $\Lambda_{\text{cs}}(\Psi_A)$  is a subset of or equal to the set of eigenvalues of the monodromy matrix  $\Psi_A[\varphi_k]$ :*

$$\Lambda_{\text{cs}}(\Psi_A) \subseteq \Lambda(\Psi_A[\varphi]) \quad \forall \varphi \in \mathbb{I}_{N_\varphi}. \quad (4.12)$$

Furthermore, for all  $\varphi \in \mathbb{I}_{N_\varphi} \setminus \{\varphi_{\min}\}$ , the remaining  $n_x[\varphi] - n_{x,\min}$  eigenvalues are located at the origin of the complex plane, such that:

$$\Lambda(\Psi_A[\varphi]) = \Lambda_{\text{cs}}(\Psi_A) \cup \{0, \dots, 0\} \quad \forall \varphi \in \mathbb{I}_{N_\varphi}. \quad (4.13)$$

□

A proof can be found in Chapters 3.1 to 3.3 of [21].

Next, the stability of periodic systems is considered by the help of the previous definitions. First, introduce the periodically time-varying state-feedback:

$$u_k = K[\varphi_k]x_k, \quad (4.14)$$

with  $K[\varphi] \in \mathbb{R}^{n_u[\varphi] \times n_x[\varphi]}$ , and define the closed-loop periodic system:

$$\mathcal{P}_{\varphi,\text{cl}} : \begin{cases} x_{k+1} = (A[\varphi_k] + B[\varphi_k]K[\varphi_k])x_k + E[\varphi_k]w_k = A_{\text{cl}}[\varphi_k]x_k + E[\varphi_k]w_k, \\ z_k = (C[\varphi_k] + D[\varphi_k]K[\varphi_k])x_k = C_{\text{cl}}[\varphi_k]x_k. \end{cases} \quad (4.15)$$

Regarding the stability of the autonomous closed-loop periodic system with  $w_k = 0$  for all  $k \in \mathbb{N}_0$ , the following result holds.

**Theorem 4.1** (cf. [21, Chap. 3]). *For the periodic system  $\mathcal{P}_{\varphi,\text{cl}}$ , let  $w_k = 0$  for all  $k \in \mathbb{N}_0$ . Then, the following statements are equivalent:*

- (a) *The periodic system  $\mathcal{P}_{\varphi,\text{cl}}$  is exponentially stable.*  
 (b) *There exists an  $N_\varphi$ -sequence of positive semi-definite matrices  $V[\varphi] \in \mathbb{S}_{\geq 0}^{n_x[\varphi]}$ , such that:*

$$V[\varphi_l] - (A[\varphi_l])^\top V[\varphi_{l+1}] A[\varphi_l] \succ 0, \quad (4.16)$$

for all  $l \in \{k, k+1, \dots, k+N_\varphi-1\}$ , with  $k \in \mathbb{N}_0$  arbitrary.

- (c) *There exist constants  $\alpha \in \mathbb{R}_{>1}$  and  $\beta \in (0, 1)$  such that:*

$$\|x_k\|_2^2 \leq \alpha \beta^k \|x_0\|_2^2 \quad \forall k \in \mathbb{N}_0, x_0 \in \mathbb{X}. \quad (4.17)$$

- (d) *The core spectrum of the monodromy matrix  $\Psi_A[\cdot]$  is in the open unit disc.*  
 (e) *The point  $x_{\text{eq}} = 0$  is the only globally asymptotically stable equilibrium point for the periodic system  $\mathcal{P}_{\varphi,\text{cl}}$ .  $\square$*

Equivalence of (a), (b), and (d) follows from [21, p.91] and Proposition 3.5 in [21, p.99]. Additionally, exponential stability of  $x_k$  as stated in (a) is equivalent to the existence of an exponentially decaying upper bound as given in (c), see for instance [40, p.359]. Equivalence of (e) and (c) can be deduced by the help of Theorem 2.1.

In the case that  $w_k \in \mathbb{W}$  is arbitrary, a notion of bounded-input/bounded-output (BIBO) stability can be established for periodic systems similar to Definition 2.8. The following result holds:

**Theorem 4.2.** *The periodic system  $\mathcal{P}_{\varphi,\text{cl}}$  with input  $w_k \in \mathbb{W}$  is BIBO stable if any of the statements in Theorem 4.1 holds. The converse does not generally hold.  $\square$*

The above result follows from [21, Chap. 5.5].

Finally, the  $\mathcal{H}_2$ -norm can be generalized to periodic systems as follows.

**Definition 4.2** (cf. [137]). *Let  $\mathbf{z}_{k,l} \in \mathbb{R}^{n_z[\varphi_k] \times n_w[\varphi_k]}$  denote the impulse response matrix of the periodic system  $\mathcal{P}_{\varphi,\text{cl}}$  at time  $k$ , with the unit pulse applied to the disturbance input  $w$  being shifted by  $l$  time-steps to the right. That is, the  $(i, j)$ -th entry of  $\mathbf{z}_{k,l}$  is given by the  $i$ -th component of  $z_k \in \mathbb{R}^{n_z[\varphi_k]}$  for  $w_l = e_j$ ,  $w_k = 0 \forall k \in \mathbb{N}_0 \setminus \{l\}$ , and  $x_0 = 0$ . Then, the generalized  $\mathcal{H}_2$ -norm of  $\mathcal{P}_{\varphi,\text{cl}}$  is defined as<sup>2</sup>:*

$$\|\mathcal{P}_{\varphi,\text{cl}}\|_{\mathcal{H}_2} := \sqrt{\frac{1}{N_\varphi} \sum_{l=0}^{N_\varphi-1} \sum_{k=0}^{\infty} \text{tr}(\mathbf{z}_{k,l}^\top \mathbf{z}_{k,l})}. \quad (4.18)$$

$\triangle$

<sup>2</sup> In literature, the generalized  $\mathcal{H}_2$ -norm for periodic systems is sometimes defined without the factor  $1/N_\varphi$ , see for instance [21, p.242]. However, the results presented in this thesis generally assume the definition stated in Eq. (4.18).

Similar to LTI Systems and to jump Markov linear systems, the  $\mathcal{H}_2$ -norm of  $\mathcal{P}_{\varphi,\text{cl}}$  is related to the performance index  $J$  as follows.

**Lemma 4.2.** *Consider a stable periodic system  $\mathcal{P}_{\varphi,\text{cl}}$  under the conditions described in Case 2.1 (see page 27). Then, the squared  $\mathcal{H}_2$ -norm and the performance index  $J$  as defined in Eq. 2.20 are equal:*

$$\|\mathcal{P}_{\varphi,\text{cl}}\|_{\mathcal{H}_2}^2 = \lim_{k_e \rightarrow \infty} \mathbb{E} \left( \frac{1}{k_e} \sum_{k=0}^{k_e-1} z_k^\top z_k \right). \quad (4.19)$$

□

A proof can be found in [21, p.243f].

**Lemma 4.3.** *Consider a stable periodic system  $\mathcal{P}_{\varphi,\text{cl}}$  under the conditions described in Case 2.2 (see page 28), and set:*

$$E[\varphi_{N_\varphi-1}] := \sqrt{N_\varphi} x_0 \in \mathbb{R}^{n_x[\varphi_0]}, \quad E[\varphi_l] := 0_{n_x[\varphi_{l+1}] \times 1} \quad \forall l \in \{0, \dots, N_\varphi - 2\}. \quad (4.20)$$

Then, the squared  $\mathcal{H}_2$ -norm and the performance index  $J$  as defined in Eq. 2.23 are equal:

$$\|\mathcal{P}_{\varphi,\text{cl}}\|_{\mathcal{H}_2}^2 = \sum_{k=0}^{\infty} z_k^\top z_k. \quad (4.21)$$

□

The proof can be found in Appendix D.1 on page 177.

## 4.3. Upper Layer Control Design

In this section, it is shown how the design problem for the cooperative asynchronous upper layer controller can be formulated and solved in the framework of periodic systems.

### 4.3.1. Modeling as Periodic System

The basic idea for designing asynchronous upper layer controllers is to model the closed-loop lower layer system  $\mathcal{P}_{\text{cl}}^\downarrow$  from the egocentric viewpoint of the  $\varphi$ -th cluster  $\mathcal{C}^\varphi$  at time-instant  $k \in \mathbb{N}_0$ . A periodic sequence of these egocentric models, comprising the periodic system  $\mathcal{P}_{\varphi}^\uparrow$ , is well-suited to represent the desired situation of local controllers being updated sequentially. The current modeling viewpoint is selected by the  $N_c$ -periodic switching function:

$$\varphi_k : \mathbb{T}^\downarrow \rightarrow \mathbb{I}_{N_c}, \quad \varphi_{k+N_c} = \varphi_k \quad \forall k \in \mathbb{N}_0, \quad (4.22)$$

determined by the choice of the variables  $\bar{k}_0^p$  from Eq. (4.4). Due to the  $N_c$ -periodicity, the switching sequence is uniquely defined by  $\varphi_0$  and by the ordered set:

$$\bar{\Phi} := \{\varphi_{k+N_c}, \dots, \varphi_{k+2}, \varphi_{k+1}\}, \quad (4.23)$$

for some  $k \in \mathbb{N}_0$ .

The input signal of each cluster controller  $\bar{\mathcal{C}}^p$  is to be held constant for  $\Delta k = N_c$  time-steps. Hence, the local control inputs  $\bar{v}_k^q$  of the  $N_c - 1$  cluster controllers  $\bar{\mathcal{C}}^q$ ,  $q \in \mathcal{N}_c \setminus \{\varphi_k\}$  which are not updated at time instant  $k$  have to be available in each egocentric model to fully specify the behavior of the overall system. Consequently, the mentioned control inputs have to become part of the extended state vector  $\bar{x}_k^\uparrow$  of the periodic system:

$$\bar{\mathcal{P}}_\varphi^\uparrow : \begin{cases} \bar{x}_{k+1}^\uparrow = \bar{A}^\uparrow[\varphi_k] \bar{x}_k^\uparrow + \bar{B}^\uparrow[\varphi_k] \bar{v}_k^\uparrow + \bar{E}^\uparrow[\varphi_k] \bar{w}_k, \\ \bar{z}_k = \bar{C}^\uparrow[\varphi_k] \bar{x}_k^\uparrow + \bar{D}^\uparrow[\varphi_k] \bar{v}_k^\uparrow. \end{cases} \quad (4.24)$$

In the sequel, it will be explained in detail how the vectors and matrices of  $\bar{\mathcal{P}}_\varphi^\uparrow$  are constructed from the variables describing  $\bar{\mathcal{P}}_{cl}^\downarrow$ . Since the purpose of  $\bar{\mathcal{P}}_\varphi^\uparrow$  is to model the controlled lower layer system  $\bar{\mathcal{P}}_{cl}^\downarrow$  from the viewpoint of the  $\varphi$ -th cluster, its input signal is selected to be the input signal associated with cluster  $\varphi$ , i.e.:

$$\bar{v}_k^\uparrow := \bar{v}_k^{\varphi_k}. \quad (4.25)$$

The periodically time-varying dimension of the signal  $\bar{v}_k^\uparrow$  is denoted by  $\bar{n}_v^\uparrow[\varphi_k] := \bar{n}_v^{\varphi_k}$ . For what follows, it will be convenient to define the ordered sets:

$$\bar{\Phi}'[\varphi_k] := \{\varphi_{k-1}, \varphi_{k-2}, \dots, \varphi_{k-N_c+1}\}, \quad (4.26)$$

$$\bar{\Phi}''[\varphi_k] := \{\varphi_{k-1}, \varphi_{k-2}, \dots, \varphi_{k-N_c+2}\}, \quad (4.27)$$

corresponding to the  $(N_c - 1)$  and  $(N_c - 2)$  previously updated clusters with respect to  $\varphi_k$ , respectively. In this context, consider the cumulated input dimensions:

$$\bar{n}_v^{\uparrow'}[\varphi_k] := \sum_{\varphi \in \bar{\Phi}'[\varphi_k]} \bar{n}_v^\uparrow[\varphi], \quad \bar{n}_v^{\uparrow''}[\varphi_k] := \sum_{\varphi \in \bar{\Phi}''[\varphi_k]} \bar{n}_v^\uparrow[\varphi]. \quad (4.28)$$

In general, it may apply that  $\bar{n}_x^\uparrow[\varphi_{k_1}] \neq \bar{n}_x^\uparrow[\varphi_{k_2}]$  for some  $\varphi_{k_1} \neq \varphi_{k_2}$ . In turn, this means that the extended state vector:

$$\bar{x}_k^\uparrow := (\bar{x}_k; \bar{v}_{k-1}^\uparrow; \dots; \bar{v}_{k-N_c+1}^\uparrow) \quad (4.29)$$

has time-varying dimension  $\bar{n}_x^\uparrow[\varphi_k] = \bar{n}_x + \bar{n}_v^{\uparrow'}[\varphi_k]$ .

The extended state vector  $\bar{x}_k^\uparrow$  consists of  $N_x^\uparrow := 2N_c - 1$  component vectors that can be associated with the  $N_c$  clusters. The assignment of these components will play a key-role when it comes to designing controllers that are structurally compatible

with  $\bar{\mathcal{P}}_\varphi^\uparrow$ , as will be explained later. In the sequel, the components  $\bar{v}_{k-l}^\uparrow$  of  $\bar{x}_k^\uparrow$  are referred to as *memory states*. At time  $k$ , they comprise the virtual quantity:

$$\bar{v}_k^{\uparrow'} := (\bar{v}_{k-1}^\uparrow; \dots; \bar{v}_{k-N_c+1}^\uparrow). \quad (4.30)$$

It is worth noting that  $\bar{v}_0^{\uparrow'}$  provides an additional degree of freedom when it comes to the initialization of the asynchronous control scheme. While the component  $\bar{x}_0$  of  $\bar{x}_0^\uparrow$  is uniquely determined by the initial state of the interconnected system  $\mathcal{P}$ , the component  $\bar{v}_k^{\uparrow'}$  is not. This point will be discussed in more detail in Sec. 4.4.

Before stating the system matrices of  $\bar{\mathcal{P}}_\varphi^\uparrow$ , a compact colon notation for addressing full block-rows or full block-columns of a partitioned matrix  $A = [A_{i,j}]$  is introduced. Let  $A$  be comprised of  $N$ -by- $N$  block-matrices. Then, for some  $l \in \mathbb{I}_N$ , define:

$$A_{l,:} := [A_{i,j}]_{i=l, j \in \mathbb{I}_N} = [A_{l,1} \quad A_{l,2} \quad \dots \quad A_{l,N}], \quad A_{:,l} := [A_{i,j}]_{i \in \mathbb{I}_N, j=l}. \quad (4.31)$$

Furthermore, for an ordered set  $\mathcal{C} \subseteq \mathbb{I}_N$ , define:

$$A_{\mathcal{C},:} := [A_{i,j}]_{i \in \mathcal{C}, j \in \mathbb{I}_N}, \quad A_{:, \mathcal{C}} := [A_{i,j}]_{i \in \mathbb{I}_N, j \in \mathcal{C}}. \quad (4.32)$$

With the above notation, for  $\bar{x}_k^\uparrow$  as defined in (4.29), the system and input matrix of  $\bar{\mathcal{P}}_\varphi^\uparrow$  are given by:

$$\bar{A}^\uparrow[\varphi_k] := \begin{bmatrix} \bar{A}_{\text{cl}}^\downarrow & \bar{B}_{:, \Phi'[\varphi_k]} \\ 0 & \bar{H}_A[\varphi_k] \end{bmatrix} \in \mathbb{R}^{\bar{n}_s^\uparrow[\varphi_{k+1}] \times \bar{n}_s^\uparrow[\varphi_k]}, \quad (4.33)$$

$$\bar{B}^\uparrow[\varphi_k] := \begin{bmatrix} \bar{B}_{:, \varphi_k} \\ \bar{H}_B[\varphi_k] \end{bmatrix} \in \mathbb{R}^{\bar{n}_s^\uparrow[\varphi_{k+1}] \times \bar{n}_v^\uparrow[\varphi_k]}, \quad (4.34)$$

respectively. The auxiliary matrices  $\bar{H}_A[\varphi_k]$  and  $\bar{H}_B[\varphi_k]$  are defined as:

$$\bar{H}_A[\varphi_k] := \begin{bmatrix} 0 & 0 \\ I_{\bar{n}_v^{\uparrow'}[\varphi_k]} & 0 \end{bmatrix} \in \mathbb{B}^{\bar{n}_v^{\uparrow'}[\varphi_{k+1}] \times \bar{n}_v^{\uparrow'}[\varphi_k]}, \quad (4.35a)$$

$$\bar{H}_B[\varphi_k] := \begin{bmatrix} I_{\bar{n}_v^\uparrow[\varphi_k]} \\ 0 \end{bmatrix} \in \mathbb{B}^{\bar{n}_v^\uparrow[\varphi_{k+1}] \times \bar{n}_v^\uparrow[\varphi_k]}. \quad (4.35b)$$

The pair  $(\bar{A}^\uparrow[\varphi_k], \bar{B}^\uparrow[\varphi_k])$  is constructed such that at time  $k$ , only the updated control input of the  $\varphi_k$ -th cluster controller  $\mathcal{C}^{\varphi_k}$  is applied to the plant. At the same time, a copy of the updated control input  $\bar{v}_k^\uparrow$  is stored in the corresponding memory state. The remaining memory states  $\bar{v}_{k-1}^\uparrow$  to  $\bar{v}_{k-N_c+1}^\uparrow$  contain the control inputs of the  $(N_c - 1)$  cluster controllers which are not updated. The influence of these control inputs on the plant is considered by the upper right block of the system matrix  $\bar{A}^\uparrow[\cdot]$ , which consists of the respective columns of the input matrix  $\bar{B}$ . The matrix  $\bar{H}_A[\varphi_k]$  causes the memory states to be shifted downwards by one position in the extended state vector  $\bar{x}_k^\uparrow$ .

The influence of the disturbance input  $\bar{w}_k$  on the state equation is described by:

$$\bar{E}^\uparrow[\varphi_k] := \begin{bmatrix} \bar{E} \\ 0_{\bar{n}_w^\uparrow[\varphi_{k+1}] \times \bar{n}_w} \end{bmatrix} \in \mathbb{R}^{\bar{n}_x^\uparrow[\varphi_{k+1}] \times \bar{n}_w}, \quad (4.36)$$

such that  $w_k$  has no direct influence on the memory states.

Finally, the equivalent description of the controlled variable  $\bar{z}_k$  in terms of the state and input of the periodic system  $\bar{\mathcal{P}}_\varphi^\uparrow$  is parametrized by:

$$\bar{C}^\uparrow[\varphi_k] := [\bar{C}_{cl}^\downarrow \quad \bar{D}_{:, \Phi^\uparrow[\varphi_k]}], \quad \bar{D}^\uparrow[\varphi_k] := \bar{D}_{:, \varphi_k}, \quad (4.37)$$

which directly follows from the considerations made so far.

Recall that for the original interconnected system (4.1), Assumption 4.1 guarantees that a unique centralized stabilizing state-feedback exists which minimizes the performance index  $J$ . The following result states that this important property is always preserved when constructing the periodic system  $\bar{\mathcal{P}}_\varphi^\uparrow$ .

**Lemma 4.4.** *Suppose that Assumption 4.1 holds. Then, the periodic system  $\bar{\mathcal{P}}_\varphi^\uparrow$  as defined in (4.24) has the following properties:*

- (a) *The periodic system  $\bar{\mathcal{P}}_\varphi^\uparrow$  is stabilizable.*
- (b) *The matrix  $\bar{D}^\uparrow[\varphi]$  has full column rank for all  $\varphi \in \mathcal{N}_c$ .*
- (c) *The periodic system  $\bar{\mathcal{P}}_\varphi^\uparrow$  does not have invariant zeros on the unit circle.*

*Properties (a) to (c) ensure the existence of a unique stabilizing  $N_c$ -periodic state-feedback control law  $\bar{v}_k^\uparrow = \bar{K}^\uparrow[\varphi_k] \bar{x}_k^\uparrow$  for  $\bar{\mathcal{P}}_\varphi^\uparrow$ , which minimizes the performance index  $J$  (see [21, Prop. 13.8]).*  $\square$

The proof of Lemma 4.4 can be found in Appendix D.2.

Summed up, the periodic system  $\bar{\mathcal{P}}_\varphi^\uparrow$  is an equivalent description of the controlled lower layer system  $\bar{\mathcal{P}}_{cl}^\downarrow$ , with the asynchronous operation of the upper layer controllers with sampling time  $\Delta k = N_c$  being already incorporated into the model. In particular, the modeling viewpoint changes periodically according to the switching function  $\varphi_k$ . This function determines which cluster controller  $\mathcal{C}^{\uparrow\varphi_k}$  is being updated at time  $k$ .

### 4.3.2. Distributed Control Design

The next step is to design an appropriate controller for  $\bar{\mathcal{P}}_\varphi^\uparrow$ . Since the goal is to design a distributed state-feedback control law for each cluster  $\varphi \in \mathcal{N}_c$ , the sought control law must have the form:

$$\bar{v}_k^\uparrow = \bar{K}^\uparrow[\varphi_k] \bar{x}_k^\uparrow = \sum_{q=1}^{N_c} \bar{K}_{1,q}^\uparrow[\varphi_k] \bar{x}_k^q + \sum_{l=1}^{N_c-1} \bar{K}_{1, N_c+l}^\uparrow[\varphi_k] \bar{v}_k^{\varphi_{k-l}}. \quad (4.38)$$



Here,  $[\bar{K}_{1,p}[\varphi_k]] = \bar{K}[\varphi_k] \in \mathbb{R}^{\bar{n}_x^\dagger[\varphi_k] \times \bar{n}_s^\dagger[\varphi_k]}$  is a periodic gain-matrix, determining the input for cluster  $\varphi_k$  as a function of the cluster states  $\bar{x}_k^p$  and the memory states  $\bar{v}_k^q$ ,  $\varphi \in \mathcal{P}[\varphi_k]$  at time  $k$ .

The structure of the feedback control law (4.38) reveals another particularity of the asynchronous scheme: compared with the synchronous scheme, the upper layer controllers  $\mathcal{C}^p$  may not only access the state information  $\bar{x}_k^q$  measured and transmitted by other controllers  $\mathcal{C}^q$ , but may also access their current control inputs  $\bar{v}_k^q$ . These  $(N_c - 1)$  additional sources of information can be modeled as additional nodes in the upper layer communication graph  $\mathcal{G}^\dagger$ , which can only send but not receive information. Thus, the corresponding rectangular adjacency matrix  $\bar{\Sigma}^\dagger = [\bar{\sigma}_{p,q}^\dagger]$  is of dimension  $N_c \times N_x^\dagger$ . For  $q \leq N_c$ , similar to the synchronous scheme,  $\bar{\sigma}_{p,q}^\dagger \in \mathbb{B}$  encodes if controller  $\mathcal{C}^p$  has access to the state  $\bar{x}_k^q$  measured by controller  $\mathcal{C}^q$ . Likewise, for  $q > N_c$ , and with  $p = \varphi_k$ ,  $\bar{\sigma}_{p,q}^\dagger$  encodes if  $\bar{v}_k^{\varphi_k - q + N_c}$  is accessible by  $\mathcal{C}^p$  or not.

In order to keep the network structure consistent, the variables  $\bar{\sigma}_{p,q}^\dagger$  with  $q > N_c$  corresponding to the memory states can be handled in two different ways. The first way is to grant  $\mathcal{C}^p$  access to the memory state of  $\mathcal{C}^q$  if and only if it has access to the state vector of  $\mathcal{C}^q$ . This leads to the constraint:

$$\bar{\sigma}_{p,q}^\dagger = \bar{\sigma}_{\varphi_k, \varphi_k - q + N_c}^\dagger \quad \forall \varphi_k \in \mathcal{N}_c, q \in \{N_c + 1, \dots, N_x^\dagger\}. \quad (4.39)$$

A second variant is to prohibit the exchange of the memory states in general:

$$\bar{\sigma}_{p,q}^\dagger = 0 \quad \forall p \in \mathcal{N}_c, q \in \{N_c + 1, \dots, N_x^\dagger\}. \quad (4.40)$$

In both cases, the matrix  $\bar{\Sigma}^\dagger$  has  $((N_c)^2 - N_c)$  degrees of freedom, as in the synchronous scheme. The corresponding set  $\bar{\Sigma}^\dagger$  of admissible communication topologies can be formed in a similar manner by using the above relations. In general, using (4.39) will result in a better closed-loop performance than using (4.40), what is due to the additional information that is being exchanged. However, there exists a class of network topologies for which both approaches yield the same performance. Characterizing these topologies by the content of an exchanged message leads to the following corollary:

**Corollary 4.1.** *Let  $\mathcal{G}^\dagger = (\mathcal{N}_c, \mathcal{E}^\dagger)$  describe an upper-layer communication graph, and denote by  $\mathcal{P}_{p,q}^\dagger$  the set of all paths in  $\mathcal{G}^\dagger$  from node  $q \in \mathcal{N}_c$  to node  $p \in \mathcal{N}_c \setminus \{q\}$ . Assume that for all  $\mathcal{P}_{p,q}^\dagger \neq \emptyset$ , there exists a path in  $\mathcal{P}_{p,q}^\dagger$  with length one. Then, the exchange of the memory states via  $\mathcal{G}^\dagger$  does not provide additional information compared to the information contained in the exchanged state vectors.  $\square$*

The result directly follows from analyzing the graph  $\mathcal{G}^\dagger$  with respect to the information contained in the memory states according to the upper-layer control law (4.38). Whenever (4.39) and (4.40) yield the same global performance, (4.40) should be the first choice, since the size of the transmitted messages is smaller than by using (4.39).

Periodic state-feedback control laws for periodic systems, which are optimized with respect to a quadratic performance index, are typically obtained by the help of periodic Riccati equations [21] or semidefinite programs (SDP) [46] [137]. Since the control law should respect the constraints imposed by the communication graph  $\mathcal{G}^\dagger$ , an SDP-formulation is used in the sequel. This allows to adopt the sufficient conditions for imposing the desired controller structure developed in [50]. In the sequel, the closed-loop system resulting from  $\tilde{\mathcal{P}}_\varphi^\dagger$  with the periodic state-feedback control law (4.38) is denoted by:

$$\tilde{\mathcal{P}}_{\varphi,\text{cl}}^\dagger : \begin{cases} \bar{x}_{k+1} = (\bar{A}^\dagger[\varphi_k] + \bar{B}^\dagger[\varphi_k]\bar{K}^\dagger[\varphi_k])\bar{x}_k^\dagger + \bar{E}^\dagger[\varphi_k] = \bar{A}_{\text{cl}}^\dagger[\varphi_k]\bar{x}_k^\dagger + \bar{E}^\dagger[\varphi_k]\bar{w}_k, \\ \bar{z}_k = \bar{C}^\dagger[\varphi_k] + \bar{D}^\dagger[\varphi_k]\bar{K}^\dagger[\varphi_k] = \bar{C}_{\text{cl}}^\dagger[\varphi_k]\bar{x}_k^\dagger. \end{cases} \quad (4.41)$$

A periodic control gain matrix  $\bar{K}^\dagger[\varphi_k]$  with the desired specifications can be determined by the help of the following theorem.

**Theorem 4.3.** *Suppose that the matrices  $\mathfrak{Z}[\varphi_l] \in \mathbb{S}_{>0}^{\bar{n}_x}$ ,  $\mathfrak{X}[\varphi_l] \in \mathbb{S}_{>0}^{\bar{n}_x^\dagger[\varphi_l]}$ ,  $\mathfrak{G}[\varphi_l] \in \mathbb{R}^{\bar{n}_x^\dagger[\varphi_l] \times \bar{n}_x^\dagger[\varphi_l]}$ ,  $\mathfrak{L}[\varphi_l] \in \mathbb{R}^{\bar{n}_x^\dagger[\varphi_l] \times \bar{n}_x^\dagger[\varphi_l]}$ , and  $\bar{\Sigma}^\dagger \in \mathbb{B}^{N_c \times N_c^\dagger}$  with  $l \in \mathcal{N}_c$  are a solution of the optimization problem:*

$$\min_{\mathfrak{Z}[\varphi_l], \mathfrak{X}[\varphi_l], \mathfrak{G}[\varphi_l], \mathfrak{L}[\varphi_l], \bar{\Sigma}^\dagger} \frac{1}{N_c} \sum_{l=1}^{N_c} \text{tr}(\mathfrak{Z}[\varphi_l]) + J^{\text{com}} \quad \text{subject to:} \quad (4.42\text{a})$$

$$\begin{bmatrix} \mathfrak{G}[\varphi_l] + (\mathfrak{G}[\varphi_l])^\top - \mathfrak{X}[\varphi_l] & \star & \star \\ \bar{A}^\dagger[\varphi_l]\mathfrak{G}[\varphi_l] + \bar{B}^\dagger[\varphi_l]\mathfrak{L}[\varphi_l] & \mathfrak{X}[\varphi_{l+1}] & \star \\ \bar{C}^\dagger[\varphi_l]\mathfrak{G}[\varphi_l] + \bar{D}^\dagger[\varphi_l]\mathfrak{L}[\varphi_l] & 0 & I \end{bmatrix} \succ 0 \quad \forall l, \quad (4.42\text{b})$$

$$\begin{bmatrix} \mathfrak{Z}[\varphi_l] & \star \\ \bar{E}^\dagger[\varphi_l] & \mathfrak{X}[\varphi_{l+1}] \end{bmatrix} \succ 0 \quad \forall l, \quad (4.42\text{c})$$

$$\mathfrak{Z}[\varphi_l] = (\mathfrak{Z}[\varphi_l])^\top \quad \forall l, \quad (4.42\text{d})$$

$$\mathfrak{X}[\varphi_l] = (\mathfrak{X}[\varphi_l])^\top \succ 0 \quad \forall l, \quad (4.42\text{e})$$

$$-M\bar{\sigma}_{\varphi_l,q}^\dagger \leq \mathfrak{L}_{1,q}[\varphi_l] \leq M\bar{\sigma}_{\varphi_l,q}^\dagger \quad \forall l, q, \quad (4.42\text{f})$$

$$-M\bar{\sigma}_{\varphi_l,q}^\dagger \leq \mathfrak{G}_{\varphi_l,q}[\varphi_l] \leq M\bar{\sigma}_{\varphi_l,q}^\dagger \quad \forall l, q, \quad (4.42\text{g})$$

$$-M(\bar{\sigma}_{\varphi_l,q}^\dagger - \bar{\sigma}_{\varphi_l,p}^\dagger + 1) \leq \mathfrak{G}_{p,q}[\varphi_l] \leq M(\bar{\sigma}_{\varphi_l,q}^\dagger - \bar{\sigma}_{\varphi_l,p}^\dagger + 1) \quad \forall l, p, q, \quad (4.42\text{h})$$

$$\bar{\Sigma}^\dagger \in \bar{\Sigma}^\dagger, \quad (4.42\text{i})$$

Eq. (4.39) or Eq. (4.40),

where  $p \in \mathcal{N}_c$ ,  $q \in \mathbb{I}_{N_c^\dagger}$ , and  $M \in \mathbb{R}_{>0}^{\star \times \star}$  denotes a matrix of suitable dimensions with entries  $M_{i,j} > \max\{\|\mathfrak{G}\|_{1,\infty}, \|\mathfrak{L}\|_{1,\infty}\}$ . Let  $\bar{K}^\dagger[\varphi_k] := \mathfrak{L}[\varphi_k](\mathfrak{G}[\varphi_k])^{-1}$ . Then, the following assertions hold:

(a) The periodic system  $\tilde{\mathcal{P}}_{\varphi,\text{cl}}^\dagger$  with  $\bar{w}_k = 0$  for all  $k \in \mathbb{N}_0$  is exponentially stable.

(b) The periodic system  $\bar{\mathcal{P}}_{\varphi, \text{cl}}^\dagger$  with input  $\bar{w}_k$  is BIBO stable.

(c) For  $J$  as defined in Case 2.1, the value of  $J + J^{\uparrow \text{com}}$  is upper-bounded by the objective function (4.42a).

(d) For  $J$  as defined in Case 2.2, and by setting:

$$\bar{E}^\dagger[\varphi_{N_c-1}] = \begin{bmatrix} \bar{x}_0 \\ \bar{v}_0^\dagger \end{bmatrix}, \quad \bar{E}^\dagger[\varphi] = 0_{\bar{n}_x^\dagger[\varphi] \times 1} \quad \forall \varphi \in \mathcal{N}_c \setminus \{\varphi_{N_c-1}\}, \quad (4.43)$$

the value of  $J + J^{\uparrow \text{com}}$  is upper-bounded by the objective function (4.42a).

(e) The periodic control law  $\bar{v}_k^\dagger = \bar{K}^\dagger[\varphi_k] \bar{x}_k^\dagger$  respects the communication topology specified by  $\Sigma^\dagger$ .  $\square$

*Proof.* Assume that (4.42b) and (4.42e) are feasible, which implies that:

$$\mathfrak{G}[\varphi] + (\mathfrak{G}[\varphi])^\top \succ \mathfrak{X}[\varphi] \succ 0 \quad \forall \varphi \in \mathcal{N}_c, \quad (4.44)$$

such that any feasible matrix  $\mathfrak{G}[\varphi]$  must be non-singular. Using:

$$\mathfrak{G}[\varphi] + (\mathfrak{G}[\varphi])^\top - \mathfrak{X}[\varphi] \preceq (\mathfrak{G}[\varphi])^\top (\mathfrak{X}[\varphi])^{-1} \mathfrak{G}[\varphi], \quad (4.45)$$

e.g. from [33], and setting  $\mathfrak{L}[\varphi] = \bar{K}^\dagger[\varphi] \mathfrak{G}[\varphi]$ , Eq. (4.42b) implies that:

$$\begin{bmatrix} (\mathfrak{G}[\varphi_l])^\top (\mathfrak{X}[\varphi_l])^{-1} \mathfrak{G}[\varphi_l] & \star & \star \\ \bar{A}^\dagger[\varphi_l] \mathfrak{G}[\varphi_l] + \bar{B}^\dagger[\varphi_l] \bar{K}^\dagger[\varphi_l] \mathfrak{G}[\varphi_l] & \mathfrak{X}[\varphi_{l+1}] & \star \\ \bar{C}^\dagger[\varphi_l] \mathfrak{G}[\varphi_l] + \bar{D}^\dagger[\varphi_l] \bar{K}^\dagger[\varphi_l] \mathfrak{G}[\varphi_l] & 0 & I \end{bmatrix} \succ 0. \quad (4.46)$$

Factoring out the regular transformation matrix  $T[\varphi] = \text{blkdiag}(\mathfrak{G}[\varphi], I, I)$  on the right-hand side and its transpose  $T[\varphi]^\top$  on the left-hand side, the above inequality is equivalent to:

$$\begin{bmatrix} (\mathfrak{X}[\varphi_l])^{-1} & \star & \star \\ \bar{A}^\dagger[\varphi_l] + \bar{B}^\dagger[\varphi_l] \bar{K}^\dagger[\varphi_l] & \mathfrak{X}[\varphi_{l+1}] & \star \\ \bar{C}^\dagger[\varphi_l] + \bar{D}^\dagger[\varphi_l] \bar{K}^\dagger[\varphi_l] & 0 & I \end{bmatrix} \succ 0. \quad (4.47)$$

Using the definitions  $\check{V}_{\text{cl}}^\dagger[\varphi] := (\mathfrak{X}[\varphi])^{-1}$  as well as  $\bar{A}_{\text{cl}}^\dagger[\varphi]$  and  $\bar{C}_{\text{cl}}^\dagger[\varphi]$  as defined in (4.41), and applying the Schur-complement (Lemma 2.5) leads to:

$$\check{V}_{\text{cl}}^\dagger[\varphi_l] - (\bar{A}_{\text{cl}}^\dagger[\varphi_l])^\top \check{V}_{\text{cl}}^\dagger[\varphi_{l+1}] \bar{A}_{\text{cl}}^\dagger[\varphi_l] - (\bar{C}_{\text{cl}}^\dagger[\varphi_l])^\top \check{V}_{\text{cl}}^\dagger[\varphi_l] \succ 0. \quad (4.48)$$

With  $(\bar{C}_{\text{cl}}^\dagger[\varphi])^\top \check{V}_{\text{cl}}^\dagger[\varphi] \succeq 0$  and  $\check{V}_{\text{cl}}^\dagger[\varphi] \succ 0$  for all  $\varphi \in \mathcal{N}_c$  due to constraint (4.42e), exponential stability of  $\bar{\mathcal{P}}_{\varphi, \text{cl}}^\dagger$  follows from Theorem 4.1. Hence, assertion (a) holds, and assertion (b) directly follows from Theorem 4.2.

Denote by  $\bar{\Phi}_{A,\text{cl}}^\dagger[\varphi_{k_1}, \varphi_{k_0}] \in \mathbb{R}^{\bar{n}_s^\dagger[\varphi_{k_1}] \times \bar{n}_s^\dagger[\varphi_{k_0}]}$  the state-transition matrix of the closed-loop system  $\bar{\mathcal{P}}_{\varphi,\text{cl}}^\dagger$ , and consider (4.48) for  $l = k + 1$ . Multiplying by  $\bar{A}_{\text{cl}}^\dagger[\varphi_k]$  from the right-hand side and by its transpose from the left-hand side leads to:

$$(\bullet)^\top (\check{V}_{\text{cl}}^\dagger[\varphi_{k+1}]) (\bar{A}_{\text{cl}}^\dagger[\varphi_k]) \succ (\bullet)^\top (\check{V}_{\text{cl}}^\dagger[\varphi_{k+2}]) (\bar{\Phi}_{A,\text{cl}}^\dagger[\varphi_{k+2}, \varphi_k]) + (\bullet)^\top (\bar{C}_{\text{cl}}^\dagger[\varphi_{k+1}] \bar{A}_{\text{cl}}^\dagger[\varphi_k]), \quad (4.49)$$

where the abbreviations  $(\bullet)^\top(BA) := A^\top B^\top BA$  and  $(\bullet)^\top(Q)(BA) := A^\top B^\top QBA$  have been used. With (4.48) evaluated for  $l = k$ , it follows that:

$$\check{V}_{\text{cl}}^\dagger[\varphi_k] \succ (\bullet)^\top (\check{V}_{\text{cl}}^\dagger[\varphi_{k+2}]) (\bar{\Phi}_{A,\text{cl}}^\dagger[\varphi_{k+2}, \varphi_k]) + \sum_{l=0}^1 (\bullet)^\top (\bar{C}_{\text{cl}}^\dagger[\varphi_{k+l}] \bar{\Phi}_{A,\text{cl}}^\dagger[\varphi_{k+l}, \varphi_k]). \quad (4.50)$$

Repeating the previous two steps ( $N_c - 2$ ) times, exploiting the  $N_c$ -periodicity of  $\check{V}_{\text{cl}}^\dagger[\varphi_k]$ , i.e.  $\check{V}_{\text{cl}}^\dagger[\varphi_k] = \check{V}_{\text{cl}}^\dagger[\varphi_{k+N_c}]$ , and using the relation  $\bar{\Phi}_{A,\text{cl}}^\dagger[\varphi_{k+N_c}, \varphi_k] = \bar{\Psi}_{A,\text{cl}}^\dagger[\varphi_k]$  leads to:

$$\check{V}_{\text{cl}}^\dagger[\varphi_k] \succ (\bullet)^\top (\check{V}_{\text{cl}}^\dagger[\varphi_k]) (\bar{\Psi}_{A,\text{cl}}^\dagger[\varphi_k]) + \sum_{l=0}^{N_c-1} (\bullet)^\top (\bar{C}_{\text{cl}}^\dagger[\varphi_{k+l}] \bar{\Phi}_{A,\text{cl}}^\dagger[\varphi_{k+l}, \varphi_k]). \quad (4.51)$$

Repeatedly multiplying (4.51) by  $\bar{\Psi}_{A,\text{cl}}^\dagger[\varphi_k]$  from the right-hand side and by its transpose from the left-hand side, and by using (4.51), one obtains for any  $n \in \mathbb{N}$ :

$$\check{V}_{\text{cl}}^\dagger[\varphi_k] \succ (\bullet)^\top (\check{V}_{\text{cl}}^\dagger[\varphi_k]) (\bar{\Psi}_{A,\text{cl}}^\dagger[\varphi_k])^n + \sum_{l=0}^{nN_c-1} (\bullet)^\top (\bar{C}_{\text{cl}}^\dagger[\varphi_{k+l}] \bar{\Phi}_{A,\text{cl}}^\dagger[\varphi_{k+l}, \varphi_k]). \quad (4.52)$$

Due to (4.48) and with Theorem 4.1 and Lemma 4.1, it follows that  $\bar{\Psi}_{A,\text{cl}}^\dagger[\varphi]$  is a Schur matrix for all  $\varphi \in \mathcal{N}_c$ . Hence, for  $n \rightarrow \infty$  one obtains from (4.52):

$$\check{V}_{\text{cl}}^\dagger[\varphi_k] \succ \sum_{l=0}^{\infty} (\bar{\Phi}_{A,\text{cl}}^\dagger[\varphi_{k+l}, \varphi_k])^\top (\bar{C}_{\text{cl}}^\dagger[\varphi_{k+l}])^\top \bar{C}_{\text{cl}}^\dagger[\varphi_{k+l}] \bar{\Phi}_{A,\text{cl}}^\dagger[\varphi_{k+l}, \varphi_k]. \quad (4.53)$$

Renaming the indices and summing over a period leads to:

$$\sum_{l=0}^{N_c-1} \check{V}_{\text{cl}}^\dagger[\varphi_{l+1}] \succ \sum_{l=0}^{N_c-1} \sum_{k=0}^{\infty} (\bullet)^\top (\bar{C}_{\text{cl}}^\dagger[\varphi_{k+l+1}] \bar{\Phi}_{A,\text{cl}}^\dagger[\varphi_{k+l+1}, \varphi_{l+1}]). \quad (4.54)$$

With the definition of the  $\mathcal{H}_2$ -norm from (4.18) (for details, see also Appendix D.1), it is now easy to see that:

$$\frac{1}{N_c} \sum_{l=0}^{N_c-1} (\bar{E}^\dagger[\varphi_l])^\top \check{V}_{\text{cl}}^\dagger[\varphi_{l+1}] \bar{E}^\dagger[\varphi_l] \succ \|\bar{\mathcal{P}}_{\varphi,\text{cl}}^\dagger\|_{\mathcal{H}_2}^2. \quad (4.55)$$

Taking the Schur-complement of LMI (4.42c) and exploiting that  $\check{V}_{\text{cl}}^\dagger[\varphi] \succ 0$  for all  $\varphi \in \mathcal{N}_c$  yields:

$$\mathfrak{Z}[\varphi_l] \succ (\bar{E}^\dagger[\varphi_l])^\top \check{V}_{\text{cl}}^\dagger[\varphi_{l+1}] \bar{E}^\dagger[\varphi_l] \succeq 0, \quad (4.56)$$

such that  $\mathfrak{Z}[\varphi] \succ 0$  for all  $\varphi \in \mathcal{N}_c$ , and:

$$\frac{1}{N_c} \sum_{l=1}^{N_c} \mathfrak{Z}[\varphi_l] = \frac{1}{N_c} \sum_{l=0}^{N_c-1} \mathfrak{Z}[\varphi_l] \succ \|\bar{\mathcal{P}}_{\varphi, \text{cl}}^\dagger\|_{\mathcal{H}_2}^2. \quad (4.57)$$

Assertions (c) and (d) now follow with Lemmas 4.2 and 4.3, respectively.

Concerning assertion (e), recall the definition of  $\bar{\Sigma}^\dagger$  on page 88, as well as the structure of the periodic control law from Eq. (4.38). Apparently, the  $\varphi$ -th row of  $\bar{\Sigma}^\dagger$  dictates the structure of  $\bar{K}^\dagger[\varphi]$ . Since  $\bar{v}_k^\dagger = \bar{v}_k^\varphi$ ,  $\bar{K}^\dagger[\varphi]$  comprises a single block-row. Thus, for ensuring structural compatibility, it must hold that:

$$\bar{\sigma}_{\varphi, q} = 0 \quad \Rightarrow \quad \bar{K}_{1, q}^\dagger[\varphi] = 0_{\bar{n}_x^\dagger[\varphi] \times \bar{n}_x^q[\varphi]} \quad (4.58)$$

for all  $\varphi \in \mathcal{N}_c$  and  $q \in \mathbb{I}_{N_x^\dagger}$ . This can be ensured by adopting the sufficient conditions from [50, Eq. (30)], leading to constraints (4.42f) to (4.42h). The consistency of the network topology is ensured either by constraint (4.39), or by constraint (4.40).  $\square$

Regarding the complexity of problem (4.42), it can be observed that the number of independent continuous optimization variables is:

$$N_{\text{cv}} = \frac{N_c}{2} ((\bar{n}_w)^2 + \bar{n}_w) + \sum_{l=0}^{N_c-1} ((\bar{n}_x^\dagger[\varphi_l])^2 + \bar{n}_x^\dagger[\varphi_l] + \bar{n}_v^\dagger[\varphi_l] \bar{n}_x^\dagger[\varphi_l]), \quad (4.59)$$

whereas the number of independent binary variables is:

$$N_{\text{bv}} = (N_c)^2 - N_c. \quad (4.60)$$

Hence, the computational time for solving the optimization problem strongly depends on the result of the clustering procedure, and therefore on the inherent interconnection structure of the interconnected system  $\mathcal{P}$ . With state-of-the-art hardware and software, the proposed method is only tractable for medium scale problems. Numerical studies showed that dimensions of up to  $\bar{n}_x^\dagger \approx 50$  and  $N_c \approx 5 \dots 8$  can be handled satisfactorily. For reducing the computational complexity, heuristics can be employed. For instance, in the light of Assumption 4.2, an optimized communication topology for the synchronous two-layer control scheme will mostly be a good (or even optimal) communication topology for the asynchronous two-layer control scheme. The design of a synchronous upper control layer is less complex than the design of an asynchronous upper control layer. Thus, the computational complexity can be reduced by optimizing the communication topology for a synchronous upper control layer, and designing an asynchronous upper control layer for this fixed communication topology. Another option is to reduce the number of continuous optimization variables by using a scaled value function instead of a fully parametrized Lyapunov matrix  $(\mathfrak{X}[\cdot])^{-1}$ . This approach is described in detail in Section 7.5.

### 4.3.3. Optimal Switching Sequence

An aspect of the asynchronous control scheme that has not yet been investigated closer is the selection of the update order of the cluster controllers, i.e. the selection of the switching sequence  $\Phi$ . It is a non-trivial problem to verify whether Assumptions 4.2 guarantee invariance of the optimal value  $J^*$  of the performance index with respect to  $\Phi$  or not. Clearly, from a control theoretic point of view, this would be a favorable property, since it would eliminate the combinatorial problem of finding an optimal switching sequence  $\Phi^*$ . However, for the case of full communication on the upper control layer, it can be verified that this invariance property does not hold. The sketch for obtaining this result is as follows: Assuming full communication allows to employ Riccati equations for calculating the value function. In particular, using a *cyclic reformulation*<sup>3</sup> of the periodic system  $\bar{\mathcal{P}}_\varphi^\uparrow$ , established tools from the theory of LTI systems can be used. In the cyclic reformulation, the choice of the switching sequence  $\Phi$  influences the order in which the periodic system matrices appear in its time-invariant counterparts. For the case  $N_\varphi = N_c = 3$ , it has been verified numerically that there exists no set of permutation matrices such that the cyclic reformulations of the only two different switching sequences are equivalent, even though they are comprised of the same set of submatrices. Hence, the solutions of the corresponding Riccati equations, and therefore the optimal performance, must be different, too. For details, the reader is referred to Sec. 6.3, 9.1, and 13.5 of [21].

In the case of full communication on the upper control layer and with values up to  $\bar{n}_x^\uparrow \approx 50$  and  $N_c \approx 5 \dots 8$  (as in Sec. 4.3), the optimal switching sequence can be determined by means of an exhaustive search. This is possible since the control problem can be efficiently solved by employing Riccati equations for time-invariant reformulations of  $\bar{\mathcal{P}}_\varphi^\uparrow$ , as sketched above. Indeed, it can easily be verified that solving a Riccati equation with MATLAB takes less than 10 seconds for an LTI system with up to  $n_x = 400$  states. The switching sequence determined by this approach can then be adopted for the procedure presented in Sec. 4.3. However, note that the optimal switching sequence for the case of full communication is not necessarily optimal for an optimized communication topology, even though a good performance can be expected.

## 4.4. Implementation

The implementation of the asynchronous hierarchical control scheme is similar to the implementation of the synchronous hierarchical control scheme: Each time-varying local control unit  $\mathcal{C}_k^i$  is comprised of a lower layer part  $\mathcal{C}^{l_i}$  and of an upper

<sup>3</sup>see Eq. (D.19) on page 180, or [21, Chap. 6.3] for details

layer part  $\mathcal{C}_k^{\uparrow i}$ . This leads to local control inputs calculated according to:

$$\mathcal{C}_k^i : u_k^i = \sum_{j=1}^{N_s} K_{i,j}^{\downarrow} x_k^j + v_k^i, \quad (4.61)$$

with  $v_k^i$  being the upper layer input to be specified in the sequel. The exchange of the local state information is accomplished by the communication network  $\mathcal{G}_k$  with periodically time-varying topology  $\Sigma_k = [\sigma_{k,i,j}] \in \mathbb{B}^{N_s \times N_s}$  given by:

$$\sigma_{k,i,j} = \begin{cases} 1 & (p(i) = p(j)) \vee ((\varphi_k = p(i)) \wedge (\bar{\sigma}_{p(i),p(j)}^{\uparrow} = 1)), \\ 0 & \text{otherwise.} \end{cases} \quad (4.62)$$

Depending on whether constraint (4.39) or (4.40) was used for the control design, the local controllers  $\mathcal{C}^i$  must transmit their local control input  $v_k^i$  in addition to their local state  $x_k^i$ .

Similar to the synchronous two-layer control scheme, the periodic upper layer control gain  $\bar{K}^{\uparrow}[\cdot]$  resulting from the MISDP (4.42) corresponds to the new subsystem order that has been identified during the clustering process (see Sec. 3.2). A reverse transformation to the original subsystem order is obtained by constructing suitable permutation matrices. Next to the permutation of the states and inputs of the original interconnected system  $\mathcal{P}$  due to the clustering procedure, the switching sequence  $\Phi$  causes a further permutation of the memory states. While the former permutation can be inverted by using the permutation matrices  $T_x$  and  $T_u$  as defined in Eq. (3.9) on page 54, an additional permutation matrix  $\bar{T}_{\Phi}[\varphi]$  is required to invert the latter permutation. With  $p \in \mathcal{N}_c$  and  $r \in \mathbb{I}_{N_c-1}$ , this matrix is given by:

$$\bar{T}_{\Phi}[\varphi] := [\bar{T}_{\Phi,p,r}[\varphi]] \in \mathbb{B}^{\bar{n}_v \times n_v^{\uparrow}[\varphi]}, \quad (4.63a)$$

$$\bar{T}_{\Phi,p,r}[\varphi_k] := \begin{cases} I_{\bar{n}_v^p} & \text{if } \text{vec}_r(\Phi^{\uparrow}[\varphi_k]) = p, \\ 0_{\bar{n}_v^p \times \bar{n}_v^{\varphi_k-r}} & \text{otherwise.} \end{cases} \quad (4.63b)$$

By the help of  $\bar{T}_{\Phi}[\varphi]$ , the extended state vector  $\bar{x}_k^{\uparrow}$  can be permuted to:

$$\begin{bmatrix} x_k \\ v_k \end{bmatrix} = \begin{bmatrix} T_x & 0 \\ 0 & T_u \bar{T}_{\Phi}[\varphi_k] \end{bmatrix} \begin{bmatrix} \bar{x}_k \\ \bar{v}_k^{\uparrow} \end{bmatrix} =: T_x^{\uparrow}[\varphi_k] \bar{x}_k^{\uparrow}. \quad (4.64)$$

Note that  $T_x^{\uparrow}[\varphi_k]$  is constructed such that the component vectors  $v_k^i = 0_{n_i^i \times 1}$  for all  $i \in \mathcal{C}^{\varphi_k}$ . This allows to write (4.64) in its current compact form without excluding these component vectors from the left-hand side of the equation, avoiding time-varying dimensions of  $v_k$ . The upper layer control gain matrix with respect to the original subsystem order is now obtained as:

$$[K^{\uparrow} \quad K_v^{\uparrow}] = T_u \begin{bmatrix} \bar{K}^{\uparrow}[1] (T_x^{\uparrow}[1])^{\top} \\ \bar{K}^{\uparrow}[2] (T_x^{\uparrow}[2])^{\top} \\ \vdots \\ \bar{K}^{\uparrow}[N_c] (T_x^{\uparrow}[N_c])^{\top} \end{bmatrix}. \quad (4.65)$$

Here,  $K_v^\dagger \in \mathbb{R}^{n_v \times n_v}$  denotes the feedback gain associated with the memory states, whose diagonal blocks are zero due to the aforementioned property of  $T_x^\dagger[\cdot]$ . Due to the concept of the asynchronous updates, the control gain in (4.65) can not be interpreted as a conventional state-feedback gain. Instead, it must be fitted into the general structure introduced in Eq. (4.5), such that:

$$\mathcal{C}^{\uparrow i} : v_k^i = \begin{cases} \sum_{q \in \bar{\mathcal{R}}^{\uparrow p(i)} \cup \{p(i)\}} \sum_{j \in \mathcal{C}^q} [K_{i,j}^\dagger & K_{v,i,j}^\dagger] \begin{bmatrix} x_k^j \\ v_k^j \end{bmatrix} & \text{if } \varphi_k = p(i), \\ v_{k-1}^i & \text{otherwise.} \end{cases} \quad (4.66)$$

Coming back to the original motivation for introducing the asynchronous control scheme, the number  $N_{m,k} \in \mathbb{N}_0$  of exchanged messages at time  $k$  will be analyzed next. Therefore, every directed information exchange between subsystems is considered as one message. The number of messages exchanged in both control schemes is related as follows:

**Corollary 4.2.** *The maximum number of messages exchanged by the asynchronous two-layer control scheme in one time step is always lower than or equal to the maximum number of messages exchanged by the synchronous two-layer control scheme in one time step.*  $\square$

*Proof.* First recall that  $\bar{N}_s^p := \text{card}(\mathcal{C}^p)$  and that  $\mathcal{N}_c^p := \mathcal{N}_c \setminus \{p\}$ . The maximum number of exchanged messages per time-step for the synchronous and for the asynchronous two-layer control scheme is given by:

$$N_{m,\max}^{\text{sy}} := \max_{k \in \mathbb{N}_0} N_{m,k}^{\text{sy}} = \sum_{p \in \mathcal{N}_c} (\bar{N}_s^p)^2 - \bar{N}_s^p + \sum_{\varphi \in \mathcal{N}_c} \sum_{q \in \mathcal{N}_c^\varphi} \bar{\sigma}_{\varphi,q}^\dagger \bar{N}_s^\varphi \bar{N}_s^q, \quad (4.67)$$

$$N_{m,\max}^{\text{as}} := \max_{k \in \mathbb{N}_0} N_{m,k}^{\text{as}} = \sum_{p \in \mathcal{N}_c} (\bar{N}_s^p)^2 - \bar{N}_s^p + \max_{\varphi \in \mathcal{N}_c} \left( \sum_{q \in \mathcal{N}_c^\varphi} \bar{\sigma}_{\varphi,q}^\dagger \bar{N}_s^\varphi \bar{N}_s^q \right), \quad (4.68)$$

respectively. Note that the number of messages exchanged by the lower control layer, which is given by the sum with summation index  $p$ , is equal in both schemes. Concerning the messages exchanged by the upper control layer, it is easy to see that:

$$\sum_{\varphi \in \mathcal{N}_c} \sum_{q \in \mathcal{N}_c^\varphi} \bar{\sigma}_{\varphi,q}^\dagger \bar{N}_s^\varphi \bar{N}_s^q \geq \max_{\varphi \in \mathcal{N}_c} \left( \sum_{q \in \mathcal{N}_c^\varphi} \bar{\sigma}_{\varphi,q}^\dagger \bar{N}_s^\varphi \bar{N}_s^q \right) \geq 0 \quad (4.69)$$

for all  $\varphi \in \mathcal{N}_c$ , which completes the proof.  $\square$

#### 4.4.1. Optimal Controller Initialization

As already mentioned in Section 4.3, the initial value  $\bar{v}_0^{\uparrow'}$  of the memory states provides an additional degree of freedom for the control designer. The component vectors of  $\bar{v}_0^{\uparrow'}$  correspond to the initial control inputs produced by the controllers



that are not updated at time  $k = 0$ . While these signals may be trivially initialized to zero, it is also possible to determine an optimal initialization  $(\bar{v}_0^{\uparrow})^*$  in terms of the global performance index  $J$ .

**Proposition 4.1.** *Consider the periodic system  $\bar{\mathcal{P}}_{\varphi, \text{cl}}^{\uparrow}$  under the conditions described in Case 2.2. Given  $\bar{x}_0 \in \mathbb{R}^{\bar{n}_x}$ , the optimal initialization  $(\bar{v}_0^{\uparrow})^* \in \mathbb{R}^{\bar{n}_v^{\uparrow}[\varphi_0]}$  of the memory states is the solution of the convex quadratic program:*

$$(\bar{v}_0^{\uparrow})^* = \arg \min_{\mathbf{v}} [\bar{x}_0^{\top} \quad \mathbf{v}^{\top}] \bar{V}_{\text{cl}}^{\uparrow}[\varphi_0] \begin{bmatrix} \bar{x}_0 \\ \mathbf{v} \end{bmatrix}. \quad (4.70)$$

Here,  $\bar{V}_{\text{cl}}^{\uparrow}[\varphi_l]$  denotes the  $N_c$ -periodic positive-semidefinite solution to the periodic Lyapunov equation (cf. [21, p.239]):

$$\bar{V}_{\text{cl}}^{\uparrow}[\varphi_l] - (\bar{A}_{\text{cl}}^{\uparrow}[\varphi_l])^{\top} \bar{V}_{\text{cl}}^{\uparrow}[\varphi_{l+1}] \bar{A}_{\text{cl}}^{\uparrow}[\varphi_l] - (\bar{C}_{\text{cl}}^{\uparrow}[\varphi_l])^{\top} \bar{C}_{\text{cl}}^{\uparrow}[\varphi_l] = 0 \quad (4.71)$$

associated with  $\bar{\mathcal{P}}_{\varphi, \text{cl}}^{\uparrow}$ , where  $l \in \{0, \dots, N_c - 1\}$ . □

*Proof.* With the  $N_c$ -periodic solution  $\bar{V}_{\text{cl}}^{\uparrow}[\varphi]$  of (4.71), it holds that [21, p.240]:

$$\|\bar{\mathcal{P}}_{\varphi, \text{cl}}^{\uparrow}\|_{\mathcal{H}_2}^2 = \frac{1}{N_c} \sum_{l=0}^{N_c-1} \text{tr}((\bar{E}^{\uparrow}[\varphi_l])^{\top} \bar{V}_{\text{cl}}^{\uparrow}[\varphi_{l+1}] \bar{E}^{\uparrow}[\varphi_l]). \quad (4.72)$$

Since  $\bar{A}_{\text{cl}}^{\uparrow}[\cdot]$  is stable according to Theorem 4.3,  $\bar{V}_{\text{cl}}^{\uparrow}[\varphi] \in \mathbb{S}_{\geq 0}^{\bar{n}_x^{\uparrow}[\varphi]}$  [21, p.239]. Thus, it can be easily verified that the QP (4.70) is convex [26, p.71, p.152f]. By the help of Lemma 4.3 and with  $\bar{V}_{\text{cl}}^{\uparrow}[\varphi_{N_c}] = \bar{V}_{\text{cl}}^{\uparrow}[\varphi_0]$ , it can be deduced that:

$$J = (\bar{x}_0^{\uparrow})^{\top} \bar{V}_{\text{cl}}^{\uparrow}[\varphi_0] \bar{x}_0^{\uparrow}. \quad (4.73)$$

Since the communication cost  $J^{\text{com}}$  does not depend on the initial state  $\bar{x}_0^{\uparrow}$ , it suffices to consider  $J$  for minimizing  $J + J^{\text{com}}$  with respect to  $\bar{x}_0^{\uparrow}$ . The QP (4.70) now follows by minimizing (4.73) with:

$$\bar{x}_0^{\uparrow} = \begin{bmatrix} \bar{x}_0 \\ \bar{v}_0^{\uparrow} \end{bmatrix}, \quad (4.74)$$

considering  $\bar{v}_0^{\uparrow}$  as optimization variable, and  $\bar{x}_0$  as a given parameter. □

Note that the optimal initialization  $(\bar{v}_0^{\uparrow})^*$  can be permuted to the original subsystem order by the help of Eq. (4.64).

### 4.4.2. Stability of the Original Interconnected System

The relation between the stability of the periodic system  $\bar{\mathcal{P}}_{\varphi, \text{cl}}^\dagger$  and the stability of the original interconnected system  $\mathcal{P}$  controlled by the asynchronous hierarchical control law is as follows:

**Theorem 4.4.** *Suppose that the periodic system  $\bar{\mathcal{P}}_{\varphi, \text{cl}}^\dagger$  is exponentially stable, and that the asynchronous hierarchical control law comprised of (4.61) and (4.66) is applied to the interconnected system  $\mathcal{P}$ . Then, the following assertions hold:*

(a) *The system  $\mathcal{P}$  with  $w_k = 0$  for all  $k \in \mathbb{N}_0$  is asymptotically stable.*

(b) *The system  $\mathcal{P}$  with input  $w_k$  is bounded-input/bounded-output stable.*  $\square$

*Proof.* With Theorem 4.1, it follows that exponential stability of  $\bar{\mathcal{P}}_{\varphi, \text{cl}}^\dagger$  implies that there exist constants  $\alpha^\dagger \in \mathbb{R}_{>1}$  and  $\beta^\dagger \in (0, 1)$  such that:

$$\|\bar{x}_k^\dagger\|_2^2 \leq \alpha^\dagger (\beta^\dagger)^k \|\bar{x}_0^\dagger\|_2^2. \quad (4.75)$$

Recall that the periodic system  $\bar{\mathcal{P}}_{\varphi, \text{cl}}^\dagger$  models the original interconnected system  $\mathcal{P}$  controlled by the asynchronous hierarchical control law. With  $\bar{x}_k^\dagger = (\bar{x}_k; \bar{v}_k^\dagger)$  and  $\|\bar{x}_k\|_2 = \|x_k\|_2$  due to  $\bar{x}_k$  being a permutation of  $x_k$ , it follows that:

$$\|\bar{x}_k^\dagger\|_2^2 = \|x_k\|_2^2 + \|\bar{v}_k^\dagger\|_2^2 \leq \alpha^\dagger (\beta^\dagger)^k (\|x_0\|_2^2 + \|\bar{v}_0^\dagger\|_2^2). \quad (4.76)$$

Exploiting that  $\|(\cdot)\|_2^2 \geq 0$ , there always exists some  $\gamma \in \mathbb{R}_{\geq 1}$  such that:

$$\|x_0\|_2^2 + \|\bar{v}_0^\dagger\|_2^2 = \gamma \|x_0\|_2^2. \quad (4.77)$$

With (4.76), this leads to:

$$\|x_k\|_2^2 \leq \|x_k\|_2^2 + \|\bar{v}_k^\dagger\|_2^2 \leq \alpha^\dagger (\beta^\dagger)^k \gamma \|x_0\|_2^2 = (\alpha^\dagger \gamma) (\beta^\dagger)^k \|x_0\|_2^2. \quad (4.78)$$

Hence, by defining:

$$\alpha := \alpha^\dagger \gamma \in \mathbb{R}_{\geq 1}, \quad \beta := \beta^\dagger \in (0, 1), \quad (4.79)$$

it follows from Theorem 2.1 that the interconnected system  $\mathcal{P}$  is asymptotically stable under the control of the asynchronous hierarchical control law, which proves assertion (a). Assertion (b) directly follows with Theorem 2.2.  $\square$

## 4.5. Numerical Example

In order to enable a comparison of the synchronous and the asynchronous two-layer control scheme, consider again the interconnected system  $\mathcal{P}$  presented in Sec. 3.6. Consistent to with the presentation of the asynchronous control scheme, the

controlled lower layer system  $\mathcal{P}_{cl}^\downarrow$  resulting from (3.78) is taken as starting point. Furthermore, the communication cost matrix  $\bar{c}^{\uparrow\text{com}}$  is adopted from (3.79) without any change. For constructing the periodic system  $\bar{\mathcal{P}}^\uparrow$ , the switching sequence is selected as:

$$\Phi = \{\varphi_{k+3}, \varphi_{k+2}, \varphi_{k+1}\} = \{3, 2, 1\}. \quad (4.80)$$

The time-varying dimensions of  $\bar{\mathcal{P}}_\varphi^\uparrow$  are given by:

$$\begin{aligned} \bar{n}_x^\uparrow[1] &= \bar{n}_x + \bar{n}_v^3 + \bar{n}_v^2 = 13, & \bar{n}_v^\uparrow[1] &= \bar{n}_v^1 = 3, \\ \bar{n}_x^\uparrow[2] &= \bar{n}_x + \bar{n}_v^1 + \bar{n}_v^3 = 14, & \bar{n}_v^\uparrow[2] &= \bar{n}_v^2 = 2, \\ \bar{n}_x^\uparrow[3] &= \bar{n}_x + \bar{n}_v^2 + \bar{n}_v^1 = 14, & \bar{n}_v^\uparrow[3] &= \bar{n}_v^3 = 2. \end{aligned} \quad (4.81)$$

The resulting periodic system matrices can be found in Appendix E.1 on p.185.

**Table 4.1.:** Comparison of the lower layer controller (left) with the synchronous (middle) and with the asynchronous (right) two-layer control scheme. For Case 2.2, it is assumed that  $x_0 \sim \mathcal{N}(0, I)$ .

upper control layer	none	synchronous	asynchronous		
topology $\bar{\Sigma}^\uparrow$	n/a	$\begin{bmatrix} 1 & 0 & 0 \\ 1 & 1 & 1 \\ 0 & 1 & 1 \end{bmatrix}$	$\begin{bmatrix} 1 & 0 & 0 & 0 & 0 \\ 1 & 1 & 1 & 0 & 0 \\ 0 & 1 & 1 & 0 & 0 \end{bmatrix}$		
initialization $\bar{v}_0^{\uparrow'}$	n/a	n/a	0	$(\bar{v}_0^{\uparrow'})^*$	
Case 2.1	$J$	296.62	289.61	290.09	290.09
	$E(J   \varphi_0 = 1)$	296.62	280.53	294.60	265.00
Case 2.2	$E(J   \varphi_0 = 2)$	296.62	295.71	287.98	273.96
	$E(J   \varphi_0 = 3)$	296.62	292.59	287.69	276.88

Table 4.1 shows the values of the performance index  $J$  for different controller structures. In every case, the lower control layer  $u_k = K^\downarrow x_k + v_k$  is applied to the system. For the upper control layer,  $v_k = 0$  (left) as well as the synchronous (middle) and the asynchronous scheme (right) are considered. All controlled systems have been rewritten as a periodic system with period  $N_\varphi = N_c = 3$  to ensure that the values of the performance index are comparable (see Appendix D.3). Furthermore, the communication topologies for the synchronous and the asynchronous upper control layer are chosen to be compatible.

Under the conditions of Case 2.1, both the synchronous and the asynchronous upper control layer show a very similar performance. Indeed, the performance of the lower control layer is improved by approximately 2.3 percent using either of the upper layer control schemes. Since  $J$  is a limit value for  $k$  approaching infinity

in this case, the initial values of  $\bar{v}_0^{\uparrow'}$  and  $\varphi_0$  have no influence on the performance index.

For  $J$  according to Case 2.2, it is assumed here that  $x_0 \sim \mathcal{N}(I, 0)$ , i.e. that  $x_0$  follows a standard normal distribution. Hence, the concept stated in Section 3.4.4 can be used to optimize the control layers with respect to the expected value  $E(J)$ . Applying only the lower control layer to the interconnected system  $\mathcal{P}$ , a performance of  $E(J) = 296.62$  is obtained. Adding the synchronous upper control layer, the performance is improved to  $E(J) = 280.53$  for  $\varphi_0 = 1$ , which corresponds to the case of all upper layer controllers being updated simultaneously at time  $k = 0$ . For  $\varphi_0 = 2$  and  $\varphi_0 = 3$ , the performance is degraded, since the first update of the upper layer controllers takes place at time  $k = 2$  and  $k = 1$ , respectively. Note that in the latter two cases, an optimal initialization of the synchronous upper layer controllers could be found by using a similar concept as proposed in Proposition 4.1. However, even with the synchronous upper layer controllers being inactive for up to two time-steps, the performance of the lower control layer is improved by the synchronous upper control layer. Similar to the synchronous scheme, the expected performance of the asynchronous scheme also depends on the choice of  $\varphi_0$ . Obviously, for  $\bar{v}_0^{\uparrow'} = 0$ , initializing either  $\mathcal{C}^{\uparrow 2}$  or  $\mathcal{C}^{\uparrow 3}$  first is beneficial in terms of the performance measure. Notably, the mean performance over all  $\varphi_0$ , which is 290.09, is similar to the mean performance of the synchronous scheme, which is 289.61. When choosing the optimal initialization  $(\bar{v}_0^{\uparrow'})^*$  according to Prop. 4.1, the mean performance is improved to 271.95.

The number of messages exchanged by the hierarchical two-layer control schemes is illustrated in Figure 4.2. As desired, the maximum number of messages exchanged in one time-step is reduced from  $N_{m,\max}^{\text{sy}} = 18$  to  $N_{m,\max}^{\text{as}} = 14$  by applying the asynchronous instead of the synchronous scheme. Furthermore, the variance of the number of messages is reduced from 48 to 16. The total number of messages exchanged over one period is  $N_m = 30$  for both schemes.

As already mentioned at the very end of Section 4.3.2, the computational complexity for designing asynchronous upper layer controllers is higher than for designing synchronous upper layer controllers, what is due to the increase of the number of continuous optimization variables. For the proposed example, designing the asynchronous upper layer controllers takes about 212 seconds, including the clustering procedure and the design of the lower control layer. On the other hand, recall from Sec. 3.6 that designing the synchronous controllers takes only about 19 seconds of computation time.

## 4.6. Discussion

In this chapter, an approach for asynchronously operating upper layer controllers was presented as an alternative to the synchronously operating upper layer controllers presented in Sec. 3.4. That is, the clustering procedure and distributed

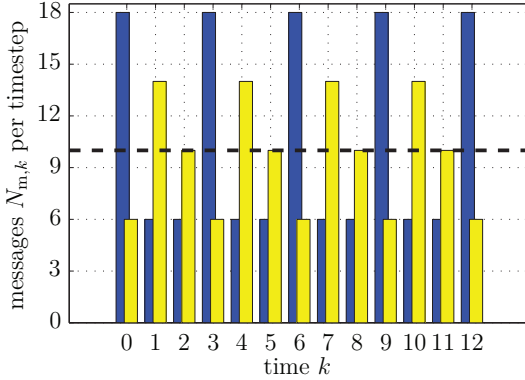


**Figure 4.2.:** Total number of messages exchanged per time-step for the synchronous scheme (blue) and for the asynchronous scheme (yellow). The dashed line shows the average number of exchanged messages per time-step, which is equal in both schemes.

lower control layer are adopted from Chapter 3. On the upper layer, similar to the synchronous scheme, each cluster is equipped with a controller that operates on a coarser timescale compared to the lower layer. However, these controllers are now updated sequentially instead of simultaneously. The problem of designing such controllers can be efficiently formulated and solved in the framework of periodic systems. By carefully selecting the controlled variable of the constructed periodic system, both control layers can be designed to cooperate for minimizing the global performance index  $J$ .

The major benefit of the asynchronously operating upper layer controllers is a significant reduction of the peak traffic in the communication network, while achieving a similar control performance compared to the synchronous scheme. The reduced peak traffic is due to the improved distribution of information exchange over time, compared to a synchronous upper layer controller. Consequently, the hardware requirements for the communication network to provide a sufficiently small transmission delay are reduced. A disadvantage of the asynchronous scheme compared to the synchronous one is its increased synthesis complexity, which is due to increased number of continuous optimization variables. However, the synthesis complexity can be reduced by employing heuristics, e.g. by adopting an optimized upper layer communication topology for the synchronous scheme.

In the case that the system under control has an initial deviation from the desired equilibrium, the performance of the asynchronous upper layer controller can be improved by initializing it in an optimal manner. As has been shown, such an optimal initialization can be found as solution to a quadratic program, which depends on

the initial state of the interconnected system. However, calculating a (sub-)optimal initialization in a distributed manner, respecting local information sets and the topology of the available communication network, remains an open question. Naturally, this problem could be tackled by using concepts from distributed model predictive control, which propose ways to solve quadratic programs in a distributed manner (see, e.g., [51] or [122]). A further aspect that has not yet been investigated is whether the performance of the closed-loop system could be further improved by directly incorporating the optimal initialization for the design of the asynchronous controller. Currently, considering the case of a non-zero initialization and zero disturbances (Case 2.2), setting up the MISDP (4.42) requires to choose a value for  $\bar{v}_0^{\uparrow}$ . Since the upper layer control law is yet unknown before solving the MISDP, the optimal initialization  $(\bar{v}_0^{\uparrow})^*$  according to Prop. 4.1 is likewise undefined. Hence, an open problem would be to break this cross-dependency, enabling to consider the option of an optimal initialization already for the control design.

As discussed in Sec. 4.3.2, the asynchronous scheme additionally allows to exchange input information between the local controllers  $\mathcal{C}^{\uparrow i}$ . For communication topologies not matching the characterization stated in Corollary 4.1, this additional information may lead to an improved performance, without affecting the communication cost  $J^{\uparrow \text{com}}$ . Thus, a further open question would be how to account for this additional information in terms of the communication cost. As a consequence, this would enable to evaluate whether an input information is worth being exchanged or not.



# 5. Application Example

This chapter compares the concepts of synchronous and asynchronous hierarchical control introduced in Chap. 3 and in Chap. 4, respectively, by means of an application example from the domain of power systems. Consisting of generator and load nodes physically interconnected via electrical transmission lines, power systems are a famous and topic example for complex interconnected systems. Due to the transmission of alternating currents and the conservation of charge and energy within the electrical network, power systems are mostly modeled by nonlinear differential algebraic equations [100]. Thus, for being able to apply the control approaches presented in the preceding chapters, a linearized dynamic model has to be derived first. Therefore, a modeling scheme originally developed in [53] and [22] is presented in Sec. 5.1. Under moderate assumptions and by employing appropriate approximations, this modeling scheme leads to a linearized time-invariant model in continuous time, which is valid around an equilibrium point. This linearized model can be employed for frequency control of power systems consisting of loads and synchronous generators with an arbitrary interconnection graph. In the second section of this chapter, the results of the synchronous and asynchronous hierarchical control design are presented. Finally, Sec. 5.3 presents the simulation results, and compares the performance and design complexity of the hierarchical control schemes with those of related approaches. Note that notation used so far is sporadically modified in this chapter to denote the physical quantities of a power system.

## 5.1. Linearized Power System Model

This section briefly reviews the modeling scheme for frequency control of a power system, as originally developed in [53] and [22]. For details, the reader is referred to these publications and the references therein.

Consider a power system consisting of  $N_s$  generator buses and  $N - N_s$  load buses, which are interconnected through a network of transmission lines. The topology of the network of transmission lines is modeled by the weighted adjacency matrix  $\Delta = \Delta^T \in \mathbb{R}^{N \times N}$  of a connected, undirected graph, where the  $N$  nodes represent the buses. Denoting the inductive reactance of the transmission line from the  $i$ -th to the  $j$ -th bus of the electrical network by  $z_{i,j} [\Omega]$ , the scalar entries  $\Delta_{i,j}$  of  $\Delta$  are defined as (cf. [53]):

$$\Delta_{i,j} = \Delta_{j,i} := -\frac{1}{z_{i,j}} = -b_{i,j} [\Omega^{-1}], \quad (5.1)$$



i.e. they correspond to the negative susceptance  $-b_{i,j}$  of the respective transmission line. If there is no transmission line between nodes  $i$  and  $j$ , then  $\Delta_{i,j} = \Delta_{j,i} = 0$ . For the  $N_s$  generator buses  $i \in \{1, \dots, N_s\}$ , the following linear differential equations modeling a steam-valve controlled synchronous generator are employed, which is a standard model for load-frequency control studies [53, Chap. 7.2]:

$$\dot{\delta}^i = \omega_i, \quad (5.2a)$$

$$\dot{\omega}^i = \frac{1}{H^i} \left( P_M^i - D^i \omega^i - P_L^i - \sum_{\{j \in \mathbb{I}_N \mid \Delta_{i,j} < 0\}} P_{i,j}^{\text{tie}} \right), \quad (5.2b)$$

$$\dot{P}_M^i = \frac{1}{\tau_T^i} (P_G^i - P_M^i), \quad (5.2c)$$

$$\dot{P}_G^i = \frac{1}{\tau_G^i} \left( P_{\text{ref}}^i - P_G^i - \frac{1}{r^i} \omega^i \right). \quad (5.2d)$$

Here,  $\delta^i$  [rad],  $\omega^i$  [rad/s], and  $P_M^i$  [MW] denote the rotor/voltage phase angle, the rotor/voltage frequency, and the amount of generated electrical power of the  $i$ -th generator, respectively, with respect to an a-priori scheduled operating point  $\delta_{\text{eq}}^i$ ,  $\omega_{\text{eq}}^i$ ,  $P_{M,\text{eq}}^i$ . The deviation of the power demand at bus  $i$  from the nominal value is modeled by the disturbance input  $P_L^i$  [MW]. Each generator is equipped with a local *turbine governor* with state  $P_G^i$  [MW] (measured w.r.t.  $P_{G,\text{eq}}^i$ ) and with reference input  $P_{\text{ref}}^i$  [MW]. Furthermore,  $H^i$ ,  $D^i$ ,  $\tau_T^i$  and  $\tau_G^i$  denote the (normalized) inertia, the damping coefficient, and the turbine and governor time constants of generator  $i$ , and  $r^i$  is the regulation constant of the decentralized primary feedback loop. The values  $P_{i,j}^{\text{tie}}$  [MW] represent the power flow from bus  $i$  to bus  $j$ .

As a first approximation, the required power flow analysis is performed by using a DC power flow model (cf. [53, Chap 7.2]), which is an acceptable approximation of a nonlinear AC power flow model for small voltage phase differences. The power flow from bus  $i$  to bus  $j$  can then be expressed as:

$$P_{i,j}^{\text{tie}} = b_{i,j}(\delta^i - \delta^j) = -P_{j,i}^{\text{tie}}. \quad (5.3)$$

As a second approximation, the phase angle dynamics of the load buses are neglected, i.e. it is assumed that their dynamics are sufficiently fast compared to the phase angle inertia of the generator buses. At the time scale relevant for frequency control, this is a suitable assumption. The power balance at the  $N - N_s$  load buses can then be expressed as:

$$0 = -P_L^i - \sum_{\{j \in \mathbb{I}_N \mid \Delta_{i,j} < 0\}} P_{i,j}^{\text{tie}}, \quad (5.4)$$

for  $i \in \{N_s + 1, \dots, N\}$ . Combining equations (5.2b), (5.3), and (5.4), the power

flow in the global power network is modeled by:

$$\begin{bmatrix} H^1 \dot{\omega}^1 \\ \vdots \\ H^{N_s} \dot{\omega}^{N_s} \\ 0 \\ \vdots \\ 0 \end{bmatrix} = \begin{bmatrix} P_M^1 - D^1 \omega^1 - P_L^1 \\ \vdots \\ P_M^{N_s} - D^{N_s} \omega^{N_s} - P_L^{N_s} \\ -P_L^{N_s+1} \\ \vdots \\ -P_L^N \end{bmatrix} - \begin{bmatrix} \Delta'_{1,1} & \Delta'_{1,2} \\ \Delta'_{2,1} & \Delta'_{2,2} \end{bmatrix} \begin{bmatrix} \delta^1 \\ \vdots \\ \delta^{N_s} \\ \delta^{N_s+1} \\ \vdots \\ \delta^N \end{bmatrix}, \quad (5.5)$$

with  $\Delta' := \Delta - \text{diag}(\Delta_{1 \times 1})$ . Employing a procedure commonly known as *Kron reduction* [49], the load voltage phase angles  $\delta^{N_s+1}$  to  $\delta^N$  can be eliminated from (5.5), leading to the reduced power flow model:

$$\begin{bmatrix} H^1 \dot{\omega}^1 \\ \vdots \\ H^{N_s} \dot{\omega}^{N_s} \end{bmatrix} = \begin{bmatrix} P_M^1 - D^1 \omega^1 \\ \vdots \\ P_M^{N_s} - D^{N_s} \omega^{N_s} \end{bmatrix} - A'_c \begin{bmatrix} \delta^1 \\ \vdots \\ \delta^{N_s} \end{bmatrix} - E'_c \begin{bmatrix} P_L^1 \\ \vdots \\ P_L^{N_s} \end{bmatrix} \quad (5.6)$$

with  $A'_c = \Delta'_{1,1} - \Delta_{1,2} \Delta_{2,2}^{-1} \Delta_{2,1}$  and  $E'_c = [I_{N_s} \quad \Delta_{1,2} \Delta_{2,2}^{-1}]$ . The power system can now be defined as an interconnection of  $N_s$  systems by taking (5.6), (5.2a), (5.2c), and (5.2d), and interpreting each generator bus as a subsystem  $\mathcal{P}^i$ . Hence, the state vector  $x^i$  and input  $u^i$  of subsystem  $\mathcal{P}^i$  are given by:

$$x^i = \begin{bmatrix} \delta^i \\ \omega^i \\ P_M^i \\ P_G^i \end{bmatrix}, \quad u^i = P_{\text{ref}}^i, \quad (5.7)$$

such that the global system is of the form:

$$\begin{bmatrix} \dot{x}^1 \\ \vdots \\ \dot{x}^{N_s} \end{bmatrix} = A_c \begin{bmatrix} x^1 \\ \vdots \\ x^{N_s} \end{bmatrix} + B_c \begin{bmatrix} u^1 \\ \vdots \\ u^{N_s} \end{bmatrix} + E_c \begin{bmatrix} w^1 \\ \vdots \\ w^N \end{bmatrix}, \quad (5.8)$$

with  $w^i = P_L^i$ . Note that the additional disturbance inputs  $w^{N_s+1}$  to  $w^N$  may be associated to the  $N_s$  subsystems according to, e.g., spatial criteria.

### Model of the 10-bus CIGRÉ Benchmark System

The power system to be modeled in this section is the well-known CIGRÉ benchmark system for frequency control [100]. The benchmark system, which is shown in Fig. 5.1, consists of a total number of  $N = 10$  interconnected load and generator buses. Buses 1 to 7 are equipped with steam-valve controlled generators and are

thus interpreted as subsystems  $\mathcal{P}^i$  with  $N_s = 7$ . Buses 8 to 10 are pure load buses. According to [53, App. E], the parameters of the benchmark system are chosen as:

$$\begin{bmatrix} H^1 & \dots & H^{N_s} \end{bmatrix} = \begin{bmatrix} 100 & 30.3 & 35.8 & 28.6 & 26 & 34.8 & 26.6 \end{bmatrix}, \quad (5.9a)$$

$$\begin{bmatrix} D^1 & \dots & D^{N_s} \end{bmatrix} = \begin{bmatrix} 0.8 & 0.85 & 0.8 & 0.8 & 0.9 & 0.7 & 0.8 \end{bmatrix}, \quad (5.9b)$$

$$\begin{bmatrix} \tau_G^1 & \dots & \tau_G^{N_s} \end{bmatrix} = \begin{bmatrix} 0.2 & 0.15 & 0.2 & 0.2 & 0.25 & 0.2 & 0.2 \end{bmatrix}, \quad (5.9c)$$

$$\begin{bmatrix} \tau_T^1 & \dots & \tau_T^{N_s} \end{bmatrix} = \begin{bmatrix} 0.5 & 0.4 & 0.5 & 0.5 & 0.4 & 0.5 & 0.5 \end{bmatrix}, \quad (5.9d)$$

$$\begin{bmatrix} r^1 & \dots & r^{N_s} \end{bmatrix} = \begin{bmatrix} \frac{1}{20} & \frac{1}{23} & \frac{1}{19} & \frac{1}{21} & \frac{1}{21} & \frac{1}{18} & \frac{1}{20} \end{bmatrix}, \quad (5.9e)$$

with transmission line susceptances given by:

$$\Delta = - \begin{bmatrix} 0 & 0 & 24.5 & 24.5 & 0 & 0 & 0 & 0 & 0 & 0 \\ 0 & 0 & 62.6 & 0 & 0 & 0 & 0 & 0 & 0 & 32.3 \\ 24.5 & 62.6 & 0 & 39.5 & 0 & 0 & 0 & 0 & 28 & 0 \\ 24.5 & 0 & 39.5 & 0 & 10 & 10 & 0 & 0 & 97 & 33 \\ 0 & 0 & 0 & 10 & 0 & 0 & 0 & 0 & 0 & 0 \\ 0 & 0 & 0 & 10 & 0 & 0 & 0 & 31.8 & 0 & 0 \\ 0 & 0 & 0 & 0 & 0 & 0 & 0 & 39.5 & 0 & 0 \\ 0 & 0 & 0 & 0 & 0 & 31.8 & 39.5 & 0 & 97 & 0 \\ 0 & 0 & 28 & 97 & 0 & 0 & 0 & 97 & 0 & 0 \\ 0 & 32.3 & 0 & 33 & 0 & 0 & 0 & 0 & 0 & 0 \end{bmatrix}. \quad (5.9f)$$

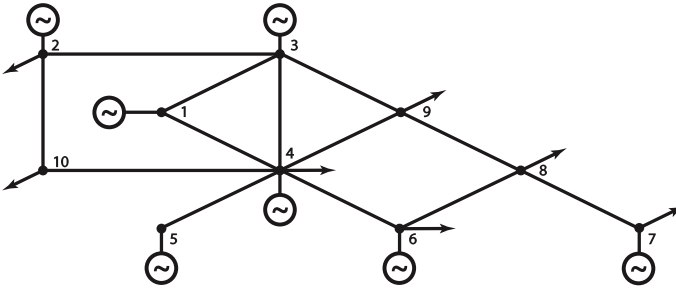


**Figure 5.1.:** Single-line representation of the 10-bus CIGRÉ benchmark system according to [53].

From the eigenvalues of the system matrix  $A_c$  of the resulting continuous-time model, the smallest time constant is found to be  $0.142 [s]$ . The model is discretized using zero-order hold with  $\Delta t = 0.1 [s]$  to capture all dynamic effects, leading

to the system matrices  $A, B$  and  $E$ . With these parameters, all subsystems are controllable. The local controlled variables are chosen as:

$$z_k^i = \begin{bmatrix} 500 & 0 & 0 & 0 \\ 0 & 500 & 0 & 0 \\ 0 & 0 & 0.01 & 0 \\ 0 & 0 & 0 & 0.01 \\ 0 & 0 & 0 & 0 \end{bmatrix} x_k^i + \begin{bmatrix} 0 \\ 0 \\ 0 \\ 0 \\ 0.1 \end{bmatrix} u_k^i, \quad (5.10)$$

for all  $i \in \{1, \dots, 7\}$ . Hence, the deviations of the local rotor phase angle and of the rotor frequency have a considerably larger influence on the global performance index  $J$  than the remaining state and the input variables. Finally, the initialization of the model is chosen as proposed in [53]:

$$\begin{aligned} x_0^1 &= \begin{bmatrix} -0.1 \\ 0.025 \\ -0.4 \\ 0.1 \end{bmatrix}, & x_0^2 &= \begin{bmatrix} 0.15 \\ -0.035 \\ 0.015 \\ 0.1 \end{bmatrix}, & x_0^3 &= \begin{bmatrix} 0.05 \\ -0.005 \\ 0 \\ 0.01 \end{bmatrix}, & x_0^4 &= \begin{bmatrix} 0.1 \\ -0.0025 \\ 0.01 \\ 0.0005 \end{bmatrix}, \\ x_0^5 &= \begin{bmatrix} -0.25 \\ 0.004 \\ 0 \\ 0.05 \end{bmatrix}, & x_0^6 &= \begin{bmatrix} -0.2 \\ 0.02 \\ -0.5 \\ 0.001 \end{bmatrix}, & x_0^7 &= \begin{bmatrix} 0.25 \\ 0.005 \\ 0.015 \\ -0.045 \end{bmatrix}. \end{aligned} \quad (5.11)$$

## 5.2. Hierarchical Control Design

As a first step of the hierarchical control design, the clustering procedure presented in Section 3.2 is applied to the interconnected system  $\mathcal{P}$ . Setting  $\gamma_{i,j} = \|A_{i,j}\|_2 + \|B_{i,j}\|$ , the following interconnection strength matrix is obtained:

$$\Gamma = \begin{bmatrix} 8.0671 & 0.0002 & 0.1072 & 0.1071 & 0.0000 & 0.0001 & 0.0001 \\ 0.0011 & 11.4486 & 1.2962 & 0.3395 & 0.0001 & 0.0003 & 0.0003 \\ 0.2852 & 0.7262 & 7.8093 & 0.6467 & 0.0002 & 0.0363 & 0.0449 \\ 0.3920 & 0.2617 & 0.8899 & 8.6701 & 0.1598 & 0.3308 & 0.2125 \\ 0.0001 & 0.0001 & 0.0003 & 0.1467 & 7.1439 & 0.0001 & 0.0001 \\ 0.0002 & 0.0002 & 0.0355 & 0.2351 & 0.0001 & 7.2813 & 0.1137 \\ 0.0002 & 0.0002 & 0.0638 & 0.2197 & 0.0001 & 0.1655 & 8.0566 \end{bmatrix}. \quad (5.12)$$

As can be deduced from the interconnection structure matrix  $\Gamma$ , the power system model possesses many weak interconnections. Choosing  $\epsilon_w = \epsilon_n = 0.25$  as threshold values for weak and negligible interconnections, the following refinement of  $\Gamma$  is obtained, what shows that the strong interconnections of the model are highly

structured:

$$\Gamma' = \begin{bmatrix} 8.0671 & 0 & 0 & 0 & 0 & 0 & 0 \\ 0 & 11.4486 & 1.2962 & 0.3395 & 0 & 0 & 0 \\ 0.2852 & 0.7262 & 7.8093 & 0.6467 & 0 & 0 & 0 \\ 0.3920 & 0.2617 & 0.8899 & 8.6701 & 0 & 0.3308 & 0 \\ 0 & 0 & 0 & 0 & 7.1439 & 0 & 0 \\ 0 & 0 & 0 & 0 & 0 & 7.2813 & 0 \\ 0 & 0 & 0 & 0 & 0 & 0 & 8.0566 \end{bmatrix}. \quad (5.13)$$

Applying the Dulmage-Mendelsohn decomposition leads to the permutation order  $\tau^T = (2 \ 3 \ 4 \ 1 \ 5 \ 6 \ 7)$ , and to the permuted matrix:

$$\Gamma'' = \begin{bmatrix} 11.4486 & 1.2962 & 0.3395 & 0 & 0 & 0 & 0 \\ 0.7262 & 7.8093 & 0.6467 & 0.2852 & 0 & 0 & 0 \\ 0.2617 & 0.8899 & 8.6701 & 0.3920 & 0 & 0.3308 & 0 \\ \hline 0 & 0 & 0 & 8.0671 & 0 & 0 & 0 \\ 0 & 0 & 0 & 0 & 7.1439 & 0 & 0 \\ 0 & 0 & 0 & 0 & 0 & 7.2813 & 0 \\ \hline 0 & 0 & 0 & 0 & 0 & 0 & 8.0566 \end{bmatrix}, \quad (5.14)$$

such that  $N_c = 3$  clusters are formed by:

$$\mathcal{C}_1 = \{2, 3, 4\}, \quad \mathcal{C}_2 = \{1, 5, 6\}, \quad \mathcal{C}_3 = \{7\}. \quad (5.15)$$

Recalling the physical interconnection structure of the generator nodes shown in Fig. 5.1, two interesting observations can be made regarding the outcome of the clustering procedure:

1. Node number 7, which appears to be a separated node, is chosen to form a separate cluster.
2. Nodes number 1 to number 6, which appear to be strongly coupled by the electrical network, are split into two (approximately) hierarchically interconnected clusters.

Hence, the algorithm conforms with intuition, and even provides some more insight into the structure of the control problem which is not obvious at first glance.

Restoring the weak interconnections that do not affect the hierarchical interconnection structure of the clusters leads to:

$$\Gamma' = \left[ \begin{array}{ccc|ccc|c} 11.4486 & 1.2962 & 0.3395 & 0.0011 & 0.0001 & 0.0003 & 0.0003 \\ 0.7262 & 7.8093 & 0.6467 & 0.2852 & 0.0002 & 0.0363 & 0.0449 \\ 0.2617 & 0.8899 & 8.6701 & 0.3920 & 0.1598 & 0.3308 & 0.2125 \\ \hline 0 & 0 & 0 & 8.0671 & 0.0000 & 0.0001 & 0.0001 \\ 0 & 0 & 0 & 0.0001 & 7.1439 & 0.0001 & 0.0001 \\ 0 & 0 & 0 & 0.0002 & 0.0001 & 7.2813 & 0.1137 \\ \hline 0 & 0 & 0 & 0 & 0 & 0 & 8.0566 \end{array} \right]. \quad (5.16)$$

Applying Theorem 3.1 leads to the lower layer controllers:

$$\begin{aligned} \mathcal{C}^{11} : u_k^1 &= -[-1.28 \quad 22.59 \quad 0.12 \quad 0.06] x_k^1 - [0.50 \quad 0.68 \quad 0.01 \quad 0.01] x_k^5 \dots \\ &\quad - [-0.29 \quad 1.22 \quad 0.02 \quad 0.01] x_k^6 + v_k^1, \\ \mathcal{C}^{12} : u_k^2 &= -[-11.70 \quad 17.87 \quad 0.30 \quad 0.12] x_k^2 - [6.18 \quad 10.85 \quad 0.16 \quad 0.07] x_k^3 \dots \\ &\quad - [3.80 \quad 4.32 \quad 0.09 \quad 0.04] x_k^4 + v_k^2, \\ \mathcal{C}^{13} : u_k^3 &= -[14.63 \quad 14.72 \quad 0.19 \quad 0.07] x_k^2 - [-26.84 \quad 17.63 \quad 0.33 \quad 0.14] x_k^3 \dots \\ &\quad - [-2.23 \quad 8.02 \quad 0.18 \quad 0.07] x_k^4 + v_k^3, \\ \mathcal{C}^{14} : u_k^4 &= -[14.32 \quad 10.22 \quad 0.12 \quad 0.04] x_k^2 - [3.87 \quad 15.00 \quad 0.20 \quad 0.08] x_k^3 \dots \\ &\quad - [-41.41 \quad 12.44 \quad 0.35 \quad 0.15] x_k^4 + v_k^4, \\ \mathcal{C}^{15} : u_k^5 &= -[1.57 \quad 3.85 \quad 0.01 \quad 0.01] x_k^1 - [13.08 \quad 45.48 \quad 0.75 \quad 0.47] x_k^5 \dots \\ &\quad - [-0.56 \quad 2.32 \quad 0.04 \quad 0.01] x_k^6 + v_k^5, \\ \mathcal{C}^{16} : u_k^6 &= -[8.23 \quad 8.73 \quad 0.03 \quad 0.01] x_k^1 - [3.20 \quad 2.75 \quad 0.03 \quad 0.02] x_k^5 \dots \\ &\quad - [-10.44 \quad 33.15 \quad 0.55 \quad 0.23] x_k^6 + v_k^6, \\ \mathcal{C}^{17} : u_k^7 &= -[-8.52 \quad 32.96 \quad 0.74 \quad 0.30] x_k^7 + v_k^7, \end{aligned} \quad (5.17)$$

which do not yet stabilize the plant. Indeed, an eigenvalue of the open-loop system which is located at  $\lambda = 1$  is moved to  $\lambda = 1.0036$  by the lower layer controller, emphasizing the need for a stabilizing upper control layer. For designing synchronous and asynchronous upper layer controllers, the communication cost function is parametrized as illustrated in Fig. 5.2. The number assigned to each directed edge of the graph corresponds to the cost that is charged for activating the communication link. For enabling a meaningful comparison between both schemes, they utilize the same upper layer communication topology, which has been optimized by using Theorem 3.3. The active communication links are illustrated by solid lines in Fig. 5.2.

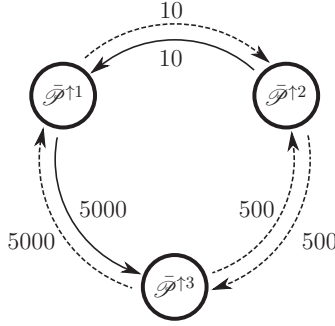


**Figure 5.2.:** Upper layer communication graph  $\mathcal{G}^{\uparrow}$ . Solid (dashed) lines denote active (inactive) communication links, and the numbers indicate the associated communication link cost.

For the depicted communication topology, the synchronous upper layer controllers are given by:

$$\begin{aligned}
 \mathcal{E}^{\uparrow 1} : v_{s\Delta k}^1 &= - [8.69 \ 47.36 \ 0.31 \ 0.13] x_{s\Delta k}^1 - [6.46 \ 5.61 \ 0.10 \ 0.06] x_{s\Delta k}^5 \dots \\
 &\quad - [7.48 \ 10.20 \ 0.19 \ 0.08] x_{s\Delta k}^6, \\
 \mathcal{E}^{\uparrow 2} : v_{s\Delta k}^2 &= - [7.39 \ 7.06 \ 0 \ 0] x_{s\Delta k}^1 - [-5.37 \ 12.50 \ 0.19 \ 0.07] x_{s\Delta k}^2 \dots \\
 &\quad - [12.00 \ 9.14 \ 0.11 \ 0.04] x_{s\Delta k}^3 - [8.63 \ 5.51 \ 0.11 \ 0.05] x_{s\Delta k}^4 \dots \\
 &\quad - [0.93 \ 0.30 \ 0 \ 0] x_{s\Delta k}^5 - [3.89 \ 1.84 \ 0.03 \ 0.01] x_{s\Delta k}^6, \\
 \mathcal{E}^{\uparrow 3} : v_{s\Delta k}^3 &= - [16.76 \ 13.25 \ 0 \ -0.01] x_{s\Delta k}^1 - [17.63 \ 15.93 \ 0.16 \ 0.05] x_{s\Delta k}^2 \dots \\
 &\quad - [-13.34 \ 11.18 \ 0.23 \ 0.09] x_{s\Delta k}^3 - [16.22 \ 8.36 \ 0.18 \ 0.08] x_{s\Delta k}^4 \dots \\
 &\quad - [2.03 \ 0.91 \ 0 \ -0.01] x_{s\Delta k}^5 - [6.92 \ 4.32 \ 0.07 \ 0.03] x_{s\Delta k}^6, \\
 \mathcal{E}^{\uparrow 4} : v_{s\Delta k}^4 &= - [18.18 \ 14.57 \ -0.02 \ -0.02] x_{s\Delta k}^1 - [15.02 \ 14.06 \ 0.14 \ 0.05] x_{s\Delta k}^2 \dots \\
 &\quad - [14.37 \ 16.09 \ 0.17 \ 0.06] x_{s\Delta k}^3 - [-9.41 \ 6.13 \ 0.31 \ 0.14] x_{s\Delta k}^4 \dots \\
 &\quad - [6.13 \ 3.28 \ 0.01 \ 0] x_{s\Delta k}^5 - [13.27 \ 9.16 \ 0.12 \ 0.05] x_{s\Delta k}^6, \\
 \mathcal{E}^{\uparrow 5} : v_{s\Delta k}^5 &= - [11.10 \ 24.04 \ 0.13 \ 0.05] x_{s\Delta k}^1 - [13.02 \ 18.84 \ 0.30 \ 0.18] x_{s\Delta k}^5 \dots \\
 &\quad - [7.05 \ 13.02 \ 0.26 \ 0.11] x_{s\Delta k}^6, \\
 \mathcal{E}^{\uparrow 6} : v_{s\Delta k}^6 &= - [17.40 \ 37.17 \ 0.19 \ 0.08] x_{s\Delta k}^1 - [10.22 \ 8.22 \ 0.16 \ 0.11] x_{s\Delta k}^5 \dots \\
 &\quad - [9.66 \ 29.95 \ 0.61 \ 0.26] x_{s\Delta k}^6, \\
 \mathcal{E}^{\uparrow 7} : v_{s\Delta k}^7 &= - [17.41 \ 9.91 \ 0.08 \ 0.03] x_{s\Delta k}^2 - [16.83 \ 14.33 \ 0.15 \ 0.05] x_{s\Delta k}^3 \dots \\
 &\quad - [10.88 \ 13.93 \ 0.24 \ 0.09] x_{s\Delta k}^4 - [20.42 \ 35.00 \ 0.87 \ 0.36] x_{s\Delta k}^7,
 \end{aligned} \tag{5.18}$$

with  $v_{s\Delta k+2}^i = v_{s\Delta k+1}^i = v_{s\Delta k}^i$  for all  $i \in \mathcal{N}$ . On the other hand, the asynchronous upper layer controllers are given by:

$$\begin{aligned}
 \mathcal{C}^{\uparrow 1} : v_{s\Delta k+1}^1 &= - \begin{bmatrix} 10.57 & 74.14 & 0.51 & 0.22 \end{bmatrix} x_{s\Delta k+1}^1 \dots \\
 &\quad - \begin{bmatrix} 9.56 & 7.36 & 0.13 & 0.08 \end{bmatrix} x_{s\Delta k+1}^5 - \begin{bmatrix} 7.49 & 12.48 & 0.26 & 0.11 \end{bmatrix} x_{s\Delta k+1}^6, \\
 \mathcal{C}^{\uparrow 2} : v_{s\Delta k}^2 &= - \begin{bmatrix} 7.07 & 11.30 & 0.03 & 0.01 \end{bmatrix} x_{s\Delta k}^1 - \begin{bmatrix} -6.06 & 19.85 & 0.32 & 0.12 \end{bmatrix} x_{s\Delta k}^2 \dots \\
 &\quad - \begin{bmatrix} 20.31 & 14.60 & 0.20 & 0.08 \end{bmatrix} x_{s\Delta k}^3 - \begin{bmatrix} 12.57 & 10.29 & 0.20 & 0.09 \end{bmatrix} x_{s\Delta k}^4 \dots \\
 &\quad - \begin{bmatrix} 0.98 & 0.80 & 0.01 & 0 \end{bmatrix} x_{s\Delta k}^5 - \begin{bmatrix} 5.64 & 4.43 & 0.07 & 0.02 \end{bmatrix} x_{s\Delta k}^6, \\
 \mathcal{C}^{\uparrow 3} : v_{s\Delta k}^3 &= - \begin{bmatrix} 19.15 & 20.61 & 0.05 & 0.01 \end{bmatrix} x_{s\Delta k}^1 - \begin{bmatrix} 32.28 & 27.03 & 0.29 & 0.10 \end{bmatrix} x_{s\Delta k}^2 \dots \\
 &\quad - \begin{bmatrix} -21.65 & 19.79 & 0.45 & 0.19 \end{bmatrix} x_{s\Delta k}^3 - \begin{bmatrix} 23.75 & 15.76 & 0.33 & 0.15 \end{bmatrix} x_{s\Delta k}^4 \dots \\
 &\quad - \begin{bmatrix} 1.96 & 2.63 & 0.02 & 0.01 \end{bmatrix} x_{s\Delta k}^5 - \begin{bmatrix} 8.92 & 9.29 & 0.13 & 0.05 \end{bmatrix} x_{s\Delta k}^6, \\
 \mathcal{C}^{\uparrow 4} : v_{s\Delta k}^4 &= - \begin{bmatrix} 20.34 & 23.44 & 0.06 & 0.01 \end{bmatrix} x_{s\Delta k}^1 - \begin{bmatrix} 27.78 & 24.63 & 0.29 & 0.10 \end{bmatrix} x_{s\Delta k}^2 \dots \\
 &\quad - \begin{bmatrix} 25.70 & 28.90 & 0.39 & 0.16 \end{bmatrix} x_{s\Delta k}^3 - \begin{bmatrix} -21.21 & 13.05 & 0.57 & 0.26 \end{bmatrix} x_{s\Delta k}^4 \dots \\
 &\quad - \begin{bmatrix} 7.17 & 6.92 & 0.06 & 0.02 \end{bmatrix} x_{s\Delta k}^5 - \begin{bmatrix} 16.50 & 16.50 & 0.18 & 0.06 \end{bmatrix} x_{s\Delta k}^6, \\
 \mathcal{C}^{\uparrow 5} : v_{s\Delta k+1}^5 &= - \begin{bmatrix} 13.36 & 32.10 & 0.16 & 0.06 \end{bmatrix} x_{s\Delta k+1}^1 \dots \\
 &\quad - \begin{bmatrix} 15.72 & 24.17 & 0.38 & 0.22 \end{bmatrix} x_{s\Delta k+1}^5 - \begin{bmatrix} 4.31 & 16.58 & 0.33 & 0.14 \end{bmatrix} x_{s\Delta k+1}^6, \\
 \mathcal{C}^{\uparrow 6} : v_{s\Delta k+1}^6 &= - \begin{bmatrix} 24.01 & 49.42 & 0.24 & 0.09 \end{bmatrix} x_{s\Delta k+1}^1 \dots \\
 &\quad - \begin{bmatrix} 13.30 & 9.87 & 0.22 & 0.15 \end{bmatrix} x_{s\Delta k+1}^5 - \begin{bmatrix} 5.95 & 41.53 & 0.88 & 0.37 \end{bmatrix} x_{s\Delta k+1}^6, \\
 \mathcal{C}^{\uparrow 7} : v_{s\Delta k+2}^7 &= - \begin{bmatrix} 22.92 & 17.67 & 0.17 & 0.06 \end{bmatrix} x_{s\Delta k+2}^2 \dots \\
 &\quad - \begin{bmatrix} 19.21 & 22.13 & 0.25 & 0.09 \end{bmatrix} x_{s\Delta k+2}^3 - \begin{bmatrix} 14.57 & 20.15 & 0.41 & 0.16 \end{bmatrix} x_{s\Delta k+2}^4 \dots \\
 &\quad - \begin{bmatrix} 19.59 & 47.72 & 1.08 & 0.44 \end{bmatrix} x_{s\Delta k+2}^7, \tag{5.19}
 \end{aligned}$$

with  $v_{s\Delta k+2}^i = v_{s\Delta k+1}^i = v_{s\Delta k}^i$  for  $i \in \mathcal{C}^1$ ,  $v_{s\Delta k+3}^i = v_{s\Delta k+2}^i = v_{s\Delta k+1}^i$  for  $i \in \mathcal{C}^2$ , and  $v_{s\Delta k+4}^i = v_{s\Delta k+3}^i = v_{s\Delta k+2}^i$  for  $i \in \mathcal{C}^3$ . The asynchronous upper layer control law does not exchange memory states, since according to Corollary 4.1, this would not lead to a performance improvement with the underlying upper layer communication graph. Both upper layer controllers have entries of significant magnitude, such that an observable cooperative influence on the lower layer can be expected.

### 5.3. Simulation Results and Discussion

With the help of the results presented in Sec. 3.4.4, the performance of the closed-loop system is measured in the sense of Case 2.2, with  $x_0 \sim \mathcal{N}(0, I)$ . For being able to compare both, the synchronous and the asynchronous hierarchical control



scheme with existing approaches, additional controllers have been designed by using standard methods from optimal control theory.

**Table 5.1.:** Comparison of different types of controllers applied to the power system model for  $x_0 \sim \mathcal{N}(0, I)$ . Even though the lower layer controller designed with neglected interconnections is unstable, both resulting hierarchical controllers are stable and yield a performance close to the (optimal) one of a centralized LQR. Note that the calculation time for the synchronous scheme includes SCT design, while the time for the asynchronous scheme does not.

controller	design model	calc. time	time domain	$E(J)$	$J^{\text{com}}$
lower layer	$\bar{\mathcal{P}}'$	5 [s]	$\mathbb{T}^\downarrow$	(unstable)	0
lower layer	$\bar{\mathcal{P}}$	5 [s]	$\mathbb{T}^\downarrow$	560632	0
hierarchical (synchronous)	$\bar{\mathcal{P}}^\uparrow$	143 [s]	$\mathbb{T}^\downarrow, \mathbb{T}^\uparrow$	399866	5010
hierarchical (asynchronous)	$\bar{\mathcal{P}}_\varphi^\uparrow$	96 [s]	$\mathbb{T}^\downarrow, \mathbb{T}^\downarrow$	388512	5010
centralized LQR	$\bar{\mathcal{P}}$	< 1 [s]	$\mathbb{T}^\downarrow$	360775	11020
centralized LQR	$\bar{\mathcal{P}}^\uparrow$ w. $\bar{K}^\downarrow = 0$	< 1 [s]	$\mathbb{T}^\uparrow$	440853	11020

Table 5.1 shows a comparison of different types of controllers applied to the discretized power system model. Regarding the expected performance  $E(J)$ , it is interesting to see that both hierarchical control schemes yield a good performance, even though their underlying lower control layer is unstable, when applied to the original system alone. Indeed, the performance is within an 11 percent range above the optimal performance obtained with a centralized linear quadratic regulator, while using only a fraction of the possible communication links. Furthermore, the performance of both hierarchical schemes is closer to the one of an LQR implemented on  $\mathbb{T}^\downarrow$  than to the one of an LQR implemented on  $\mathbb{T}^\uparrow$ . Hence, the lower control layer obviously plays an important part in the two-layer scheme. Additionally, the performance of a sole lower layer controller that has been designed considering all plant interconnections is significantly worse than those of the hierarchical control schemes. Consequently, one can deduce that the presented two-layer concept indeed makes sense from the viewpoint of closed-loop performance, since both control layers truly cooperate for maximizing the performance.

Concerning computation time, the LMI-based methods are clearly outperformed by the LQR design, which is due to the computational efficacy of the Riccati equation. However, the LQR design is not able to consider communication constraints. For SCT design, computing the synchronous hierarchical controller takes about 2.5

minutes, meaning that the approach has the potential to be applied to larger systems. This computation time is a significant improvement compared to single layer approaches which rely on mixed-integer programming. For instance, the approach presented in [50] typically takes several hours for finding a distributed single layer controller for the power system model. Due to the periodic model, which requires a larger number of linear matrix inequalities for constructing a suitable Lyapunov function, the asynchronous hierarchical scheme requires more computation time than the synchronous approach. However, for the power system example, designing an asynchronous hierarchical controller for a given upper layer communication topology also just took about 1.5 minutes.

With a parametrization of the communication cost function  $J^{\text{com}}$  as shown in Fig. 5.2, the communication topology that has been optimized within the synchronous hierarchical control framework only uses one third of the available communication links. Interestingly, the link  $\bar{\sigma}_{2,1}^{\downarrow}$  is not being used, although its cost is very cheap compared to the other communication links. On the other hand,  $\bar{\sigma}_{3,1}^{\uparrow}$  is activated despite its high cost. Hence, one can deduce that the information transmitted via  $\bar{\sigma}_{3,1}^{\uparrow}$  is far more important for the global closed-loop performance than the information transmitted via  $\bar{\sigma}_{2,1}^{\downarrow}$ . The different contributions of the single communication links is also emphasized by the following calculation: Recall from Table 5.1 that the performance when using either all, or none, of the upper layer communication links is 360755, or 560632, respectively. Assuming that all communication links equally contribute to the global closed-loop performance, one would expect a performance of about 427381 when using one third of the available links. However, the performance of the hierarchical control schemes is better than this expectation.

In the sequel, the time behavior of the power system is analyzed for selected types of controllers. To this end, a series of simulations has been performed with the power system model, assuming the initial state given in Eq. (5.11). Each of the following figures shows the trajectories of the local frequencies  $\omega_k^i$  at nodes 1 to 7 for 200 time steps, which is an important indicator for the synchronization of the generator buses. The finite sum:

$$\check{J} := \sum_{k=0}^{2000} \bar{z}_k^T \bar{z}_k < J \quad (5.20)$$

and the largest frequency magnitude for  $k \geq 170$  are taken as finite horizon performance indicators.

Fig. 5.3 shows the frequency trajectories of the uncontrolled system, which is marginally stable due to a pole at  $\lambda = 1$ . Nevertheless, it can be seen that the frequencies slowly approach the equilibrium point. After 170 time-steps, the largest frequency magnitude has a value of 0.0772, and  $\check{J} = 5837$ . In Fig. 5.4, it is shown how the performance of the closed-loop system can be improved by a lower layer controller designed with  $\bar{\mathcal{P}}$ , i.e. under consideration of all interconnections. The largest frequency magnitude after 170 time-steps is 0.0498, and  $\check{J}$  has been decreased

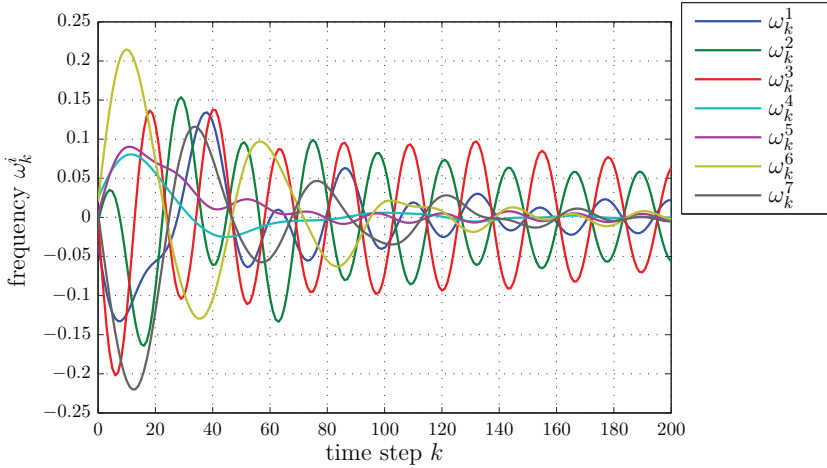


**Figure 5.3.:** Trajectories of the frequencies  $\omega_k^i$  for the first 200 time steps of the uncontrolled system. The largest magnitude of the frequency deviation for  $k \geq 170$  is 0.0772.

to  $\check{J} = 3.3727$ .

Figures 5.5 and 5.6 show the frequency trajectories obtained with the synchronous and the asynchronous hierarchical control scheme, respectively. The largest frequency magnitude after 170 time-steps and the value of  $\check{J}$  are, respectively, 0.0346 and 0.0268 as well as 3212 and 3109. Hence, the chosen finite horizon performance indicators qualitatively match the expected infinite horizon performance stated in Table 5.1. Finally, Fig. 5.7 shows the trajectories obtained with a linear quadratic regulator implemented on  $\mathbb{T}^\downarrow$ . Here, the largest frequency magnitude after 170 time-steps is 0.0152, and  $\check{J} = 2924.2$ .

Finally, in Fig. 5.8, the different control schemes are analyzed with consideration of communication time delay. For simplicity, it is assumed here that the time delay is constant and equal for all communication links, which suffices to demonstrate that the hierarchical control schemes possess a certain robustness against communication time delay. The duration of the delay is varied from zero up to 70 percent of the discretization time  $T = 0.1$  [s]. As can be seen, all considered control schemes manage to stabilize the power system model, even under the influence of the largest time delay<sup>1</sup>. Furthermore, the finite horizon performance index  $\check{J}$  increases only moderately up to 1.7 percent.

<sup>1</sup>The closed-loop system is still stable for time-delays greater than  $0.7T$ . The critical value was not determined here.

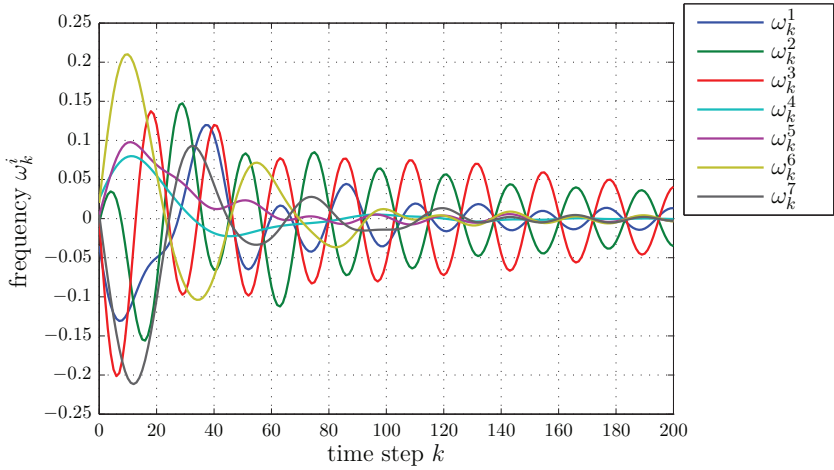


**Figure 5.4.:** Trajectories of the frequencies  $\omega_k^i$  for the first 200 time steps with the lower layer controller designed with  $\mathcal{P}$ . The largest magnitude of the frequency deviation for  $k \geq 170$  is 0.0498, and  $\bar{J} = 3372.7$ .

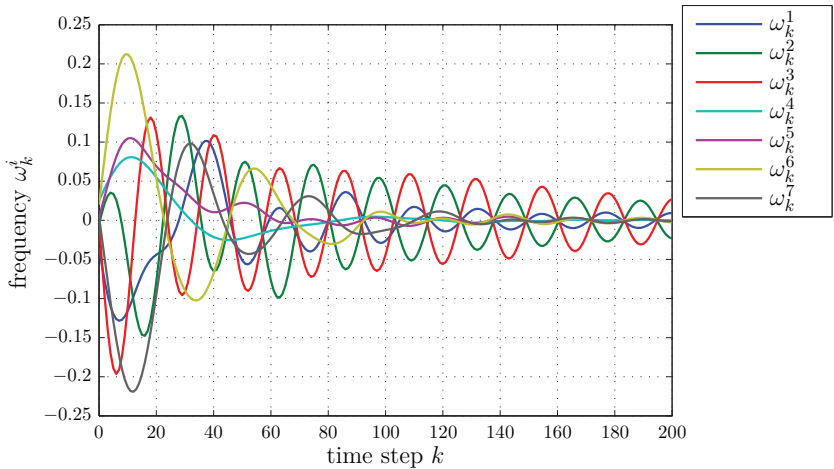


**Figure 5.5.:** Trajectories of the frequencies  $\omega_k^i$  for the first 200 time steps with the synchronous hierarchical controller. The largest magnitude of the frequency deviation for  $k \geq 170$  is 0.0346, and  $\bar{J} = 3212$ .

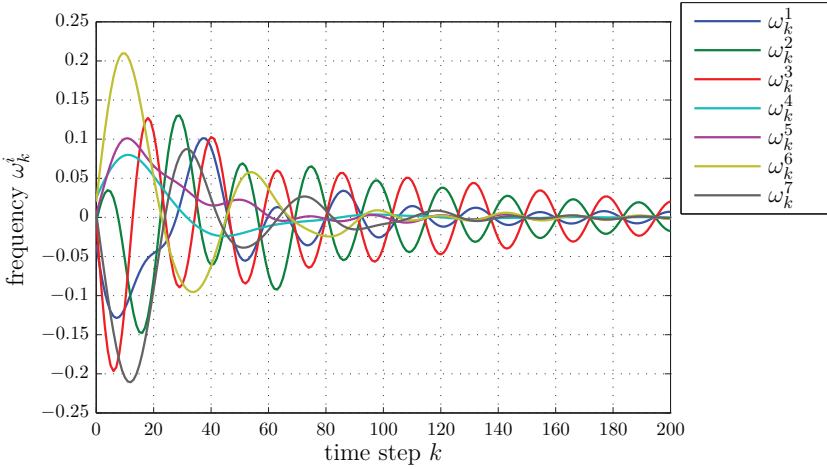


**Figure 5.6.:** Trajectories of the frequencies  $\omega_k^i$  for the first 200 time steps with the asynchronous hierarchical controller. The largest magnitude of the frequency deviation for  $k \geq 170$  is 0.0268, and  $\check{J} = 3109$ .

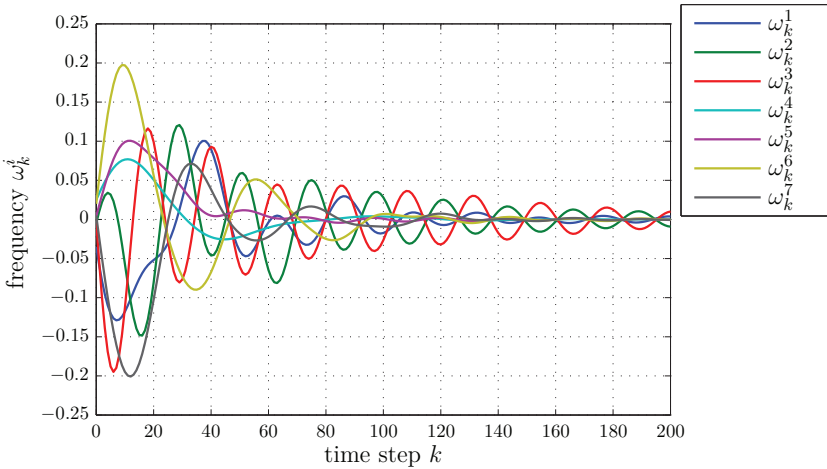


**Figure 5.7.:** Trajectories of the frequencies  $\omega_k^i$  for the first 200 time steps with the centralized linear quadratic regulator implemented on  $\mathbb{T}^4$ . The largest magnitude of the frequency deviation for  $k \geq 170$  is 0.0152, and  $\check{J} = 2924.2$ .

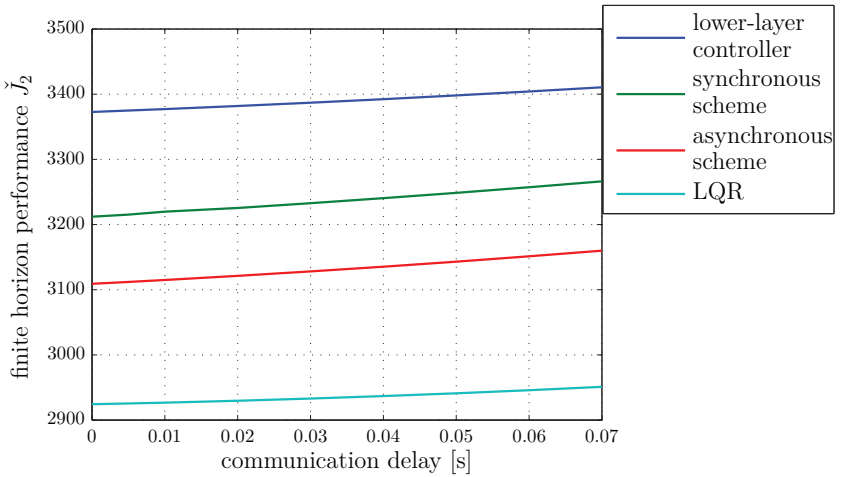


**Figure 5.8.:** Finite horizon performance index  $\check{J}$  of the investigated control schemes as a function of the communication time delay. All control schemes manage to stabilize the system under constant time delay, while the finite horizon performance  $\check{J}$  degrades up to 1.7 percent.



## **Part III.**

# **Distributed and Hierarchical Control of Uncertain Systems**





# 6. Distributed Control of Interconnected Jump Markov Systems

The second part of this thesis focused on interconnected systems with linear, time-invariant dynamics. In this chapter, as well as in the subsequent one, the approaches presented so far are extended to a more general class of dynamic systems, namely the class of jump Markov systems. These are a class of hybrid dynamic systems, where the modeling parameters (e.g., the matrices  $A$  to  $E$  of a linear system) depend on a time-varying variable which is taken from a discrete finite set. Jump Markov systems are particularly suited to model abrupt and random changes in system behavior, like component failures, communication link breakdowns, packet losses, or environmental changes, to name a few. The probabilistic occurrence of such events is modeled by a Markov chain, which selects the current parameters or *mode* of the dynamic model. Thus, in contrast to the periodic systems introduced in Chap. 4, the temporal evolution of the model parameters is uncertain.

This chapter presents an approach for designing distributed state-feedback controllers for interconnected jump Markov systems with linear dynamics. That is, each subsystem is modeled by a local Markov chain, determining its stochastic parameter evolution. In contrast to the second part of this thesis, a notion of different modeling and control layers is not established here, as a focus is on the treatment of uncertain communication links. Thus, the layer indicators  $(\cdot)^\downarrow$  and  $(\cdot)^\uparrow$  are not required. In large parts, the contents of this chapter are based on results previously presented in [128]. Starting with a set of interconnected jump Markov systems, the approach adopts and refines a procedure which was already sketched in [82] and [139]. The main idea of this first step towards distributed control design is to transform the subsystems into a partitioned centralized model, which is afterwards used as basis for the actual control design. Furthermore, the stochastic framework underlying the jump Markov systems allows to consider probabilistic communication uncertainties already in the control design. Together with the basic setup, this will be explained in more detail in the following section. Afterwards, Sec. 6.2 presents the construction of the centralized model, which serves as basis for the development of the control synthesis conditions in Sec. 6.3. Finally, in Sec. 6.4, the effectiveness of the approach is shown by means of a numerical example, followed by a concluding discussion in Sec. 6.5.

## 6.1. Problem Setup

The class of dynamic models considered in this chapter are interconnected discrete-time jump Markov linear systems  $\{\mathcal{P}_\theta^i\}_{i \in \mathcal{N}_s}$ , consisting of  $N_s$  interconnected subsystems of the form:

$$\mathcal{P}_\theta^i : \begin{cases} x_{k+1}^i = A_{i,i}[\theta_k^i]x_k^i + B_{i,i}[\theta_k^i]u_k^i + E_{i,i}[\theta_k^i]w_k^i + r_{x,k}^i[\theta_k^i], \\ z_k^i = C_{i,i}[\theta_k^i]x_k^i + D_{i,i}[\theta_k^i]u_k^i + r_{z,k}^i[\theta_k^i], \\ \mathcal{M}^i = (\Theta^i, P^i, \mu_0^i), \end{cases} \quad (6.1)$$

with local controlled variables  $z_k^i \in \mathbb{R}^{n_z^i}$  and local Markov chains  $\mathcal{M}^i$ . The states  $\theta_k^i \in \Theta^i$  of these Markov chains correspond to the local modes of the subsystems. The signals  $r_{x,k}^i[\theta_k^i]$  and  $r_{z,k}^i[\theta_k^i]$  model the interconnections between the subsystems, and are defined as:

$$r_{x,k}^i[\theta_k^i] = \sum_{j \in \mathcal{N}_s^i} A_{i,j}[\theta_k^i]x_k^j + B_{i,j}[\theta_k^i]u_k^j + E_{i,j}[\theta_k^i]w_k^j, \quad (6.2a)$$

$$r_{z,k}^i[\theta_k^i] = \sum_{j \in \mathcal{N}_s^i} C_{i,j}[\theta_k^i]x_k^j + D_{i,j}[\theta_k^i]u_k^j. \quad (6.2b)$$

The state of each subsystem is fully described by the local hybrid state  $\zeta_k^i = (x_k^i, \theta_k^i)$ , which is assumed to be measurable by  $\mathcal{P}_\theta^i$ . Hence, each subsystem must be equipped with suitable sensing equipment to measure its local state variables. Since the local mode often models component failures, the subsystems need to perform online failure detection.

The goal pursued in this chapter is to design a distributed control law for  $\{\mathcal{P}_\theta^i\}_{i \in \mathcal{N}_s}$  which minimizes the performance index  $J$  according to Case 2.1 or Case 2.2. In contrast to Chapters 3 and 4, SCT design will not be considered, such that a communication cost does not need to be taken into account. The reason for this will be explained later. Recall that  $\mathcal{R}_k^i \subseteq \mathcal{N}_s$  denotes the index set of subsystems transmitting their local (hybrid) state  $\zeta_k^i$  to the subsystem  $\mathcal{P}_\theta^i$  at time  $k$ . With the help of  $\mathcal{R}_k^i$ , the general form of an admissible distributed control law can be stated as:

$$\mathcal{E}^i : u_k^i = \kappa^i(\zeta_k^i), \quad (6.3)$$

where

$$\zeta_k^i := \{\zeta_k^i = (x_k^i, \theta_k^i) \mid i \in \mathcal{R}_k^i\} \quad (6.4)$$

denotes the set of hybrid states available to  $\mathcal{P}_\theta^i$  at time  $k$ .

In contrast to the previous approaches, communication uncertainties are explicitly considered within this approach. To this end, the communication network model is extended by stochastic communication link failures as explained in detail in Sec.

2.2. The evolution of the network topology over time is modeled by the state  $\theta_{\Sigma,k}$  of a Markov chain  $\mathcal{M}_{\Sigma}$ , see Eq. (2.37) on page 33. Hence, the communication network topology is captured by the time-varying adjacency matrix:

$$\Sigma[\theta_{\Sigma,k}] \in \Sigma \subset \mathbb{B}^{N_s \times N_s}, \quad (6.5)$$

such that:

$$\mathcal{R}_k^i := \mathcal{R}^i[\theta_{\Sigma,k}] = \{j \in \mathcal{N}_s \mid \sigma_{i,j}[\theta_{\Sigma,k}] = 1\}. \quad (6.6)$$

Focusing on linear control laws as in the previous chapters, the sought local control laws  $\mathcal{E}^i$  thus take the specific form:

$$\mathcal{E}^i : u_k^i = K_{i,i}[\theta_k^1, \dots, \theta_k^{N_s}, \theta_{\Sigma,k}] x_k^i + \sum_{j \in \mathcal{R}_k^i \setminus \{i\}} K_{i,j}[\theta_k^1, \dots, \theta_k^{N_s}, \theta_{\Sigma,k}] x_k^j, \quad (6.7)$$

where  $K_{i,j}[\cdot] \in \mathbb{R}^{n_i \times n_j}$  denotes the block-entries of a matrix  $K[\cdot] = [K_{i,j}[\cdot]]$ . The associated time-varying communication graph is denoted by  $\mathcal{G}_k$ . Figure 6.1 illustrates the resulting distributed control structure for  $N_s = 3$  interconnected subsystems  $\mathcal{P}_{\theta}^i$ .

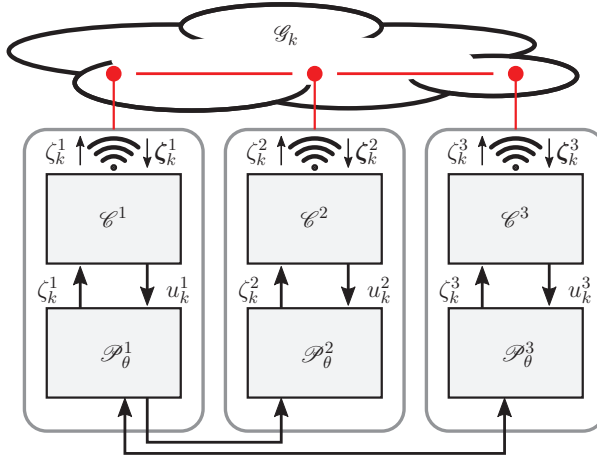


**Figure 6.1.:** Implementation of the distributed control scheme for the exemplary case of  $N_s = 3$  subsystems.

## 6.2. Centralized Modeling of Interconnected JMLS

In the sequel, a procedure is introduced which allows to model an interconnected jump Markov linear system  $\{\mathcal{P}_{\theta}^i\}_{i \in \mathcal{N}_s}$  in a centralized manner. In contrast to a

monolithic JMLS, this modeling procedure leads to a *partitioned* JMLS  $\mathcal{P}_\theta$ , containing additional information which allow to recover the original subsystem structure. As a first step of the procedure, a parallel composition of the Markov chains  $\mathcal{M}^i$  is performed, resulting in an extended Markov chain  $\mathcal{M}$  with combined Markov state  $\theta_k$ . Then, in a second step, the matrices describing the partitioned JMLS are constructed as a function of  $\theta_k$  and  $\theta_{\Sigma,k}$ .

Since the transitions of the single Markov chains  $\mathcal{M}^i$  may occur independently, all possible combinations of the elements of the local discrete state-spaces  $\Theta^i$  have to be taken into account when constructing the extended Markov chain  $\mathcal{M}$ . By the help of the cartesian product, the state-space  $\Theta$  of the extended Markov chain can thus be constructed as:

$$\Theta := \Theta^1 \times \dots \times \Theta^{N_s} = \times_{i=1}^{N_s} \Theta^i. \quad (6.8)$$

Consequently,  $\Theta$  contains  $N_\theta := \text{card}(\Theta) = \prod_{i=1}^{N_s} N_\theta^i$  elements. For the construction of the corresponding transition probability matrix  $P$  and initial distribution  $\mu_0$ , consider the special case  $N_s = 2$  first: In this case, each transition from  $\theta_k$  to  $\theta_{k+1}$  of the extended Markov state, denoted by  $\theta_k \rightarrow \theta_{k+1}$ , corresponds to a combination of simultaneous transitions  $\theta_k^1 \rightarrow \theta_{k+1}^1$  and  $\theta_k^2 \rightarrow \theta_{k+1}^2$ . The corresponding transition probabilities for these simultaneous transitions follow from the product of the corresponding entries of  $P^1$  and  $P^2$ . The initial distribution is determined in a similar manner. For the construction of the extended Markov state given in Eq. (6.8), the overall transition probability matrix  $P$  and the initial distribution  $\mu_0$  can be conveniently constructed by the help of the Kronecker product. Hence, the parallel composition of two local Markov chains  $\mathcal{M}^1$  and  $\mathcal{M}^2$ , which is denoted by  $\mathcal{M}^1 \parallel \mathcal{M}^2$ , is given by:

$$\mathcal{M}^1 \parallel \mathcal{M}^2 := (\Theta^1 \times \Theta^2, P^1 \otimes P^2, \mu_0^1 \otimes \mu_0^2). \quad (6.9)$$

Similar schemes exist for the parallel composition of continuous-time Markov processes [68] and of Markov reward chains [89]. For the general case of  $N_s > 2$ , simply letting:

$$\mathcal{M} := (((\mathcal{M}^1 \parallel \mathcal{M}^2) \parallel \mathcal{M}^3) \parallel \dots) \parallel \mathcal{M}^{N_s}, \quad (6.10)$$

and applying Eq. (6.9) multiple times leads to:

$$\mathcal{M} = (\times_{i=1}^{N_s} \Theta^i, \otimes_{i=1}^{N_s} P^i, \otimes_{i=1}^{N_s} \mu_0^i). \quad (6.11)$$

From the definition of the cartesian product, the elements  $\theta$  of  $\Theta$  take the form of  $N_s$ -tuples  $(\theta^1, \dots, \theta^{N_s})$ . To conform with the basic definition of a JMLS, the extended Markov states  $\theta$  may be relabeled with natural numbers, such that  $\Theta = \mathbb{I}_{N_\theta}$ . For being able to recover the original subsystem structure later, a bijective function

$\Psi(\cdot)$  is introduced as proposed in [139]. This function maps the relabeled extended Markov state to the corresponding  $N_s$ -tuple of local Markov states:

$$\Psi : \Theta \rightarrow \Theta^1 \times \dots \times \Theta^{N_s}, \quad \theta \mapsto (\theta^1, \dots, \theta^{N_s}). \quad (6.12)$$

In contrast to [139], explicit formulas for constructing  $\Psi(\cdot)$  are given in the sequel. Furthermore, the function:

$$\Psi_i : \Theta \rightarrow \Theta^i, \quad \theta \mapsto \theta^i, \quad (6.13)$$

with  $i \in \mathcal{N}_s$  is introduced, which extracts the  $i$ -th local Markov state from  $\theta_k$ . Both,  $\Psi$  and  $\Psi_i$  will be required later for constructing the partitioned JMLS, and for implementing the distributed control law.

**Definition 6.1** ([128]). *For  $\mathcal{M}$  constructed according to Eq. (6.11), and  $\theta \in \Theta = \mathbb{I}_{N_\theta}$ , the function  $\Psi_i$  with  $i \in \mathcal{N}_s$  is given by:*

$$\Psi_i(\theta) := \left\lceil \frac{\theta}{\prod_{j=i+1}^{N_s} N_\theta^j} \right\rceil \bmod_1 N_\theta^i. \quad (6.14)$$

Here,  $\lceil \cdot \rceil$  denotes the ceil function, i.e. rounding up to the next integer, and  $\bmod_1$  is a shifted modulus function, defined as:

$$n \bmod_1 m := ((n - 1) \bmod m) + 1, \quad (6.15)$$

such that  $n \bmod_1 n = n$ . □

The function  $\Psi_i(\theta)$  can be derived as follows: From the definition of the cartesian product of ordered sets, the local Markov state  $\theta^{N_s}$  and the extended Markov state  $\theta$  are related according to:

$$\theta = m N_\theta^{N_s} + \theta^{N_s} \quad (6.16)$$

for  $\theta^{N_s} \in \Theta^{N_s}$  and  $m \in \mathbb{N}_0$ . Thus:

$$\theta^{N_s} = ((\theta - 1) \bmod N_\theta^{N_s}) + 1 = \theta \bmod_1 N_\theta^{N_s}. \quad (6.17)$$

Suppose now that  $\theta^i$  is the Markov state to be extracted from  $\theta$ . Assuming that the value of  $\theta$  is increased, it follows from the structure of  $\Theta$  that one has to traverse all combinations of Markov states  $\theta^j$  with  $i, j \in \mathcal{N}_s$  and  $j > i$ , until  $\theta^i$  is either incremented or reset to one. In contrast, recall that for  $\theta^{N_s}$  being the state of interest, every change of  $\theta$  causes a change of  $\theta^{N_s}$ , which allows to extract  $\theta^{N_s}$  by means of Eq. (6.14). Motivated by this observation, consider the virtual extended Markov state:

$$\theta'(i) := \left\lceil \frac{\theta}{\prod_{j=i+1}^{N_s} N_\theta^j} \right\rceil, \quad (6.18)$$

which changes its value if and only if the value of  $\theta^i$  in  $\theta$  is changed. This is accomplished by dividing  $\theta$  by the number of the aforementioned combinations of Markov states, and by rounding up the resulting quotient to the next integer. In particular, note that  $\theta'(N_s) = \theta$ . Due to the construction of  $\theta'(i)$ , it holds that:

$$\theta'(i) = mN_\theta^i + \theta^i \quad (6.19)$$

for  $\theta^i \in \Theta^i$  and  $m \in \mathbb{N}_0$ . Solving for  $\theta^i$  in a similar manner as in Eq. (6.17) leads to Eq. (6.14).

Since  $\Psi = (\Psi_1, \dots, \Psi_{N_s})$ , Definition 6.1 can also be used for calculating  $\Psi$ .

**Definition 6.2** ([128]). *The inverse of the function  $\Psi(\cdot)$  is defined as:*

$$\Psi^{-1} : \Theta^1 \times \dots \times \Theta^{N_s} \rightarrow \Theta, \quad (\theta^1, \dots, \theta^{N_s}) \mapsto \theta, \quad (6.20)$$

and is given by:

$$\Psi^{-1}(\theta^1, \dots, \theta^{N_s}) := \theta^{N_s} + \sum_{i=1}^{N_s-1} \left( (\theta^i - 1) \prod_{j=i+1}^{N_s} N_\theta^j \right). \quad (6.21)$$

□

The inverse function  $\Psi^{-1}(\cdot)$  is obtained by enumerating the ordered set  $\Theta = \Theta^1 \times \dots \times \Theta^{N_s}$ , which leads to the correspondence:

$$\begin{aligned} (\theta^1, \dots, \theta^{N_s}) \triangleq & \theta^{N_s} + (\theta^{N_s-1} - 1)N_\theta^{N_s} + (\theta^{N_s-2} - 1)N_\theta^{N_s}N_\theta^{N_s-1} + \dots \\ & + (\theta^1 - 1)N_\theta^{N_s}N_\theta^{N_s-1} \dots N_\theta^2 = \Psi^{-1}(\theta^1, \dots, \theta^{N_s}). \end{aligned} \quad (6.22)$$

Rewriting the middle part of the equation directly leads to Eq. (6.21).

For constructing the partitioned JMLS  $\mathcal{P}_\theta$ , introduce the partitioned state vector:

$$x_k := (x_k^1; \dots; x_k^{N_s}) \in \mathbb{R}^{n_x}, \quad (6.23)$$

with  $n_x = \sum_{i=1}^{N_s} n_x^i$ . The partitioned input vector  $u_k \in \mathbb{R}^{n_u}$ , the partitioned disturbance vector  $w_k \in \mathbb{R}^{n_w}$ , and the partitioned vector of controlled variables  $z_k \in \mathbb{R}^{n_z}$ , as well as their respective dimensions, are analogously defined. Arranging the matrices describing the subsystems  $\mathcal{P}_\theta^i$  according to the definitions of  $\theta_k$  and the vectors  $x_k$ ,  $u_k$ ,  $w_k$ , and  $z_k$ , the partitioned JMLS is obtained as:

$$\mathcal{P}_\theta : \begin{cases} x_{k+1} = A[\theta_k]x_k + B[\theta_k]u_k + E[\theta_k]w_k, \\ z_k = C[\theta_k]x_k + D[\theta_k]u_k, \\ \mathcal{M} = (\Theta, P, \mu_0), \\ x_0 = (x_0^1; \dots; x_0^{N_s}). \end{cases} \quad (6.24)$$

The corresponding matrices are constructed as:

$$A[\theta_k] = \begin{bmatrix} A_{1,1}[\Psi_1(\theta_k)] & \dots & A_{1,N_s}[\Psi_1(\theta_k)] \\ \vdots & \ddots & \vdots \\ A_{N_s,1}[\Psi_{N_s}(\theta_k)] & \dots & A_{N_s,N_s}[\Psi_{N_s}(\theta_k)] \end{bmatrix}, \quad (6.25)$$

with analogous definitions for  $B[\theta_k]$  to  $E[\theta_k]$ .

**Remark 6.1.** For the subsequent control synthesis, it will be necessary that  $\mathcal{M}$  is a homogeneous Markov chain. This is ensured by assuming all local Markov chains  $\mathcal{M}^i$  to be homogeneous. However, as stated in [139], this assumption is sufficient but not necessary for  $\mathcal{M}$  to be homogeneous. Indeed, there may exist interdependencies between the local Markov states  $\theta^i$ , which can be captured by a homogeneous Markov chain  $\mathcal{M}$ . However, in such a case, the construction formulas for the functions  $\Psi(\cdot)$  and  $\Psi^{-1}(\cdot)$  will not be valid anymore.  $\triangle$

### 6.3. Distributed Controller Design

In this section, an approach to the optimization-based design of a distributed, time-varying state-feedback controller for the interconnected JMLS  $\{\mathcal{P}_\theta^i\}_{i \in N_s}$  will be presented. To this end, the partitioned JMLS  $\mathcal{P}_\theta$  will be used as an equivalent description of the interconnected JMLS. In terms of  $\mathcal{P}_\theta$ , the sought linear control law stated in (6.7) takes the simplified matrix form:

$$\begin{bmatrix} u_k^1 \\ \vdots \\ u_k^{N_s} \end{bmatrix} = \begin{bmatrix} K_{1,1}[\theta_k, \theta_{\Sigma,k}] & \dots & K_{1,N_s}[\theta_k, \theta_{\Sigma,k}] \\ \vdots & \ddots & \vdots \\ K_{N_s,1}[\theta_k, \theta_{\Sigma,k}] & \dots & K_{N_s,N_s}[\theta_k, \theta_{\Sigma,k}] \end{bmatrix} \begin{bmatrix} x_k^1 \\ \vdots \\ x_k^{N_s} \end{bmatrix}, \quad (6.26)$$

with gain matrices  $K_{i,j}[\theta_k, \theta_{\Sigma,k}] \in \mathbb{R}^{n_u^i \times n_x^j}$ . Hence, the closed-loop system  $\mathcal{P}_{\theta,\text{cl}}$  resulting from  $\mathcal{P}_\theta$  with controller (6.26) depends on the states of the Markov chains  $\mathcal{M}$  and  $\mathcal{M}_\Sigma$ :

$$\mathcal{P}_{\theta,\text{cl}} : \begin{cases} x_{k+1} = (A[\theta_k] + B[\theta_k]K[\theta_k, \theta_{\Sigma,k}])x_k + E[\theta_k]w_k = A_{\text{cl}}[\theta_k, \theta_{\Sigma,k}]x_k + E[\theta_k]w_k, \\ z_k = (C[\theta_k] + D[\theta_k]K[\theta_k, \theta_{\Sigma,k}])x_k = C_{\text{cl}}[\theta_k, \theta_{\Sigma,k}]x_k, \\ \mathcal{M} = (\Theta, P, \mu_0), \mathcal{M}_\Sigma = (\Theta_\Sigma, P_\Sigma, \mu_{\Sigma,0}), \\ x_0 = (x_0^1; \dots; x_0^{N_s}). \end{cases} \quad (6.27)$$

It will be essential to ensure that the local controllers  $\mathcal{C}^i$  only use the information that is actually available to them according to the current topology  $\Sigma[\theta_{\Sigma,k}]$  of the communication network. Hence, each local control input  $u_k^i$  must only depend on the set  $\zeta_k^i$  of hybrid states that are transmitted to  $\mathcal{C}^i$  at time  $k$ . The dependency



of  $u_k^i$  on local states  $x_k^j$  with  $j \in \mathcal{N}_s^i$  can be restricted to those  $x_k^j$  with  $j \in \mathcal{R}^i[\theta_{\Sigma,k}]$  by ensuring that:

$$\sigma_{i,j}[\theta_{\Sigma,k}] = 0 \quad \Rightarrow \quad K_{i,j}[\theta_k, \theta_{\Sigma,k}] = 0_{n_i^i \times n_x^j} \quad (6.28)$$

for all  $i, j \in \mathcal{N}_s$ ,  $\theta \in \Theta$ , and  $\theta_{\Sigma} \in \Theta_{\Sigma}$ . For restricting the dependency of  $u_k^i$  on the local Markov states  $\theta^j$  with  $j \in \mathcal{N}_s^i$  to those  $\theta^j$  with  $j \in \mathcal{R}^i[\theta_{\Sigma,k}]$ , temporarily assume that  $\theta_{\Sigma,k} = \theta_{\Sigma}$  is constant. This assumption will later be dropped again and thus, does not lead to any restrictions. For any fixed  $\theta_{\Sigma} \in \Theta_{\Sigma}$ , it must be ensured that:

$$K_{i,:}[\theta_k, \theta_{\Sigma}] = K_{i,:}[\theta_{k+1}, \theta_{\Sigma}] \quad (6.29)$$

for any two extended Markov states  $\theta_k \neq \theta_{k+1}$  which can not be distinguished by the local controller  $\mathcal{C}^i$ . This situation occurs whenever a transition  $\theta_k \rightarrow \theta_{k+1}$  does not affect the local Markov states  $\theta_k^j$  with  $j \in \mathcal{R}^i[\theta_{\Sigma,k}]$  which are transmitted to the controller  $\mathcal{C}^i$ . Thus, the controller  $\mathcal{C}^i$  is not aware of the transition  $\theta_k \rightarrow \theta_{k+1}$ . In this context, consider the following result:

**Lemma 6.1.** *Given a constant communication topology  $\Sigma[\theta_{\Sigma}] \in \Sigma$ , the local controller  $\mathcal{C}^i$  is aware of the transition  $\theta_k \rightarrow \theta_{k+1}$  of the extended Markov state, i.e. it can distinguish  $\theta_k$  and  $\theta_{k+1}$ , if and only if:*

$$\gamma_i(\theta_k, \theta_{k+1}, \theta_{\Sigma}) := \sum_{j=1}^{N_s} \sigma_{i,j}[\theta_{\Sigma}] \|\Psi_j(\theta_k) - \Psi_j(\theta_{k+1})\| > 0. \quad (6.30)$$

□

*Proof.* The value of the  $j$ -th local Markov state  $\theta_k^j$  changes from time  $k$  to time  $k+1$  if and only if:

$$\|\theta_k^j - \theta_{k+1}^j\| > 0. \quad (6.31)$$

Substituting  $\theta_k^j$  by  $\Psi_j(\theta_k)$ , the above equation can be expressed in terms of the extended Markov state  $\theta_k$ . Hence, a transition  $\theta_k \rightarrow \theta_{k+1}$  of the extended Markov state includes a change of the local Markov state  $\theta_k^j$  to  $\theta_{k+1}^j \neq \theta_k^j$  if and only if:

$$\|\Psi_j(\theta_k) - \Psi_j(\theta_{k+1})\| > 0. \quad (6.32)$$

According to the definition of the adjacency matrix  $\Sigma[\theta_{\Sigma}]$ , the local Markov state  $\theta_k^j$  can be transmitted to controller  $\mathcal{C}^i$  if and only if  $\sigma_{i,j}[\theta_{\Sigma}] > 0$ . Hence, controller  $\mathcal{C}^i$  is aware of the transition  $\theta_k \rightarrow \theta_{k+1}$  if:

$$\sigma_{i,j}[\theta_{\Sigma}] \|\Psi_j(\theta_k) - \Psi_j(\theta_{k+1})\| > 0, \quad (6.33)$$

i.e. if the value of  $\theta_k^j$  changes and is transmitted to  $\mathcal{C}^i$ . Since changes of any local Markov state received by  $\mathcal{C}^i$  can be recognized, controller  $\mathcal{C}^i$  is aware of a transition  $\theta_k \rightarrow \theta_{k+1}$  if (6.30) holds.

To prove necessity, assume that  $\gamma_i(\theta_k, \theta_{k+1}, \theta_\Sigma) = 0$  and that  $\mathcal{C}^i$  is aware of  $\theta_k \rightarrow \theta_{k+1}$  with  $\theta_{k+1} \neq \theta_k$ . Since  $\gamma_i(\theta_k, \theta_{k+1}, \theta_\Sigma) = 0$ , either  $\sigma_{i,j}[\theta_\Sigma] = 0$  or  $\theta_k^j = \theta_{k+1}^j$  for all  $j \in \mathcal{N}_s$ . Hence, all local Markov states received by  $\mathcal{C}^i$  (including  $\theta_k^i$ ) do not change, which is a contradiction to the assumptions made before.  $\square$

Lemma 6.1 can now be used to state the condition for requesting constraint (6.29), leading to the implication:

$$\gamma_i(\theta, \theta', \theta_\Sigma) = 0 \quad \Rightarrow \quad K_{i,:}[\theta, \theta_\Sigma] = K_{i,:}[\theta', \theta_\Sigma], \quad (6.34)$$

which needs to be satisfied by the  $K_{i,j}[\cdot]$  for all  $i \in \mathcal{N}_s$ ,  $\theta, \theta' \in \Theta$ , and  $\theta_\Sigma \in \Theta_\Sigma$ .

For restricting the dependency of  $u_k^i$  on the communication topology  $\Sigma[\theta_\Sigma]$  to those communication topologies  $\Sigma[\theta_\Sigma] \in \Sigma$  which can be distinguished by controller  $\mathcal{C}^i$ , temporarily assume now that  $\theta_k = \theta$  is constant. Like the previous temporary assumption, this assumption will be dropped again in the sequel. From an implementational viewpoint, it is practical and reasonable to assume that the set of controllers  $\mathcal{C}^j$  transmitting information to controller  $\mathcal{C}^i$  is known by the latter. Indeed, each controller can easily check if expected information from controller  $\mathcal{C}^j$  is available at time  $k$  or not, such that each  $\mathcal{C}^i$  is aware of the index set  $\mathcal{R}^i[\theta_{\Sigma,k}]$ . As a consequence of this assumption, each local control law must not change for any two values of  $\theta_{\Sigma,k}$  which do not affect  $\mathcal{R}^i[\theta_{\Sigma,k}]$ . Equivalently, it must hold that:

$$\mathcal{R}^i[\theta_\Sigma] = \mathcal{R}^i[\theta'_\Sigma] \quad \Rightarrow \quad K_{i,:}[\theta, \theta_\Sigma] = K_{i,:}[\theta, \theta'_\Sigma] \quad (6.35)$$

for all  $i \in \mathcal{N}_s$ ,  $\theta \in \Theta$ , and  $\theta_\Sigma, \theta'_\Sigma \in \Theta_\Sigma$ .

Dropping the temporary assumptions  $\theta_k = \theta$  and  $\theta_{\Sigma,k} = \theta_\Sigma$  imposed before means that both Markov states may change in one time step, requiring to consider combined transitions  $(\theta_k, \theta_{\Sigma,k}) \rightarrow (\theta_{k+1}, \theta_{\Sigma,k+1})$ . As before, controller  $\mathcal{C}^i$  must not adjust its control law if it is not aware of this combined transition. Note that any combined transition  $(\theta, \theta_\Sigma) \rightarrow (\theta', \theta'_\Sigma)$  can be interpreted as a sequence of the form:

$$(\theta, \theta_\Sigma) \rightarrow (\theta', \theta_\Sigma) \rightarrow (\theta', \theta'_\Sigma). \quad (6.36)$$

It must thus hold that:

$$(\gamma_i(\theta, \theta', \theta_\Sigma) = 0) \wedge (\mathcal{R}^i[\theta_\Sigma] = \mathcal{R}^i[\theta'_\Sigma]) \quad \Rightarrow \quad K_{i,:}[\theta, \theta_\Sigma] = K_{i,:}[\theta', \theta'_\Sigma] \quad (6.37)$$

for all  $\theta, \theta' \in \Theta$ ,  $\theta_\Sigma, \theta'_\Sigma \in \Theta_\Sigma$ , and  $i \in \mathcal{N}_s$ .

**Lemma 6.2.** *For each combined Markov state transition  $(\theta, \theta_\Sigma) \rightarrow (\theta', \theta'_\Sigma)$  of  $\mathcal{M}$  and  $\mathcal{M}_\Sigma$ , the implications (6.34) and (6.35) ensure that implication (6.37) holds.  $\square$*

*Proof.* Assume that both conditions of implication (6.37) are satisfied. Then, it follows from implication (6.34) and from (6.35) evaluated for  $\theta'$  that:

$$\gamma_i(\theta, \theta', \theta_\Sigma) = 0 \quad \Rightarrow \quad K_{i,:}[\theta, \theta_\Sigma] = K_{i,:}[\theta', \theta_\Sigma], \quad (6.38)$$

$$\mathcal{R}^i[\theta_\Sigma] = \mathcal{R}^i[\theta'_\Sigma] \quad \Rightarrow \quad K_{i,:}[\theta', \theta_\Sigma] = K_{i,:}[\theta', \theta'_\Sigma]. \quad (6.39)$$

Combining the above implications directly leads to (6.37).  $\square$

### 6.3.1. Synthesis Problem

By the help of the above considerations, the distributed control design problem can be transformed into an SDP. To this end, consider the following generalization of the operator  $\mathcal{D}_n(\mathbf{V})$  with  $\mathbf{V} \in \mathbb{H}^{N_\theta}(\mathbb{R}^{n_x \times n_x})$  introduced in Sec. 2.3:

$$\mathcal{D}_{\theta, \theta_\Sigma}(\mathbf{V}) := \sum_{m=1}^{N_\theta} \sum_{n=1}^{N_\Sigma} p_{m, \theta} p_{\Sigma, n, \theta_\Sigma} V[m, n]. \quad (6.40)$$

**Theorem 6.1.** *Suppose that the matrices  $\mathfrak{Z}[\theta, \theta_\Sigma] \in \mathbb{S}_{>0}^{n_\theta}$ ,  $\mathfrak{X}[\theta, \theta_\Sigma] \in \mathbb{S}_{>0}^{n_x}$ ,  $\mathfrak{G}[\theta, \theta_\Sigma] \in \mathbb{R}^{n_x \times n_x}$ , and  $\mathfrak{L}[\theta, \theta_\Sigma] \in \mathbb{R}^{n_v \times n_x}$  with  $\theta \in \Theta$  and  $\theta_\Sigma \in \Theta_\Sigma$  are a solution of the optimization problem:*

$$\min_{\mathfrak{Z}[\theta, \theta_\Sigma], \mathfrak{X}[\theta, \theta_\Sigma], \mathfrak{G}[\theta, \theta_\Sigma], \mathfrak{L}[\theta, \theta_\Sigma]} \sum_{\theta=1}^{N_\theta} \sum_{\theta_\Sigma=1}^{N_\Sigma} \text{tr}(\mathfrak{Z}[\theta, \theta_\Sigma]) \quad \text{subject to:} \quad (6.41a)$$

$$\left[ \begin{array}{c} \mathfrak{X}[\theta, \theta_\Sigma] - \mu_{0, \theta} \mu_{0, \theta_\Sigma} E[\theta](E[\theta])^\top \\ \star \end{array} \quad \begin{array}{c} A[\theta] \mathfrak{G}[\theta, \theta_\Sigma] + B[\theta] \mathfrak{L}[\theta, \theta_\Sigma] \\ \mathfrak{G}[\theta, \theta_\Sigma] + (\mathfrak{G}[\theta, \theta_\Sigma])^\top - \mathcal{D}_{\theta, \theta_\Sigma}(\mathfrak{X}) \end{array} \right] \succ 0, \quad (6.41b)$$

$$\left[ \begin{array}{c} \mathfrak{Z}[\theta, \theta_\Sigma] \quad C[\theta] \mathfrak{G}[\theta, \theta_\Sigma] + D[\theta] \mathfrak{L}[\theta, \theta_\Sigma] \\ \star \quad \mathfrak{G}[\theta, \theta_\Sigma] + (\mathfrak{G}[\theta, \theta_\Sigma])^\top - \mathcal{D}_{\theta, \theta_\Sigma}(\mathfrak{X}) \end{array} \right] \succ 0, \quad (6.41c)$$

$$\mathfrak{X}[\theta, \theta_\Sigma] = (\mathfrak{X}[\theta, \theta_\Sigma])^\top \succ 0, \quad (6.41d)$$

$$\mathfrak{Z}[\theta, \theta_\Sigma] = (\mathfrak{Z}[\theta, \theta_\Sigma])^\top, \quad (6.41e)$$

$$\mathfrak{L}_{i,j}[\theta, \theta_\Sigma] = 0_{n_x^i \times n_x^j} \quad \text{if } \sigma_{i,j}[\theta_\Sigma] = 0, \quad (6.41f)$$

$$\mathfrak{G}_{i,j}[\theta, \theta_\Sigma] = 0_{n_x^i \times n_x^j} \quad \text{if } \sigma_{i,j}[\theta_\Sigma] = 0, \quad (6.41g)$$

$$\mathfrak{G}_{h,j}[\theta, \theta_\Sigma] = 0_{n_x^h \times n_x^j} \quad \text{if } (\sigma_{i,j}[\theta_\Sigma] = 0) \wedge (\sigma_{i,h}[\theta_\Sigma] = 1), \quad (6.41h)$$

$$\mathfrak{L}_{i,:}[\theta, \theta_\Sigma] = \mathfrak{L}_{i,:}[\theta', \theta_\Sigma] \quad \text{if } \gamma_i(\theta, \theta', \theta_\Sigma) = 0, \quad (6.41i)$$

$$\mathfrak{G}[\theta, \theta_\Sigma] = \mathfrak{G}[\theta', \theta_\Sigma] \quad \text{if } \prod_{i=1}^{N_s} \gamma_i(\theta, \theta', \theta_\Sigma) = 0, \quad (6.41j)$$

$$\mathfrak{L}_{i,:}[\theta, \theta_\Sigma] = \mathfrak{L}_{i,:}[\theta', \theta'_\Sigma] \quad \text{if } \mathcal{R}^i[\theta_\Sigma] = \mathcal{R}^i[\theta'_\Sigma], \quad (6.41k)$$

$$\mathfrak{G}[\theta, \theta_\Sigma] = \mathfrak{G}[\theta', \theta'_\Sigma] \quad \text{if } \exists i \in \mathcal{N}_s : \mathcal{R}^i[\theta_\Sigma] = \mathcal{R}^i[\theta'_\Sigma], \quad (6.41l)$$

for all  $i, j, h \in \mathcal{N}_s$ ,  $\theta, \theta' \in \Theta$ , and  $\theta_\Sigma, \theta'_\Sigma \in \Theta_\Sigma$ . Let:

$$K[\theta, \theta_\Sigma] := \mathfrak{L}[\theta, \theta_\Sigma](\mathfrak{G}[\theta, \theta_\Sigma])^{-1}. \quad (6.42)$$

Then, the following assertions hold:

- (a) The JMLS  $\mathcal{P}_{\theta,\text{cl}}$  with  $w_k = 0$  for all  $k \in \mathbb{N}_0$  is mean-square stable.
- (b) The JMLS  $\mathcal{P}_{\theta,\text{cl}}$  with input  $w_k$  is BIBO stable in the mean-square sense.
- (c) The value of the  $\mathcal{H}_2$ -norm as defined in Def. (2.15) is upper-bounded by the objective function (6.41a).
- (d) For  $J$  as defined in Case 2.1, and by setting  $\mu_0 := \mu_\infty$ , the value of  $J$  is upper-bounded by the objective function (6.41a).
- (e) For  $J$  as defined in Case 2.2, and by setting  $E[\theta] := x_0 \forall \theta \in \Theta$ , the value of  $J$  is upper-bounded by the objective function (6.41a).
- (f) The control law  $u_k = K[\theta_k, \theta_{\Sigma,k}]x_k$  is consistent to the communication topology specified by  $\Sigma[\theta_{\Sigma,k}]$ .  $\square$

*Proof.* By using the parallel composition according to Eq. (6.9), the Markov chain governing the combined Markov state  $(\theta_k, \theta_{\Sigma,k})$  is obtained as:

$$\mathcal{M} \parallel \mathcal{M}_\Sigma = (\Theta \times \Theta_\Sigma, P \otimes P_\Sigma, \mu_0 \times \mu_{\Sigma,0}). \quad (6.43)$$

Hence, the operator  $\mathcal{D}_\theta(\cdot)$  defined in (2.47) naturally extends to (6.40). At this point, Theorem 6 from [37] can be employed, which states that the SDP comprised of (6.41a) to (6.41e) ensures mean-square stability of the corresponding closed-loop system  $\mathcal{P}_{\theta,\text{cl}}$ , and that  $\|\mathcal{P}_{\theta,\text{cl}}\|_{\mathcal{H}_2}^2$  is upper-bounded by the objective function (6.41a). Hence, assertions (a) and (c) hold, and assertions (b), (d), and (e) follow with Theorem 2.4, with Lemma 2.2, and with Lemma 2.4, respectively.

Concerning the structure of the distributed control law, implications (6.28), (6.34), and (6.35) have to be formulated in terms of the nonlinear controller parametrization given by the matrices  $\mathfrak{G}[\theta, \theta_\Sigma]$  and  $\mathfrak{L}[\theta, \theta_\Sigma]$ . The constraints (6.41f) to (6.41h), which are sufficient for implication (6.28) to hold, can be adopted from [50]. For ensuring that  $K_{i,:}[\theta, \theta_\Sigma] = K_{i,:}[\theta', \theta'_\Sigma]$  for some  $\theta, \theta' \in \Theta$  and  $\theta_\Sigma, \theta'_\Sigma \in \Theta_\Sigma$ , it suffices to set [52]:

$$\mathfrak{L}_{i,:}[\theta, \theta_\Sigma] = \mathfrak{L}_{i,:}[\theta', \theta'_\Sigma], \quad (6.44)$$

$$\mathfrak{G}[\theta, \theta_\Sigma] = \mathfrak{G}[\theta', \theta'_\Sigma]. \quad (6.45)$$

Considering the corresponding conditions of implications (6.34) and (6.35) leads to the constraints (6.41i) to (6.41l).  $\square$

As already mentioned in Sec. 6.1, SCT design is not considered in this chapter. One reason for this becomes apparent when analyzing Problem (6.41) with respect to the binary variables  $\sigma_{i,j}[\theta_\Sigma]$ . When implementing constraints (6.41f) to (6.41l) by the help of the Big-M method [136], the logical conditions for constraints (6.41j) to (6.41l) become nonlinear in the binary variables  $\sigma_{i,j}[\theta_\Sigma]$ . Consequently, the problem becomes non-convex if the binary variables are relaxed to the interval

$[0, 1]$ , prohibiting the usage of branch-and-bound techniques for efficiently solving the MISDP.

The number of continuous optimization variables in Problem (6.41) is:

$$N_{cv} = \frac{N_\theta N_\Sigma}{2} ((n_z)^2 + n_z + 3(n_x)^2 + 3n_x + 2n_u n_x). \quad (6.46)$$

Note that no binary variables are required to set up Problem (6.41), since the set of constraints (6.41f) to (6.41l) is dictated by  $\Sigma$ . Numerical studies revealed that, besides the number of optimization variables, several other quantities influence the required time for solving the SDP (6.41). In particular, it was observed that the calculation time varied up to 20% for two different interconnected JMLS with identical system dimensions. Hence, besides the number of optimization variables, the number of constraints which are generated by the adjacency matrices  $\Sigma[\cdot]$  has a significant impact on the complexity of the optimization problem.

Regarding the scalability of Problem (6.41), the limiting factor is the number of Markov states  $N_\theta^i$  of the jump Markov linear subsystems  $\mathcal{P}_\theta^i$ . Due to the combinatorics of the parallel composition, even moderate changes of the number of local Markov states may lead to significant changes of the number of extended Markov states.

### 6.3.2. Implementation

The distributed control law follows from (6.26) with gain matrix  $K[\theta, \theta_\Sigma]$  from the solution of the SDP (6.41). In the light of Eq. (6.7), the local controller of the  $i$ -th subsystem  $\mathcal{P}_\theta^i$  is given by:

$$\mathcal{C}^i : u_k^i = \sum_{j \in \mathcal{N}_s} K_{i,j} [\Psi^{-1}(\theta_k^1, \dots, \theta_k^{N_s}), \theta_{\Sigma,k}], x_k^j. \quad (6.47)$$

For implementing  $\mathcal{C}^i$ , every controller  $\mathcal{C}^j$  with  $j \in \mathcal{R}^i[\theta_{\Sigma,k}]$  must transmit its local hybrid state  $\zeta_k^j$  to the controller  $\mathcal{C}^i$  at time  $k$ . Due to constraint (6.34), every local Markov state  $\theta_k^j$  with  $j \in \mathcal{N}_s^i \setminus \mathcal{R}^i[\theta_{\Sigma,k}]$  can be set to  $\theta_k^j = 1$  without any restriction. Concerning  $\theta_{\Sigma,k}$ , constraint (6.35) ensures that controller  $\mathcal{C}^i$  may choose any  $\theta_{\Sigma,k} \in \Theta_\Sigma$  with  $\mathcal{R}^i[\theta_{\Sigma,k}^i] = \mathcal{R}^i[\theta_{\Sigma,k}]$ . The set  $\mathcal{R}^i[\theta_{\Sigma,k}]$  can easily be determined by each local controller  $\mathcal{C}^i$  by tracking the senders of the received hybrid states.

**Remark 6.2.** *The results presented in this chapter can be generalized to the case of separate communication topologies  $\Sigma_{x,k}$  and  $\Sigma_{\theta,k}$  for the local states  $x_k^i$  and for the local Markov states  $\theta_k^i$ , respectively. However, it seems more reasonable from the viewpoint of the implementation to assume that both states,  $x_k^i$  and  $\theta_k^i$ , are always transmitted together.*

## 6.4. Numerical Example

For showing the effectiveness of the presented approach, consider the following set of  $N_s = 3$  interconnected jump Markov linear subsystems  $\mathcal{P}_\theta^i$ , parametrized by:

$\theta^1$	$A_{1,:}[\theta^1]$	$B_{1,:}[\theta^1]$	$C_{1,:}[\theta^1]$	$D_{1,:}[\theta^1]$
1	$\begin{bmatrix} 0.2 & -1 & 0.4 & 1.3 & 0 & 0.4 \\ 0.2 & 0.8 & 1.2 & 0.1 & 0.6 & 0.1 \end{bmatrix}$	$\begin{bmatrix} 0 & 0 & 0 \\ 1 & 0 & 0.2 \end{bmatrix}$	$\begin{bmatrix} 8 & 0 & 0 & 0 & 0 & 0 \\ 0 & 5 & 0 & 0 & 0 & 0 \end{bmatrix}$	$\begin{bmatrix} 2 & 1 & 1 \\ 1.5 & 0 & 0 \end{bmatrix}$
2	$\begin{bmatrix} 0.9 & 0 & 0.2 & 1.3 & 0.2 & 0.3 \\ 0.4 & 0.7 & 1 & 0.1 & 1.4 & 0.1 \end{bmatrix}$	$\begin{bmatrix} 0 & 0 & 0 \\ 0.1 & 0.1 & 0 \end{bmatrix}$	$\begin{bmatrix} 8 & 0 & 0 & 0 & 0 & 0 \\ 0 & 5 & 0 & 0 & 0 & 0 \end{bmatrix}$	$\begin{bmatrix} 2 & 1 & 1 \\ 1.5 & 0 & 0 \end{bmatrix}$
$\theta^2$	$A_{2,:}[\theta^2]$	$B_{2,:}[\theta^2]$	$C_{2,:}[\theta^2]$	$D_{2,:}[\theta^2]$
1	$\begin{bmatrix} 0.2 & 0 & 1 & 0.3 & 0 & 0 \\ 0 & 0.1 & 0.7 & 1.8 & 0 & 0.1 \end{bmatrix}$	$\begin{bmatrix} 0 & 1 & 0.1 \\ 0 & 2 & 0 \end{bmatrix}$	$\begin{bmatrix} 0 & 0 & 8 & 0 & 0 & 0 \\ 0 & 0 & 0 & 5 & 0 & 0 \end{bmatrix}$	$\begin{bmatrix} 1 & 2 & 1 \\ 0 & 1.5 & 0 \end{bmatrix}$
2	$\begin{bmatrix} 0.4 & 0 & 0.9 & 1 & 0.3 & -0.2 \\ 0.2 & 0 & 0.5 & -1 & 0.2 & 0 \end{bmatrix}$	$\begin{bmatrix} 0 & 1 & 0 \\ 0 & 0.3 & 0 \end{bmatrix}$	$\begin{bmatrix} 0 & 0 & 8 & 0 & 0 & 0 \\ 0 & 0 & 0 & 5 & 0 & 0 \end{bmatrix}$	$\begin{bmatrix} 1 & 2 & 1 \\ 0 & 1.5 & 0 \end{bmatrix}$
$\theta^3$	$A_{3,:}[\theta^3]$	$B_{3,:}[\theta^3]$	$C_{3,:}[\theta^3]$	$D_{3,:}[\theta^3]$
1	$\begin{bmatrix} 0.6 & -0.8 & 0.2 & 1 & 1.1 & 0 \\ 0.5 & 0.3 & 0 & 0.1 & 0.2 & 0.8 \end{bmatrix}$	$\begin{bmatrix} 0 & 0 & 0 \\ 0 & 0 & 1 \end{bmatrix}$	$\begin{bmatrix} 0 & 0 & 0 & 0 & 8 & 0 \\ 0 & 0 & 0 & 0 & 0 & 5 \end{bmatrix}$	$\begin{bmatrix} 1 & 1 & 2 \\ 0 & 0 & 1.5 \end{bmatrix}$

Furthermore,  $E_{i,i}[\theta^i] = I_2$  and  $E_{i,j}[\theta^i] = 0_{2 \times 2}$  for all  $i, j \in \mathcal{N}_s$  and all  $\theta^i \in \Theta^i$ . The dimensions of the interconnected JMLS are thus given by  $n_x^i = n_w^i = n_z^i = 2$  and  $n_u^i = 1$  for all  $i \in \mathcal{N}_s$ . Note that the third subsystem  $\mathcal{P}_\theta^3$  only has one local Markov state, such that it is governed by the trivial Markov chain  $\mathcal{M}^3 = (\{1\}, 1, 1)$ . Hence,  $\mathcal{P}_\theta^3$  can be interpreted as an LTI subsystem. The Markov chains of subsystems  $\mathcal{P}_\theta^1$  and  $\mathcal{P}_\theta^2$  are parametrized by:

$$\mathcal{M}^1 = \left( \{1, 2\}, \begin{bmatrix} 0.9 & 0.1 \\ 0.9 & 0.1 \end{bmatrix}, \begin{bmatrix} 0.8 \\ 0.2 \end{bmatrix} \right), \quad \mathcal{M}^2 = \left( \{1, 2\}, \begin{bmatrix} 0.6 & 0.4 \\ 0.7 & 0.3 \end{bmatrix}, \begin{bmatrix} 0.5 \\ 0.5 \end{bmatrix} \right). \quad (6.48)$$

The failure prone communication topology is modeled by the following Markov chain and adjacency matrices:

$$\mathcal{M}_\Sigma = \left( \{1, 2\}, \begin{bmatrix} 0.95 & 0.05 \\ 0.95 & 0.05 \end{bmatrix}, \begin{bmatrix} 1 \\ 0 \end{bmatrix} \right), \quad \Sigma[1] = \begin{bmatrix} 1 & 1 & 1 \\ 1 & 1 & 1 \\ 1 & 0 & 1 \end{bmatrix}, \quad \Sigma[2] = \begin{bmatrix} 1 & 0 & 1 \\ 1 & 1 & 1 \\ 1 & 0 & 1 \end{bmatrix}. \quad (6.49)$$

Thus, at each time instant  $k \in \mathbb{N}_0$ , the communication link  $\sigma_{1,2}$  from controller  $\mathcal{C}^2$  to controller  $\mathcal{C}^1$  has a five percent likelihood to fail.

Applying the modeling procedure presented in Sec. 6.2 leads to the extended Markov chain:

$$\mathcal{M} = \left( \{1, 2, 3, 4\}, \begin{bmatrix} 0.54 & 0.36 & 0.06 & 0.04 \\ 0.63 & 0.27 & 0.07 & 0.03 \\ 0.54 & 0.36 & 0.06 & 0.04 \\ 0.63 & 0.27 & 0.07 & 0.03 \end{bmatrix}, \begin{bmatrix} 0.4 \\ 0.4 \\ 0.1 \\ 0.1 \end{bmatrix} \right). \quad (6.50)$$

Furthermore, the mapping  $\Psi(\theta) = (\theta^1, \theta^2)$  from the extended Markov state  $\theta$  to the local Markov states  $\theta^i$  is given by:

$$\Psi(1) = (1, 1), \quad \Psi(2) = (1, 2), \quad \Psi(3) = (2, 1), \quad \Psi(4) = (2, 2). \quad (6.51)$$

The construction of the state-space matrices  $A[\theta]$  to  $E[\theta]$  of  $\mathcal{P}_\theta$  is now performed according to Eq. (6.25), and is exemplarily shown for the following two cases:

$$A[2] = \begin{bmatrix} A_{1,1}[1] & A_{1,2}[1] & A_{1,3}[1] \\ A_{2,1}[2] & A_{2,2}[2] & A_{2,3}[2] \\ A_{3,1}[1] & A_{3,2}[1] & A_{3,3}[1] \end{bmatrix}, \quad A[3] = \begin{bmatrix} A_{1,1}[2] & A_{1,2}[2] & A_{1,3}[2] \\ A_{2,1}[1] & A_{2,2}[1] & A_{2,3}[1] \\ A_{3,1}[1] & A_{3,2}[1] & A_{3,3}[1] \end{bmatrix}. \quad (6.52)$$

A subset of the optimized gain matrices  $K[\theta, \theta_\Sigma]$  obtained for the above parametrization is:

$$K[1, 1] = \begin{bmatrix} 0.45 & -1.93 & -0.61 & 1.23 & 0.20 & 0.27 \\ 0.02 & -0.08 & -0.29 & -0.90 & 0.02 & -0.05 \\ -0.43 & -0.13 & 0 & 0 & -0.12 & -0.76 \end{bmatrix}, \quad (6.53a)$$

$$K[2, 1] = \begin{bmatrix} 0.38 & -1.85 & -0.78 & 1.29 & 0.16 & 0.29 \\ -0.58 & 0.09 & -1.14 & 0.77 & -0.55 & 0.11 \\ -0.43 & -0.13 & 0 & 0 & -0.12 & -0.76 \end{bmatrix}, \quad (6.53b)$$

$$K[1, 2] = \begin{bmatrix} 0.38 & -1.88 & 0 & 0 & 0.21 & 0.31 \\ 0.02 & -0.08 & -0.29 & -0.90 & 0.02 & -0.05 \\ -0.43 & -0.13 & 0 & 0 & -0.12 & -0.76 \end{bmatrix}, \quad (6.53c)$$

$$K[2, 2] = \begin{bmatrix} 0.38 & -1.88 & 0 & 0 & 0.21 & 0.31 \\ -0.58 & 0.09 & -1.14 & 0.77 & -0.55 & 0.11 \\ -0.43 & -0.13 & 0 & 0 & -0.12 & -0.76 \end{bmatrix}. \quad (6.53d)$$

The above numerical values for  $K[\theta, \theta_\Sigma]$  demonstrate that the local controllers  $\mathcal{C}^i$  only make use of the state information  $x_k^j$  available to them at time  $k$  according to the topology of communication network  $\mathcal{G}_k$ . For instance,  $K_{3,2}[\theta, \theta_\Sigma]$  is equal to  $0_{1 \times 2}$  for all  $\theta \in \theta$  and  $\theta_\Sigma \in \Theta_\Sigma$ , since the corresponding communication link is unavailable for all  $\theta_\Sigma \in \Theta_\Sigma$ . For the same reason, controller  $\mathcal{C}^3$  is not aware of the local Markov state  $\theta_k^2$ , which results in  $K_{3,:}[1, \theta_\Sigma] = K_{3,:}[2, \theta_\Sigma]$ . Thus, controller

$\mathcal{C}^3$  can always assume an arbitrary value  $\theta_k^2 \in \Theta^2$ . The gain matrices  $K[1, 2]$  and  $K[2, 2]$  demonstrate the effect of the defective communication link, which is inactive for  $\theta_\Sigma = 2$ . Hence, the corresponding gain  $K_{1,2}[\theta, 2]$  is zero for all  $\theta \in \Theta$ , and both the first and the third subsystem can not distinguish the Markov states  $\theta = 1 = \Psi^{-1}(1, 1)$  and  $\theta = 2 = \Psi^{-1}(1, 2)$ . Thus,  $K_{1,:}[1, 2] = K_{1,:}[2, 2]$ , and  $K_{3,:}[1, 2] = K_{3,:}[2, 2]$ .

For comparing the performance of the interconnected system  $\{\mathcal{P}_\theta^i\}_{i \in \mathcal{N}_s}$  with different controllers, the  $\mathcal{H}_2$ -norm as defined in Def. 2.15 (see p.38) is considered as performance measure for the resulting closed-loop system. The performance of a centralized linear quadratic regulator is 30.12. However, this control law can not be implemented for the considered system, since it ignores the probabilistic information constraints imposed by the communication network  $\mathcal{G}_k$ . Furthermore, stability of the closed-loop system can not be guaranteed in case of communication link failure. A stabilizing fully decentralized control law, on the other hand, does not exist for the considered interconnected system, since subsystem  $\mathcal{P}_\theta^3$  can not be stabilized with local information only. In contrast, the proposed distributed control scheme achieves a  $\mathcal{H}_2$ -norm of 36.17, while respecting the communication constraints and using the information transmitted via the defective communication link whenever it is available. This clearly demonstrates the advantages of the proposed distributed control scheme.

The evolution of the state trajectory of the interconnected system  $\{\mathcal{P}_\theta^i\}_{i \in \mathcal{N}_s}$  controlled by the presented distributed controllers is characterized in Fig. 6.2. The figure shows the envelopes and the quadratic mean of the state trajectories of 2500 simulation runs of 60 time-steps each. For each simulation run, the initial state was:

$$x_0 = [10 \ 10 \ -10 \ -10 \ -10 \ 10]^\top, \quad (6.54)$$

and  $w_k$  was white Gaussian noise. The trajectories of the Markov states  $\theta_k$  and  $\theta_{\Sigma,k}$  have been sampled according to  $P$ ,  $\mu_0$  and  $P_\Sigma$ ,  $\mu_{\Sigma,0}$ , respectively. It can be seen that the state  $x_k$  is attracted to the equilibrium, indicating that the closed-loop system is indeed mean-square stable.

## 6.5. Discussion

An approach to the design of distributed state-feedback controllers for interconnected jump Markov linear subsystems with uncertain communication was presented in this chapter. In a first step, the interconnected system is recast into a partitioned centralized jump Markov linear system  $\mathcal{P}_\theta$ , depending on both the parallel composition of the local Markov chains and a Markov chain governing the timely evolution of the communication topology. Preserving the structural information of the interconnected subsystems, the partitioned jump Markov linear system allows to formulate an SDP for the design of a distributed, mode-dependent state-feedback controller. Compared to online methods like model predictive control, a



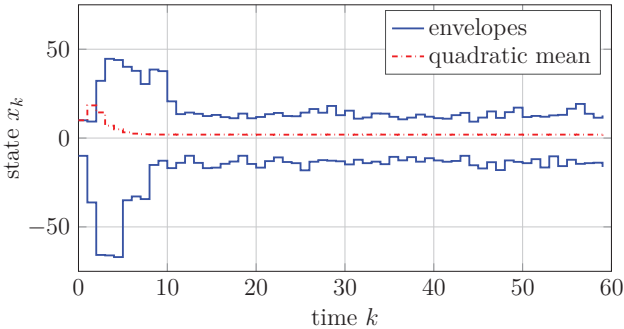


**Figure 6.2.:** Envelopes and quadratic mean of the closed-loop system state  $x_k$  for white Gaussian noise  $w_k$  and  $x_0 = [10 \ 10 \ -10 \ -10 \ -10 \ 10]^T$ .

particular advantage of such a control law is its low implementation complexity, making it particularly suited for fast processes.

A special focus was on the derivation of structural constraints which ensure that the resulting controllers respect the current topology of the communication network. In particular, the local controllers are able to reconfigure themselves when expected information transmitted over defective communication links is missing or delayed. However, due to nonlinear dependencies of the binary variables, performing simultaneous control and communication topology design within the presented framework is not recommended. Hence, the development of simplified linear synthesis conditions remains an open question.

A further topic of future research would be to make the hierarchical scheme presented in the second part of this thesis amenable to interconnected jump Markov systems. In order to get an invariant interconnection measure for the purpose of structural analysis, one may introduce an interconnection measure which considers, e.g., the worst case interconnection strength over all extended Markov states  $\theta \in \Theta$ . Similar to the two-layer scheme introduced for LTI systems, a lower control layer which is decentralized w.r.t. the identified clusters could be designed in a first step. For the design of an upper control layer, the main challenge will then be to find an efficient formulation for dealing with the uncertainty induced when considering a coarser time-scale. Otherwise, the combinatorics would dramatically increase the synthesis complexity on the upper layer, since any possible  $\Delta k$ -sequence of Markov states would constitute a new Markov state for the upper layer system. An imaginable remedy to this problem would be to derive a polytopic model for each Markov state, which raises the question of conservativeness of such an approach. Alternatively, one may think of an uncertain (e.g., polytopic) system description which incorporates a probability density function describing the probability distribution of the model uncertainty.

# 7. Hierarchical Control of Interconnected Semi-Markov Systems

In this chapter, it will be shown how the hierarchical approach developed in Chap. 3 can be extended to a generalized class of jump Markov systems (JMS). Despite their considerable modeling flexibility, jump Markov systems have limitations concerning the underlying distribution of the events over time. More specifically, using a Markov chain for modeling the evolution of the events over time requires them to follow a geometrical distribution, which does not apply for many practical scenarios. This observation has motivated the development of a more general class of jump Markov systems, which are called jump semi-Markov systems (JSMS) [141]. While for classical JMS, it is assumed that the transition probabilities of the Markov chain are time-invariant, the transition probabilities of a JSMS may vary over time. An article of Zhang et al. provides a comprehensive overview of several special cases that have been considered in literature [141]. So far, JSMS have usually been investigated in the context of centralized settings [56] [112], such that the approach to be presented next is one of the first dealing with distributed control of this system class. Note that large parts of this chapter have previously been published in [61].

In the sequel, a scenario is considered in which the semi-Markov chain is modeled as a global entity, with the global Markov state being measurable by the subsystems. For a practical application, this may be interpreted as a centralized entity for failure detection, with the resulting information being transmitted to the subsystems. A distributed two-layer control structure similar to the one presented in Chap. 3 will be developed, which is particularly suitable for controlling this type of dynamic systems. According to the existing hierarchical concept, the structure of the distributed two-layer controller is adjusted to the inherent interconnection topology of the plant. In accordance with the hybrid dynamic model, both layers of the distributed controller operate on different time-scales: fast time constants and strong subsystem interconnections are managed by local controllers on a lower control layer, which are coordinated by an upper control layer operating on a coarser time-scale. Furthermore, the upper control layer accounts for the handling of the discrete events.

## 7.1. Problem Setup

Consider a set of  $N_s \in \mathbb{N}$  interconnected uncertain subsystems  $\mathcal{P}_\theta^i$ ,  $i \in \mathcal{N}_s$ , where the dynamics of the  $i$ -th subsystem is given by:

$$\mathcal{P}_\theta^i = \begin{cases} x_{k+1}^i = \sum_{j=1}^{N_s} A_{i,j}[\theta_k] x_k^j + B_{i,j}[\theta_k] u_k^j + E_{i,j}[\theta_k] w_k^j, \\ z_k^i = \sum_{j=1}^{N_s} C_{i,j}[\theta_k] x_k^j + D_{i,j}[\theta_k] u_k^j. \end{cases} \quad (7.1)$$

In order to simplify the presentation, it is assumed here that the state-space matrices  $A_{i,j}[\cdot]$  to  $E_{i,j}[\cdot]$  parametrizing the subsystems depend on the state  $\theta_k \in \Theta$  of a global Markov chain  $\mathcal{M}_k = (\Theta, P_k, \mu_0)$ . The variable  $\theta_k$  will also be called the global *mode* of the interconnected system  $\{\mathcal{P}_\theta^i\}_{i \in \mathcal{N}_s}$ . In cases where the state-space matrices depend on local Markov states  $\theta_k^i$ , the procedure presented in Sec. 6.2 can be adopted for combining them to a global Markov chain. As mentioned before,  $\mathcal{M}_k$  is evaluated on a coarser time-scale compared to the sampling time of the subsystem dynamics  $\mathcal{P}_\theta^i$ . This assumption is modeled by a periodically time-varying transition probability matrix:

$$P_k = \begin{cases} P & \exists s \in \mathbb{N}_0 \mid s\Delta k = k, \\ I & \text{otherwise,} \end{cases} \quad (7.2)$$

with a constant  $\Delta k \in \mathbb{N}_{>1}$ . Hence, the Markov chain  $\mathcal{M}_k$  basically acts on the upper layer time-domain  $\mathbb{T}^\dagger$ . The basic structure of the interconnected system  $\{\mathcal{P}_\theta^i\}_{i \in \mathcal{N}_s}$  is illustrated in Fig. 7.1.

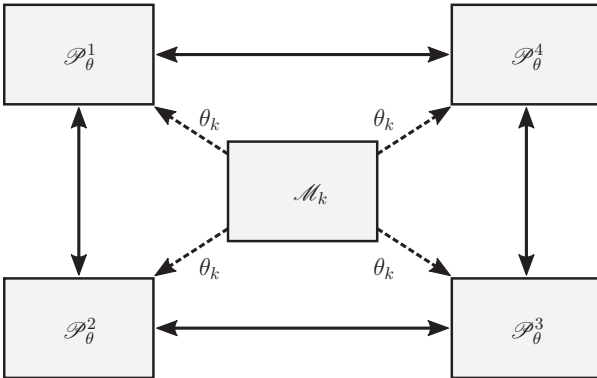


**Figure 7.1.:** Basic structure of interconnected uncertain subsystems  $\mathcal{P}_\theta^i$  with a global Markov chain  $\mathcal{M}_k$ . The solid lines between the subsystems indicate the physical interconnections, while dashed lines indicate the influence of the global Markov state  $\theta_k$ .

Within this setting, the two different time-scales are motivated by physical systems which require a small sampling time  $\Delta t$  to account for all relevant time-constants, but where discrete events influencing the system dynamics occur (or can be modeled more accurately) on a coarser time-scale. For instance, referring to Chap. 5, modeling a power system requires discretization times of fractions of seconds, while events like power-line failures are rather modeled on a coarser time-scale.

Applying Equations (6.23) and (6.25) to  $x_k^i$ ,  $u_k^i$ ,  $w_k^i$ ,  $z_k^i$ , and  $A_{i,j}[\cdot]$  to  $E_{i,j}[\cdot]$ , respectively, the interconnection of the  $N_s$  subsystems  $\mathcal{P}_\theta^i$  leads to the centralized partitioned system:

$$\mathcal{P}_\theta = \begin{cases} x_{k+1} = A[\theta_k]x_k + B[\theta_k]u_k + E[\theta_k]w_k, \\ z_k = C[\theta_k]x_k + D[\theta_k]u_k, \\ \mathcal{M}_k = (\Theta, P_k, \mu_0), \\ x_0 = (x_0^1; \dots; x_0^{N_s}). \end{cases} \quad (7.3)$$

### Hierarchical Controller Structure

The two different time-scales of the continuous- and the discrete-valued part of the dynamics, as well as the distributed character of the model, lead to a relatively high complexity regarding control synthesis. In the sequel, it will be shown how this complexity can be efficiently managed with an extension of the basic concepts introduced in Chap. 3.

In a first step prior to the control design, the interconnection structure of the uncertain plant is analyzed, and strongly coupled subsystems are grouped into clusters. This procedure is an extension of the subsystem clustering presented in Sec. 3.2. As before, each cluster is described by an index set  $\mathcal{C}^p[\theta] \subseteq \mathbb{I}_N$  with  $p \in \mathbb{I}_{N_c[\theta]}$ , which now additionally depends on the global mode  $\theta \in \Theta$ . Hence, the number  $N_c[\theta] \in \mathbb{N}_{\leq N_s}$  of identified clusters may be different in each mode. As a consequence, the permutation order of the signal vectors depends on the mode  $\theta$ . This is indicated by the following notation:

$$\bar{x}_k^p[\theta] := [x_k^i]_{i \in \mathcal{C}^p[\theta]}, \quad (7.4)$$

with analogous definitions for  $u_k$ ,  $w_k$ , and  $z_k$ , respectively.

In a second step, a lower control layer is designed, which operates on the time-domain  $\mathbb{T}^\downarrow$  and addresses fast dynamics and strong interconnections between the subsystems. This lower layer controller is of the form:

$$\bar{u}_k^p[\theta_k] = \bar{K}_{p,p}^\downarrow[\theta_k] \bar{x}_k^p[\theta_k] + \bar{v}_k^p[\theta_k], \quad (7.5)$$

where  $\bar{v}_k \in \mathbb{R}^n$  denotes the upper layer input to be chosen later. As established in Chap. 3, the lower layer controller has a decentralized structure w.r.t. the clusters.

Consequently, full communication between all subsystems  $i \in \mathcal{C}^p[\theta]$  belonging to the same cluster is required, while communication between the clusters is prohibited. In a third and final step, the upper control layer is chosen as:

$$\bar{v}_{s\Delta k}^p[\theta_{s\Delta k}] = \sum_{q=1}^{N_c[\theta_{s\Delta k}]} \bar{K}_{p,q}^\uparrow[\theta_{s\Delta k}] \bar{x}_s^q[\theta_{s\Delta k}]. \quad (7.6)$$

The task of the upper control layer is to implement communication between the clusters, and to account for the weak interconnections that have been neglected for the design of the lower control layer. Additionally, for the present case of jump semi-Markov systems, the upper control layer is responsible for the handling of the global mode transitions.

In order to set up the simultaneous controller and communication topology design on the upper control layer, the mode-dependent directed graph:

$$\mathcal{G}^\uparrow[\theta] = (\mathbb{I}_{N_c[\theta]}, \mathcal{E}^\uparrow[\theta]) \quad (7.7)$$

is defined, which is associated with the clustered subsystems. As usual, each cluster represents a node in the graph. However, since the sets  $\mathcal{C}^p[\theta]$  are a function of  $\theta$ , the upper layer communication topology also becomes a function of  $\theta$ . The corresponding adjacency matrix  $\bar{\Sigma}^\uparrow[\theta] = [\bar{\sigma}_{p,q}^\uparrow[\theta]] \in \mathbb{B}^{N_c[\theta] \times N_c[\theta]}$  is defined as:

$$\bar{\sigma}_{p,q}^\uparrow[\theta] := \begin{cases} 1 & \text{if } (q, p) \in \mathcal{E}^\uparrow[\theta], \\ 0 & \text{otherwise.} \end{cases} \quad (7.8)$$

The quality of a given topology  $\bar{\Sigma}^\uparrow[\theta]$  is evaluated by the help of a communication cost function:

$$J^{\uparrow\text{com}}(\bar{\Sigma}^\uparrow[\theta]) := \sum_{p \in \mathbb{I}_{N_c[\theta]}} \sum_{q \in \mathbb{I}_{N_c[\theta]}} \bar{c}_{p,q}^{\uparrow\text{com}}[\theta] \bar{\sigma}_{p,q}^\uparrow[\theta], \quad (7.9)$$

with parameters  $\bar{c}_{p,q}^{\uparrow\text{com}}[\theta] \in \mathbb{R}_{\geq 0}$  parametrizing the cost for activating the link from cluster  $q$  to cluster  $p$ .

## 7.2. Subsystem Clustering

The following algorithm analyzes the structure of the interconnected system  $\mathcal{P}_\theta^i$ ,  $i \in \mathcal{N}_s$ , allowing to incorporate the interconnection structure for the design of the distributed control law. The main idea is to apply the clustering procedure presented in Sec. 3.2 separately for each mode  $\theta \in \Theta$ , which results in the following steps:

- (a) The interconnection structure and interconnection strength between the subsystems  $\mathcal{P}_\theta^i$  is mapped into an  $N_\theta$ -sequence of matrices  $\mathbf{\Gamma} = (\Gamma[1], \dots, \Gamma[N_\theta]) \in \mathbb{H}^{N_\theta}(\mathbb{R}_{\geq 0}^{n_s \times n_s})$ . The scalar entries  $\gamma_{i,j}[\theta]$  of  $\Gamma[\theta]$  are chosen according to:

$$\gamma_{i,j}[\theta] := \|A_{i,j}[\theta]\|_2 + \|B_{i,j}[\theta]\|_2 \quad (7.10)$$

for all  $i, j \in \mathcal{N}_s$  and all  $\theta \in \Theta$ .

- (b) Define small non-negative numbers  $\epsilon_w, \epsilon_n \in \mathbb{R}_{\geq 0}$  such that  $\epsilon_w \geq \epsilon_n$ . These design parameters determine if an interconnection between two subsystems  $\mathcal{P}_\theta^i$  and  $\mathcal{P}_\theta^j$  is considered to be weak during the structural analysis ( $\gamma_{i,j}[\theta] \leq \epsilon_w$ ), or is even neglected completely for designing the lower control layer ( $\gamma_{i,j}[\theta] \leq \epsilon_n$ ).
- (c) The interconnection structure resulting from the strong interconnections is stored in the  $N_\theta$ -sequence of matrices  $\mathbf{\Gamma}' \in \mathbb{H}^{N_\theta}(\mathbb{R}_{\geq 0}^{n_x \times n_x})$ , which is defined by:

$$\gamma'_{i,j}[\theta] := \begin{cases} \gamma_{i,j}[\theta] & \text{if } \gamma_{i,j}[\theta] > \epsilon_w, \\ 2\epsilon_w & \text{if } i = j, \\ 0 & \text{otherwise.} \end{cases} \quad (7.11)$$

- (d) The Dulmage-Mendelsohn decomposition [102] is applied separately to each matrix  $\Gamma'[\theta]$ , with  $\theta \in \Theta$ . The resulting UBT matrix is denoted by  $\Gamma''[\theta]$ , comprising the  $N_\theta$ -sequence  $\mathbf{\Gamma}''$ . The index vector  $\tau[\theta] \in \mathbb{N}^{N_s}$  contains the permuted subsystem order for each mode, such that:

$$\gamma''_{i,j}[\theta] = \gamma'_{\tau_i[\theta], \tau_j[\theta]}[\theta] =: \gamma'_{\tau_i, \tau_j}[\theta]. \quad (7.12)$$

The second equality is established as a shorthand for simplifying the notation.

- (e) For fixed  $\theta \in \Theta$ , denote the number of blocks on the diagonal of the UBT matrix  $\Gamma''[\theta]$  by  $N_c[\theta]$ . For all  $p \in \mathcal{N}_c[\theta] := \mathbb{I}_{N_c[\theta]}$  and all  $\theta \in \Theta$ , the indices  $i \in \mathcal{N}_s$  of the subsystems belonging to the  $p$ -th diagonal block of  $\Gamma''[\theta]$  are stored in an index set  $\mathcal{C}^p[\theta] \subseteq \mathcal{N}_s$ .
- (f) Optionally, the clusters may be joined for fixed  $\theta$ , while respecting user-defined bounds on the cluster size. For details, the reader is referred to step (f) of the clustering procedure presented in Sec. 3.2 (see p.52).
- (g) All entries of  $\Gamma'[\theta]$  that are smaller than  $\epsilon_w$  but larger than or equal to  $\epsilon_n$  are restored to their original values. Similarly, those entries of  $\Gamma'[\theta]$  that are smaller than  $\epsilon_n$  but do not affect the hierarchical interconnection structure of the clusters, are restored, too:

- 1: **Given:**  $\mathbf{\Gamma}, \mathbf{\Gamma}', N_s, \{\mathcal{C}^p[\theta]\}$
- 2: **for**  $\theta = 1$  **to**  $N_\theta$  **do**
- 3:   set:  $h := 1, p := 1$
- 4:   **for**  $i = 1$  **to**  $N_s$  **do**
- 5:     **if**  $i \geq h + \text{card}(\mathcal{C}^p[\theta])$  **then**
- 6:       set:  $h := i, p := p + 1$
- 7:     **end if**
- 8:     **for**  $j = 1$  **to**  $N_s$  **do**
- 9:       **if**  $(\gamma_{\tau_i, \tau_j}[\theta] - \gamma'_{\tau_i, \tau_j}[\theta] > 0)$  **then**
- 10:         **if**  $(j \geq h) \vee (\gamma_{\tau_i, \tau_j}[\theta] \geq \epsilon_n)$  **then**

```

11:         set:  $\gamma'_{\tau_i, \tau_j}[\theta] := \gamma_{\tau_i, \tau_j}[\theta]$ 
12:     end if
13: end if
14: end for
15: end for
16: end for
17: return  $\Gamma'$ 
    
```

The outcome of the clustering procedure is the  $N_\theta$ -sequence of matrices  $\Gamma' \in \mathbb{H}^{N_\theta}(\mathbb{R}_{\geq 0}^{N_s \times N_s})$ , characterizing the mode-dependent interconnection structure of the subsystems. The subsystem clusters are defined by the index sets  $\mathcal{C}^p[\theta]$ , which are disjoint for fixed  $\theta \in \Theta$ .

The new subsystem order is encoded by the vector  $\tau[\theta] \in \mathbb{N}^{N_s}$ . This vector can be used for constructing the permutation matrices  $T_x[\theta]$ ,  $T_u[\theta]$ ,  $T_w[\theta]$ , and  $T_z[\theta]$  of dimension  $T_\bullet[\theta] = [T_\bullet^{i,j}[\theta]] \in \mathbb{B}^{n_\bullet \times n_\bullet}$  according to:

$$T_\bullet^{i,j}[\theta] = \begin{cases} I_{n_\bullet^{\tau_j[\theta]}} & \text{if } \tau_j[\theta] = i, \\ 0 & \text{otherwise.} \end{cases} \quad (7.13)$$

The above variables can be used to construct the aggregate subsystems  $\bar{\mathcal{P}}_\theta^p$  according to the index sets  $\mathcal{C}^p[\theta]$ . To this end, define the partitioned matrices:

$$\bar{A}[\theta] = [\bar{A}_{p,q}[\theta]] := T_x^T[\theta]A[\theta]T_x[\theta] \in \mathbb{R}^{n_x \times n_x}, \quad (7.14a)$$

$$\bar{B}[\theta] = [\bar{B}_{p,q}[\theta]] := T_x^T[\theta]B[\theta]T_u[\theta] \in \mathbb{R}^{n_x \times n_u}, \quad (7.14b)$$

$$\bar{C}[\theta] = [\bar{C}_{p,q}[\theta]] := T_z^T[\theta]C[\theta]T_x[\theta] \in \mathbb{R}^{n_z \times n_x}, \quad (7.14c)$$

$$\bar{D}[\theta] = [\bar{D}_{p,q}[\theta]] := T_z^T[\theta]D[\theta]T_u[\theta] \in \mathbb{R}^{n_z \times n_u}, \quad (7.14d)$$

$$\bar{E}[\theta] = [\bar{E}_{p,q}[\theta]] := T_x^T[\theta]E[\theta]T_w[\theta] \in \mathbb{R}^{n_x \times n_w}. \quad (7.14e)$$

Since the clusters depend on the current Markov state, the state, input, and output signals of the aggregate subsystems become functions of  $\theta_k$ , such that:

$$\bar{\mathcal{P}}_\theta^p : \begin{cases} \bar{x}_{k+1}^p[\theta_k] = \sum_{q=1}^{N_s} \bar{A}_{p,q}[\theta_k] \bar{x}_k^q[\theta_k] + \bar{B}_{p,q}[\theta_k] \bar{u}_k^q[\theta_k] + \bar{E}_k[\theta_k] w_k^q[\theta_k], \\ \bar{z}_k^p[\theta_k] = \sum_{q=1}^{N_s} \bar{C}_{p,q}[\theta_k] \bar{x}_k^q[\theta_k] + \bar{D}_{p,q}[\theta_k] \bar{u}_k^q[\theta_k], \\ \bar{x}_0^p[\theta_0] = [x_0^i]_{i \in \mathcal{C}^p[\theta_0]}, \end{cases} \quad (7.15)$$

for  $\theta_k \in \Theta$ .

In order to ensure that the lower layer control design problem is well-posed, the following assumption is imposed:

**Assumption 7.1.** *The pair  $(\bar{A}_{p,p}[\theta], \bar{B}_{p,p}[\theta])$  is stabilizable for all  $p \in \mathcal{N}_c[\theta]$ ,  $\theta \in \Theta$ .*

With Lemma 2.6, it thus follows that the uncertain dynamic system  $\bar{\mathcal{P}}_\theta$  is stabilizable by decentralized state-feedback for any fixed mode  $\theta \in \Theta$ .

### 7.3. Lower Layer Control Design

The design of the lower control layer is performed independently for each mode  $\theta \in \Theta$ . This is motivated by the fact that mode switches may only occur every  $\Delta k$ -th time-step, such that the overall behavior of the system consists of sequences of fixed modes. Adverse effects induced by mode-transitions, like performance degradation or even instability of the controlled system, are handled by the upper control layer.

In order to enable a sequential design of the lower and of the upper control layer, the upper layer input signal  $\bar{v}_k[\theta]$  is assumed to be zero during the lower layer control design. For constructing the lower layer synthesis problems, the overall system is written in terms of the clusters for each mode  $\theta \in \Theta$ , and neglected interconnections are removed from the system matrices. This leads to the aggregate subsystems:

$$\bar{\mathcal{P}}_\theta^{pp} : \begin{cases} \bar{x}_{k+1}^p[\theta_k] = \sum_{q=1}^{N_s} \bar{A}'_{p,q}[\theta_k] \bar{x}_k^q[\theta_k] + \bar{B}'_{p,q}[\theta_k] \bar{u}_k^q[\theta_k] + \bar{E}_{p,q}[\theta_k] \bar{w}_k^q[\theta_k], \\ \bar{z}_k^p[\theta_k] = \sum_{q=1}^{N_s} \bar{C}'_{p,q}[\theta_k] \bar{x}_k^q[\theta_k] + \bar{D}_{p,q}[\theta_k] \bar{u}_k^q[\theta_k], \\ \bar{x}_0^p[\theta_0] = [x_0^i]_{i \in \mathcal{C}^p[\theta_0]}, \end{cases} \quad (7.16)$$

for  $p, q \in \mathcal{N}_c[\theta]$  and with:

$$\bar{A}'_{p,q}[\theta] := [A'_{i,j}[\theta]]_{i \in \mathcal{C}^p[\theta], j \in \mathcal{C}^q[\theta]}, \quad A'_{i,j}[\theta] := \begin{cases} A_{i,j} & \text{if } \gamma'_{i,j}[\theta] > 0, \\ 0_{n_i^x \times n_j^x} & \text{otherwise,} \end{cases} \quad (7.17a)$$

$$\bar{B}'_{p,q}[\theta] := [B'_{i,j}[\theta]]_{i \in \mathcal{C}^p[\theta], j \in \mathcal{C}^q[\theta]}, \quad B'_{i,j}[\theta] := \begin{cases} B_{i,j} & \text{if } \gamma'_{i,j}[\theta] > 0, \\ 0_{n_i^x \times n_j^i} & \text{otherwise.} \end{cases} \quad (7.17b)$$

Applying Theorem 3.1 to the clustered system  $\bar{\mathcal{P}}_\theta'$  separately for each  $\theta \in \Theta$  leads to the semidefinite programs:

$$\min_{\mathfrak{G}[\theta], \mathfrak{L}[\theta], \mathfrak{X}[\theta], \mathfrak{Z}[\theta]} \text{tr}(\mathfrak{Z}[\theta]) \quad (7.18a)$$

$$\text{subject to: } \begin{bmatrix} \mathfrak{Z}[\theta] & \star \\ \bar{E}[\theta] & \mathfrak{X}[\theta] \end{bmatrix} \succ 0, \quad (7.18b)$$

$$\begin{bmatrix} \mathfrak{G}[\theta] + (\mathfrak{G}[\theta])^\top - \mathfrak{X}[\theta] & \star & \star \\ A'[\theta] \mathfrak{G}[\theta] + \bar{B}'[\theta] \mathfrak{L}[\theta] & \mathfrak{X}[\theta] & \star \\ \bar{C}'[\theta] \mathfrak{G}[\theta] + \bar{D}[\theta] \mathfrak{L}[\theta] & 0 & I \end{bmatrix} \succ 0, \quad (7.18c)$$

$$\mathfrak{X}[\theta] = (\mathfrak{X}[\theta])^\top \succ 0, \quad (7.18d)$$

$$\mathfrak{G}[\theta] = \text{blkdiag}(\mathfrak{G}_{p,p}[\theta]), \quad (7.18e)$$

$$\mathfrak{L}[\theta] = \text{blkdiag}(\mathfrak{L}_{p,p}[\theta]). \quad (7.18f)$$

From the solution of Problem (7.18), the lower layer controller gain matrices  $\bar{K}^\perp[\theta]$  are obtained as:

$$\bar{K}^\perp[\theta] = \mathfrak{L}[\theta](\mathfrak{G}[\theta])^{-1}, \quad \theta \in \Theta. \quad (7.19)$$



Under the control of  $\bar{u}_k^p[\theta_k] = \bar{K}_{p,p}^\downarrow[\theta_k]\bar{x}_k^p[\theta_k]$  with  $p \in \mathcal{N}_c[\theta_k]$ , the clustered system  $\bar{\mathcal{P}}_\theta$  becomes a system with input  $\bar{v}_k$ :

$$\bar{\mathcal{P}}_{\theta,\text{cl}}^\downarrow : \begin{cases} \bar{x}_{k+1}[\theta_k] = (\bar{A}[\theta_k] + \bar{B}[\theta_k]\bar{K}^\downarrow[\theta_k])\bar{x}_k[\theta_k] + \bar{B}[\theta_k]\bar{v}_k[\theta_k] + \bar{E}[\theta_k]\bar{w}_k[\theta_k], \\ \bar{z}_k[\theta_k] = (\bar{C}[\theta_k] + \bar{D}[\theta_k]\bar{K}^\downarrow[\theta_k])\bar{x}_k[\theta_k] + \bar{D}[\theta_k]\bar{v}_k[\theta_k]. \end{cases} \quad (7.20)$$

In accordance with established notation, define:

$$\bar{A}_{\text{cl}}^\downarrow[\theta] := (\bar{A}[\theta] + \bar{B}[\theta]\bar{K}^\downarrow[\theta]), \quad \bar{C}_{\text{cl}}^\downarrow[\theta] := (\bar{C}[\theta] + \bar{D}[\theta]\bar{K}^\downarrow[\theta]). \quad (7.21)$$

Due to the neglected interconnections in  $\bar{A}'[\cdot]$  and  $\bar{B}'[\cdot]$  and the neglected mode transitions, the lower layer controller does neither ensure mean-square stability nor  $\mathcal{H}_2$ -performance for the lower layer closed-loop system  $\bar{\mathcal{P}}_{\theta,\text{cl}}^\downarrow$ . However, by carefully designing a suitable upper layer controller, the composite two-layer controller provides guarantees concerning both, MSS and performance. Furthermore, it offers a good tradeoff between communication effort and closed-loop performance.

## 7.4. Upper Layer Control Design

For the design of the upper control layer, the weak interconnections and mode-transitions are explicitly taken into account. In addition, communication between the clusters is implemented. Before designing the upper layer control law, the controlled lower layer system  $\bar{\mathcal{P}}_{\theta,\text{cl}}$  is first time-lifted to the upper layer time-domain  $\mathbb{T}^\uparrow$ , preserving its partitioning with respect to the clusters. To this end, recall the notation  $\hat{\theta}_s = \theta_{s\Delta k}$ , such that the clustered upper layer system can be stated as:

$$\bar{\mathcal{P}}_\theta^\uparrow : \begin{cases} \hat{x}_{s+1}[\hat{\theta}_s] = \bar{A}^\uparrow[\hat{\theta}_s]\hat{x}_s[\hat{\theta}_s] + \bar{B}^\uparrow[\hat{\theta}_s]\hat{u}_s[\hat{\theta}_s] + \bar{E}^\uparrow[\hat{\theta}_s]\hat{w}_s[\hat{\theta}_s], \\ \hat{z}_s[\hat{\theta}_s] = \bar{C}^\uparrow[\hat{\theta}_s]\hat{x}_s[\hat{\theta}_s] + \bar{D}^\uparrow[\hat{\theta}_s]\hat{u}_s[\hat{\theta}_s] + \bar{F}^\uparrow[\hat{\theta}_s]\hat{w}_s[\hat{\theta}_s]. \end{cases} \quad (7.22a)$$

The matrices  $\bar{A}^\uparrow[\cdot]$  to  $\bar{F}^\uparrow[\cdot]$  are defined as:

$$\bar{A}^\uparrow[\hat{\theta}_s] := (\bar{A}_{\text{cl}}^\downarrow[\hat{\theta}])^{\Delta k} \in \mathbb{R}^{n_x \times n_x}, \quad (7.22b)$$

$$\bar{B}^\uparrow[\hat{\theta}_s] := \sum_{h=0}^{\Delta k-1} (\bar{A}_{\text{cl}}^\downarrow[\hat{\theta}])^h \bar{B}[\hat{\theta}] \in \mathbb{R}^{n_x \times n_u}, \quad (7.22c)$$

$$\bar{C}^\uparrow[\hat{\theta}_s] := \begin{bmatrix} \bar{C}_{\text{cl}}^\downarrow[\hat{\theta}] \\ \bar{C}_{\text{cl}}^\downarrow[\hat{\theta}] \bar{A}_{\text{cl}}^\downarrow[\hat{\theta}] \\ \vdots \\ \bar{C}_{\text{cl}}^\downarrow[\hat{\theta}] (\bar{A}_{\text{cl}}^\downarrow[\hat{\theta}])^{\Delta k-1} \end{bmatrix} \in \mathbb{R}^{\bar{n}_z^\uparrow \times n_x}, \quad (7.22d)$$

$$\bar{D}^\uparrow[\hat{\theta}_s] := \begin{bmatrix} \bar{D}[\hat{\theta}] \\ \bar{C}_{\text{cl}}^\downarrow[\hat{\theta}] \bar{B}[\hat{\theta}] + \bar{D}[\hat{\theta}] \\ \vdots \\ \bar{C}_{\text{cl}}^\downarrow[\hat{\theta}] (\sum_{h=0}^{\Delta k-2} (\bar{A}_{\text{cl}}^\downarrow[\hat{\theta}])^h) \bar{B}[\hat{\theta}] + \bar{D}[\hat{\theta}] \end{bmatrix} \in \mathbb{R}^{\bar{n}_z^\uparrow \times n_u}, \quad (7.22e)$$

$$\bar{E}^\uparrow[\hat{\theta}_s] := [(\bar{A}_{\text{cl}}^\downarrow[\hat{\theta}])^{\Delta k-1} \bar{E}[\hat{\theta}] \quad \dots \quad \bar{A}_{\text{cl}}^\downarrow[\hat{\theta}] \bar{E}[\hat{\theta}] \quad \bar{E}[\hat{\theta}]] \in \mathbb{R}^{n_x \times \bar{n}_w^\uparrow}, \quad (7.22f)$$

$$\bar{F}^\uparrow[\hat{\theta}_s] := \begin{bmatrix} 0 & 0 & \dots & 0 \\ \bar{C}_{\text{cl}}^\downarrow[\hat{\theta}] \bar{E}[\hat{\theta}] & \ddots & \ddots & \vdots \\ \vdots & \ddots & \ddots & 0 \\ \bar{C}_{\text{cl}}^\downarrow[\hat{\theta}] (\bar{A}_{\text{cl}}^\downarrow[\hat{\theta}])^{\Delta k-2} \bar{E}[\hat{\theta}] & \dots & \bar{C}_{\text{cl}}^\downarrow[\hat{\theta}] \bar{E}[\hat{\theta}] & 0 \end{bmatrix} \in \mathbb{R}^{n_x \times \bar{n}_w^\uparrow}, \quad (7.22g)$$

and the lifted disturbance vector is constructed as:

$$\hat{w}_s[\hat{\theta}_s] = \begin{bmatrix} \bar{w}_s \Delta k[\hat{\theta}_s] \\ \vdots \\ \bar{w}_{(s+1)\Delta k-1}[\hat{\theta}_s] \end{bmatrix} \in \mathbb{R}^{\bar{n}_w^\uparrow}. \quad (7.23)$$

For the dimensions, it holds that  $\bar{n}_z^\uparrow = n_z \Delta k$  and  $\bar{n}_w^\uparrow = n_w \Delta k$ .

The major advantage of time-lifting the dynamics is that, from the viewpoint of the upper layer time-domain  $\mathbb{T}^\uparrow$ , the original semi-Markov chain becomes a homogeneous Markov chain. Consequently, the upper layer system  $\bar{\mathcal{P}}_\theta^\uparrow$  is a regular jump Markov system with Markov chain:

$$\mathcal{M}^\uparrow = (\Theta, P, \mu_0). \quad (7.24)$$

Adding an upper layer controller of the form (7.6) to the time-lifted system  $\bar{\mathcal{P}}_\theta^\uparrow$  results in the controlled JMS  $\bar{\mathcal{P}}_{\theta, \text{cl}}^\uparrow$ . The connection between the performance measure of the lower layer and the upper layer system is as follows:

**Proposition 7.1.** *For system  $\bar{\mathcal{P}}_\theta^\uparrow$ , choose:*

$$\bar{E}^\uparrow[\hat{\theta}] = (\bar{A}_{\text{cl}}^\downarrow[\hat{\theta}])^{\Delta k-1} \bar{E}[\hat{\theta}], \quad \bar{F}^\uparrow[\hat{\theta}] = \begin{bmatrix} 0 \\ \bar{C}_{\text{cl}}^\downarrow[\hat{\theta}] \bar{E}[\hat{\theta}] \\ \vdots \\ \bar{C}_{\text{cl}}^\downarrow[\hat{\theta}] (\bar{A}_{\text{cl}}^\downarrow[\hat{\theta}])^{\Delta k-2} \bar{E}[\hat{\theta}] \end{bmatrix}, \quad (7.25)$$

for all  $\hat{\theta} \in \Theta$ . Then, it holds that:

$$\|\bar{\mathcal{P}}_{\hat{\theta}}^{\uparrow}\|_{\mathcal{H}_2} = \|\bar{\mathcal{P}}_{\hat{\theta},\text{cl}}^{\downarrow}\|_{\mathcal{H}_2}. \quad (7.26)$$

□

*Proof.* According to Definition 2.15, the  $\mathcal{H}_2$ -norm of system  $\bar{\mathcal{P}}_{\hat{\theta},\text{cl}}^{\downarrow}$  is defined as:

$$\|\bar{\mathcal{P}}_{\hat{\theta},\text{cl}}^{\downarrow}\|_{\mathcal{H}_2}^2 = \sum_{m=1}^{N_{\theta}} \sum_{k=0}^{\infty} \mu_{0,m} \mathbb{E}(\text{tr}((\bar{\mathbf{z}}_k^{\downarrow})^{\top} \bar{\mathbf{z}}_k^{\downarrow}) | \theta_0 = m), \quad (7.27)$$

where  $\bar{\mathbf{z}}_k^{\downarrow}$  denotes the corresponding impulse response matrix. Since the right-hand side of expression (7.27) is summed up from  $k = 0$  to  $k = \infty$ , it can be equivalently expressed in terms of  $s$ , leading to:

$$\sum_{k=0}^{\infty} \mu_{0,m} \mathbb{E}(\text{tr}((\bar{\mathbf{z}}_k^{\downarrow})^{\top} \bar{\mathbf{z}}_k^{\downarrow}) | \theta_0 = m) = \mu_{0,m} \sum_{s=0}^{\infty} \sum_{l=0}^{\Delta k-1} \mathbb{E}(\text{tr}((\bullet)^{\top} \bar{\mathbf{z}}_{s\Delta k+l}^{\downarrow}) | \theta_0 = m). \quad (7.28)$$

Due to the execution of the semi-Markov chain according to Eq. (7.2), it holds that  $\theta_{s\Delta k} = \dots = \theta_{(s+1)\Delta k-1} = \hat{\theta}_s$ . Hence:

$$\sum_{l=0}^{\Delta k-1} \mathbb{E}(\text{tr}((\bullet)^{\top} \bar{\mathbf{z}}_{s\Delta k+l}^{\downarrow}) | \theta_0 = m) = \mathbb{E}(\text{tr}(\sum_{l=0}^{\Delta k-1} (\bullet)^{\top} \bar{\mathbf{z}}_{s\Delta k+l}^{\downarrow}) | \theta_0 = m). \quad (7.29)$$

With the impulse response matrix  $\bar{\mathbf{z}}_k^{\downarrow}$ ,  $k \in \mathbb{N}_0$  being given by:

$$\bar{\mathbf{z}}_k^{\downarrow} = \begin{cases} 0 & \text{if } k = 0, \\ C[\theta_k]A[\theta_{k-1}] \cdots A[\theta_1]E[\theta_0] & \text{otherwise,} \end{cases} \quad (7.30)$$

it can be deduced that the impulse response matrix  $\hat{\mathbf{z}}_s^{\uparrow}$ ,  $s \in \mathbb{N}_0$  of system  $\bar{\mathcal{P}}_{\hat{\theta}}^{\uparrow}$  is given by:

$$\hat{\mathbf{z}}_s^{\uparrow} = \begin{bmatrix} \bar{\mathbf{z}}_{s\Delta k}^{\downarrow} \\ \vdots \\ \bar{\mathbf{z}}_{(s+1)\Delta k-1}^{\downarrow} \end{bmatrix} = \begin{cases} \bar{F}^{\uparrow}[\hat{\theta}_0] & \text{if } s = 0, \\ \bar{C}^{\uparrow}[\hat{\theta}_s] \bar{A}^{\uparrow}[\hat{\theta}_{s-1}] \cdots \bar{A}^{\uparrow}[\hat{\theta}_1] \bar{E}^{\uparrow}[\hat{\theta}_0] & \text{otherwise.} \end{cases} \quad (7.31)$$

Consequently:

$$\mathbb{E}(\text{tr}(\sum_{l=0}^{\Delta k-1} (\bullet)^{\top} \bar{\mathbf{z}}_{s\Delta k+l}^{\downarrow}) | \theta_0 = m) = \mathbb{E}(\text{tr}((\hat{\mathbf{z}}_s^{\uparrow})^{\top} \hat{\mathbf{z}}_s^{\uparrow}) | \theta_0 = m), \quad (7.32)$$

which completes the proof. □

By the help of Proposition 7.1, the synthesis of the upper layer controller can be formulated as an MISDP. To this end, a binary matrix variable  $\bar{\Sigma}^{\uparrow}[\hat{\theta}]$  is introduced, which accounts for the simultaneous optimization of the network topology.

**Theorem 7.1.** Let  $\mathfrak{G}[\hat{\theta}]$ ,  $\mathfrak{X}[\hat{\theta}] \in \mathbb{R}^{n_x \times n_x}$ ,  $\mathfrak{L}[\hat{\theta}] \in \mathbb{R}^{n_u \times n_x}$ ,  $\mathfrak{Z}[\hat{\theta}] \in \mathbb{R}^{\bar{n}_w^\dagger \times \bar{n}_w^\dagger}$ , and  $\bar{\Sigma}^\dagger[\hat{\theta}] \in \mathbb{B}^{N_c[\hat{\theta}] \times N_c[\hat{\theta}]}$  with  $\hat{\theta} \in \Theta$  be the solution of the MISDP:

$$\min_{\substack{\mathfrak{G}[\hat{\theta}], \mathfrak{L}[\hat{\theta}], \mathfrak{Z}[\hat{\theta}], \bar{\Sigma}^\dagger[\hat{\theta}] \\ \hat{\theta}=1}} \sum_{\hat{\theta}=1}^{N_\theta} \mu_{0,\hat{\theta}} \operatorname{tr}(\mathfrak{Z}[\hat{\theta}]) + J^{\operatorname{com}}(\bar{\Sigma}^\dagger[\hat{\theta}]) \quad \text{subject to:} \quad (7.33a)$$

$$\begin{bmatrix} \mathfrak{Z}[\hat{\theta}] & \star & \star \\ \bar{E}^\dagger[\hat{\theta}] & \mathfrak{X}[\hat{\theta}] & \star \\ \bar{F}^\dagger[\hat{\theta}] & 0 & I \end{bmatrix} \succ 0 \quad \forall \hat{\theta}, \quad (7.33b)$$

$$\begin{bmatrix} \mathfrak{G}[\hat{\theta}] + (\mathfrak{G}[\hat{\theta}])^\top - \mathfrak{X}[\hat{\theta}] & \star & \star \\ P'[\hat{\theta}](\bar{A}^\dagger[\hat{\theta}]\mathfrak{G}[\hat{\theta}] + \bar{B}^\dagger[\hat{\theta}]\mathfrak{L}[\hat{\theta}]) & \operatorname{blkdiag}_h(\mathfrak{X}[h]) & \star \\ \bar{C}^\dagger[\hat{\theta}]\mathfrak{G}[\hat{\theta}] + \bar{D}^\dagger[\hat{\theta}]\mathfrak{L}[\hat{\theta}] & 0 & I \end{bmatrix} \succ 0 \quad \forall \hat{\theta}, \quad (7.33c)$$

$$\bar{\Sigma}^\dagger[\hat{\theta}] \in \bar{\Sigma}^\dagger[\hat{\theta}] \quad \forall \hat{\theta}, \quad (7.33d)$$

$$-M\bar{\sigma}_{p,q}^\dagger[\hat{\theta}] \leq \mathfrak{L}_{p,q}[\hat{\theta}] \leq M\bar{\sigma}_{p,q}^\dagger[\hat{\theta}] \quad \forall \hat{\theta}, p, q, \quad (7.33e)$$

$$-M\bar{\sigma}_{p,q}^\dagger[\hat{\theta}] \leq \mathfrak{G}_{p,q}[\hat{\theta}] \leq M\bar{\sigma}_{p,q}^\dagger[\hat{\theta}] \quad \forall \hat{\theta}, p, q, \quad (7.33f)$$

$$-M(\bar{\sigma}_{p,q}^\dagger[\hat{\theta}] - \bar{\sigma}_{p,r}^\dagger[\hat{\theta}] + 1) \leq \mathfrak{G}_{r,q}[\hat{\theta}] \leq M(\bar{\sigma}_{p,q}^\dagger[\hat{\theta}] - \bar{\sigma}_{p,r}^\dagger[\hat{\theta}] + 1) \quad \forall \hat{\theta}, p, q, r, \quad (7.33g)$$

where  $\hat{\theta} \in \Theta$  and  $p, q, r \in \mathcal{N}_c[\hat{\theta}]$ . Furthermore,  $M \in \mathbb{R}_{>0}^{\star \times \star}$  denotes a matrix of suitable dimensions with entries  $M_{i,j} > \max\{\|\mathfrak{G}\|_{1,\infty}, \|\mathfrak{L}\|_{1,\infty}\}$ , and the matrix  $P'[\hat{\theta}] \in \mathbb{B}^{N_\theta n_x \times n_x}$  is defined as:

$$P'[\hat{\theta}] := \begin{bmatrix} T_x^\top[1]T_x[\hat{\theta}]\sqrt{P_{\hat{\theta},1}} \\ \vdots \\ T_x^\top[N_\theta]T_x[\hat{\theta}]\sqrt{P_{\hat{\theta},N_\theta}} \end{bmatrix}. \quad (7.34)$$

Let  $\bar{K}^\dagger[\hat{\theta}] := \mathfrak{L}[\hat{\theta}](\mathfrak{G}[\hat{\theta}])^{-1}$ . Then, the following assertions hold:

- The jump Markov linear system  $\bar{\mathcal{P}}_{\theta,\text{cl}}^\dagger$  with  $\bar{w}_k = 0$  for all  $k \in \mathbb{N}_0$  is mean-square stable.
- The jump Markov linear system  $\bar{\mathcal{P}}_{\theta,\text{cl}}^\dagger$  with input  $\bar{w}_k$  is BIBO stable in the mean-square sense.
- For  $J$  as defined in Case 2.1, and by setting  $\mu_0 := \mu_\infty$  and  $\bar{E}^\dagger[\hat{\theta}]$ ,  $\bar{F}^\dagger[\hat{\theta}]$  as stated in Prop. 7.1, the value of  $J + J^{\operatorname{com}}$  is upper-bounded by the objective function (7.33a).
- For  $J$  as defined in Case 2.2, and by setting  $\bar{E}^\dagger[\hat{\theta}]$  and  $\bar{F}^\dagger[\hat{\theta}]$  as stated in Prop. 7.1 with  $\bar{E}[\hat{\theta}] = \bar{x}_0[\hat{\theta}]$ , the value of  $J + J^{\operatorname{com}}$  is upper-bounded by the objective function (7.33a).
- The hierarchical two-layer controller comprised of Eq. (7.5) and Eq. (7.6) respects the communication topology encoded by  $\bar{\Sigma}^\dagger[\hat{\theta}]$ .  $\square$

*Proof.* Assume that a solution to Problem (7.33) exists. The upper left block entry of (7.33c) implies that:

$$\mathfrak{G}[\hat{\theta}] + (\mathfrak{G}[\hat{\theta}])^\top \succ \mathfrak{X}[\hat{\theta}] \succ 0 \quad (7.35)$$

for all  $\hat{\theta} \in \Theta$ , such that any feasible matrix  $\mathfrak{G}[\hat{\theta}]$  must be non-singular. Using relation (4.45) and substituting  $\mathfrak{L}[\hat{\theta}] = \bar{K}^\dagger[\hat{\theta}]\mathfrak{G}[\hat{\theta}]$  in Eq. (7.33c) leads to:

$$\begin{bmatrix} (\mathfrak{G}[\hat{\theta}])^\top (\mathfrak{X}[\hat{\theta}])^{-1} \mathfrak{G}[\hat{\theta}] & \star & \star \\ P'[\hat{\theta}](\bar{A}^\dagger[\hat{\theta}]\mathfrak{G}[\hat{\theta}] + \bar{B}^\dagger[\hat{\theta}]\bar{K}^\dagger[\hat{\theta}]\mathfrak{G}[\hat{\theta}]) & \text{blkdiag}_h(\mathfrak{X}[h]) & \star \\ \bar{C}^\dagger[\hat{\theta}]\mathfrak{G}[\hat{\theta}] + \bar{D}^\dagger[\hat{\theta}]\bar{K}^\dagger[\hat{\theta}]\mathfrak{G}[\hat{\theta}] & 0 & I \end{bmatrix} \succ 0. \quad (7.36)$$

Factoring out the non-singular matrix  $T[\hat{\theta}] = \text{blkdiag}(\mathfrak{G}[\hat{\theta}], I_{n_x}, I_{n_x})$  on the right-hand side and its transpose  $(T[\hat{\theta}])^\top$  on the left-hand side, inequality (7.36) is equivalent to:

$$\begin{bmatrix} (\mathfrak{X}[\hat{\theta}])^{-1} & \star & \star \\ P'[\hat{\theta}](\bar{A}^\dagger[\hat{\theta}] + \bar{B}^\dagger[\hat{\theta}]\bar{K}^\dagger[\hat{\theta}]) & \text{blkdiag}_h(\mathfrak{X}[h]) & \star \\ \bar{C}^\dagger[\hat{\theta}] + \bar{D}^\dagger[\hat{\theta}]\bar{K}^\dagger[\hat{\theta}] & 0 & I \end{bmatrix} \succ 0. \quad (7.37)$$

Forming the Schur-complement and substituting the definitions of  $\bar{A}_{\text{cl}}^\dagger[\hat{\theta}]$  and  $\bar{C}_{\text{cl}}^\dagger[\hat{\theta}]$  leads to:

$$(\mathfrak{X}[\hat{\theta}])^{-1} - (\bullet)^\top (\text{blkdiag}_h((\mathfrak{X}[h])^{-1})) (P'[\hat{\theta}]\bar{A}_{\text{cl}}^\dagger[\hat{\theta}]) - (\bullet)^\top (\bar{C}_{\text{cl}}^\dagger[\hat{\theta}]) \succ 0. \quad (7.38)$$

With the help of Eq. (7.34), it can easily be verified that:

$$(P'[\hat{\theta}])^\top \text{blkdiag}_h((\mathfrak{X}[h])^{-1}) P'[\hat{\theta}] = T_x^\top[\hat{\theta}] \sum_{h=1}^{N_\theta} p_{\hat{\theta},h} T_x[h] (\mathfrak{X}[h])^{-1} T_x^\top[h] T_x[\hat{\theta}], \quad (7.39)$$

where the permutation matrices  $T_x[\cdot]$  account for the  $\hat{\theta}$ -dependent permutation of the state vector. Substituting the above expression into Eq. (7.38) and making use of the operator  $\mathcal{E}(\cdot)$  as defined in Eq. (2.47) (see page 36) yields:

$$(\mathfrak{X}[\hat{\theta}])^{-1} - (\bar{A}_{\text{cl}}^\dagger[\hat{\theta}])^\top \mathcal{E}_\theta(\mathfrak{X}^{-1}) \bar{A}_{\text{cl}}^\dagger[\hat{\theta}] - (\bar{C}_{\text{cl}}^\dagger[\hat{\theta}])^\top \bar{C}_{\text{cl}}^\dagger[\hat{\theta}] \succ 0, \quad (7.40)$$

where:

$$\mathfrak{X}^{-1} := ((\mathfrak{X}[1])^{-1}, \dots, (\mathfrak{X}[N_\theta])^{-1}). \quad (7.41)$$

Making use of Theorems 2.3 and 2.4, assertions (a) and (b) follow.

Multiplying (7.40) by  $\sqrt{p_{h,\hat{\theta}}}\bar{A}_{\text{cl}}^\dagger[h]$  from the right-hand side and by its transpose from the left-hand side and summing up over all  $\hat{\theta} \in \Theta$  leads to:

$$\begin{aligned} (\bar{A}_{\text{cl}}^\dagger[h])^\top \mathcal{E}_h(\mathfrak{X}^{-1}) \bar{A}_{\text{cl}}^\dagger[h] &\succ (\bar{A}_{\text{cl}}^\dagger[h])^\top \sum_{\hat{\theta} \in \Theta} p_{h,\hat{\theta}} (\bar{A}_{\text{cl}}^\dagger[\hat{\theta}])^\top \mathcal{E}_\theta(\mathfrak{X}^{-1}) \bar{A}_{\text{cl}}^\dagger[\hat{\theta}] \bar{A}_{\text{cl}}^\dagger[h] \dots \\ &+ (\bar{A}_{\text{cl}}^\dagger[h])^\top \sum_{\hat{\theta} \in \Theta} p_{h,\hat{\theta}} (\bar{C}_{\text{cl}}^\dagger[\hat{\theta}])^\top \bar{C}_{\text{cl}}^\dagger[\hat{\theta}] \bar{A}_{\text{cl}}^\dagger[h]. \end{aligned} \quad (7.42)$$

Swapping  $h$  and  $\hat{\theta}$  in the above inequality and substituting the left-hand side by inequality (7.40), one obtains:

$$\begin{aligned} (\mathfrak{X}[\hat{\theta}])^{-1} \succ & (\bar{A}_{\text{cl}}^\dagger[\hat{\theta}])^\top \sum_{h \in \Theta} p_{\hat{\theta}, h} (\bar{A}_{\text{cl}}^\dagger[h])^\top \mathfrak{E}_h (\mathfrak{X}^{-1}) \bar{A}_{\text{cl}}^\dagger[h] \bar{A}_{\text{cl}}^\dagger[\hat{\theta}] \dots \\ & + (\bar{A}_{\text{cl}}^\dagger[\hat{\theta}])^\top \sum_{h \in \Theta} p_{\hat{\theta}, h} (\bar{C}_{\text{cl}}^\dagger[h])^\top \bar{C}_{\text{cl}}^\dagger[h] \bar{A}_{\text{cl}}^\dagger[\hat{\theta}] + (\bar{C}_{\text{cl}}^\dagger[\hat{\theta}])^\top \bar{C}_{\text{cl}}^\dagger[\hat{\theta}]. \end{aligned} \quad (7.43)$$

In terms of expected values, this inequality can equivalently be expressed as:

$$\begin{aligned} (\mathfrak{X}[\hat{\theta}_0])^{-1} \succ & \mathbb{E}((\bar{A}_{\text{cl}}^\dagger[\hat{\theta}_0])^\top (\bar{A}_{\text{cl}}^\dagger[\hat{\theta}_1])^\top (\mathfrak{X}[\hat{\theta}_2])^{-1} \bar{A}_{\text{cl}}^\dagger[\hat{\theta}_1] \bar{A}_{\text{cl}}^\dagger[\hat{\theta}_0]) \dots \\ & + \mathbb{E}((\bar{A}_{\text{cl}}^\dagger[\hat{\theta}_0])^\top (\bar{C}_{\text{cl}}^\dagger[\hat{\theta}_1])^\top \bar{C}_{\text{cl}}^\dagger[\hat{\theta}_1] \bar{A}_{\text{cl}}^\dagger[\hat{\theta}_0]) + (\bar{C}_{\text{cl}}^\dagger[\hat{\theta}_0])^\top \bar{C}_{\text{cl}}^\dagger[\hat{\theta}_0]. \end{aligned} \quad (7.44)$$

Repeating these steps ( $n - 2$ ) times leads to:

$$\begin{aligned} (\mathfrak{X}[\hat{\theta}_0])^{-1} \succ & \mathbb{E}((\bullet)^\top ((\mathfrak{X}[\hat{\theta}_n])^{-1}) (\bar{A}_{\text{cl}}^\dagger[\hat{\theta}_{n-1}] \dots \bar{A}_{\text{cl}}^\dagger[\hat{\theta}_0])) \dots \\ & + \mathbb{E}\left(\sum_{s=1}^{n-1} (\bullet)^\top (\bar{C}_{\text{cl}}^\dagger[\hat{\theta}_s] \bar{A}_{\text{cl}}^\dagger[\hat{\theta}_{s-1}] \dots \bar{A}_{\text{cl}}^\dagger[\hat{\theta}_0])\right) + (\bar{C}_{\text{cl}}^\dagger[\hat{\theta}_0])^\top \bar{C}_{\text{cl}}^\dagger[\hat{\theta}_0]. \end{aligned} \quad (7.45)$$

Taking the limit  $n \rightarrow \infty$ , the first term on the right hand side approaches zero, since the closed-loop system is mean-square stable (see also [31, Chap. 3]). Hence, it follows that:

$$(\mathfrak{X}[\hat{\theta}_0])^{-1} \succ \mathbb{E}\left(\sum_{s=1}^{\infty} (\bullet)^\top (\bar{C}_{\text{cl}}^\dagger[\hat{\theta}_s] \bar{A}_{\text{cl}}^\dagger[\hat{\theta}_{s-1}] \dots \bar{A}_{\text{cl}}^\dagger[\hat{\theta}_0])\right) + (\bar{C}_{\text{cl}}^\dagger[\hat{\theta}_0])^\top \bar{C}_{\text{cl}}^\dagger[\hat{\theta}_0]. \quad (7.46)$$

Forming the Schur-complement of LMI (7.33b):

$$\mathfrak{Z}[\hat{\theta}] - (\bar{E}^\dagger[\hat{\theta}])^\top (\mathfrak{X}[\hat{\theta}]^{-1}) \bar{E}^\dagger[\hat{\theta}] - (\bar{F}^\dagger[\hat{\theta}])^\top \bar{F}^\dagger[\hat{\theta}] \succ 0. \quad (7.47)$$

Evaluating this equation for  $\hat{\theta} = \hat{\theta}_0$  and rearranging the summands yields:

$$\mathfrak{Z}[\hat{\theta}_0] \succ (\bar{E}^\dagger[\hat{\theta}_0])^\top (\mathfrak{X}[\hat{\theta}_0]^{-1}) \bar{E}^\dagger[\hat{\theta}_0] + (\bar{F}^\dagger[\hat{\theta}_0])^\top \bar{F}^\dagger[\hat{\theta}_0]. \quad (7.48)$$

Considering the initial distribution  $\mu_0$  of  $\hat{\theta}_0$  leads to:

$$\sum_{\hat{\theta}=1}^{N_\theta} \mu_{0, \hat{\theta}} \mathfrak{Z}[\hat{\theta}] \succ \sum_{\hat{\theta}=1}^{N_\theta} \mu_{0, \hat{\theta}} ((\bar{E}^\dagger[\hat{\theta}])^\top (\mathfrak{X}[\hat{\theta}]^{-1}) \bar{E}^\dagger[\hat{\theta}] + (\bar{F}^\dagger[\hat{\theta}])^\top \bar{F}^\dagger[\hat{\theta}]). \quad (7.49)$$

Taking Inequality (7.46) into account and taking the trace of  $\mathfrak{Z}[\hat{\theta}]$  reveals that:

$$\sum_{\hat{\theta}=1}^{N_\theta} \mu_{0, \hat{\theta}} \text{tr}(\mathfrak{Z}[\hat{\theta}]) > \|\bar{\mathcal{P}}_{\hat{\theta}, \text{cl}}^\dagger\|_{\mathcal{H}_2}, \quad (7.50)$$

see Definition 2.15 on page 38. Making use of Prop. 7.1 reveals that if  $\bar{E}^\uparrow[\hat{\theta}]$  and  $\bar{F}^\uparrow[\hat{\theta}]$  are chosen according to Eq. (7.25), it holds that:

$$\sum_{\hat{\theta}=1}^{N_\theta} \mu_{0,\hat{\theta}} \text{tr}(\mathfrak{Z}[\hat{\theta}]) > \|\bar{\mathcal{P}}_{\theta,\text{cl}}^\uparrow\|_{\mathcal{H}_2} = \|\bar{\mathcal{P}}_{\theta,\text{cl}}^\downarrow\|_{\mathcal{H}_2}. \quad (7.51)$$

Assertions (c) and (d) now follow by establishing the connection between  $\|\bar{\mathcal{P}}_{\theta,\text{cl}}^\downarrow\|_{\mathcal{H}_2}$ ,  $J_1$  and  $J_2$  by using Lemmas 2.2 and 2.4, respectively.

Finally, assertion (e) follows by applying the structural constraints presented in [50] to the matrix variables  $\mathfrak{G}[\hat{\theta}]$  and  $\mathfrak{L}[\hat{\theta}]$  separately for all  $\theta \in \Theta$ , leading to the constraints (7.33e) to (7.33g).  $\square$

For implementing the two-layer controller at the original system, the upper layer and lower layer control gains have to be permuted according to:

$$K^\downarrow[\theta] = [K_{i,j}^\downarrow[\theta]] = T_u[\theta] \bar{K}^\downarrow[\theta] T_x^\top[\theta], \quad (7.52a)$$

$$K^\uparrow[\theta] = [K_{i,j}^\uparrow[\theta]] = T_u[\theta] \bar{K}^\uparrow[\theta] T_x^\top[\theta]. \quad (7.52b)$$

In terms of the original subsystem order, the hierarchical distributed control law is then given by:

$$u_k^i = \sum_{j=1}^{N_s} K_{i,j}^\downarrow[\theta_k] x_k^j + K_{i,j}^\uparrow[\theta_k] x_{s\Delta k}^j. \quad (7.53)$$

## 7.5. Reducing the Synthesis Complexity

Despite the fact that the clustering procedure significantly reduces the combinatorial complexity of the SCT design on the upper control layer, the problem is still fairly complex. Therefore, the following approach inspired by [23] and [52] can be used to further reduce the complexity of the upper layer control design.

The underlying idea is as follows: In a first step, the upper layer control design is performed without structural constraints. Since the resulting problem is a standard centralized  $\mathcal{H}_2$ -problem for JMLS, it can be efficiently solved by solving a set of coupled algebraic Riccati equations (CARE) associated with  $\bar{\mathcal{P}}_\theta^\uparrow$ , see [31, Chap.4]. Scaling the value function that is obtained from the solution of the CARE by a scalar factor  $(\mathfrak{a}[\hat{\theta}])^{-1} \in \mathbb{R}_{\geq 1}$ , it can be used for designing a structured control law with inferior performance compared to the optimal control law. Denoting the solution of the CARE by  $\bar{V}^\uparrow[\hat{\theta}] \in \mathbb{S}_{>0}^{N_c[\hat{\theta}]}$ ,  $\hat{\theta} \in \Theta$ , and assuming that  $\bar{V}^\uparrow[\hat{\theta}]$  is invertible, leads to the following result:

**Theorem 7.2.** Suppose that  $\mathbf{a}[\hat{\theta}] \in \mathbb{R}_{>0}$ ,  $\mathfrak{L}[\hat{\theta}] \in \mathbb{R}^{n_u \times n_x}$ ,  $\bar{\Sigma}^\uparrow[\hat{\theta}] \in \mathbb{B}^{\bar{N}_c[\hat{\theta}] \times \bar{N}_c[\hat{\theta}]}$ , and  $\mathfrak{Z}[\hat{\theta}] \in \mathbb{R}^{\bar{n}_w^\uparrow \times \bar{n}_w^\uparrow}$  with  $\hat{\theta} \in \Theta$  denote the solution of the optimization problem:

$$\min_{\mathbf{a}[\hat{\theta}], \mathfrak{L}[\hat{\theta}], \mathfrak{Z}[\hat{\theta}], \bar{\Sigma}^\uparrow[\hat{\theta}]} \sum_{\hat{\theta}=1}^{N_\theta} \mu_{0,\hat{\theta}} \operatorname{tr}(\mathfrak{Z}[\hat{\theta}]) + J^{\text{com}}(\bar{\Sigma}^\uparrow[\hat{\theta}]) \text{ subject to:} \quad (7.54a)$$

$$\bar{\Sigma}^\uparrow[\hat{\theta}] \in \bar{\Sigma}^\uparrow[\hat{\theta}] \quad \forall \hat{\theta}, \quad (7.54b)$$

$$\begin{bmatrix} \mathfrak{Z}[\hat{\theta}] & \star & \star \\ \bar{E}^\uparrow[\hat{\theta}] & \mathbf{a}[\hat{\theta}](\bar{V}^\uparrow[\hat{\theta}])^{-1} & \star \\ \bar{F}^\uparrow[\hat{\theta}] & 0 & I \end{bmatrix} \succ 0 \quad \forall \hat{\theta}, \quad (7.54c)$$

$$\begin{bmatrix} \mathbf{a}[\hat{\theta}]\bar{V}^\uparrow[\hat{\theta}] & \star & \star \\ P'[\hat{\theta}](\mathbf{a}[\hat{\theta}]\bar{A}^\uparrow[\hat{\theta}] + \bar{B}^\uparrow[\hat{\theta}]\mathfrak{L}[\hat{\theta}]) & \operatorname{blkdiag}_h(\mathbf{a}[h](\bar{V}^\uparrow[h])^{-1}) & \star \\ \mathbf{a}[\hat{\theta}]\bar{C}^\uparrow[\hat{\theta}] + \bar{D}^\uparrow[\hat{\theta}]\mathfrak{L}[\hat{\theta}] & 0 & I \end{bmatrix} \succ 0 \quad \forall \hat{\theta}, \quad (7.54d)$$

$$-M\bar{\sigma}_{p,q}^\uparrow[\hat{\theta}]\mathbf{1}_{\bar{n}_a^p \times \bar{n}_x^q} \leq \mathfrak{L}_{p,q}[\hat{\theta}] \leq M\bar{\sigma}_{p,q}^\uparrow[\hat{\theta}]\mathbf{1}_{\bar{n}_a^p \times \bar{n}_x^q} \quad \forall \hat{\theta}, p, q, \quad (7.54e)$$

with  $\hat{\theta} \in \Theta$ ,  $p, q \in \mathcal{N}_c[\hat{\theta}]$ , and  $\bar{V}^\uparrow[\hat{\theta}] \succ 0$ . Then, the assertions of Theorem 7.1 also hold with:

$$\bar{K}^\uparrow[\hat{\theta}] := (\mathbf{a}[\hat{\theta}])^{-1}\mathfrak{L}[\hat{\theta}]. \quad (7.55)$$

□

*Proof.* Forming the Schur-complement of LMI (7.54d) and substituting  $\mathfrak{L}[\hat{\theta}] = \mathbf{a}[\hat{\theta}]\bar{K}^\uparrow[\hat{\theta}]$  results in:

$$\begin{aligned} & \mathbf{a}[\hat{\theta}]\bar{V}^\uparrow[\hat{\theta}] - (\mathbf{a}[\hat{\theta}])^2(\bullet)^\top (\operatorname{blkdiag}_h((\mathbf{a}[h])^{-1}\bar{V}^\uparrow[h]))((P'[\hat{\theta}])(\bar{A}^\uparrow[\hat{\theta}] + \bar{B}^\uparrow[\hat{\theta}]\bar{K}^\uparrow[\hat{\theta}])) \dots \\ & - (\mathbf{a}[\hat{\theta}])^2(\bullet)^\top (\bar{C}^\uparrow[\hat{\theta}] + \bar{D}^\uparrow[\hat{\theta}]\bar{K}^\uparrow[\hat{\theta}]) \succ 0. \end{aligned} \quad (7.56)$$

Define  $\bar{V}_a^\uparrow[\hat{\theta}] := (\mathbf{a}[\hat{\theta}])^{-1}\bar{V}^\uparrow[\hat{\theta}]$  and  $\bar{V}_a^\uparrow := (\bar{V}_a^\uparrow[1], \dots, \bar{V}_a^\uparrow[N_\theta])$ . Dividing Eq. (7.56) by  $(\mathbf{a}[\hat{\theta}])^2 > 0$  and using Eq. (7.39) leads to:

$$\bar{V}_a^\uparrow[\hat{\theta}] - (\bullet)^\top (\mathcal{E}_\theta(\bar{V}_a^\uparrow))(\bar{A}^\uparrow[\hat{\theta}] + \bar{B}^\uparrow[\hat{\theta}]\bar{K}^\uparrow[\hat{\theta}]) - (\bullet)^\top (\bar{C}^\uparrow[\hat{\theta}] + \bar{D}^\uparrow[\hat{\theta}]\bar{K}^\uparrow[\hat{\theta}]) \succ 0. \quad (7.57)$$

Since it is assumed that  $\bar{V}_a^\uparrow[\hat{\theta}] \succ 0$ , the argumentation to show that assertions (a) to (c) hold is now very similar to the one that has been used from Eq. (7.40) to Eq. (7.50) in the proof of Theorem 7.1. Note that there is no need to constrain  $\mathbf{a}[\hat{\theta}]$  to positive values, since this is implicitly ensured by the upper left entry of LMI (7.54d).

The scaling by  $(\mathbf{a}[\hat{\theta}])^{-1}$  (see Eq. (7.55)) does not influence the structure of the gain matrix. Hence, the structural constraints can directly be formulated as linear constraints on  $\mathfrak{L}[\hat{\theta}]$ , leading to constraint (7.54e). □



Since the precomputed Lyapunov matrix  $\bar{V}^\uparrow[\hat{\theta}]$  is only scaled by the factor  $\mathbf{a}[\theta]$ , there is no need for a nonlinear controller parametrization in Theorem 7.2. Compared to Theorem 7.1, this leads to two major advantages: First, a smaller number of continuous optimization variables is required, which reduces the computational complexity of the problem. Furthermore, an approximation similar to Eq. (4.45) is not required for deriving the synthesis conditions. The second major advantage is that the scaled upper layer control gain matrices  $\mathfrak{L}[\hat{\theta}] = \mathbf{a}[\hat{\theta}]\bar{K}^\uparrow[\hat{\theta}]$  appear as an optimization variable. This allows to formulate the necessary and sufficient constraints (7.54e) to enforce a controller structure which is compatible with  $\bar{\Sigma}^\uparrow[\theta]$ . In contrast, the constraint set (7.33e) to (7.33g) used in Theorem 7.1 is only sufficient for  $\bar{K}^\uparrow[\hat{\theta}]$  being structurally compatible with  $\bar{\Sigma}^\uparrow[\theta]$ .

## 7.6. Numerical Example

The following academic example borrowed from [61] illustrates the principles of the presented approach. The considered interconnected system  $\{\mathcal{P}_\theta^i\}_{i \in \mathcal{N}_s}$  consists of  $N_s = 5$  subsystems with dimensions  $n_x^i = 2$  and  $n_u^i = 2$  for all  $i \in \mathcal{N}_s$ , and  $n_z^1 = n_z^4 = 3$ ,  $n_z^2 = n_z^3 = n_z^5 = 4$ . The global Markov chain  $\mathcal{M}_k$  is parameterized by:

$$P = \begin{bmatrix} 0.9 & 0.1 & 0 \\ 0.2 & 0.5 & 0.3 \\ 0 & 0.2 & 0.8 \end{bmatrix}, \quad \mu_0^\top = \begin{bmatrix} 1 \\ 0 \\ 0 \end{bmatrix}, \quad \Theta = \mathbb{I}_3, \quad (7.58)$$

with  $\Delta k = 5$ . The complete set of system matrices can be found in Appendix E.2.

The uncontrolled interconnected system  $\{\mathcal{P}_\theta^i\}_{i \in \mathcal{N}_s}$  is unstable in every single mode, and is not mean-square stable. The matrices  $\Gamma[\theta]$  describing the mode-dependent interconnection strength and structure are given by:

$$\begin{aligned} \Gamma[1] &= \begin{bmatrix} 2.43 & 2.21 & 0.71 & 0.20 & 0.20 \\ 3.00 & 3.08 & 0.30 & 0.10 & 1.73 \\ 0 & 0.10 & 1.60 & 4.01 & 0.50 \\ 0 & 0 & 1.13 & 2.45 & 4.00 \\ 0.10 & 0.46 & 0.63 & 0.40 & 3.24 \end{bmatrix}, & \Gamma[2] &= \begin{bmatrix} 4.14 & 0.81 & 1.77 & 0.20 & 0.20 \\ 0.40 & 5.11 & 0.10 & 0.30 & 2.14 \\ 0 & 0 & 6.83 & 4.01 & 0.60 \\ 0.20 & 0 & 1.13 & 2.45 & 2.40 \\ 0.10 & 0.42 & 0.63 & 1.00 & 3.24 \end{bmatrix}, \\ \Gamma[3] &= \begin{bmatrix} 3.74 & 1.71 & 2.23 & 0.50 & 0.20 \\ 0.60 & 7.74 & 0.40 & 0.30 & 1.38 \\ 0 & 0 & 3.94 & 4.01 & 0.60 \\ 0 & 0.20 & 1.32 & 2.48 & 0.60 \\ 0.10 & 1.15 & 0.63 & 1.00 & 3.24 \end{bmatrix}. \end{aligned} \quad (7.59)$$

At first glance, no particular interconnection structure can be identified from  $\Gamma[\cdot]$ . However, it can be observed that some interconnections are considerably weaker

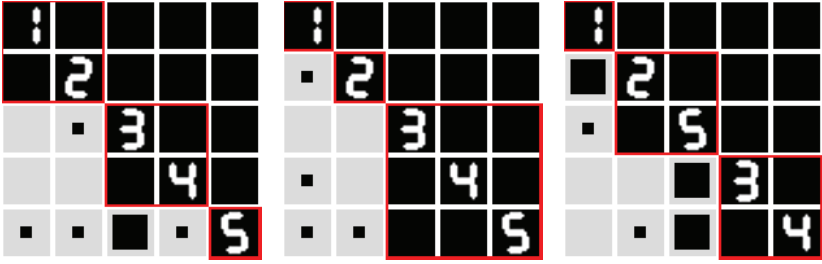


**Figure 7.2.:** Results of the clustering procedure visualized for  $\theta = 1$  (left) to  $\theta = 3$  (right). Large black squares denote strong interconnections, medium-sized black squares denote weak interconnections, and small black squares denote neglected interconnections, respectively. In each mode,  $N_c[\theta] = 3$  clusters are obtained, which are enframed in red.

than others, for instance  $\Gamma_{3,2}[1]$  versus  $\Gamma_{2,1}[1]$ . By the help of the clustering procedure presented in Sec. 7.2, an approximate hierarchical interconnection structure of the subsystems can be identified. Fig. 7.2 illustrates the results of the clustering procedure for  $\epsilon_n = 0.5$  and  $\epsilon_w = 0.65$ . In the figure, a strong interconnection ( $\gamma_{i,j}[\theta] > \epsilon_w$ ) is represented by a black square, a weak interconnection ( $\epsilon_n < \gamma_{i,j}[\theta] \leq \epsilon_w$ ) is represented by a medium-sized black square, and a neglected interconnection ( $\gamma_{i,j}[\theta] \leq \epsilon_n$ ) is represented by a small black square. A grey square represents a non-existing interconnection. In mode  $\theta = 1$  and  $\theta = 2$ , four interconnections are neglected, and one interconnection is considered to be weak in mode  $\theta = 1$ . In mode  $\theta = 3$ , two interconnections are neglected, and three interconnections are considered to be weak. In all three modes,  $N_c[\theta] = 3$  clusters are identified, which are parametrized by the index sets:

$$\begin{aligned}
 \mathcal{C}^1[1] &= \{1, 2\}, & \mathcal{C}^2[1] &= \{3, 4\}, & \mathcal{C}^3[1] &= \{5\}, \\
 \mathcal{C}^1[2] &= \{1\}, & \mathcal{C}^2[2] &= \{2\}, & \mathcal{C}^3[2] &= \{3, 4, 5\}, \\
 \mathcal{C}^1[3] &= \{1\}, & \mathcal{C}^2[3] &= \{2, 5\}, & \mathcal{C}^3[3] &= \{3, 4\}.
 \end{aligned} \tag{7.60}$$

Since the members of each cluster change as a function of the global mode  $\theta$ , the topology of the hierarchical controller also varies over time. Hence, in contrast to conventional control schemes, not only the controller parametrization, but also the controller structure reacts to the stochastic changes of the system behavior.

From the viewpoint of SCT design, the clustering procedure has reduced the number of independent communication links from  $N_l = 0.5 N_\theta (N_s^2 - N_s) = 60$  to  $N_l^\dagger = 0.5 \sum_{\theta \in \Theta} (N_c[\theta])^2 - N_c[\theta] = 18$ . As a consequence, the number of possible communication topologies is reduced from  $2^{60}$  to  $2^{18}$ , resulting in an improved scalability for the hierarchical approach compared to single layer SCT design. By

employing suitable and efficient algorithms like, e.g., branch-and-bound, the combinatorial complexity can be further reduced, since only a subset of the nodes of the underlying search tree has to be taken into account.

A comparison of the performance measure  $J$  according to Case 2.2 and the computation time of different types of controllers is performed in Table 7.1. The first and the last row contain the results of centralized controllers that have been separately designed for a comparison with the hierarchical control scheme. The lower layer controller in the first row is designed to be robust against the time-varying transition probabilities, considering the transition probability matrix as a matrix polytope  $P(\alpha) = \alpha P + (1 - \alpha)I$  with  $\alpha \in [0, 1]$ . For details on this approach, the reader is referred to [101]. The bad performance of the centralized upper layer controller in the last row of the table is due to the upper layer model being badly conditioned, when no lower control layer is present. Concerning overall performance, the proposed hierarchical control scheme outperforms every single-layer control scheme, while providing a tradeoff between performance and communication cost. As a drawback, the hierarchical design requires a computation time of almost an hour, while the design of conventional centralized controllers only takes a few seconds<sup>1</sup>. This increase in computation time is mainly due to the incorporated SCT design and the structural constraints imposing the distributed controller structure. By using Theorem 7.2 instead of Theorem 7.1, the computation time for the hierarchical control scheme can be reduced by more than a factor ten. Notably, both Theorems result in different controller parametrizations with different communication topologies, although the parametrization of the optimization problem is the same. This discrepancy is due to the fact that both approaches use different upper bounds on the performance measure, and that the structural constraints used in Thm. 7.2 are less conservative than those used in Thm. 7.1. The parameters of the hierarchical controllers can be found in Appendix E.2.

## 7.7. Discussion

This chapter considered a class of interconnected semi-Markov jump systems with fast continuous dynamics and a global Markov chain being evaluated on a coarser time scale. Thus, spatially distributed subsystems with small time constants and abrupt changes occurring in larger time intervals can be efficiently modeled in this framework. Assuming that the Markov chain is evaluated after a fixed number of discrete time steps, it is shown that a hierarchical two-layer controller structure similar to the one presented in the second part of this thesis is particularly suited to control such types of dynamic systems. An algorithm was presented which groups the subsystems into clusters, depending on the global mode of the system. This results in a reduced combinatorial complexity when performing simultaneous control

---

<sup>1</sup>The computations were performed with an AMD Phenom II X4-920 processor with 4Gb of RAM, using Matlab, YALMIP [79], and the MOSEK optimization software [95].

**Table 7.1.:** Comparison of different controller types for  $\mathcal{P}_\theta$ . The first and the last row contain separately designed centralized controllers for the lower layer and for the upper layer time domain, respectively. For the hierarchical design, Thm. 7.1 is used in the third row, and Thm. 7.2 is used in the fourth row. The performance index  $J$  is interpreted according to Case 2.2.

#	controller	design model	calc. time	time domain	$J$	$J^{\uparrow\text{com}}$
1	lower layer	$\bar{\mathcal{P}}_\theta$	2.5 [s]	$\mathbb{T}^\downarrow$	21.97	0
2	lower layer	$\bar{\mathcal{P}}'_\theta$	4 [s]	$\mathbb{T}^\downarrow$	29.49	0
3	hierarchical	$\bar{\mathcal{P}}'_\theta, \bar{\mathcal{P}}_\theta^\uparrow$	2964 [s]	$\mathbb{T}^\downarrow, \mathbb{T}^\uparrow$	5.52	0.5
4	—, Thm. 7.2	$\bar{\mathcal{P}}'_\theta, \bar{\mathcal{P}}_\theta^\uparrow$	273 [s]	$\mathbb{T}^\downarrow, \mathbb{T}^\uparrow$	5.50	2.25
5	upper layer	$\bar{\mathcal{P}}_\theta^\uparrow$ w. $\bar{K}^\downarrow[\cdot] = 0$	40 [s]	$\mathbb{T}^\uparrow$	10712	3

and network topology design, and furthermore allows to adopt the structure of the distributed controllers depending on the global system mode. In total, the resulting two-layer control scheme provides a good and parametrizable tradeoff between closed-loop performance and communication effort.

The design of each control layer can be formulated by means of independent semidefinite programs, which can be solved sequentially. The controller derived from the solutions of these optimization problems satisfies sufficient conditions regarding controller structure. Furthermore, it guarantees stability and performance of the controlled system. For the upper control layer, it was shown that the synthesis complexity can be further reduced by using a Lyapunov function with a single degree of freedom. This Lyapunov function is the scaled value function obtained from the coupled algebraic Riccati equations associated with the centralized optimal control problem. A particular advantage that comes with this approach is that necessary and sufficient constraints for enforcing the controller structure can be formulated. However, the optimization results in a different optimized controller structure, since an other upper bound for the performance of the controlled system is used.

So far, the hierarchical approach pursued in this chapter is restricted to  $\Delta k$  being constant. Extending the construction of the upper layer system and the corresponding synthesis conditions for control design to incorporate time-varying values of  $\Delta k$  thus remains an open question. Similar to Chap. 6, the main challenge will be to find an efficient solution for handling the additional source of uncertainty in the upper layer model.



## 8. Discussion and Outlook

In this thesis, different approaches to distributed feedback control of interconnected discrete-time systems are presented. A special focus is on the development of hierarchical control structures and the integration of structural analysis and decomposition methods within the control design, which allows to deal with large systems of high complexity. More specifically, Chapter 3 presents a hierarchical two-layer feedback control scheme which groups strongly coupled subsystems on a lower control layer and coordinates these weakly coupled groups on an upper control layer with lower sampling frequency. This concept is extended in Chapter 4, where the distributed upper layer controllers are now designed to operate sequentially instead of simultaneously by employing concepts from periodic system theory. In Chapter 5, both two-layer control schemes are compared and applied to an example system from the domain of power systems. Chapter 6 presents an approach to distributed control of jump Markov linear systems with local Markov chains. In particular, it is shown how uncertain communication links can be taken into account already during the control design phase. Finally, the hierarchical two-layer control scheme developed in Chapter 3 and Chapter 4 is extended to a class of jump semi-Markov linear systems in Chapter 7. In this chapter, the results of the previous chapters are summarized and discussed. Afterwards, some directions for future research are presented.

### 8.1. Summary and Comparison of the Presented Approaches

The main goal pursued in this thesis is to combine the ideas and advantages from the fields of system decomposition, hierarchical feedback control, and SCT design for being able to design distributed control laws for complex interconnected systems. Instead of designing a single distributed control layer for the overall system, the idea is to analyse and decompose the system structure in a first step. The actual control task should be performed by multiple control layers in a cooperative manner, where a particular goal is that both control layers cooperatively optimize a global performance index. In the sequel, the developed approaches are summarized and compared against each other.

In Chapter 3, a distributed hierarchical two-layer control structure is presented as an alternative to distributed single-layer feedback control structures with optimized communication network topology. The basic idea is to simplify the communication

topology optimization performed during the control design by incorporating information about the interconnection structure of the dynamical subsystems. To this end, a structural analysis is performed prior to the control design, which groups strongly coupled subsystems into clusters. These clusters are controlled by a distributed lower control layer, which exchanges information only between subsystems that are in the same cluster. A super-ordinated upper control layer is responsible for the coordination of the clusters, and accounts for neglected interconnections between them. Combining the communication topology optimization with the design of the upper control layer, a tradeoff between global closed-loop performance and communication effort is achieved. At the same time, the combinatorial complexity of the communication topology optimization is significantly reduced, since the clustering reduces the number of possible communication topologies. The clustering procedure does not lead to a pre-determined result, but provides some degrees of freedom to the control designer. More specifically, the thresholds for classifying weak and negligible interconnections and the criterion for joining clusters have to be chosen. These thresholds influence the structure and performance of the resulting two-layer controller. Therefore, the clustering procedure is seen as a supportive tool for the control design process. The qualitative influence of the design parameters is discussed in detail in Sec. 3.2. Since the identified clusters are only weakly coupled, the upper control layer can be implemented on a coarser time-scale compared to the lower control layer. This further reduces the communication effort. Numerical results show that the closed-loop performance of this control scheme is close to the optimal performance of a linear quadratic regulator, while enabling a distributed implementation with a sparse communication graph.

Chapter 4 directly builds on the results of Chapter 3, and addresses the distribution of the communication load within the two-layer scheme. Since the distributed upper layer controllers proposed in Chapter 3 update their controlled variables synchronously, the amount of data exchanged via the communication network possesses high periodic peaks. In order to avoid these peaks, upper layer controllers performing sequential updates are proposed in Chapter 4. This way, the communication load is equably distributed over time. The main contribution of Chapter 4 is the development of a modeling scheme which transforms the distributed upper layer control problem to the framework of periodic systems. This allows to formulate the control design problem as an optimization problem. Within this new approach, new questions concerning the upper control layer arise, such as the optimal controller update sequence, the optimal initialization of the controllers, and the benefits of exchanging the local controlled variables. Simulation results show that the performance of the synchronous and the asynchronous scheme is comparable, while the latter requires more computational resources.

In Chapter 5, the synchronous and asynchronous hierarchical control scheme are applied to a dynamic model from the domain of power systems. More specifically, a linearized model of the popular 10-bus CIGRÉ benchmark system serves as an application example for both two-layer control schemes. A remarkable result pre-

sented in this chapter is that even an unstable lower layer controller contributes to the overall system performance when combined with a stabilizing upper control layer. Furthermore, the performance of both two-layer control schemes is in between the optimal performance achieved by an LQR on the lower and on the upper control layer. Finally, it has been shown that the two-layer control schemes are robust against communication delays. This has been verified for constant delays of up to 70 percent of one sampling period.

Chapter 6 deals with distributed control of interconnected jump Markov linear subsystems. In contrast to the other approaches, a single-layer control scheme is considered in this chapter, as a special focus is on stability and performance robustness against communication link failures. For developing sufficient conditions for control synthesis, the subsystems as well as the stochastic model of the availability of the communication links are combined to a structured jump Markov system. The control synthesis results in a set of controllers for each subsystem. During the execution of the distributed control scheme, the appropriate local control laws are selected depending on the information that is available to each subsystem at the current time-step. Thus, in contrast to the hierarchical distributed control schemes presented in Chapters 3 and 4, the local controllers are able to adapt to time-varying communication topologies. However, the structure of the optimization problem used for control synthesis makes it difficult to incorporate SCT design.

Finally, the distributed two-layer control scheme presented in the second part of this thesis is extended to a class of interconnected jump semi-Markov linear systems in Chapter 7. It is shown that if the Markov chain is evaluated on a coarser time-scale than the dynamics, a two-layer control scheme is particularly suited to control such a semi-Markov system, since each layer handles different control tasks: The lower control layer is optimized for to perform well for fixed modes and coordinates the strongly coupled subsystems within each cluster, while the upper control layer handles the mode transitions and coordinates the weakly coupled clusters. A further contribution of Chapter 7 is an optimization-based approach for control synthesis which reduces the required computation effort. This is accomplished by scaling the value function obtained from the coupled algebraic Riccati equations by a scalar factor. This way, the number of continuous optimization variables is significantly reduced. Furthermore, new constraints on the controller structure can be formulated which are less restrictive compared to the ones used before. Not surprisingly, different numerical results are obtained with this simplified approach, which emphasizes the influence of the employed approximation for the closed-loop performance and the structural constraints.

The contributions of this thesis can be summarized as follows:

- A distributed hierarchical two-layer feedback control scheme for interconnected LTI systems is developed. It builds on a structural analysis of the interconnected system and groups strongly coupled subsystems into clusters. These clusters are controlled by a distributed lower control layer, which is designed



by neglecting the interconnections between the clusters. The coordination of the clusters is performed by a super-ordinated upper control layer, which cooperates with the lower control layer for optimizing a global performance index. Optionally, the communication topology of the upper control layer can be optimized during the control synthesis, leading to an approximation of single-layer SCT design problems with reduced combinatorial complexity.

- For interconnected jump Markov linear systems, a synthesis procedure for distributed state feedback control is presented. In particular, the distributed controller structure respects a given topology of the communication network, and is able to adapt to stochastic communication link failure or package dropouts based on locally available information only.
- All presented approaches are provided with rigorous stability and performance guarantees, which are verified with explicit and detailed mathematical proofs. The considered performance criteria and optimization problems employed for control synthesis are presented in a unified and versatile mathematical framework. Furthermore, every control approach is exemplarily applied to a numerical example.
- The synchronous and asynchronous hierarchical two-layer control schemes are applied to a common benchmark model for the frequency control of power systems. The proposed control schemes are compared against the optimal centralized solutions, which reveals that they provide a good tradeoff between performance and communication effort.

## 8.2. Outlook

Large parts of the presented approaches are independent of a particular mathematical framework, and are therefore amenable to various extensions. For instance, the general concept of two cooperating distributed control layers could be generalized to further classes of dynamic systems, like nonlinear or parameter-varying dynamics. On the other hand, when dealing with linear dynamics, the LMI-based synthesis framework chosen in this thesis also provides much flexibility.

Besides the extension to other classes of dynamic systems, another open problem is to generalize the presented concepts to the case of static output feedback or dynamic output feedback. A first step in this direction was taken in the master thesis [42], which proposes an extension of the LMI-based synthesis framework. However, it turned out that especially for the case of dynamic output feedback, the state of the art optimization algorithms suffer from massive numerical problems when applied to the resulting semidefinite programs. This effect can already be observed for trivial dynamics with two state variables. The problem is closer investigated in [118] and in [43], where a direct search algorithm and an approach based on the

alternating direction method of multipliers (ADMM), respectively, are proposed as a remedy. Another option could be to use a simplified LMI formulation similar to the one presented in Sec. 7.5, which may increase the numerical robustness.

A particular question that has not yet been addressed for the proposed hierarchical feedback controllers is how to incorporate constraints on the input variables of the interconnected system. For single-layer state feedback controllers, such constraints have already been implemented in the versatile LMI framework, see for instance [25, Sec. 7.2.3]. That approach, as well as similar ones, could serve well as a starting point for finding suitable constraints for the case of hierarchical state feedback. Similarly, the ideas presented in Chapter 7, namely the explicit consideration of uncertain communication links during control synthesis, could be generalized to the hierarchical two-layer concept. Notably, the two-layer scheme already exhibits a certain degree of robustness against permanent communication link failures: In case that the lower control layer already stabilizes the interconnected system, the upper control layer could simply be disabled if some of the associated communication links fail.

As has already been mentioned in the previous section, the asynchronous hierarchical feedback scheme presented in Chapter 4 raised many new questions compared to the synchronous scheme of Chapter 3. For instance, the distributed computation of an optimal initialization of the local upper layer controllers is still an open problem. Here, ideas from distributed optimization or distributed model predictive control may lead the way towards a solution. From a control theoretic point of view, another interesting question would be whether the optimal upper layer controllers depend on their initialization or not.

Another line of thought concerns the clustering procedures presented in Sec. 3.2 and in Sec. 7.2, which is currently limited to the interconnections of the states and inputs of the dynamics. Thus, it remains an open question if the clustering could additionally or even completely be performed from the perspective of the global performance criterion. This would mean to form clusters which are weakly coupled in terms of the global performance criterion instead of the global closed-loop stability.



# Appendix A. Equivalence of Output Variance and $\mathcal{H}_2$ -Norm

The following proofs belong to Lemma 2.1 and to Lemma 2.3, which can be found on p.39 and on p.40, respectively.

## A.1. Proof of Lemma 2.1

*Proof.* Recall the closed-loop dynamic system  $\mathcal{P}_{\text{cl}}$  with input  $w_k$  and output  $z_k$  as stated in Eq. (2.51):

$$\mathcal{P}_{\text{cl}} = \begin{cases} x_{k+1} = (A + BK)x_k + Ew_k = A_{\text{cl}}x_k + Ew_k, \\ z_k = (C + DK)x_k + Fw_k = C_{\text{cl}}x_k + Fw_k, \end{cases} \quad (\text{A.1})$$

and assume that  $A$  is a Schur matrix. Next, consider the performance index  $J$  as defined in Eq. (2.20). Exploiting the linearity of the expected value and the basic properties of the trace leads to:

$$\begin{aligned} J &= \lim_{k_e \rightarrow \infty} \mathbb{E} \left( \frac{1}{k_e} \sum_{k=0}^{k_e-1} z_k^\top z_k \right) = \lim_{k_e \rightarrow \infty} \mathbb{E} \left( \frac{1}{k_e} \sum_{k=0}^{k_e-1} \text{tr}(z_k^\top z_k) \right) \\ &= \lim_{k_e \rightarrow \infty} \mathbb{E} \left( \frac{1}{k_e} \sum_{k=0}^{k_e-1} \text{tr}(z_k z_k^\top) \right) = \lim_{k_e \rightarrow \infty} \text{tr} \left( \frac{1}{k_e} \sum_{k=0}^{k_e-1} \mathbb{E}(z_k z_k^\top) \right). \end{aligned} \quad (\text{A.2})$$

Recall that  $w_k$  is assumed to be independent of  $x_0$ , with  $\mathbb{E}(w_k) = 0$  and  $\mathbb{E}(w_k w_l^\top) = 0$  for all  $k, l \in \mathbb{N}_0$  with  $k \neq l$ . It follows that:

$$\begin{aligned} \mathbb{E}(x_k w_k^\top) &= \mathbb{E}((A_{\text{cl}} x_{k-1} + Ew_{k-1})w_k^\top) = A_{\text{cl}} \mathbb{E}(x_{k-1} w_k^\top) \\ &= (A_{\text{cl}})^k \mathbb{E}(x_0 w_k^\top) = 0. \end{aligned} \quad (\text{A.3})$$

With  $\mathbb{E}(w_k w_k^\top) = I$ , it now holds for the covariance of  $z_k$  that:

$$\mathbb{E}(z_k z_k^\top) = C_{\text{cl}} \mathbb{E}(x_k x_k^\top) C_{\text{cl}}^\top + F F^\top. \quad (\text{A.4})$$

Defining  $X_k := \mathbb{E}(x_k x_k^\top)$ , the performance index  $J$  is thus equivalent to:

$$J = \lim_{k_e \rightarrow \infty} \text{tr} \left( \frac{1}{k_e} \sum_{k=0}^{k_e-1} C_{\text{cl}} X_k C_{\text{cl}}^\top + F F^\top \right). \quad (\text{A.5})$$

Due to the assumptions on  $w_k$ , the covariance matrix  $X_k$  of the state  $x_k$  evolves according to (see [65, Thm. 6.22] or [4, Sec. 4.3]):

$$X_{k+1} = A_{\text{cl}}X_kA_{\text{cl}}^{\text{T}} + EE^{\text{T}}, \quad (\text{A.6})$$

with  $X_0 = 0_{n_x \times n_x}$ . For  $k_e \rightarrow \infty$ , the performance index converges to (see [65, Thm. 6.23, Thm. 6.24] or [4, Thm. 3.1]):

$$J = \text{tr} \left( C_{\text{cl}}XC_{\text{cl}}^{\text{T}} + FF^{\text{T}} \right), \quad (\text{A.7})$$

with  $X$  denoting the unique solution to the Lyapunov equation:

$$X = A_{\text{cl}}XA_{\text{cl}}^{\text{T}} + EE^{\text{T}}. \quad (\text{A.8})$$

It follows from (A.7) and (A.8) that  $J = \|\mathcal{P}_{\text{cl}}\|_{\mathcal{H}_2}^2$ , see e.g. [142, p.561].  $\square$

## A.2. Proof of Lemma 2.3

*Proof.* Consider the squared  $\mathcal{H}_2$ -norm of an LTI system  $\mathcal{P}_{\text{cl}}$  with  $E := x_0$  and  $F := 0_{n_z \times n_w}$ :

$$\begin{aligned} \|\mathcal{P}_{\text{cl}}\|_{\mathcal{H}_2}^2 &= \sum_{k=0}^{\infty} \text{tr}(\mathbf{z}_k^{\text{T}}\mathbf{z}_k) \\ &= \sum_{k=0}^{\infty} \text{tr}((C_{\text{cl}}(A_{\text{cl}})^{k-1}x_0)^{\text{T}}(C_{\text{cl}}(A_{\text{cl}})^{k-1}x_0)) \\ &= \sum_{k=0}^{\infty} \text{tr}(x_k^{\text{T}}C_{\text{cl}}^{\text{T}}C_{\text{cl}}x_k) \\ &= \sum_{k=0}^{\infty} \text{tr}(z_k^{\text{T}}z_k) \\ &= J. \end{aligned} \quad (\text{A.9})$$

$\square$

# Appendix B. Expected Performance for Stochastic Initial States

The purpose of this chapter is to prove the following lemma, which can be used to formulate the expected quadratic cost in the case that the initial state  $x_0$  is uniformly distributed over an ellipsoid, as shown in Sec. 3.4.4 (see p.67).

**Lemma B.1.** *Assume that  $x \sim \mathcal{U}(\mathcal{E}_x)$  is uniformly distributed over the ellipsoid:*

$$\mathcal{E}_x := \{x \in \mathbb{R}^{n_x} \mid (x - \mu_x)^\top \Sigma_x^{-1} (x - \mu_x) \leq 1\}, \quad (\text{B.1})$$

and let  $P \in \mathbb{S}_{>0}^n$ . Then, it holds that:

$$\mathbb{E}(x^\top P x) = \frac{1}{n_x + 2} \text{tr}(\Sigma_x P) + \mu_x^\top P \mu_x. \quad (\text{B.2})$$

□

In order to proof the above result, first consider the following two lemmas.

**Lemma B.2.** *Consider the infinite sequence  $(s_n)_{n \in \mathbb{N}}$  defined by:*

$$s_n := \int_0^\pi \sin^n(\xi) d\xi. \quad (\text{B.3})$$

For all  $m, n \in \mathbb{N}$ , it holds that:

$$s_n = \begin{cases} \frac{n-1}{n} \frac{n-3}{n-2} \frac{n-5}{n-4} \cdots \frac{5}{6} \frac{3}{4} \frac{\pi}{2} & \text{if } n = 2m, \\ \frac{n-1}{n} \frac{n-3}{n-2} \frac{n-5}{n-4} \cdots \frac{4}{5} \frac{2}{3} & \text{if } n = 2m - 1, \end{cases} \quad (\text{B.4})$$

which implies that  $0 < s_n \leq 2 \forall n \in \mathbb{N}$ . □

*Proof.* Exploiting that:

$$\int_0^\pi \sin^n(\xi) d\xi = 2 \int_0^{\frac{\pi}{2}} \sin^n(\xi) d\xi, \quad (\text{B.5})$$

Eq. (6) of [28, p.1050] can be used to show the claim. □

**Lemma B.3.** Let  $P \in \mathbb{S}_{>0}^n$  be a symmetric positive definite matrix, and let  $\bar{\mathcal{E}}(r, \mu, \Sigma)$  with  $r \in \mathbb{R}_{\geq 0}$ ,  $\mu \in \mathbb{R}^n$ , and  $\Sigma \in \mathbb{S}_{>0}^n$  denote a closed set defined as:

$$\bar{\mathcal{E}}(r, \mu, \Sigma) := \{x \in \mathbb{R}^n \mid (x - \mu)^\top \Sigma^{-1} (x - \mu) = r^2\}. \quad (\text{B.6})$$

Then, there exist functions:

$$\alpha(r, n) := r^{n+1} \prod_{j=1}^n s_j \geq 0, \quad \beta(r, n) := 2\pi r^{n-1} \prod_{j=1}^{n-2} s_j \geq 0, \quad (\text{B.7})$$

and a positive definite matrix  $V \in \mathbb{R}_{>0}^{n \times n}$  with  $VV^\top = \Sigma$  such that:

$$\int_{\bar{\mathcal{E}}(r, \mu, \Sigma)} x^\top P x \, dx = \det(V) \left[ \alpha(r, n) \operatorname{tr}(P\Sigma) + \beta(r, n) \mu^\top P \mu \right]. \quad (\text{B.8})$$

□

*Proof.* Since  $\Sigma \in \mathbb{S}_{>0}^n$ , one can always find  $V \in \mathbb{R}_{>0}^{n \times n}$  such that  $\Sigma = VV^\top$ , e.g. by applying the Cholesky decomposition to  $\Sigma$  (see [28, p.890]). Using the invertible linear variable transformation  $y = V^{-1}(x - \mu)$ , the integral in Eq. (B.8) can be rewritten as:

$$\int_{\bar{\mathcal{E}}(r, \mu, \Sigma)} x^\top P x \, dx = \det(V) \int_{\bar{\mathcal{E}}(r, 0, I)} y^\top V^\top P V y + 2y^\top V^\top P \mu + \mu^\top P \mu \, dy, \quad (\text{B.9})$$

with  $\det(V) > 0$ . In the remainder of the proof, the integral on the right-hand side is split into three summands, each of which are considered separately in the sequel. Since  $P \in \mathbb{S}_{>0}^n$  and  $V \in \mathbb{R}_{>0}^{n \times n}$ , it holds that  $V^\top P V \in \mathbb{S}_{>0}^n$ . Hence, there always exists an orthogonal transformation matrix  $T \in \mathbb{R}^{n \times n}$  with  $T^\top T = TT^\top = I$  and  $\det(T) = 1$  (see [28, p.257, p.280f]) such that:

$$T^\top V^\top P V T = D, \quad (\text{B.10})$$

where  $D = \operatorname{diag}(d_{i,i}) \in \mathbb{S}_{>0}^n$  is a diagonal matrix. Letting  $z = T^\top y$ , it holds that:

$$\int_{\bar{\mathcal{E}}(r, 0, I)} y^\top V^\top P V y \, dy = \int_{\bar{\mathcal{E}}(r, 0, I)} z^\top D z \det(T) \, dz = \int_{\bar{\mathcal{E}}(r, 0, I)} z^\top D z \, dz. \quad (\text{B.11})$$

Note that the set  $\bar{\mathcal{E}}(r, 0, I)$  is not altered due to this transformation, since:

$$y^\top y = z^\top T^\top T z = z^\top z. \quad (\text{B.12})$$

Since  $\bar{\mathcal{E}}(r, 0, I)$  describes the surface of a hyperball, it is convenient to perform a coordinate transformation for the right-hand side of (B.11) from kartesian into  $n$ -dimensional polar coordinates [2, p.199], which leads to (B.14) (see page 167). Substituting the absolute value of the functional determinant [2, p.200]:

$$\det(J) = \frac{\partial(z_1, \dots, z_n)}{\partial(r, \varphi, \theta_1, \dots, \theta_{n-2})} = (-1)^n r^{n-1} \sin(\theta_1) \sin^2(\theta_2) \cdots \sin^{n-2}(\theta_{n-2}), \quad (\text{B.13})$$

and excluding the factor  $r^{n+1}$  leads to (B.15).

$$\begin{aligned}
\int_{\mathcal{E}(r,0,t)} z^T D z dz &= \int_{-\pi}^{\pi} \int_0^{\pi} \int_0^{\pi} \int_0^{\pi} \dots \int_0^{\pi} [r^2 \cos^2(\varphi) \sin^2(\theta_1) \sin^2(\theta_2) \sin^2(\theta_3) \dots \sin^2(\theta_{n-2}) \sin^2(\theta_{n-1})] d_{1,1} \dots \\
&+ r^2 \sin^2(\varphi) \sin^2(\theta_1) \sin^2(\theta_2) \sin^2(\theta_3) \dots \sin^2(\theta_{n-3}) \sin^2(\theta_{n-2}) d_{2,2} \dots \\
&+ r^2 \cos^2(\theta_1) \sin^2(\theta_2) \sin^2(\theta_3) \dots \sin^2(\theta_{n-3}) \sin^2(\theta_{n-2}) d_{3,3} \dots \\
&+ r^2 \cos^2(\theta_2) \sin^2(\theta_3) \dots \sin^2(\theta_{n-3}) \sin^2(\theta_{n-2}) d_{4,4} + \dots \\
&+ \dots + \dots \\
&+ r^2 \cos^2(\theta_{n-3}) \sin^2(\theta_{n-2}) p_{n-1,n-1} + r^2 \cos^2(\theta_{n-2}) d_{n,n} \Big] |\det(\mathcal{J})| \dots \\
&d\theta_1 d\theta_2 d\theta_3 \dots d\theta_{n-3} d\theta_{n-2} d\varphi
\end{aligned} \tag{B.14}$$

$$\begin{aligned}
\int_{\bar{\mathcal{E}}(r,0,t)} z^T D z dz &= r^{n+1} \int_{-\pi}^{\pi} \int_0^{\pi} \int_0^{\pi} \dots \int_0^{\pi} \cos^2(\varphi) \sin^3(\theta_1) \sin^4(\theta_2) \sin^5(\theta_3) \dots \sin^{n-1}(\theta_{n-3}) \sin^n(\theta_{n-2}) d_{1,1} \dots \\
&+ \sin^2(\varphi) \sin^3(\theta_1) \sin^4(\theta_2) \sin^5(\theta_3) \dots \sin^{n-1}(\theta_{n-3}) \sin^n(\theta_{n-2}) d_{2,2} \dots \\
&+ \cos^2(\theta_1) \sin(\theta_1) \sin^4(\theta_2) \sin^5(\theta_3) \dots \sin^{n-1}(\theta_{n-3}) \sin^n(\theta_{n-2}) d_{3,3} \dots \\
&+ \cos^2(\theta_2) \sin(\theta_1) \sin^2(\theta_2) \sin^5(\theta_3) \dots \sin^{n-1}(\theta_{n-3}) \sin^n(\theta_{n-2}) d_{4,4} \dots \\
&+ \dots + \dots \\
&+ \cos^2(\theta_{n-3}) \sin(\theta_1) \sin^2(\theta_2) \sin^3(\theta_3) \dots \sin^{n-3}(\theta_{n-3}) \sin^n(\theta_{n-2}) d_{n-1,n-1} \dots \\
&+ \cos^2(\theta_{n-2}) \sin(\theta_1) \sin^2(\theta_2) \sin^3(\theta_3) \dots \sin^{n-3}(\theta_{n-3}) \sin^{n-2}(\theta_{n-2}) d_{n,n} \dots \\
&d\theta_1 d\theta_2 d\theta_3 \dots d\theta_{n-3} d\theta_{n-2} d\varphi
\end{aligned} \tag{B.15}$$

$$\int_{\bar{\mathcal{E}}(r,0,t)} z^T D z dz = r^{n+1} \left[ \prod_{j=3}^n s_j \int_{-\pi}^{\pi} \cos^2(\varphi) d\varphi d_{1,1} + \int_{-\pi}^{\pi} \sin^2(\varphi) d\varphi d_{2,2} \right] + \sum_{i=3}^n \prod_{j=1}^{s_j} \int_{-\pi}^{\pi} s_l \int_{-\pi}^{\pi} \cos^2(\theta_{l-2}) \sin^{i-2}(\theta_{l-2}) d\theta_{l-2} d\varphi d_{i,i} \tag{B.16}$$



Exploiting the linearity of integration, the multiple integral is split into a sum of  $n$  multiple integrals, each containing one diagonal element  $d_{i,i}$  of  $D$ . Furthermore, since the integration limits are constant and the integrand is a product of functions depending on a scalar variable, each multiple integral can be rewritten as a product of independent integrals. Altogether, by using the definition (B.3), Equation (B.15) can be rewritten as (B.16), where the product operator is defined by:

$$\prod_{i=j}^l s_i := \begin{cases} 1 & \text{if } (l < j), \\ s_j & \text{if } (l = j), \\ s_j s_{j+1} \cdots s_{l-1} s_l & \text{if } (l > j), \end{cases} \quad (\text{B.17})$$

for  $j, l \in \mathbb{N}_0$ . It can easily be verified that:

$$\int_{-\pi}^{\pi} \cos^2(\varphi) d\varphi = \int_{-\pi}^{\pi} \sin^2(\varphi) d\varphi = s_1 s_2 = \pi, \quad (\text{B.18})$$

such that the factors of  $d_{1,1}$  and  $d_{2,2}$  in (B.16) are equal to  $\alpha(r, n)$ . Assume that the coefficients of the remaining  $d_{i,i}$  with  $i \in \{3, \dots, n\}$  in (B.16) are all equal to  $\alpha(r, n)$ , which results in:

$$r^{n+1} \prod_{j=1}^n s_j \stackrel{!}{=} r^{n+1} \prod_{j=1}^{i-3} s_j \prod_{l=i+1}^n s_l \int_{-\pi}^{\pi} \int_0^{\pi} \cos^2(\theta_{i-2}) \sin^{i-2}(\theta_{i-2}) d\theta_{i-2} d\varphi. \quad (\text{B.19})$$

Obviously, the above equation holds in the trivial case that  $r^{n+1} = 0$ . In the case that  $r^{n+1} > 0$ , dividing both sides by:

$$r^{n+1} \prod_{j=1}^{i-3} s_j \prod_{l=i+1}^n s_l > 0, \quad (\text{B.20})$$

changing the integration order, and performing the change of variables  $\xi := \theta_{i-2}$ , it remains to show that:

$$s_{i-2} s_{i-1} s_i \stackrel{!}{=} \int_{-\pi}^{\pi} \int_0^{\pi} \cos^2(\xi) \sin^{i-2}(\xi) d\xi d\varphi \quad \forall i \in \{3, \dots, n\}. \quad (\text{B.21})$$

Consider the following relation, obtained by partial integration of  $s_i$  for  $i \geq 2$ :

$$s_i = \int_0^{\pi} \sin^{i-1}(\xi) \sin(\xi) d\xi = (i-1) \int_0^{\pi} \cos^2(\xi) \sin^{i-2}(\xi) d\xi. \quad (\text{B.22})$$

Substituting (B.22) into (B.19) and integrating the right-hand side:

$$s_{i-2} s_{i-1} s_i \stackrel{!}{=} \int_{-\pi}^{\pi} \frac{s_i}{i-1} d\varphi. \quad (\text{B.23})$$

Dividing by  $s_i > 0$  leads to:

$$s_{i-2}s_{i-1} \stackrel{!}{=} \frac{2\pi}{i-1}, \quad (\text{B.24})$$

which can be easily verified by the help of Lemma B.2. Hence, it holds that:

$$\int_{\bar{\mathcal{E}}(r,0,I)} y^\top V^\top P V y dy = \int_{\bar{\mathcal{E}}(r,0,I)} z^\top D z = \alpha(r, n) \sum_{i=1}^n d_{i,i} = \alpha(r, n) \text{tr}(D). \quad (\text{B.25})$$

With  $D = T^\top V^\top P V T$ ,  $T T^\top = I$ , and  $\Sigma = V V^\top$ , as well as with some basic properties of the trace, it follows that:

$$\int_{\bar{\mathcal{E}}(r,0,I)} y^\top V^\top P V y dy = \alpha(r, n) \text{tr}(D) = \alpha(r, n) \text{tr}(V^\top P V) = \alpha(r, n) \text{tr}(P \Sigma). \quad (\text{B.26})$$

Performing a coordinate transformation for the second summand in (B.9) into polar coordinates leads to (B.32) (see page 170). Substituting the functional determinant  $\det(J)$  as defined in (B.13) and using definitions (B.3) and:

$$\tilde{\mu}_i := \sum_{j=1}^n \tilde{p}_{i,j} \mu_j \quad (\text{B.27})$$

leads to (B.33). For the coefficients of  $\tilde{\mu}_1$  and  $\tilde{\mu}_2$ , it is easily verified that:

$$\int_{-\pi}^{\pi} \cos(\varphi) d\varphi = \int_{-\pi}^{\pi} \sin(\varphi) d\varphi = 0. \quad (\text{B.28})$$

For  $i \in \{3, \dots, n\}$  and  $\xi := \theta_{i-2}$ , the coefficient of  $\tilde{\mu}_i$  contains the factor:

$$\int_{-\pi}^{\pi} \int_0^{\pi} \cos(\xi) \sin^{i-2}(\xi) d\xi d\varphi = 2\pi \int_0^{\pi} \cos(\xi) \sin^{i-2}(\xi) d\xi = 2\pi \left[ \frac{1}{i-1} \sin^{i-1}(\xi) \right]_{\xi=0}^{\xi=\pi} = 0, \quad (\text{B.29})$$

where the antiderivative is obtained by means of partial integration. Hence:

$$2 \int_{\bar{\mathcal{E}}(r,0,I)} y^\top V^\top P \mu dy = 0. \quad (\text{B.30})$$

Transforming the third summand of (B.9) to polar coordinates leads to:

$$\begin{aligned} \int_{\bar{\mathcal{E}}(r,0,I)} \mu^\top P \mu dy &= \mu^\top P \mu \int_{-\pi}^{\pi} \int_0^{\pi} \cdots \int_0^{\pi} |\det(J)| d\theta_1 \cdots d\theta_{n-2} d\varphi \\ &= \mu^\top P \mu \int_{-\pi}^{\pi} r^{n-1} s_1 \cdots s_{n-2} d\varphi \\ &= 2\pi r^{n-1} \prod_{j=1}^{n-2} s_j \mu^\top P \mu \\ &= \beta(r, n) \mu^\top P \mu. \end{aligned} \quad (\text{B.31})$$

$$\begin{aligned}
 2 \int_{\mathcal{E}(r,0,t)} y^\top V^\top P \mu \, dy &= 2 \int_{\mathcal{E}(r,0,t)} y^\top \tilde{P} \mu \, dy \\
 &= 2 \int_{-\pi}^{\pi} \int_0^{\pi} \int_0^{\pi} \dots \int_0^{\pi} \left[ r \cos(\varphi) \sin(\theta_1) \sin(\theta_2) \cdots \sin(\theta_{n-2}) \sum_{j=1}^n \tilde{p}_{1,j} \mu_j \cdots \right. \\
 &\quad + r \sin(\varphi) \sin(\theta_1) \sin(\theta_2) \cdots \sin(\theta_{n-2}) \sum_{j=1}^n \tilde{p}_{2,j} \mu_j \cdots \\
 &\quad + r \cos(\theta_1) \sin(\theta_2) \cdots \sin(\theta_{n-2}) \sum_{j=1}^n \tilde{p}_{3,j} \mu_j \cdots + \\
 &\quad + \dots + \dots \\
 &\quad \left. + r \cos(\theta_{n-3}) \sin(\theta_{n-2}) \sum_{j=1}^n \tilde{p}_{n-1,j} \mu_j + r \cos(\theta_{n-2}) \sum_{j=1}^n \tilde{p}_{n,j} \mu_j \right] |\det(J)| \dots \\
 &\quad d\theta_1 d\theta_2 \cdots d\theta_{n-2} d\varphi
 \end{aligned} \tag{B.32}$$

$$\begin{aligned}
 2 \int_{\mathcal{E}(r,0,t)} y^\top \tilde{P} \mu \, dy &= 2r^n \left[ \prod_{l=2}^{n-1} s_l \int_{-\pi}^{\pi} \cos(\varphi) d\varphi \tilde{\mu}_1 + \int_{-\pi}^{\pi} \sin(\varphi) d\varphi \tilde{\mu}_2 \right] \\
 &\quad + \sum_{i=3}^n \prod_{j=1}^{i-3} s_j \prod_{l=i}^{n-1} s_l \int_{-\pi}^{\pi} \int_{-\pi}^{\pi} \cos(\theta_{i-2}) \sin^{i-2}(\theta_{i-2}) d\theta_{i-2} d\varphi \tilde{\mu}_i
 \end{aligned} \tag{B.33}$$

Recalling Eq. (B.9) and the results obtained for the three summands:

$$\int_{\mathcal{E}(r,\mu,\Sigma)} x^\top P x dx = \det(V) \left[ \alpha(r, n) \operatorname{tr}(P\Sigma) + \beta(r, n) \mu^\top P \mu \right]. \quad (\text{B.34})$$

Note that  $\alpha(r, n) > 0$ ,  $\beta(r, n) > 0$  if and only if  $r > 0$ , and  $\alpha(r, n) = 0$ ,  $\beta(r, n) = 0$  otherwise, which follows directly with  $s_j > 0 \forall j \in \mathbb{N}$ , cf. Lemma B.2.  $\square$

By the help of Lemma B.3, it can now be shown that the original claim stated in Lemma B.1 holds.

*Proof.* Since the random variable  $x \sim \mathcal{U}(\mathcal{E}_x)$  is uniformly distributed over the ellipsoid  $\mathcal{E}_x$ , the corresponding probability density function is obtained as:

$$p_x(x) = \begin{cases} p_x := \frac{1}{\int_{\mathcal{E}_x} 1 dx} & \text{if } x \in \mathcal{E}_x, \\ 0 & \text{otherwise.} \end{cases} \quad (\text{B.35})$$

In the sequel, the Gamma function<sup>1</sup> is denoted by  $\Gamma(x) : \mathbb{C} \setminus \mathbb{Z}_{\leq 0} \rightarrow \mathbb{C}$ , where  $\Gamma(x+1) = x!$  [28, p.459]. With  $y = V^{-1}(x - \mu_x)$  and the expression for the integral over the unit ball  $\mathcal{E}(1, 0, I)$  from [48, p.620], it holds that:

$$\frac{1}{p_x} = \int_{\mathcal{E}_x} 1 dx = \det(V) \int_{\mathcal{E}(1,0,I)} 1 dy = \det(V) \frac{\sqrt{\pi^n}}{\Gamma(\frac{n}{2} + 1)}. \quad (\text{B.36})$$

Recall the definition of the expected value:

$$\mathbb{E}(x^\top P x) = \int_{\mathbb{R}^n} x^\top P x p_x dx = p_x \int_0^1 \int_{\mathcal{E}(r,\mu_x,\Sigma_x)} x^\top P x dx dr. \quad (\text{B.37})$$

Determine  $V \in \mathbb{R}_{>0}^{n \times n}$  such that  $VV^\top = \Sigma_x$ . Applying Lemma B.3 to the inner integral yields:

$$\mathbb{E}(x^\top P x) = p_x \det(V) \int_0^1 r^{n+1} \prod_{j=1}^n s_j \operatorname{tr}(P\Sigma_x) + 2\pi r^{n-1} \prod_{j=1}^{n-2} s_j \mu_x^\top P \mu_x dr. \quad (\text{B.38})$$

Exploiting that  $s_{n-1}s_n = 2\pi/n$  according to (B.24) and performing the integration:

$$\mathbb{E}(x^\top P x) = 2\pi p_x \det(V) \prod_{j=1}^{n-2} s_j \int_0^1 \frac{r^{n+1}}{n} \operatorname{tr}(P\Sigma_x) + r^{n-1} \mu_x^\top P \mu_x dr \quad (\text{B.39})$$

$$= \frac{2\pi}{n} p_x \det(V) \prod_{j=1}^{n-2} s_j \left[ \frac{1}{n+2} \operatorname{tr}(P\Sigma_x) + \mu_x^\top P \mu_x \right]. \quad (\text{B.40})$$

<sup>1</sup>The Gamma function is also referred to as Euler Integral of the Second Kind, see [28, p.459] for a definition.

Let  $n = 2m$  with  $m \in \mathbb{N}$  and consider the following relation, where  $s_{2l-1}s_{2l} = \pi/l$  is used to establish the following relation (see (B.24)):

$$\prod_{j=1}^{n-2} s_j = \prod_{l=1}^{m-1} s_{2l-1}s_{2l} = \prod_{l=1}^{m-1} \frac{\pi}{l} = \frac{\pi^{m-1}}{(m-1)!} = \frac{m}{\pi} \frac{\sqrt{\pi^{2m}}}{m!} = \frac{n}{2\pi} \frac{\sqrt{\pi^n}}{\Gamma(\frac{n}{2} + 1)}. \quad (\text{B.41})$$

For  $n = 2m - 1$ ,  $m \in \mathbb{N}$ , a similar relation can be obtained, starting with:

$$\prod_{j=1}^{n-2} s_j = s_1 \prod_{l=1}^{m-2} s_{2l}s_{2l+1} = 2 \prod_{l=1}^{m-2} \frac{2\pi}{2l+1} = 2 \prod_{l=1}^{m-2} \frac{2^2\pi l}{2l(2l+1)} = \frac{2^{2m-3}\pi^{m-2}(m-2)!}{(2m-3)!}. \quad (\text{B.42})$$

Using the following relation for the Gamma function from [28, p.460]:

$$\Gamma(m + \frac{1}{2}) = \frac{(2m)! \sqrt{\pi}}{m! 2^{2m}}, \quad (\text{B.43})$$

and  $n = 2m - 1$ , Eq. (B.42) can be rewritten as:

$$\begin{aligned} \frac{2^{2m-3}\pi^{m-2}(m-2)!}{(2m-3)!} &= \frac{\sqrt{\pi^{2m-1}}}{2\pi} \frac{m! 2^{2m}}{(2m)! \sqrt{\pi}} \frac{2m(2m-1)(2m-2)}{2^2m(m-1)} \\ &= \frac{\sqrt{\pi^{2m-1}}}{2\pi} \frac{1}{\Gamma(m + \frac{1}{2})} (2m-1) \\ &= \frac{n}{2\pi} \frac{\sqrt{\pi^n}}{\Gamma(\frac{n}{2} + 1)}. \end{aligned} \quad (\text{B.44})$$

Inserting either (B.41) or (B.44) into (B.40) leads to:

$$E(x^\top P x) = p_x \det(V) \frac{\sqrt{\pi^n}}{\Gamma(\frac{n}{2} + 1)} \left[ \frac{1}{n+2} \text{tr}(P\Sigma_x) + \mu_x^\top P \mu_x \right]. \quad (\text{B.45})$$

Substituting  $p_x$  from Eq. (B.36) into the above relation completes the proof.  $\square$

# Appendix C. Comparison of Interconnection Measures

Concerning the clustering procedure presented in Section 3.2, it seems appropriate to discuss the suitability of the interconnection measure introduced in Eq. (3.6), especially since various alternatives exist (e.g. [5] [6] [27] [30] [138]). To this end, a Monte-Carlo-Simulation has been performed. In each simulation run, a random stable discrete-time LTI system  $\mathcal{P}$  is first generated using the function `drss` provided by MATLAB. Next, this system is partitioned into  $N_s = 5$  subsystems with  $n_x^i = 4$  and  $n_u^i = 3$  for all  $i \in \mathcal{N}_s$ . Then, the interconnection matrix  $\Gamma \in \mathbb{R}_{>0}^{N_s \times N_s}$  is calculated, where six different interconnection measures are used. With  $\mathcal{P}_{u^i, x^j}$  denoting the global system  $\mathcal{P}$  with input  $u^i$  and output  $x^j$ , these measures are defined as follows:

$$(I.1) \quad \gamma_{i,j} = \|\mathcal{P}_{u^i, x^j}\|_{\mathcal{H}_\infty},$$

$$(I.3) \quad \gamma_{i,j} = \|A_{i,j}\|_2 + \|B_{i,j}\|_2,$$

$$(I.5) \quad \gamma_{i,j} = \|A_{i,j}\|_2,$$

$$(I.2) \quad \gamma_{i,j} = \|\mathcal{P}_{u^i, x^j}\|_{\mathcal{H}_2},$$

$$(I.4) \quad \gamma_{i,j} = \|A_{i,j}\|_\infty + \|B_{i,j}\|_\infty,$$

$$(I.6) \quad \gamma_{i,j} = \|A_{i,j}\|_\infty.$$

According to these measures, the  $N_n \in \mathbb{N}$  weakest nonzero interconnections are set to zero. Then, different measures for the quality of the obtained approximation are evaluated, which enables a comparison of the interconnection measures. The measures for the quality of the approximation are defined as follows:

- (M.1) open-loop eigenvalues: the eigenvalues of the original system matrix  $A$  and of the approximated system matrix  $A'$  are stacked into two separate vectors. The Euclidean norm of the difference vector serves as approximation measure.
- (M.2) closed-loop eigenvalues (1): interconnections are only removed from the system matrix  $A$  (yielding  $A'$ ). Next, two linear quadratic regulators are calculated with respect to the same random controlled variable:  $K'$  is calculated using  $A'$ ,  $B$ ,  $C$ , and  $D$ , and  $K$  is calculated using  $A$ ,  $B$ ,  $C$ , and  $D$ . Then, the eigenvalues of the closed-loop system matrices  $A + BK$  and  $A + BK'$  are compared as described in (M.1).
- (M.3) closed-loop eigenvalues (2): like (M.2), but interconnections are removed in both  $A$  and  $B$ .

(M.4) closed-loop performance (1): like (M.2), but closed-loop performance is compared instead of closed-loop eigenvalues.

(M.5) closed-loop eigenvalues (2): like (M.4), but interconnections are removed in both  $A$  and  $B$ .

Another criterion used to evaluate the quality of the obtained approximation is the stability of the resulting closed-loop system:

(S.1) number of simulations where the matrix  $A+BK'$  as constructed for calculating (M.2) is a Schur matrix.

(S.2) number of simulations where the matrix  $A+BK'$  as constructed for calculating (M.3) is a Schur matrix.

The following tables compare the quality of the approximation obtained for the different interconnection measures. In order to rate the interconnection measures, two different rating numbers are employed. As a first rating number, the percentage of simulation runs at which each interconnection measure performed best is stated in Tables C.1 and C.4. In Tables C.2 and C.5, a weighted rating number is used instead. This rating number is calculated as follows: Suppose that for the  $r$ -th simulation run, the quality measure (M. $h$ ) obtained for the interconnection measure (I.1) to (I.6) is contained in a vector  $m(r, h) \in \mathbb{R}_{\geq 0}^6$ , where the  $i$ -th component is denoted by  $m_i(r, h) \in \mathbb{R}_{\geq 0}$ . Then, the  $i$ -th component of the weighted rating number is obtained as:

$$100 \sum_{r=1}^{15000} \frac{m_i(r, h) - \min_j m_j(r, h)}{\sum_{i=1}^6 m_i(r, h) - \min_j m_j(r, h)}. \quad (\text{C.1})$$

In order to avoid divisions by zero, the contribution of the  $r$ -th simulation run is set to zero if the sum in the denominator is zero.

As can be deduced from Table C.1, the interconnection measures (I.3) and (I.5) perform very well for a small number of neglected entries. The weighted rating number stated in Table C.2 confirms this conclusion. Furthermore, both tables show that the 2-norm and  $\infty$ -norm based interconnection measures (I.3) and (I.4) considering both the  $A$  and  $B$  matrix perform better when entries of both matrices are deleted, as it applies for (M.3) and (M.5). Accordingly, the measures (I.5) and (I.6) only considering the matrix  $A$  perform better in the measures (M.2) and (M.4), where only the entries of the  $A$  matrix are deleted. The values obtained for  $N_n = 10$  neglected entries confirm these observations, see Tables C.4 and C.5.

A further advantage of the measures (I.3) to (I.6) is that they can be applied to unstable systems without any difficulty. In addition, the computational burden for calculating these measures is considerably smaller than for calculating the  $\mathcal{H}_2$ - and  $\mathcal{H}_\infty$ -based interconnection measures (I.1) and (I.2). Concerning stability of the closed-loop systems that is obtained when plugging in the controller designed for the

approximate system to the original system, Tables C.3 and C.6 state that utilizing the  $p$ -norm based interconnection measures more often leads to stable closed-loop systems than utilizing the  $\mathcal{H}$ -norm based interconnection measures.

A drawback of interconnection measures (I.3) to (I.6) is that they depend on the current state-space representation, particularly on the selected scaling of the state variables. If necessary, this drawback can be easily circumvented by normalizing the model parameters before applying the clustering procedure. A suitable procedure is to apply the MATLAB function `balance` to the system matrix  $A$ . This function returns a similarity transformation such that the transformed system matrix  $A$  has approximately equal row and column norms. Since the corresponding transformation matrix is diagonal, the structure of the involved state space matrices is not affected.

	input to state				state to state	
	(I.1)	(I.2)	(I.3)	(I.4)	(I.5)	(I.6)
(M.1)	0.61	0.85	1.51	1.11	<u>68.92</u>	27.00
(M.2)	20.95	12.77	10.21	7.60	<u>27.49</u>	20.98
(M.3)	20.49	19.91	<u>21.69</u>	13.77	13.35	10.78
(M.4)	13.13	9.41	10.50	7.87	<u>34.25</u>	24.83
(M.5)	12.11	18.18	<u>28.65</u>	17.31	13.63	10.11

**Table C.1.:** Percentage of the best interconnection measure for  $N_n = 3$ .

	input to state				state to state	
	(I.1)	(I.2)	(I.3)	(I.4)	(I.5)	(I.6)
(M.1)	6.78	7.82	10.94	11.39	<u>32.97</u>	30.10
(M.2)	17.11	15.07	12.52	12.64	21.28	<u>21.37</u>
(M.3)	16.40	18.70	<u>18.96</u>	18.24	13.91	13.80
(M.4)	13.71	13.26	13.35	13.48	<u>23.46</u>	22.74
(M.5)	12.97	17.93	<u>21.41</u>	20.53	13.75	13.40

**Table C.2.:** Weighted rating number of interconnection measures for  $N_n = 3$ .



	input to state				state to state	
	(I.1)	(I.2)	(I.3)	(I.4)	(I.5)	(I.6)
(S.1)	14998	14999	14999	14999	<u>15000</u>	<u>15000</u>
(S.2)	14952	14984	14985	<u>14988</u>	14939	14939

**Table C.3.:** Absolute number of stable closed-loop systems for  $N_n = 3$ .

	input to state				state to state	
	(I.1)	(I.2)	(I.3)	(I.4)	(I.5)	(I.6)
(M.1)	0.77	0.73	1.31	1.49	<u>68.82</u>	26.87
(M.2)	17.10	10.49	8.27	7.89	<u>28.89</u>	27.36
(M.3)	17.37	18.88	<u>23.23</u>	18.58	11.05	10.89
(M.4)	11.06	8.00	8.86	8.91	<u>32.90</u>	30.27
(M.5)	11.89	17.80	<u>28.82</u>	22.15	9.30	9.85

**Table C.4.:** Percentage of the best performing interconnection measure for  $N_n = 10$ .

	input to state				state to state	
	(I.1)	(I.2)	(I.3)	(I.4)	(I.5)	(I.6)
(M.1)	5.78	7.58	12.88	12.88	<u>32.80</u>	28.08
(M.2)	15.99	14.37	11.77	11.93	<u>23.22</u>	22.73
(M.3)	15.70	18.61	<u>20.46</u>	19.06	13.15	13.01
(M.4)	13.33	13.25	13.16	13.43	<u>23.88</u>	22.95
(M.5)	14.13	18.22	<u>21.51</u>	20.39	12.77	12.76

**Table C.5.:** Weighted rating number of interconnection measures for  $N_n = 10$ .

	input to state				state to state	
	(I.1)	(I.2)	(I.3)	(I.4)	(I.5)	(I.6)
(S.1)	14963	14969	14983	14980	14991	<u>14992</u>
(S.2)	13883	14205	<u>14430</u>	14376	13792	13725

**Table C.6.:** Absolute number of stable closed-loop systems for  $N_n = 10$ .

# Appendix D. Asynchronous Hierarchical Control

The proofs presented in the following two sections belong to Lemma 4.3 and to Lemma 4.4 of Chapter 4, which can be found on p.84 and on p.87, respectively. Finally, Sec. D.3 shows how to formulate a closed-loop system using the synchronous two-layer control scheme of Chap. 3 as a periodic system. This procedure is used in Sec. 4.5 to compare the performance of the synchronous and asynchronous two-layer control scheme (see p.97).

## D.1. Proof of Lemma 4.3

*Proof.* According to Definition 4.2, for  $k \in \mathbb{N}_0$  and with  $l \in \{0, \dots, N_c - 1\}$ , the impulse response matrix of the periodic system  $\mathcal{P}_{p,cl}$  is given by (cf. [21, p.242]):

$$\mathbf{z}_{k,l} = \begin{cases} C_{cl}[\varphi_k] A_{cl}[\varphi_{k-1}] A_{cl}[\varphi_{k-2}] \cdots A_{cl}[\varphi_{l+1}] E[\varphi_l] & \text{if } k > l, \\ 0_{n_z[\varphi_k] \times n_v[\varphi_l]} & \text{otherwise.} \end{cases} \quad (\text{D.1})$$

With  $E[\varphi_k]$  as defined in Eq. (4.20) on p.84, it follows that:

$$\mathbf{z}_{k,l} = \begin{cases} \sqrt{N_\varphi} C_{cl}[\varphi_k] A_{cl}[\varphi_{k-1}] \cdots A_{cl}[\varphi_{N_\varphi}] x_0 & \text{if } l = N_\varphi - 1, k > l, \\ 0_{n_z[\varphi_k] \times 1} & \text{otherwise.} \end{cases} \quad (\text{D.2})$$

Let  $k' := k - N_\varphi$  to obtain:

$$\mathbf{z}_{k'+N_\varphi,l} = \begin{cases} \sqrt{N_\varphi} C_{cl}[\varphi_{k'+N_\varphi}] A_{cl}[\varphi_{k'+N_\varphi-1}] \cdots A_{cl}[\varphi_{N_\varphi}] x_0 & \text{if } l = N_\varphi - 1, k' \geq 0, \\ 0_{n_z[\varphi_{k'+N_\varphi}] \times 1} & \text{otherwise.} \end{cases} \quad (\text{D.3})$$

Due to the  $N_\varphi$ -periodicity of the switching function  $\varphi_k$ , it holds that:

$$\mathbf{z}_{k'+N_\varphi,l} = \begin{cases} \sqrt{N_\varphi} C_{cl}[\varphi_{k'}] A_{cl}[\varphi_{k'-1}] \cdots A_{cl}[\varphi_0] x_0 & \text{if } l = N_\varphi - 1, k' \geq 0, \\ 0_{n_z[\varphi_{k'}] \times 1} & \text{otherwise.} \end{cases} \quad (\text{D.4})$$

Hence, for all  $k' \in \mathbb{N}_0$ , it holds that:

$$\sum_{l=0}^{N_\varphi-1} \mathbf{z}_{k'+N_\varphi,l}^\top \mathbf{z}_{k'+N_\varphi,l} = N_\varphi z_{k'}^\top z_{k'}. \quad (\text{D.5})$$

The claim now follows with the definition of the  $\mathcal{H}_2$ -norm for periodic systems in Eq. (4.18) and with  $\mathbf{z}_{k,l} = 0$  for all  $0 \leq k < N_\varphi$  and all  $l \in \{0, \dots, N_c - 1\}$ .  $\square$

## D.2. Proof of Lemma 4.4

**Claim (a): The periodic system  $\bar{\mathcal{P}}_\varphi^\uparrow$  is stabilizable**

*Proof.* Recall the structure of the pair  $(\bar{A}^\uparrow[\varphi], \bar{B}^\uparrow[\varphi])$ , where the symbol  $*$  denotes the respective block-columns of the matrix  $\bar{B}$ :

$$\bar{A}^\uparrow[\varphi] = \begin{bmatrix} \bar{A}_{\text{cl}}^\downarrow & * \\ 0 & \bar{H}_\Lambda[\varphi] \end{bmatrix}, \quad \bar{B}^\uparrow[\varphi] = \begin{bmatrix} \bar{B}_{:, \varphi} \\ \bar{H}_\text{B}[\varphi] \end{bmatrix}. \quad (\text{D.6})$$

Since  $\bar{A}^\uparrow[\varphi]$  is in upper block-triangular form and  $\bar{H}_\Lambda[\varphi]$  is a Schur matrix for all  $\varphi \in \mathcal{N}_c$ , it suffices to show that the reduced periodic system  $(\bar{A}^\uparrow[\varphi], \bar{B}^\uparrow[\varphi])$  with:

$$\bar{A}^\uparrow[\varphi] := \bar{A}_{\text{cl}}^\downarrow, \quad \bar{B}^\uparrow[\varphi] := \bar{B}_{:, \varphi}, \quad \varphi \in \mathcal{N}_c \quad (\text{D.7})$$

is stabilizable. According to [21, Prop. 4.11], the pair  $(\bar{A}^\uparrow[\varphi], \bar{B}^\uparrow[\varphi])$  is stabilizable if and only if for all characteristic multipliers  $\lambda \in \mathbb{C}_{\geq 1}$  of  $\bar{A}_{\text{cl}}^\downarrow$  and a vector  $\xi \in \mathbb{R}^{n_x}$ , the conditions:

$$\xi^\top (\bar{A}_{\text{cl}}^\downarrow)^{N_c} = \xi^\top \lambda, \quad \xi^\top (\bar{A}_{\text{cl}}^\downarrow)^{\varphi-1} \bar{B}_{:, \varphi} = 0 \quad \forall \varphi \in \mathcal{N}_c \quad (\text{D.8})$$

imply  $\xi = 0$ . Recall that the pair  $(A, B)$  is assumed to be stabilizable, which implies that the matrix  $[A - \lambda I \quad B]$  has full row rank for all  $\lambda \in \mathbb{C}_{\geq 1}$  [142, Theorem 21.2]. Hence, the matrix:

$$T_x^\top [A - \lambda I \quad B] \begin{bmatrix} T_x \\ T_u \end{bmatrix} = [\bar{A} - \lambda I \quad \bar{B}] \quad (\text{D.9})$$

has full row rank for all  $\lambda \in \mathbb{C}_{\geq 1}$ , since  $T_x$  and  $T_u$  are permutation matrices as defined in (3.9). It follows that the matrix:

$$[\bar{A} + \bar{B}\bar{K}^\downarrow - \lambda I \quad \bar{B}] = [\bar{A}_{\text{cl}}^\downarrow - \lambda I \quad \bar{B}] \quad (\text{D.10})$$

has full row rank for all  $\lambda \in \mathbb{C}_{\geq 1}$ , since it can be obtained from (D.9) via elementary column operations. Equivalently, it applies for all  $\lambda \in \mathbb{C}_{\geq 1}$  that:

$$\left. \begin{array}{l} \xi^\top \bar{A}_{\text{cl}}^\downarrow = \xi^\top \lambda \\ \xi^\top \bar{B} = 0 \end{array} \right\} \Rightarrow \xi = 0. \quad (\text{D.11})$$

Exploiting that a multiplication of  $\bar{B}$  by  $\lambda \in \mathbb{C}_{\geq 1}$  is a collection of elementary column operations and using the first condition of (D.11) recursively, the latter equation can be expressed as:

$$\left. \begin{array}{l} \xi^\top (\bar{A}_{\text{cl}}^\downarrow)^{h_1} = \xi^\top \lambda^{h_1} \\ \lambda^{h_2} \xi^\top \bar{B} = \xi^\top (\bar{A}_{\text{cl}}^\downarrow)^{h_2} \bar{B} = 0 \end{array} \right\} \Rightarrow \xi = 0, \quad (\text{D.12})$$

for all  $h_1, h_2 \in \mathbb{N}$ . The first line implies that a left eigenvector  $\xi$  of  $\bar{A}_{\text{cl}}^\downarrow$  with the eigenvalue  $\lambda \in \mathbb{C}_{\geq 1}$  is a left eigenvector of  $(\bar{A}_{\text{cl}}^\downarrow)^{h_1}$  with the eigenvalue  $\lambda^{h_1} \in \mathbb{C}_{\geq 1}$ . The second line of (D.11) is equivalent to:

$$\xi^\top \bar{B} = 0 \quad \Leftrightarrow \quad \xi^\top \bar{B}_{:,1} = \dots = \xi^\top \bar{B}_{:,N_c} = 0. \quad (\text{D.13})$$

Combining (D.12) and (D.13), the conditions (D.11) can be equivalently expressed as:

$$\left. \begin{aligned} \xi^\top \bar{A}_{\text{cl}} \downarrow = \xi^\top \lambda &\quad \Leftrightarrow \quad \xi^\top (\bar{A}_{\text{cl}}^\downarrow)^{N_c} = \xi^\top \lambda^{N_c} \\ \xi^\top \bar{B}_{:,1} &= 0 \\ \xi^\top \bar{B}_{:,2} = 0 &\quad \Leftrightarrow \quad \xi^\top (\bar{A}_{\text{cl}}^\downarrow)^{N_c} \bar{B}_{:,2} = 0 \\ &\quad \vdots \\ \xi^\top \bar{B}_{:,N_c} = 0 &\quad \Leftrightarrow \quad \xi^\top (\bar{A}_{\text{cl}}^\downarrow)^{N_c-1} \bar{B}_{:,N_c} = 0 \end{aligned} \right\} \Rightarrow \xi = 0. \quad (\text{D.14})$$

Since it holds that:

$$\{\lambda \mid \lambda \in \mathbb{C}_{\geq 1}\} = \{\lambda^h \mid \lambda \in \mathbb{C}_{\geq 1}, h \in \mathbb{N}\}, \quad (\text{D.15})$$

Equation (D.14) implies that the conditions (D.8) hold for all  $\lambda \in \mathbb{C}_{\geq 1}$ . Hence, the pair  $(\bar{A}^\uparrow[\varphi], \bar{B}^\uparrow[\varphi])$  is stabilizable, implying the original claim.  $\square$

**Claim (b): The matrix  $\bar{D}^\uparrow[\varphi]$  has full column rank for all  $\varphi \in \mathcal{N}_c$**

*Proof.* This property of  $\bar{D}^\uparrow[\varphi]$  directly follows from its definition in Eq. (4.37) and from Assumption 4.1.  $\square$

**Claim (c): The periodic system  $\bar{\mathcal{P}}_\varphi^\uparrow$  has no invariant zeros on  $\mathbb{C}_1$**

In order to simplify the presentation on the subsequent pages, the *forward shift operator*  $\varsigma$  for a vector  $\eta^\top = [\eta_1 \ \dots \ \eta_m] \in \mathbb{C}^n$ , or for an ordered set  $\mathcal{I} = \{i_1, i_2, \dots, i_n\}$  is defined as follows:

$$\varsigma \eta := [\eta_m \ \eta_1 \ \eta_2 \ \dots \ \eta_{m-1}]^\top, \quad \varsigma \mathcal{I} := \{i_n, i_1, i_2, \dots, i_{n-1}\}. \quad (\text{D.16})$$

The following properties of the index shift operator  $\varsigma$  will be relevant, where  $l \in \mathbb{Z}_{\neq 0}$ :

$$\varsigma^l \eta := \varsigma^{l-1}(\varsigma \eta), \quad \varsigma^0 \eta := \eta, \quad \varsigma^m \eta = \eta, \quad \varsigma^l \eta^\top := (\varsigma^l \eta)^\top. \quad (\text{D.17})$$

*Proof.* For the system  $\bar{\mathcal{P}}_\varphi^\uparrow$  to have no invariant zeros on the unit circle, the matrix:

$$\mathring{P}_0(\lambda) := \begin{bmatrix} \mathring{A} - \lambda I & \mathring{B} \\ \mathring{C} & \mathring{D} \end{bmatrix}, \quad (\text{D.18})$$

must have full column rank for all  $\lambda \in \mathbb{C}_1$ , see [21, p.215f]. Here, the matrices denoted by  $\mathring{(\cdot)}$  are defined as<sup>1</sup>:

$$\mathring{A} := \begin{bmatrix} 0 & \bar{A}^\dagger[\varphi_{N_c}] \\ \text{blkdiag}(\bar{A}^\dagger[\varphi_1], \dots, \bar{A}^\dagger[\varphi_{N_c-1}]) & 0 \end{bmatrix}, \quad (\text{D.19a})$$

$$\mathring{B} := \begin{bmatrix} 0 & \bar{B}^\dagger[\varphi_{N_c}] \\ \text{blkdiag}(\bar{B}^\dagger[\varphi_1], \dots, \bar{B}^\dagger[\varphi_{N_c-1}]) & 0 \end{bmatrix}, \quad (\text{D.19b})$$

$$\mathring{C} := \text{blkdiag}(\bar{C}^\dagger[\varphi_1], \dots, \bar{C}^\dagger[\varphi_{N_c}]), \quad (\text{D.19c})$$

$$\mathring{D} := \text{blkdiag}(\bar{D}^\dagger[\varphi_1], \dots, \bar{D}^\dagger[\varphi_{N_c}]). \quad (\text{D.19d})$$

The corresponding dimensions are defined as:

$$\mathring{n}_x := \sum_{l=1}^{N_c} \bar{n}_x^\dagger[\varphi_l], \quad \mathring{n}_v := \sum_{l=1}^{N_c} \bar{n}_v^\dagger[\varphi_l]. \quad (\text{D.20})$$

Then, given a vector  $[\xi^\top \ \chi^\top]^\top$  with  $\xi \in \mathbb{R}^{\mathring{n}_x}$  and  $\chi \in \mathbb{R}^{\mathring{n}_v}$ , one has to show that:

$$\begin{bmatrix} \mathring{A} - \lambda I & \mathring{B} \\ \mathring{C} & \mathring{D} \end{bmatrix} \begin{bmatrix} \xi \\ \chi \end{bmatrix} = \begin{bmatrix} 0 \\ 0 \end{bmatrix} \Rightarrow \begin{bmatrix} \xi \\ \chi \end{bmatrix} = \begin{bmatrix} 0 \\ 0 \end{bmatrix} \quad \forall \lambda \in \mathbb{C}_1. \quad (\text{D.21})$$

Partition both,  $\xi$  and  $\chi$  into  $N_c$  subvectors  $\xi[\varphi] \in \mathbb{R}^{\bar{n}_x}$  and  $\chi[\varphi] \in \mathbb{R}^{\bar{n}_v^\dagger[\varphi]}$ , respectively, with  $\varphi \in \mathcal{N}_c$ . Hence:

$$\xi = \begin{bmatrix} \xi[\varphi_1] \\ \vdots \\ \xi[\varphi_{N_c}] \end{bmatrix}, \quad \chi = \begin{bmatrix} \chi[\varphi_1] \\ \vdots \\ \chi[\varphi_{N_c}] \end{bmatrix}. \quad (\text{D.22})$$

These subvectors can be associated with the inherent block-structure of the matrix  $\mathring{P}_0(\lambda)$ . Next, partition each subvector  $\xi[\varphi]$  again into two subvectors  $\xi_1[\varphi] \in \mathbb{R}^{\bar{n}_x}$  and  $\xi_2[\varphi] \in \mathbb{R}^{\bar{n}_v^\dagger[\varphi]}$ , such that:

$$\xi[\varphi] = \begin{bmatrix} \xi_1[\varphi] \\ \xi_2[\varphi] \end{bmatrix}. \quad (\text{D.23})$$

For  $l \in \mathcal{N}_c$ , the following equations are obtained from the last  $\bar{n}_v^\dagger[\varphi_{l+1}]$  rows of the  $l$ -th block-row of (D.21) when using (4.35) and the periodicity of  $\varphi_k$ , i.e.  $\varphi_0 = \varphi_{N_c}$ :

$$\lambda \xi_2[\varphi_l] = \bar{H}_A[\varphi_{l-1}] \xi_2[\varphi_{l-1}] + \bar{H}_B[\varphi_{l-1}] \chi[\varphi_{l-1}]. \quad (\text{D.24})$$

Exploiting that  $\lambda \neq 0$  and starting from  $l = N_c$ , induction for (D.24) leads to:

$$\begin{aligned} \lambda \xi_2[\varphi_0] &= \sum_{l=2}^{N_c-1} \lambda^{l-1} \bar{H}_A[\varphi_{N_c-1}] \cdots \bar{H}_A[\varphi_{N_c-l+1}] \bar{H}_B[\varphi_{N_c-l}] \chi[\varphi_{N_c-l}] \cdots \\ &\quad + \lambda^{1-N_c} \bar{H}_A[\varphi_{N_c-1}] \cdots \bar{H}_A[\varphi_1] (\bar{H}_A[\varphi_0] \xi_2[\varphi_0] + \bar{H}_B[\varphi_0] \chi[\varphi_0]) \cdots \\ &\quad + \bar{H}_B[\varphi_{N_c-1}] \chi[\varphi_{N_c-1}]. \end{aligned} \quad (\text{D.25})$$

<sup>1</sup>The matrices  $\mathring{A}$  to  $\mathring{D}$  compose a so-called *cyclic reformulation* of the periodic system  $\bar{\mathcal{P}}^\dagger$ , see [21, Chap. 6.3].

Taking into account the properties of the matrices  $\bar{H}_A[\varphi]$  and  $\bar{H}_B[\varphi]$ , it turns out that the second line in (D.25) equals zero, and that the remaining part of the equation reduces to:

$$(\lambda \xi_2[\varphi_0])^\top = [\lambda^0(\chi[\varphi_{N_c-1}])^\top \quad \dots \quad \lambda^{2-N_c}(\chi[\varphi_1])^\top]. \quad (\text{D.26})$$

Recall the definition of the ordered set  $\Phi'[\varphi]$  from Eq. (4.26) on page 85, and note that  $\Phi'[\varphi_l] = \Phi'[\varphi_{l+N_c}]$ . Substituting (D.26) into (D.24) for  $l = 1$  and solving the recursion for  $2 \leq l \leq N_c - 1$  leads to:

$$\lambda(\xi_2[\varphi_l])^\top = [\lambda^0(\chi[\text{vec}_1(\Phi'[\varphi_l])])^\top \quad \dots \quad \lambda^{2-N_c}(\chi[\text{vec}_{N_c-1}(\Phi'[\varphi_l])])^\top]. \quad (\text{D.27})$$

In particular, (D.27) equals (D.26) for  $l = N_c$ . The main purpose of Eq. (D.27) is that it decouples the interdependency of the  $\xi_2[\varphi_l]$  for  $1 \leq l \leq N_c$  given in (D.24), and relates them to the components of  $\chi$  instead. Evaluating the first  $\bar{n}_x$  rows of the  $l$ -th block-row of (D.21) for  $l \in \mathcal{N}_c$  yields:

$$\lambda \xi_1[\varphi_l] = \bar{A}_{\text{cl}}^\downarrow \xi_1[\varphi_{l-1}] + \bar{B}_{:, \Phi'[\varphi_{l-1}]} \xi_2[\varphi_{l-1}] + \bar{B}_{:,\varphi_{l-1}} \chi[\varphi_{l-1}]. \quad (\text{D.28})$$

Consider the following circulant matrix:

$$\kappa = [\kappa_{p,q}] := \begin{bmatrix} \kappa_0 \\ \zeta^1 \kappa_0 \\ \vdots \\ \zeta^{N_c-1} \kappa_0 \end{bmatrix} \in \mathbb{N}_0^{N_c \times N_c}, \quad \kappa_0 := [N_c - 1 \quad \dots \quad 2 \quad 1 \quad 0]. \quad (\text{D.29})$$

Using  $\kappa$ , (D.27) and (D.28) leads to:

$$\lambda \xi_1[\varphi_l] = \bar{A}_{\text{cl}}^\downarrow \xi_1[\varphi_{l-1}] + \sum_{q=1}^{N_c} \bar{B}_{:,\varphi_q} \lambda^{-\kappa_{l,q}} \chi[\varphi_q]. \quad (\text{D.30})$$

A similar approach for the  $(N_c + l)$ -th block row of (D.21) for  $l \in \mathcal{N}_c$  yields:

$$0 = \bar{C}_{\text{cl}}^\downarrow \xi_1[\varphi_{l-1}] + \sum_{q=1}^{N_c} \bar{D}_{:,\varphi_q} \lambda^{-\kappa_{l,q}} \chi[\varphi_q]. \quad (\text{D.31})$$

Introducing the matrix:

$$\bar{D}(\lambda, l) := [\bar{D}_{:,\varphi_1} \lambda^{-\kappa_{l,1}} \quad \dots \quad \bar{D}_{:,\varphi_{N_c}} \lambda^{-\kappa_{l,N_c}}], \quad (\text{D.32})$$

with  $\lambda^{-\kappa_{l,q}} \in \mathbb{C}_1$  for all  $l, q \in \mathcal{N}_c$ , Eq. (D.31) can equivalently be written as:

$$0 = \bar{C}_{\text{cl}}^\downarrow \xi_1[\varphi_{l-1}] + \bar{D}(\lambda, l) \chi. \quad (\text{D.33})$$

Without loss of generality, assume now that  $\bar{D}^\top \bar{C}_{\text{cl}}^\downarrow = 0$  (see, e.g., Remark 4.1 in [31, p.74]). With the properties of the scalar product of two vectors in an Euclidean

vector space, this implies that the column vectors of  $\bar{C}_{\text{cl}}^\downarrow$  and  $\bar{D}$  are pairwise orthogonal. Hence, the column vectors of  $\bar{C}_{\text{cl}}^\downarrow$  and  $\bar{D}$  are linearly independent. Since  $\bar{D}(\lambda, l)$  can be obtained from  $\bar{D}$  via elementary column operations for all  $l \in \mathcal{N}_c$  and all  $\lambda \in \mathbb{C}_1$ , it follows that the same property must hold for the matrix  $\bar{D}(\lambda, l)$ , i.e.  $(\bar{D}(\lambda, l))^\top \bar{C}_{\text{cl}}^\downarrow = 0$ . Consequently, since  $\bar{D}$  has full column rank,  $\bar{D}(\lambda, l)$  has full column rank for all  $l \in \mathcal{N}_c$  and all  $\lambda \in \mathbb{C}_1$ . Hence, for any  $l \in \mathcal{N}_c$ , Eq. (D.33) implies that  $\chi = 0$ .

Combining (D.30) and (D.31) and substituting  $\chi = 0$  yields:

$$\begin{bmatrix} \lambda \xi_1[\varphi_l] \\ 0 \end{bmatrix} = \begin{bmatrix} \bar{A}_{\text{cl}}^\downarrow \\ \bar{C}_{\text{cl}}^\downarrow \end{bmatrix} \xi_1[\varphi_{l-1}]. \quad (\text{D.34})$$

Since  $\lambda \neq 0$ , using induction for (D.34) leads to:

$$\begin{bmatrix} \lambda^{N_c} \xi_1[\varphi_l] \\ 0 \end{bmatrix} = \begin{bmatrix} (\bar{A}_{\text{cl}}^\downarrow)^{N_c} \\ \bar{C}_{\text{cl}}^\downarrow \end{bmatrix} \xi_1[\varphi_l]. \quad (\text{D.35})$$

Due to Assumption 4.1 (see p.78), the matrix:

$$\begin{bmatrix} A - \lambda I & B \\ C & D \end{bmatrix} \quad (\text{D.36})$$

has full column rank for all  $\lambda \in \mathbb{C}_1$ . Hence, the matrix:

$$\begin{bmatrix} \bar{A} + \bar{B}\bar{K}^\downarrow - \lambda I & \bar{B} \\ \bar{C} + \bar{D}\bar{K}^\downarrow & \bar{D} \end{bmatrix} = \begin{bmatrix} \bar{A}_{\text{cl}}^\downarrow - \lambda I & \bar{B} \\ \bar{C}_{\text{cl}}^\downarrow & \bar{D} \end{bmatrix} \quad (\text{D.37})$$

must have full column rank for all  $\lambda \in \mathbb{C}_1$ , since it can be obtained from (D.36) via elementary row and column operations. This implies that the first block column of (D.37) must have full column rank, leading to:

$$\begin{bmatrix} \lambda \xi_1[\varphi_l] \\ 0 \end{bmatrix} = \begin{bmatrix} \bar{A}_{\text{cl}}^\downarrow \\ \bar{C}_{\text{cl}}^\downarrow \end{bmatrix} \xi_1[\varphi_l] \Rightarrow \xi_1[\varphi_l] = 0. \quad (\text{D.38})$$

The first block row of (D.38) claims  $\xi_1[\varphi_l]$  to be an eigenvector of  $\bar{A}_{\text{cl}}^\downarrow$  with corresponding eigenvalue  $\lambda \in \mathbb{C}_1$ . Similar to (D.12), it is easy to show that for any  $h \in \mathbb{N}$ :

$$(\bar{A}_{\text{cl}}^\downarrow)^h \xi_1[\varphi_l] = \lambda^h \xi_1[\varphi_l], \quad (\text{D.39})$$

i.e. if  $\xi_1[\varphi_l]$  is a right eigenvector of  $\bar{A}_{\text{cl}}^\downarrow$  with the eigenvalue  $\lambda \in \mathbb{C}_1$ , then, at the same time,  $\xi_1[\varphi_l]$  is a right eigenvector of  $(\bar{A}_{\text{cl}}^\downarrow)^h$  with the eigenvalue  $\lambda^h \in \mathbb{C}_1$ . It directly follows that (D.35) implies  $\xi_1[\varphi_l] = 0$  for all  $l \in \mathcal{N}_c$ , which completes the proof.  $\square$

### D.3. Numerical Example

Formulation of a system  $\mathcal{P}$  controlled by a synchronous two-layer controller with  $\Delta k = 3$  as a periodic system:

$$\bar{\mathcal{P}}_{\text{p,cl}}^\dagger : \begin{cases} \bar{x}_{k+1}^\uparrow = \bar{A}_{\text{cl}}^\dagger[\varphi_k] \bar{x}_k^\uparrow + \bar{E}^\dagger \bar{w}_k, \\ \bar{z}_k = \bar{C}_{\text{cl}}^\dagger[\varphi_k] \bar{x}_k^\uparrow, \end{cases} \quad (\text{D.40})$$

with state vector:

$$\bar{x}_k^\uparrow := \begin{bmatrix} \bar{x}_k \\ \bar{v}_k \end{bmatrix}, \quad (\text{D.41})$$

switching sequence:

$$\Phi = \{\varphi_{k+3}, \varphi_{k+2}, \varphi_{k+1}\} = \{3, 2, 1\}, \quad (\text{D.42})$$

and matrices:

$$\begin{aligned} \bar{A}_{\text{cl}}^\dagger[1] &= \begin{bmatrix} \bar{A}_{\text{cl}}^\downarrow + \bar{B} \bar{K}^\uparrow & 0 \\ \bar{K}^\uparrow & 0_{\bar{n}_v \times \bar{n}_v} \end{bmatrix}, & \bar{A}_{\text{cl}}^\dagger[2] = \bar{A}_{\text{cl}}^\dagger[3] &= \begin{bmatrix} \bar{A}_{\text{cl}}^\uparrow & \bar{B} \\ 0 & I_{\bar{n}_v} \end{bmatrix}, & \bar{E}^\dagger &= \begin{bmatrix} \bar{E} \\ 0 \end{bmatrix}, \\ \bar{C}_{\text{cl}}^\dagger[1] &= \begin{bmatrix} \bar{C}_{\text{cl}}^\downarrow + \bar{D} \bar{K}^\uparrow & 0_{\bar{n}_z \times \bar{n}_v} \end{bmatrix}, & \bar{C}_{\text{cl}}^\dagger[2] = \bar{C}_{\text{cl}}^\dagger[3] &= \begin{bmatrix} \bar{C}_{\text{cl}}^\downarrow & \bar{D} \end{bmatrix}. \end{aligned} \quad (\text{D.43})$$





# Appendix E. Numerical Values

## E.1. Numerical Values of Section 4.5

On the following pages, the state-space matrices  $\bar{A}^\uparrow[\varphi]$  to  $\bar{D}^\uparrow[\varphi]$  corresponding to the periodic system  $\bar{\mathcal{P}}_\varphi^\uparrow$  constructed in Sec. 4.5 are shown. These matrices are obtained by applying the modeling procedure described in Sec. 4.3.1 and using the numerical values stated in Sec. 3.6. The remaining matrices  $\bar{E}^\uparrow[\varphi]$  are obtained as:

$$\begin{aligned}\bar{E}^\uparrow[1] &= \begin{bmatrix} I_9 \\ 0_{5 \times 9} \end{bmatrix} \\ \bar{E}^\uparrow[2] &= \begin{bmatrix} I_9 \\ 0_{5 \times 9} \end{bmatrix} \\ \bar{E}^\uparrow[3] &= \begin{bmatrix} I_9 \\ 0_{4 \times 9} \end{bmatrix}.\end{aligned}$$

$$\left[ \begin{array}{c|c} \bar{A}^\dagger[1] & \bar{B}^\dagger[1] \\ \hline \bar{C}^\dagger[1] & \bar{D}^\dagger[1] \end{array} \right] =$$

-0.21	0.01	0.03	-0.06	0.10	0	0.20	0	0	0	0	0	0.30	0.70	0
0.82	0.29	0.08	0.05	-0.10	0.10	-0.10	0	0	0	0	0	-0.20	0	0
0.26	-0.01	0.03	0.10	0.10	0	0.20	0	0	0	0	0	0	0	-0.90
0.58	-0.10	0.09	0.30	-0.10	0.10	-0.10	0	0	0	0	0	0	0	0.30
0	0	0.20	0	0.25	-0.31	0.34	0.70	-0.40	0.40	0	0	0	0	0
0.10	0	0	0	0.40	1.10	-1.30	0	0.90	0	0	0	0	0	0
0	0.20	0	0	0.26	0.49	-0.58	0	0.90	0	0.60	0	0	0	0
0	0	0	0	0	0	0	-0.20	0.22	0	0	-1.50	0	0	0
0	0	0	0	0	0	0	-0.10	-0.04	0	0	0	0	0	0
0	0	0	0	0	0	0	0	0	0	0	0	1.00	0	0
0	0	0	0	0	0	0	0	0	0	0	0	0	1.00	0
0	0	0	0	0	0	0	0	0	0	0	0	0	0	1.00
0	0	0	0	0	0	0	0	0	1.00	0	0	0	0	0
1.90	0.54	-0.39	-0.23	0	0	0	0	0	0	0	0	1.00	0	0
1.00	0	0	0	0	0	0	0	0	0	0	0	0	0	0
-0.12	-0.50	-1.36	-0.98	0	0	0	0	0	0	0	0	0	1.00	0
0	2.00	0	0	0	0	0	0	0	0	0	0	0	0	0
1.93	0.35	0.30	-0.00	0	0	0	0	0	0	0	0	0	0	1.00
0	0	0	0	-2.87	0.71	-0.66	0	0	1.00	0	0	0	0	0
0	0	2.65	0	0	0	0	0	0	0	0	0	0	0	0
0	0	0	3.16	0	0	0	0	0	0	0	0	0	0	0
0	0	0	0	0.44	0.48	-0.29	0	0	1.00	0	0	0	0	0
0	0	0	0	3.61	0	0	0	0	0	0	0	0	0	0
0	0	0	0	0	0	0	0.00	-0.08	0	0	1.00	0	0	0
0	0	0	0	0	4.00	0	0	0	0	0	0	0	0	0
0	0	0	0	0	0	4.36	0	0	0	0	0	0	0	0
0	0	0	0	0	0	0	0.08	-0.53	0	0	0	0	0	1.00
0	0	0	0	0	0	0	4.69	0	0	0	0	0	0	0
0	0	0	0	0	0	0	0	5.00	0	0	0	0	0	0





## E.2. Numerical Values of Section 7.6

### E.2.1. Subsystem Dynamics

Subsystem dynamics and controlled variables for mode  $\theta = 1$ :

$$x_{k+1}^1 = \begin{bmatrix} 1.2 & 0.5 \\ 0.3 & 0.7 \end{bmatrix} x_k^1 + \begin{bmatrix} 0.2 & 0.1 \\ 2 & 0 \end{bmatrix} x_k^2 + \begin{bmatrix} 0 & 0.1 \\ 0.6 & 0.1 \end{bmatrix} x_k^3 + \begin{bmatrix} 0.2 & 0 \\ 0 & 0 \end{bmatrix} x_k^4 \dots \\ + \begin{bmatrix} 1 \\ 0 \end{bmatrix} u_k^1 + \begin{bmatrix} 0.2 & 0 \\ 0 & 0 \end{bmatrix} u_k^2 + \begin{bmatrix} 0 & 0 \\ 0 & 0.1 \end{bmatrix} u_k^3 + \begin{bmatrix} 0 & 0.2 \\ 0 & 0 \end{bmatrix} u_k^5 + \begin{bmatrix} 1 & 0 \\ 0 & 1 \end{bmatrix} w_k^1,$$

$$x_{k+1}^2 = \begin{bmatrix} 0 & 0.1 \\ 3 & 0 \end{bmatrix} x_k^1 + \begin{bmatrix} 1.4 & 0.1 \\ 0.3 & 0.7 \end{bmatrix} x_k^2 + \begin{bmatrix} 0.3 & 0 \\ 0 & 0 \end{bmatrix} x_k^3 + \begin{bmatrix} 0.1 & 0 \\ 0 & 0 \end{bmatrix} x_k^4 + \begin{bmatrix} 0.3 & 0.1 \\ 0 & 0.1 \end{bmatrix} x_k^5 \dots \\ + \begin{bmatrix} 1 & 0 \\ 1 & -1 \end{bmatrix} u_k^2 + \begin{bmatrix} 0 & 0 \\ 1 & 1 \end{bmatrix} u_k^5 + \begin{bmatrix} 1 & 0 \\ 0 & 1 \end{bmatrix} w_k^2,$$

$$x_{k+1}^3 = \begin{bmatrix} 0 & 0 \\ 0.1 & 0 \end{bmatrix} x_k^2 + \begin{bmatrix} 0.6 & 0 \\ 0 & 0.1 \end{bmatrix} x_k^3 + \begin{bmatrix} 0.2 & 1 \\ 2 & 0 \end{bmatrix} x_k^4 + \begin{bmatrix} 0 & 0 \\ 0.4 & 0 \end{bmatrix} x_k^5 \dots \\ + \begin{bmatrix} 0 & 1 \\ 0 & 0 \end{bmatrix} u_k^3 + \begin{bmatrix} 0 & 2 \\ 2 & 0 \end{bmatrix} u_k^4 + \begin{bmatrix} 0 & 0.1 \\ 0 & 0 \end{bmatrix} u_k^5 + \begin{bmatrix} 1 & 0 \\ 0 & 1 \end{bmatrix} w_k^3,$$

$$x_{k+1}^4 = \begin{bmatrix} 0.6 & 0.2 \\ 0 & 1.1 \end{bmatrix} x_k^3 + \begin{bmatrix} 1 & 0.1 \\ 0.2 & 0.3 \end{bmatrix} x_k^4 + \begin{bmatrix} 0 & 2 \\ 0.4 & 0 \end{bmatrix} x_k^5 \dots \\ + \begin{bmatrix} 1 & -1 \\ 0.2 & 0 \end{bmatrix} u_k^4 + \begin{bmatrix} 0 & 2 \\ 0 & 0 \end{bmatrix} u_k^5 + \begin{bmatrix} 2 & 1 \\ 1 & 2 \end{bmatrix} w_k^4,$$

$$x_{k+1}^5 = \begin{bmatrix} 0.1 & 0 \\ 0 & 0 \end{bmatrix} x_k^1 + \begin{bmatrix} 0 & 0.2 \\ 0 & 0.3 \end{bmatrix} x_k^2 + \begin{bmatrix} 0.6 & 0.2 \\ 0 & 0 \end{bmatrix} x_k^3 + \begin{bmatrix} 0 & 0.4 \\ 0.2 & 0 \end{bmatrix} x_k^4 + \begin{bmatrix} 0.3 & 1.2 \\ 0.4 & 0 \end{bmatrix} x_k^5 \dots \\ + \begin{bmatrix} 0.1 & 0 \\ 0 & 0 \end{bmatrix} u_k^2 + \begin{bmatrix} 0 & 2 \\ 1 & 0 \end{bmatrix} u_k^5 + \begin{bmatrix} 1 & 1 \\ 0 & 1 \end{bmatrix} w_k^5,$$

$$z_k^1 = \begin{bmatrix} 4 & 0 \\ 0 & 4 \\ 0 & 0 \end{bmatrix} x_k^1 + \begin{bmatrix} 1 & 3 \\ 0 & 0 \\ 0 & 0 \end{bmatrix} x_k^2 + \begin{bmatrix} 0 \\ 0 \\ 6 \end{bmatrix} u_k^1 + \begin{bmatrix} 0 & 0 \\ 0 & 0 \\ 0.1 & 0 \end{bmatrix} u_k^2,$$

$$z_k^2 = \begin{bmatrix} 2 & 0 \\ 0 & 2 \\ 0 & 0 \\ 0 & 0 \end{bmatrix} x_k^1 + \begin{bmatrix} 5 & -1 \\ 0 & 4 \\ 0 & 0 \\ 0 & 0 \end{bmatrix} x_k^2 + \begin{bmatrix} 0 & 0 \\ 0 & 1 \\ 0 & 0 \\ 0 & 0 \end{bmatrix} x_k^4 + \begin{bmatrix} 0 \\ 1 \\ 0 \end{bmatrix} u_k^1 + \begin{bmatrix} 0 & 0 \\ 0 & 0 \\ 4 & 0 \\ 0 & 2 \end{bmatrix} u_k^2,$$

$$z_k^3 = \begin{bmatrix} 2 & 0 \\ 0 & 2 \\ 0 & 0 \\ 0 & 0 \end{bmatrix} x_k^1 + \begin{bmatrix} 1 & -1 \\ 0 & 0 \\ 0 & 0 \\ 0 & 0 \end{bmatrix} x_k^2 + \begin{bmatrix} 0 & 4 \\ 5 & 0 \\ 0 & 0 \\ 0 & 0 \end{bmatrix} x_k^3 + \begin{bmatrix} 0 \\ 0 \\ 2 \\ 0 \end{bmatrix} u_k^1 + \begin{bmatrix} 0 & 0 \\ 0 & 0 \\ 0.4 & 0 \\ 0 & 1 \end{bmatrix} u_k^2 + \begin{bmatrix} 0 & 0 \\ 0 & 0 \\ 4 & 0 \\ 0 & 3 \end{bmatrix} u_k^3,$$

$$z_k^4 = \begin{bmatrix} 4 & 0 \\ 0 & 2 \\ 0 & 0 \end{bmatrix} x_k^1 + \begin{bmatrix} 1 & 3 \\ 0 & 0 \\ 0 & 0 \end{bmatrix} x_k^2 + \begin{bmatrix} 0 & 1 \\ 0 & 2 \\ 0 & 0 \end{bmatrix} x_k^3 + \begin{bmatrix} 2 & 3 \\ 0 & 0 \\ 0 & 0 \end{bmatrix} x_k^4 \dots$$

$$+ \begin{bmatrix} 0 \\ 0 \\ 6 \end{bmatrix} u_k^1 + \begin{bmatrix} 0 & 0 \\ 0 & 0 \\ 0.1 & 0 \end{bmatrix} u_k^2 + \begin{bmatrix} 0 & 0 \\ 0 & 0 \\ 0.3 & 0 \end{bmatrix} u_k^3 + \begin{bmatrix} 0 & 0 \\ 0.2 & 0 \\ 0 & 0.1 \end{bmatrix} u_k^4,$$

$$z_k^5 = \begin{bmatrix} 2 & 0 \\ 0 & 2 \\ 0 & 0 \\ 0 & 0 \end{bmatrix} x_k^1 + \begin{bmatrix} 1 & -1 \\ 0 & 1 \\ 0 & 0 \\ 0 & 0 \end{bmatrix} x_k^2 + \begin{bmatrix} 0 & 1 \\ 0 & 2 \\ 0 & 0 \\ 0 & 0 \end{bmatrix} x_k^3 + \begin{bmatrix} 0 \\ 0 \\ 1 \\ 0 \end{bmatrix} u_k^1 + \begin{bmatrix} 0 & 0 \\ 0 & 0 \\ 4 & 0 \\ 0 & 2 \end{bmatrix} u_k^2 + \begin{bmatrix} 0 & 0 \\ 0 & 0 \\ 0.3 & 0 \\ 0 & 2 \end{bmatrix} u_k^3.$$

Subsystem dynamics and controlled variables for mode  $\theta = 2$ :

$$x_{k+1}^1 = \begin{bmatrix} 0.2 & 0.8 \\ 0.4 & 0.7 \end{bmatrix} x_k^1 + \begin{bmatrix} 0.1 & 0.6 \\ 0.4 & 0 \end{bmatrix} x_k^2 + \begin{bmatrix} 0.4 & 1.1 \\ 0.6 & 0.5 \end{bmatrix} x_k^3 + \begin{bmatrix} 0.2 & 0 \\ 0 & 0 \end{bmatrix} x_k^4 \dots$$

$$+ \begin{bmatrix} 3 \\ 0 \end{bmatrix} u_k^1 + \begin{bmatrix} 0.2 & 0 \\ 0 & 0 \end{bmatrix} u_k^2 + \begin{bmatrix} 0 & 0 \\ 0 & 0.4 \end{bmatrix} u_k^3 + \begin{bmatrix} 0 & 0.2 \\ 0 & 0 \end{bmatrix} u_k^5 + \begin{bmatrix} 1 & 0 \\ 0 & 1 \end{bmatrix} w_k^1,$$

$$x_{k+1}^2 = \begin{bmatrix} 0 & 0.4 \\ 0 & 0 \end{bmatrix} x_k^1 + \begin{bmatrix} 2.8 & 0.3 \\ 0.1 & 0.7 \end{bmatrix} x_k^2 + \begin{bmatrix} 0.1 & 0 \\ 0 & 0 \end{bmatrix} x_k^3 + \begin{bmatrix} 0.3 & 0 \\ 0 & 0 \end{bmatrix} x_k^4 + \begin{bmatrix} 0.7 & 0.2 \\ 0 & 0.1 \end{bmatrix} x_k^5 \dots$$

$$+ \begin{bmatrix} 1 & 0 \\ 1 & 2 \end{bmatrix} u_k^2 + \begin{bmatrix} 0 & 0 \\ 1 & 1 \end{bmatrix} u_k^5 + \begin{bmatrix} 1 & 0 \\ 0 & 1 \end{bmatrix} w_k^2,$$

$$x_{k+1}^3 = \begin{bmatrix} 0.9 & 0.2 \\ 0 & 1.7 \end{bmatrix} x_k^3 + \begin{bmatrix} 0.2 & 0.2 \\ 2 & 0 \end{bmatrix} x_k^4 + \begin{bmatrix} 0 & 0 \\ 0.4 & 0 \end{bmatrix} x_k^5 \dots$$

$$+ \begin{bmatrix} 5 & 1 \\ 0 & 2 \end{bmatrix} u_k^3 + \begin{bmatrix} 0 & 0 \\ 2 & 0 \end{bmatrix} u_k^4 + \begin{bmatrix} 0 & 0.2 \\ 0 & 0 \end{bmatrix} u_k^5 + \begin{bmatrix} 1 & 0 \\ 0 & 1 \end{bmatrix} w_k^3,$$

$$x_{k+1}^4 = \begin{bmatrix} 0 & 0.2 \\ 0 & 0 \end{bmatrix} x_k^1 + \begin{bmatrix} 0.6 & 0.2 \\ 0 & 1.1 \end{bmatrix} x_k^3 + \begin{bmatrix} 1 & 0.1 \\ 0.2 & 0.3 \end{bmatrix} x_k^4 + \begin{bmatrix} 0 & 0 \\ 0.4 & 0 \end{bmatrix} x_k^5 \dots$$

$$+ \begin{bmatrix} 1 & -1 \\ 0.2 & 0 \end{bmatrix} u_k^4 + \begin{bmatrix} 0 & 2 \\ 0 & 0 \end{bmatrix} u_k^5 + \begin{bmatrix} 2 & 1 \\ 1 & 2 \end{bmatrix} w_k^4,$$

$$x_{k+1}^5 = \begin{bmatrix} 0.1 & 0 \\ 0 & 0 \end{bmatrix} x_k^1 + \begin{bmatrix} 0 & 0.1 \\ 0 & 0.3 \end{bmatrix} x_k^2 + \begin{bmatrix} 0.6 & 0.2 \\ 0 & 0 \end{bmatrix} x_k^3 + \begin{bmatrix} 0 & 1 \\ 0.1 & 0 \end{bmatrix} x_k^4 + \begin{bmatrix} 0.3 & 1.2 \\ 0.4 & 0 \end{bmatrix} x_k^5 \dots$$

$$+ \begin{bmatrix} 0.1 & 0 \\ 0 & 0 \end{bmatrix} u_k^2 + \begin{bmatrix} 0 & 2 \\ 1 & 0 \end{bmatrix} u_k^5 + \begin{bmatrix} 1 & 1 \\ 0 & 1 \end{bmatrix} w_k^5,$$

$$z_k^1 = \begin{bmatrix} 4 & 0 \\ 0 & 2 \\ 0 & 0 \end{bmatrix} x_k^1 + \begin{bmatrix} 1 & 3 \\ 0 & 0 \\ 0 & 0 \end{bmatrix} x_k^2 + \begin{bmatrix} 0 \\ 0 \\ 6 \end{bmatrix} u_k^1 + \begin{bmatrix} 0 & 0 \\ 0 & 0 \\ 0.1 & 0 \end{bmatrix} u_k^2,$$

$$z_k^2 = \begin{bmatrix} 2 & 0 \\ 0 & 2 \\ 0 & 0 \\ 0 & 0 \end{bmatrix} x_k^1 + \begin{bmatrix} 5 & -1 \\ 0 & 4 \\ 0 & 0 \\ 0 & 0 \end{bmatrix} x_k^2 + \begin{bmatrix} 0 & 0 \\ 0 & 1 \\ 0 & 0 \\ 0 & 0 \end{bmatrix} x_k^4 + \begin{bmatrix} 0 \\ 1 \\ 0 \end{bmatrix} u_k^1 + \begin{bmatrix} 0 & 0 \\ 0 & 0 \\ 4 & 0 \\ 0 & 2 \end{bmatrix} u_k^2,$$

$$z_k^3 = \begin{bmatrix} 2 & 0 \\ 0 & 2 \\ 0 & 0 \\ 0 & 0 \end{bmatrix} x_k^1 + \begin{bmatrix} 1 & -1 \\ 0 & 0 \\ 0 & 0 \\ 0 & 0 \end{bmatrix} x_k^2 + \begin{bmatrix} 0 & 4 \\ 5 & 0 \\ 0 & 0 \\ 0 & 0 \end{bmatrix} x_k^3 + \begin{bmatrix} 0 \\ 0 \\ 2 \\ 0 \end{bmatrix} u_k^1 + \begin{bmatrix} 0 & 0 \\ 0 & 0 \\ 0.4 & 0 \\ 0 & 1 \end{bmatrix} u_k^2 + \begin{bmatrix} 0 & 0 \\ 0 & 0 \\ 4 & 0 \\ 0 & 3 \end{bmatrix} u_k^3,$$

$$z_k^4 = \begin{bmatrix} 4 & 0 \\ 0 & 2 \\ 0 & 0 \end{bmatrix} x_k^1 + \begin{bmatrix} 1 & 3 \\ 0 & 0 \\ 0 & 0 \end{bmatrix} x_k^2 + \begin{bmatrix} 0 & 1 \\ 0 & 2 \\ 0 & 0 \end{bmatrix} x_k^3 + \begin{bmatrix} 2 & 3 \\ 0 & 0 \\ 0 & 0 \end{bmatrix} x_k^4 \dots$$

$$+ \begin{bmatrix} 0 \\ 0 \\ 6 \end{bmatrix} u_k^1 + \begin{bmatrix} 0 & 0 \\ 0 & 0 \\ 0.1 & 0 \end{bmatrix} u_k^2 + \begin{bmatrix} 0 & 0 \\ 0 & 0 \\ 0.3 & 0 \end{bmatrix} u_k^3 + \begin{bmatrix} 0 & 0 \\ 0.2 & 0 \\ 0 & 0.1 \end{bmatrix} u_k^4,$$

$$z_k^5 = \begin{bmatrix} 2 & 0 \\ 0 & 2 \\ 0 & 0 \\ 0 & 0 \end{bmatrix} x_k^1 + \begin{bmatrix} 1 & -1 \\ 0 & 1 \\ 0 & 0 \\ 0 & 0 \end{bmatrix} x_k^2 + \begin{bmatrix} 0 & 1 \\ 0 & 2 \\ 0 & 0 \\ 0 & 0 \end{bmatrix} x_k^5 + \begin{bmatrix} 0 \\ 0 \\ 1 \\ 0 \end{bmatrix} u_k^1 + \begin{bmatrix} 0 & 0 \\ 0 & 0 \\ 4 & 0 \\ 0 & 2 \end{bmatrix} u_k^2 + \begin{bmatrix} 0 & 0 \\ 0 & 0 \\ 0.3 & 0 \\ 0 & 2 \end{bmatrix} u_k^5.$$

Subsystem dynamics and controlled variables for mode  $\theta = 3$ :

$$x_{k+1}^1 = \begin{bmatrix} 1.2 & 1.8 \\ 0.4 & 1.7 \end{bmatrix} x_k^1 + \begin{bmatrix} 0.2 & 1.6 \\ 0.1 & 0 \end{bmatrix} x_k^2 + \begin{bmatrix} 0.1 & 2.1 \\ 0.6 & 0.3 \end{bmatrix} x_k^3 + \begin{bmatrix} 0.2 & 0 \\ 0 & 0 \end{bmatrix} x_k^4 \dots$$

$$+ \begin{bmatrix} 1 \\ 0.1 \end{bmatrix} u_k^1 + \begin{bmatrix} 0.1 & 0 \\ 0 & 0 \end{bmatrix} u_k^2 + \begin{bmatrix} 0 & 0 \\ 0 & 0.1 \end{bmatrix} u_k^3 + \begin{bmatrix} 0.3 & 0 \\ 0 & 0 \end{bmatrix} u_k^4 + \begin{bmatrix} 0 & 0.2 \\ 0 & 0 \end{bmatrix} u_k^5 + \begin{bmatrix} 1 & 0 \\ 0 & 1 \end{bmatrix} w_k^1,$$

$$x_{k+1}^2 = \begin{bmatrix} 0 & 0.6 \\ 0 & 0 \end{bmatrix} x_k^1 + \begin{bmatrix} 1.8 & 0.3 \\ 0.7 & 0.9 \end{bmatrix} x_k^2 + \begin{bmatrix} 0.4 & 0 \\ 0 & 0 \end{bmatrix} x_k^3 + \begin{bmatrix} 0.3 & 0 \\ 0 & 0 \end{bmatrix} x_k^4 + \begin{bmatrix} 0.3 & 0.2 \\ 0 & 0.1 \end{bmatrix} x_k^5 \dots$$



$$+ \begin{bmatrix} 2 & 0 \\ 5 & 2 \end{bmatrix} u_k^2 + \begin{bmatrix} 0 & 0 \\ 0.2 & 1 \end{bmatrix} u_k^5 + \begin{bmatrix} 1 & 0 \\ 0 & 1 \end{bmatrix} w_k^2,$$

$$x_{k+1}^3 = \begin{bmatrix} 1.9 & 0.2 \\ 0 & 1.7 \end{bmatrix} x_k^3 + \begin{bmatrix} 0.2 & 0.1 \\ 2 & 0 \end{bmatrix} x_k^4 + \begin{bmatrix} 0 & 0 \\ 0.4 & 0 \end{bmatrix} x_k^5 \dots \\ + \begin{bmatrix} 1 & 0 \\ 0 & 2 \end{bmatrix} u_k^3 + \begin{bmatrix} 0 & 2 \\ 2 & 0 \end{bmatrix} u_k^4 + \begin{bmatrix} 0 & 0.2 \\ 0 & 0 \end{bmatrix} u_k^5 + \begin{bmatrix} 1 & 0 \\ 0 & 1 \end{bmatrix} w_k^3,$$

$$x_{k+1}^4 = \begin{bmatrix} 0.6 & 0.2 \\ 0 & 1.3 \end{bmatrix} x_k^3 + \begin{bmatrix} 1 & 0.1 \\ 0.2 & 0.3 \end{bmatrix} x_k^4 + \begin{bmatrix} 0 & 0 \\ 0.4 & 0 \end{bmatrix} x_k^5 \dots \\ + \begin{bmatrix} 0.2 & 0 \\ 0 & 0 \end{bmatrix} u_k^2 + \begin{bmatrix} 1 & -1 \\ 0.4 & 0 \end{bmatrix} u_k^4 + \begin{bmatrix} 0 & 0.2 \\ 0 & 0 \end{bmatrix} u_k^5 + \begin{bmatrix} 2 & 1 \\ 1 & 2 \end{bmatrix} w_k^4,$$

$$x_{k+1}^5 = \begin{bmatrix} 0.1 & 0 \\ 0 & 0 \end{bmatrix} x_k^1 + \begin{bmatrix} 0 & 0.4 \\ 1 & 0.3 \end{bmatrix} x_k^2 + \begin{bmatrix} 0.6 & 0.2 \\ 0 & 0 \end{bmatrix} x_k^3 + \begin{bmatrix} 0 & 1 \\ 0.3 & 0 \end{bmatrix} x_k^4 + \begin{bmatrix} 0.3 & 1.2 \\ 0.4 & 0 \end{bmatrix} x_k^5 \dots \\ + \begin{bmatrix} 0.1 & 0 \\ 0 & 0 \end{bmatrix} u_k^2 + \begin{bmatrix} 0 & 2 \\ 1 & 0 \end{bmatrix} u_k^5 + \begin{bmatrix} 1 & 1 \\ 0 & 1 \end{bmatrix} w_k^5,$$

$$z_k^1 = \begin{bmatrix} 4 & 0 \\ 0 & 4 \\ 0 & 0 \end{bmatrix} x_k^1 + \begin{bmatrix} 1 & 3 \\ 0 & 0 \\ 0 & 0 \end{bmatrix} x_k^2 + \begin{bmatrix} 0 \\ 0 \\ 6 \end{bmatrix} u_k^1 + \begin{bmatrix} 0 & 0 \\ 0 & 0 \\ 0.1 & 0 \end{bmatrix} u_k^2,$$

$$z_k^2 = \begin{bmatrix} 2 & 0 \\ 0 & 2 \\ 0 & 0 \\ 0 & 0 \end{bmatrix} x_k^1 + \begin{bmatrix} 5 & -1 \\ 0 & 4 \\ 0 & 0 \\ 0 & 0 \end{bmatrix} x_k^2 + \begin{bmatrix} 0 & 0 \\ 0 & 1 \\ 0 & 0 \\ 0 & 0 \end{bmatrix} x_k^4 + \begin{bmatrix} 0 \\ 0 \\ 1 \\ 0 \end{bmatrix} u_k^1 + \begin{bmatrix} 0 & 0 \\ 0 & 0 \\ 4 & 0 \\ 0 & 2 \end{bmatrix} u_k^2,$$

$$z_k^3 = \begin{bmatrix} 2 & 0 \\ 0 & 2 \\ 0 & 0 \\ 0 & 0 \end{bmatrix} x_k^1 + \begin{bmatrix} 1 & -1 \\ 0 & 0 \\ 0 & 0 \\ 0 & 0 \end{bmatrix} x_k^2 + \begin{bmatrix} 0 & 4 \\ 5 & 0 \\ 0 & 0 \\ 0 & 0 \end{bmatrix} x_k^3 + \begin{bmatrix} 0 \\ 0 \\ 2 \\ 0 \end{bmatrix} u_k^1 + \begin{bmatrix} 0 & 0 \\ 0 & 0 \\ 0.4 & 0 \\ 0 & 1 \end{bmatrix} u_k^2 + \begin{bmatrix} 0 & 0 \\ 0 & 0 \\ 4 & 0 \\ 0 & 3 \end{bmatrix} u_k^3,$$

$$z_k^4 = \begin{bmatrix} 4 & 0 \\ 0 & 2 \\ 0 & 0 \end{bmatrix} x_k^1 + \begin{bmatrix} 1 & 3 \\ 0 & 0 \\ 0 & 0 \end{bmatrix} x_k^2 + \begin{bmatrix} 0 & 1 \\ 0 & 2 \\ 0 & 0 \end{bmatrix} x_k^3 + \begin{bmatrix} 2 & 3 \\ 0 & 0 \\ 0 & 0 \end{bmatrix} x_k^4 \dots \\ + \begin{bmatrix} 0 \\ 0 \\ 6 \end{bmatrix} u_k^1 + \begin{bmatrix} 0 & 0 \\ 0 & 0 \\ 0.1 & 0 \end{bmatrix} u_k^2 + \begin{bmatrix} 0 & 0 \\ 0 & 0 \\ 0.3 & 0 \end{bmatrix} u_k^3 + \begin{bmatrix} 0 & 0 \\ 0.2 & 0 \\ 0 & 0.1 \end{bmatrix} u_k^4,$$

$$z_k^5 = \begin{bmatrix} 2 & 0 \\ 0 & 2 \\ 0 & 0 \\ 0 & 0 \end{bmatrix} x_k^1 + \begin{bmatrix} 1 & -1 \\ 0 & 1 \\ 0 & 0 \\ 0 & 0 \end{bmatrix} x_k^2 + \begin{bmatrix} 0 & 1 \\ 0 & 2 \\ 0 & 0 \\ 0 & 0 \end{bmatrix} x_k^5 + \begin{bmatrix} 0 \\ 0 \\ 1 \\ 0 \end{bmatrix} u_k^1 + \begin{bmatrix} 0 & 0 \\ 0 & 0 \\ 4 & 0 \\ 0 & 2 \end{bmatrix} u_k^2 + \begin{bmatrix} 0 & 0 \\ 0 & 0 \\ 0.3 & 0 \\ 0 & 2 \end{bmatrix} u_k^5.$$

### E.2.2. Lower Layer Controllers

Lower layer controllers of the hierarchical control scheme. When used separately, as in the second row of Table 7.1, set  $v_k^i = 0$  for all  $i \in \mathcal{N}_s$ .

Values for mode  $\theta = 1$ :

$$u_k^1 = \begin{bmatrix} -0.9893 & -0.3475 \end{bmatrix} x_k^1 + \begin{bmatrix} 0.0399 & -0.0646 \end{bmatrix} x_k^2 + v_k^1,$$

$$u_k^2 = \begin{bmatrix} -0.1305 & -0.3363 \\ 2.8591 & -0.0460 \end{bmatrix} x_k^1 + \begin{bmatrix} -1.9142 & -0.1058 \\ -1.0192 & 0.5105 \end{bmatrix} x_k^2 + v_k^2,$$

$$u_k^3 = \begin{bmatrix} 0.1051 & -0.1905 \\ -0.8820 & -0.4904 \end{bmatrix} x_k^3 + \begin{bmatrix} 0.0860 & -0.0670 \\ -0.1431 & 0.0337 \end{bmatrix} x_k^4 + v_k^3,$$

$$u_k^4 = \begin{bmatrix} -0.1684 & -0.2197 \\ -0.0092 & 0.2578 \end{bmatrix} x_k^3 + \begin{bmatrix} -1.0597 & -0.1383 \\ -0.0170 & -0.5246 \end{bmatrix} x_k^4 + v_k^4,$$

$$u_k^5 = \begin{bmatrix} -0.1136 & 0.1240 \\ -0.1604 & -0.6237 \end{bmatrix} x_k^5 + v_k^5.$$

Values for mode  $\theta = 2$ :

$$u_k^1 = \begin{bmatrix} -0.1000 & -0.3163 \end{bmatrix} x_k^1 + v_k^1,$$

$$u_k^2 = \begin{bmatrix} -2.6036 & -0.3292 \\ 1.2245 & -0.2155 \end{bmatrix} x_k^2 + v_k^2,$$

$$u_k^3 = \begin{bmatrix} -0.1463 & 0.1295 \\ -0.3498 & -0.9669 \end{bmatrix} x_k^3 + \begin{bmatrix} 0.0223 & -0.0410 \\ -0.3233 & 0.0288 \end{bmatrix} x_k^4 + \begin{bmatrix} 0.0499 & -0.0186 \\ -0.3348 & -0.0421 \end{bmatrix} x_k^5 + v_k^3,$$

$$u_k^4 = \begin{bmatrix} 0.3272 & 0.0554 \\ 0.0479 & 0.6036 \end{bmatrix} x_k^3 + \begin{bmatrix} -0.6474 & -0.0056 \\ 0.5238 & -0.8738 \end{bmatrix} x_k^4 + \begin{bmatrix} 0.2355 & 0.1617 \\ 0.4814 & -0.2274 \end{bmatrix} x_k^5 + v_k^4,$$

$$u_k^5 = \begin{bmatrix} -0.1315 & -0.3156 \\ -0.3093 & -0.0059 \end{bmatrix} x_k^3 + \begin{bmatrix} 0.0790 & 0.2827 \\ -0.0292 & -0.5119 \end{bmatrix} x_k^4 + \begin{bmatrix} -0.3155 & 0.0594 \\ -0.1208 & -0.4748 \end{bmatrix} x_k^5 + v_k^5.$$

Values for mode  $\theta = 3$ :

$$u_k^1 = \begin{bmatrix} -1.7375 & -5.3393 \end{bmatrix} x_k^1 + v_k^1,$$

$$\begin{aligned}
 u_k^2 &= \begin{bmatrix} -0.5691 & -0.0799 \\ 0.6473 & -0.4932 \end{bmatrix} x_k^2 + \begin{bmatrix} -0.1747 & 0.0173 \\ 0.5382 & 0.1485 \end{bmatrix} x_k^5 + v_k^2, \\
 u_k^3 &= \begin{bmatrix} -0.4280 & 1.0858 \\ 1.4602 & 0.7431 \end{bmatrix} x_k^3 + \begin{bmatrix} -0.0893 & -0.1605 \\ -0.1229 & 0.0017 \end{bmatrix} x_k^4 + v_k^3, \\
 u_k^4 &= \begin{bmatrix} -1.3536 & -1.5917 \\ -0.8908 & -0.7188 \end{bmatrix} x_k^3 + \begin{bmatrix} -0.8398 & -0.0695 \\ -0.0946 & 0.0801 \end{bmatrix} x_k^4 + v_k^4, \\
 u_k^5 &= \begin{bmatrix} -0.6098 & 0.3488 \\ 0.1269 & 0.0271 \end{bmatrix} x_k^2 + \begin{bmatrix} -0.8478 & -0.2842 \\ -0.2417 & -0.5499 \end{bmatrix} x_k^5 + v_k^5,
 \end{aligned}$$

### E.2.3. Upper Layer Controllers

Upper layer controllers designed with Theorem 7.1.

Values for mode  $\theta = 1$ :

$$\begin{aligned}
 v_{s\Delta k}^1 &= [0.0863 \quad 0.0515] x_{s\Delta k}^1 + [0.0793 \quad 0.0213] x_{s\Delta k}^2, \\
 v_{s\Delta k}^2 &= \begin{bmatrix} -0.0121 & -0.0110 \\ -0.2561 & 0.0209 \end{bmatrix} x_{s\Delta k}^1 + \begin{bmatrix} 0.0084 & -0.0066 \\ 0.2196 & 0.0517 \end{bmatrix} x_{s\Delta k}^2, \\
 v_{s\Delta k}^3 &= \begin{bmatrix} 0.1264 & 0.0721 \\ -0.0979 & -0.0191 \end{bmatrix} x_{s\Delta k}^1 + \begin{bmatrix} 0.0896 & 0.0198 \\ -0.1912 & 0.0274 \end{bmatrix} x_{s\Delta k}^2 \cdots \\
 &\quad + \begin{bmatrix} 0.1009 & 0.0594 \\ -0.0043 & 0.0024 \end{bmatrix} x_{s\Delta k}^3 + \begin{bmatrix} 0.0408 & 0.0147 \\ 0.0010 & -0.0517 \end{bmatrix} x_{s\Delta k}^4, \\
 v_{s\Delta k}^4 &= \begin{bmatrix} 0.0646 & 0.0081 \\ 0.1289 & 0.0140 \end{bmatrix} x_{s\Delta k}^1 + \begin{bmatrix} -0.0712 & -0.0031 \\ 0.0694 & -0.0250 \end{bmatrix} x_{s\Delta k}^2 \cdots \\
 &\quad + \begin{bmatrix} 0.0008 & 0.0005 \\ 0.0014 & -0.0009 \end{bmatrix} x_{s\Delta k}^3 + \begin{bmatrix} -0.0005 & 0.0130 \\ -0.0017 & 0.0275 \end{bmatrix} x_{s\Delta k}^4, \\
 v_{s\Delta k}^5 &= \begin{bmatrix} -0.0372 & -0.0238 \\ 0.0092 & 0.0008 \end{bmatrix} x_{s\Delta k}^1 + \begin{bmatrix} -0.0717 & -0.0378 \\ 0.0987 & -0.0060 \end{bmatrix} x_{s\Delta k}^2 + \begin{bmatrix} -0.0095 & 0.0311 \\ 0.0007 & -0.0028 \end{bmatrix} x_{s\Delta k}^5,
 \end{aligned}$$

with  $v_{s\Delta k+l}^i = v_{s\Delta k}^i$  for all  $i \in \mathcal{N}_s$  and  $l \in \{1, 2, 3, 4\}$ .

Values for mode  $\theta = 2$ :

$$v_{s\Delta k}^1 = [-0.1181 \quad -0.0787] x_{s\Delta k}^1,$$

$$\begin{aligned}
 v_{s\Delta k}^2 &= \begin{bmatrix} -0.0070 & -0.0015 \\ 0.0253 & 0.0051 \end{bmatrix} x_{s\Delta k}^2, \\
 v_{s\Delta k}^3 &= \begin{bmatrix} 0.1178 & 0.0361 \\ -0.5952 & -0.2281 \end{bmatrix} x_{s\Delta k}^3 + \begin{bmatrix} 0.0298 & -0.0503 \\ -0.1570 & 0.2394 \end{bmatrix} x_{s\Delta k}^4 \dots \\
 &\quad + \begin{bmatrix} 0.0509 & -0.0117 \\ -0.2433 & 0.0692 \end{bmatrix} x_{s\Delta k}^5, \\
 v_{s\Delta k}^4 &= \begin{bmatrix} 0.5325 & 0.2835 \\ 0.2705 & 0.3478 \end{bmatrix} x_{s\Delta k}^3 + \begin{bmatrix} 0.1571 & -0.1890 \\ 0.1283 & -0.1086 \end{bmatrix} x_{s\Delta k}^4 \dots \\
 &\quad + \begin{bmatrix} 0.1978 & -0.0868 \\ 0.0602 & -0.1477 \end{bmatrix} x_{s\Delta k}^5, \\
 v_{s\Delta k}^5 &= \begin{bmatrix} -0.1189 & -0.2514 \\ -0.0531 & 0.0153 \end{bmatrix} x_{s\Delta k}^3 + \begin{bmatrix} -0.0715 & -0.0401 \\ -0.0050 & 0.0062 \end{bmatrix} x_{s\Delta k}^4 \dots \\
 &\quad + \begin{bmatrix} 0.0022 & 0.0497 \\ -0.0267 & -0.0161 \end{bmatrix} x_{s\Delta k}^5,
 \end{aligned}$$

with  $v_{s\Delta k+l}^i = v_{s\Delta k}^i$  for all  $i \in \mathcal{N}_s$  and  $l \in \{1, 2, 3, 4\}$ .

Values for mode  $\theta = 3$ :

$$\begin{aligned}
 v_{s\Delta k}^1 &= \begin{bmatrix} 0.0831 & 0.2525 \end{bmatrix} x_{s\Delta k}^1 + \begin{bmatrix} 0.1460 & -0.0677 \end{bmatrix} x_{s\Delta k}^2 \dots \\
 &\quad + \begin{bmatrix} -0.2532 & -0.2286 \end{bmatrix} x_{s\Delta k}^3 + \begin{bmatrix} -0.0725 & 0.0943 \end{bmatrix} x_{s\Delta k}^4 \dots \\
 &\quad + \begin{bmatrix} -0.1221 & 0.0660 \end{bmatrix} x_{s\Delta k}^5, \\
 v_{s\Delta k}^2 &= \begin{bmatrix} -0.0547 & -0.2167 \\ 0.1992 & 0.7280 \end{bmatrix} x_{s\Delta k}^1 + \begin{bmatrix} -0.1844 & -0.0361 \\ 0.6393 & 0.1018 \end{bmatrix} x_{s\Delta k}^2 \dots \\
 &\quad + \begin{bmatrix} 0.0474 & 0.0454 \\ -0.2370 & -0.2301 \end{bmatrix} x_{s\Delta k}^3 + \begin{bmatrix} 0.0267 & -0.0386 \\ -0.1192 & 0.1837 \end{bmatrix} x_{s\Delta k}^4 \dots \\
 &\quad + \begin{bmatrix} 0.0982 & -0.0514 \\ -0.3525 & 0.1926 \end{bmatrix} x_{s\Delta k}^5, \\
 v_{s\Delta k}^3 &= \begin{bmatrix} -0.0200 & -0.2158 \\ -0.0292 & -0.2180 \end{bmatrix} x_{s\Delta k}^1 + \begin{bmatrix} -0.0840 & 0.0720 \\ 0.0522 & 0.0458 \end{bmatrix} x_{s\Delta k}^2 \dots \\
 &\quad + \begin{bmatrix} -0.6426 & 0.3384 \\ -0.3716 & -0.0040 \end{bmatrix} x_{s\Delta k}^3 + \begin{bmatrix} 0.0000 & -0.1536 \\ -0.0077 & -0.0741 \end{bmatrix} x_{s\Delta k}^4 \dots
 \end{aligned}$$

$$\begin{aligned}
 & + \begin{bmatrix} 0.0806 & -0.0099 \\ -0.1081 & 0.0254 \end{bmatrix} x_{s\Delta k}^5, \\
 v_{s\Delta k}^4 & = \begin{bmatrix} 0.0266 & 0.2008 \\ 0.0023 & 0.0766 \end{bmatrix} x_{s\Delta k}^1 + \begin{bmatrix} -0.0156 & -0.0405 \\ 0.0175 & -0.0441 \end{bmatrix} x_{s\Delta k}^2 \dots \\
 & + \begin{bmatrix} 0.3484 & -0.0412 \\ 0.3227 & -0.1728 \end{bmatrix} x_{s\Delta k}^3 + \begin{bmatrix} 0.0058 & 0.0702 \\ 0.0040 & 0.0715 \end{bmatrix} x_{s\Delta k}^4 \dots \\
 & + \begin{bmatrix} 0.0617 & -0.0142 \\ -0.0299 & -0.0007 \end{bmatrix} x_{s\Delta k}^5, \\
 v_{s\Delta k}^5 & = \begin{bmatrix} 0.0738 & -0.0487 \\ 0.0270 & 0.2120 \end{bmatrix} x_{s\Delta k}^1 + \begin{bmatrix} 0.1804 & -0.0107 \\ 0.0811 & 0.0216 \end{bmatrix} x_{s\Delta k}^2 \dots \\
 & + \begin{bmatrix} -0.1510 & -0.3933 \\ 0.0173 & 0.0827 \end{bmatrix} x_{s\Delta k}^3 + \begin{bmatrix} -0.1649 & 0.3810 \\ 0.0235 & -0.0690 \end{bmatrix} x_{s\Delta k}^4 \dots \\
 & + \begin{bmatrix} -0.1647 & 0.1060 \\ -0.0136 & 0.0054 \end{bmatrix} x_{s\Delta k}^5,
 \end{aligned}$$

with  $v_{s\Delta k+l}^i = v_{s\Delta k}^i$  for all  $i \in \mathcal{N}_s$  and  $l \in \{1, 2, 3, 4\}$ .

Upper layer controllers designed with Theorem 7.2.

Values for mode  $\theta = 1$ :

$$\begin{aligned}
 v_{s\Delta k}^1 & = [0.1323 \quad 0.0534] x_{s\Delta k}^1 + [0.0674 \quad 0.0190] x_{s\Delta k}^2 + [0.1241 \quad -0.0326] x_{s\Delta k}^3 \dots \\
 & + [0.0037 \quad 0.0166] x_{s\Delta k}^4 + [0.0380 \quad 0.0661] x_{s\Delta k}^5, \\
 v_{s\Delta k}^2 & = - \begin{bmatrix} 0.0495 & 0.0165 \\ 0.2625 & 0.0749 \end{bmatrix} x_{s\Delta k}^1 - \begin{bmatrix} 0.0163 & 0.0071 \\ 0.0121 & 0.0073 \end{bmatrix} x_{s\Delta k}^2 + \begin{bmatrix} -0.0713 & 0.0212 \\ -0.1524 & 0.2127 \end{bmatrix} x_{s\Delta k}^3 \dots \\
 & + \begin{bmatrix} -0.0140 & -0.0128 \\ -0.0325 & 0.0729 \end{bmatrix} x_{s\Delta k}^4 - \begin{bmatrix} 0.0490 & 0.0416 \\ 0.1152 & 0.1612 \end{bmatrix} x_{s\Delta k}^5, \\
 v_{s\Delta k}^3 & = \begin{bmatrix} 0.1142 & 0.0697 \\ 0.0205 & -0.0348 \end{bmatrix} x_{s\Delta k}^1 + \begin{bmatrix} 0.0845 & 0.0076 \\ -0.1638 & 0.0298 \end{bmatrix} x_{s\Delta k}^2 + \begin{bmatrix} -0.0000 & 0.0750 \\ 0.1798 & -0.0380 \end{bmatrix} x_{s\Delta k}^3 \dots \\
 & + \begin{bmatrix} 0.0129 & 0.0152 \\ 0.0349 & 0.0325 \end{bmatrix} x_{s\Delta k}^4 + \begin{bmatrix} 0.0175 & -0.0397 \\ 0.0158 & 0.0655 \end{bmatrix} x_{s\Delta k}^5,
 \end{aligned}$$

$$\begin{aligned}
 v_{s\Delta k}^4 &= \begin{bmatrix} 0.0760 & -0.0072 \\ 0.0370 & 0.0193 \end{bmatrix} x_{s\Delta k}^1 + \begin{bmatrix} -0.0967 & 0.0258 \\ 0.0327 & -0.0070 \end{bmatrix} x_{s\Delta k}^2 + \begin{bmatrix} 0.0860 & 0.0022 \\ -0.0812 & 0.0026 \end{bmatrix} x_{s\Delta k}^3 \cdots \\
 &+ \begin{bmatrix} 0.0128 & 0.0521 \\ -0.0290 & -0.0181 \end{bmatrix} x_{s\Delta k}^4 - \begin{bmatrix} 0.1390 & 0.0322 \\ 0.1188 & 0.0582 \end{bmatrix} x_{s\Delta k}^5, \\
 v_{s\Delta k}^5 &= \begin{bmatrix} -0.0628 & -0.0309 \\ -0.0395 & 0.0211 \end{bmatrix} x_{s\Delta k}^1 + \begin{bmatrix} -0.0659 & -0.0363 \\ 0.1121 & -0.0238 \end{bmatrix} x_{s\Delta k}^2 - \begin{bmatrix} 0.0137 & 0.0427 \\ 0.1083 & 0.0050 \end{bmatrix} x_{s\Delta k}^3 \cdots \\
 &+ \begin{bmatrix} -0.0124 & 0.0174 \\ -0.0225 & -0.0603 \end{bmatrix} x_{s\Delta k}^4 + \begin{bmatrix} -0.0306 & 0.0253 \\ 0.0853 & 0.0104 \end{bmatrix} x_{s\Delta k}^5,
 \end{aligned}$$

with  $v_{s\Delta k+l}^i = v_{s\Delta k}^i$  for all  $i \in \mathcal{N}_s$  and  $l \in \{1, 2, 3, 4\}$ .

Values for mode  $\theta = 2$ :

$$\begin{aligned}
 v_{s\Delta k}^1 &= \begin{bmatrix} 0.0084 & -0.0423 \end{bmatrix} x_{s\Delta k}^1 + \begin{bmatrix} -0.0628 & -0.1172 \end{bmatrix} x_{s\Delta k}^3 \cdots \\
 &+ \begin{bmatrix} -0.0333 & 0.0394 \end{bmatrix} x_{s\Delta k}^4 + \begin{bmatrix} -0.0408 & 0.0216 \end{bmatrix} x_{s\Delta k}^5, \\
 v_{s\Delta k}^2 &= \begin{bmatrix} 0.0034 & -0.0006 \\ 0.0124 & 0.0003 \end{bmatrix} x_{s\Delta k}^2 + \begin{bmatrix} -0.0393 & 0.0100 \\ 0.1057 & -0.0258 \end{bmatrix} x_{s\Delta k}^3 \cdots \\
 &+ \begin{bmatrix} -0.0107 & -0.0431 \\ 0.0483 & 0.1154 \end{bmatrix} x_{s\Delta k}^4 + \begin{bmatrix} -0.1227 & -0.0751 \\ 0.3201 & 0.2038 \end{bmatrix} x_{s\Delta k}^5, \\
 v_{s\Delta k}^3 &= \begin{bmatrix} 0.0430 & 0.0847 \\ -0.2182 & -0.4335 \end{bmatrix} x_{s\Delta k}^1 + \begin{bmatrix} 0.0273 & -0.0479 \\ -0.1451 & 0.2173 \end{bmatrix} x_{s\Delta k}^3 \cdots \\
 &+ \begin{bmatrix} -0.0161 & -0.0150 \\ 0.0737 & 0.0681 \end{bmatrix} x_{s\Delta k}^4 + \begin{bmatrix} -0.0293 & -0.0057 \\ 0.1215 & 0.0255 \end{bmatrix} x_{s\Delta k}^5, \\
 v_{s\Delta k}^4 &= \begin{bmatrix} 0.1774 & 0.3836 \\ 0.0203 & 0.0865 \end{bmatrix} x_{s\Delta k}^1 + \begin{bmatrix} 0.1336 & -0.1276 \\ -0.0193 & 0.0046 \end{bmatrix} x_{s\Delta k}^3 \cdots \\
 &+ \begin{bmatrix} -0.0440 & -0.0622 \\ 0.0171 & -0.0734 \end{bmatrix} x_{s\Delta k}^4 - \begin{bmatrix} 0.0909 & 0.0532 \\ 0.2804 & 0.2297 \end{bmatrix} x_{s\Delta k}^5, \\
 v_{s\Delta k}^5 &= - \begin{bmatrix} 0.0195 & 0.0969 \\ 0.0327 & 0.0739 \end{bmatrix} x_{s\Delta k}^1 + \begin{bmatrix} -0.0635 & -0.0849 \\ -0.0402 & 0.0029 \end{bmatrix} x_{s\Delta k}^3 \cdots \\
 &+ \begin{bmatrix} -0.0788 & -0.0382 \\ 0.0149 & 0.0028 \end{bmatrix} x_{s\Delta k}^4 - \begin{bmatrix} 0.1235 & 0.0238 \\ 0.0604 & 0.0357 \end{bmatrix} x_{s\Delta k}^5,
 \end{aligned}$$

with  $v_{s\Delta k+l}^i = v_{s\Delta k}^i$  for all  $i \in \mathcal{N}_s$  and  $l \in \{1, 2, 3, 4\}$ .

Values for mode  $\theta = 3$ :

$$v_{s\Delta k}^1 = \begin{bmatrix} 0.0710 & 0.1947 \end{bmatrix} x_{s\Delta k}^1 + \begin{bmatrix} 0.1341 & -0.0644 \end{bmatrix} x_{s\Delta k}^2 - \begin{bmatrix} 0.2604 & 0.2218 \end{bmatrix} x_{s\Delta k}^3 \dots \\ + \begin{bmatrix} -0.0818 & 0.1039 \end{bmatrix} x_{s\Delta k}^4 + \begin{bmatrix} -0.1191 & 0.0636 \end{bmatrix} x_{s\Delta k}^5,$$

$$v_{s\Delta k}^2 = \begin{bmatrix} -0.0369 & -0.1602 \\ 0.1379 & 0.5267 \end{bmatrix} x_{s\Delta k}^1 + \begin{bmatrix} -0.1892 & -0.0444 \\ 0.6533 & 0.1332 \end{bmatrix} x_{s\Delta k}^2 \dots \\ + \begin{bmatrix} 0.0445 & 0.0336 \\ -0.2263 & -0.1845 \end{bmatrix} x_{s\Delta k}^3 + \begin{bmatrix} 0.0258 & -0.0335 \\ -0.1192 & 0.1696 \end{bmatrix} x_{s\Delta k}^4 \dots \\ + \begin{bmatrix} 0.1005 & -0.0532 \\ -0.3595 & 0.1980 \end{bmatrix} x_{s\Delta k}^5,$$

$$v_{s\Delta k}^3 = \begin{bmatrix} 0.0198 & -0.0508 \\ 0.0012 & -0.1153 \end{bmatrix} x_{s\Delta k}^1 + \begin{bmatrix} -0.0744 & 0.0779 \\ 0.0514 & 0.0510 \end{bmatrix} x_{s\Delta k}^2 + \begin{bmatrix} -0.5371 & 0.3233 \\ -0.3258 & -0.0050 \end{bmatrix} x_{s\Delta k}^3 \dots \\ + \begin{bmatrix} 0.0043 & -0.1427 \\ -0.0121 & -0.0583 \end{bmatrix} x_{s\Delta k}^4 + \begin{bmatrix} 0.0717 & -0.0137 \\ -0.1123 & 0.0212 \end{bmatrix} x_{s\Delta k}^5,$$

$$v_{s\Delta k}^4 = \begin{bmatrix} -0.0016 & 0.1031 \\ -0.0154 & 0.0020 \end{bmatrix} x_{s\Delta k}^1 + \begin{bmatrix} -0.0157 & -0.0448 \\ 0.0124 & -0.0484 \end{bmatrix} x_{s\Delta k}^2 + \begin{bmatrix} 0.3024 & -0.0383 \\ 0.2698 & -0.1670 \end{bmatrix} x_{s\Delta k}^3 \dots \\ + \begin{bmatrix} 0.0089 & 0.0566 \\ 0.0022 & 0.0662 \end{bmatrix} x_{s\Delta k}^4 + \begin{bmatrix} 0.0657 & -0.0105 \\ -0.0251 & 0.0010 \end{bmatrix} x_{s\Delta k}^5,$$

$$v_{s\Delta k}^5 = \begin{bmatrix} 0.0543 & -0.1499 \\ 0.0173 & 0.1864 \end{bmatrix} x_{s\Delta k}^1 + \begin{bmatrix} 0.1812 & 0.0243 \\ 0.0812 & 0.0173 \end{bmatrix} x_{s\Delta k}^2 + \begin{bmatrix} -0.1534 & -0.3345 \\ 0.0142 & 0.0748 \end{bmatrix} x_{s\Delta k}^3 \dots \\ + \begin{bmatrix} -0.1811 & 0.3930 \\ 0.0263 & -0.0737 \end{bmatrix} x_{s\Delta k}^4 + \begin{bmatrix} -0.1643 & 0.1047 \\ -0.0146 & 0.0066 \end{bmatrix} x_{s\Delta k}^5,$$

with  $v_{s\Delta k+l}^i = v_{s\Delta k}^i$  for all  $i \in \mathcal{N}_s$  and  $l \in \{1, 2, 3, 4\}$ .

# List of Symbols

## Equalities, Inequalities and Definitions

$\mathcal{A} := \mathcal{B}$	$\mathcal{A}$ is defined to be $\mathcal{B}$
$\mathcal{A} = \mathcal{B}, \mathcal{A} \neq \mathcal{B}$	$\mathcal{A}$ is equal to $\mathcal{B}, \mathcal{A}$ is not equal to $\mathcal{B}$
$\mathcal{A} \in \mathcal{B}, \mathcal{A} \notin \mathcal{B}$	$\mathcal{A}$ is an element of a set $\mathcal{B}, \mathcal{A}$ is not an element of a set $\mathcal{B}$
$\mathcal{A} \subset \mathcal{B}, \mathcal{A} \subseteq \mathcal{B}$	a set $\mathcal{A}$ is a subset of a set $\mathcal{B}, \mathcal{A}$ is a subset of or equal to the set $\mathcal{B}$
$\mathcal{A} < \mathcal{B}, \mathcal{A} \leq \mathcal{B}$	component wise inequality of matrices $\mathcal{A} = [a_{i,j}] \in \mathbb{R}^{m \times n}$ and $\mathcal{B} = [b_{i,j}] \in \mathbb{R}^{m \times n}$ : $a_{i,j} < b_{i,j}$ for all $(i,j) \in \{1, \dots, m\} \times \{1, \dots, n\}$ , $a_{i,j} \leq b_{i,j}$ for all $(i,j) \in \{1, \dots, m\} \times \{1, \dots, n\}$
$\mathcal{A} \prec \mathcal{B}, \mathcal{A} \preceq \mathcal{B}$	inequality of symmetric positive definite matrices $\mathcal{A} \in \mathbb{R}^{n \times n}$ and $\mathcal{B} \in \mathbb{R}^{n \times n}$ : $y^\top \mathcal{A} y < y^\top \mathcal{B} y$ for all $y \in \mathbb{R}^n$ , $y^\top \mathcal{A} y \leq y^\top \mathcal{B} y$ for all $y \in \mathbb{R}^n$
$(\bullet)^\top(\mathcal{B}\mathcal{A})$	Abbreviation of symmetric products of matrices $\mathcal{A} \in \mathbb{R}^{m \times n}$ and $\mathcal{B} \in \mathbb{R}^{p \times m}$ : $\bullet^\top(\mathcal{A}\mathcal{B}) := \mathcal{A}^\top \mathcal{B}^\top \mathcal{B} \mathcal{A}$
$(\bullet)^\top(\mathcal{R})(\mathcal{B}\mathcal{A})$	Abbreviation of symmetric products of matrices $\mathcal{A} \in \mathbb{R}^{m \times n}$ , $\mathcal{B} \in \mathbb{R}^{p \times m}$ , and $\mathcal{R} \in \mathbb{R}^{p \times p}$ : $(\bullet)^\top(\mathcal{R})(\mathcal{B}\mathcal{A}) := \mathcal{A}^\top \mathcal{B}^\top \mathcal{R} \mathcal{B} \mathcal{A}$

## Functions

$\lceil \cdot \rceil : \mathbb{R} \rightarrow \mathbb{Z}$	ceil function, $\lceil y \rceil := \min_{i \in \mathbb{Z}} i \geq y$
$\lfloor \cdot \rfloor : \mathbb{R} \rightarrow \mathbb{Z}$	floor function, $\lfloor y \rfloor := \max_{i \in \mathbb{Z}} i \leq y$
$p : \mathcal{N}_s \rightarrow \mathcal{N}_c$	cluster $\mathcal{C}^p$ containing subsystem $\mathcal{P}^i$ : $p(i) := q \in \mathcal{N}_c \mid i \in \mathcal{C}^q$
$\varphi : \mathbb{T} \rightarrow \mathbb{I}_{N_\varphi}$	$N_\varphi$ -periodic switching function
$\text{sgn} : \mathbb{R} \rightarrow \{\pm 1\}$	signum function
$\mathcal{V} : \mathbb{X} \rightarrow \mathbb{R}_{\geq 0}$	Lyapunov function



## General

$(\cdot)_k$	piecewise-constant signal sampled at time $t = k\Delta t$ : $\omega_k = \omega(k\Delta t)$
$(\cdot)_{[k_1:k_2]}$	time sequence from $k_1$ to $k_2$ : $\omega_{[k_1:k_2]}^\top = [\omega_{k_1}^\top, \dots, \omega_{k_2}^\top]$
$(\cdot)^i$	value associated with subsystem $\mathcal{P}^i$ or controller $\mathcal{C}^i$
$(\bar{\cdot})^p$	value associated with cluster $\bar{\mathcal{P}}^p$ or cluster controller $\bar{\mathcal{C}}^p$
$(\cdot)^\downarrow$	value associated with the lower control layer
$(\cdot)^\uparrow$	value associated with the upper control layer
$(\bar{\cdot})$	permuted and/or re-partitioned vector, matrix, or set
$(\check{\cdot})$	lower or upper bound of a value
$(\hat{\cdot})$	piecewise-constant signal defined on the upper layer time-domain
$(\cdot)_{[\varphi]}$	value depending on a periodic switching function $\varphi$
$(\hat{\cdot})_s$	piecewise-constant signal sampled at time $t = s\Delta k\Delta t$ : $\omega_s = \omega(s\Delta k\Delta t)$
$(\cdot)^*$	optimal value, e.g. optimal value of the performance index: $J^*$
$(\cdot)_{[\theta]}$	value depending on a Markov state $\theta \in \Theta \subset \mathbb{N}$
$\mathcal{C}^i$	controller of subsystem $i$
$\Delta k$	multiple of the sampling time $\Delta t$
$\Delta t$	sampling time, i.e. time increment for each time step $k$
$\mathcal{E}$	edges of the communication graph $\mathcal{G}$ : $\mathcal{E} \subseteq \mathcal{N} \times \mathcal{N}$
$\mathcal{G}$	communication graph: $\mathcal{G} = (\mathcal{N}, \mathcal{E})$
$J$	performance index
$k$	discrete time $k$
$\mathcal{M}$	Markov chain: $\mathcal{M} = (\Theta, P, \mu_0)$
$n_\bullet$	dimension of a signal vector, e.g. state dimension $n_x$
$n_\bullet^i$	dimension of a signal vector of subsystem $i$ , e.g. subsystem state dimension $n_x^i$

---

$N_c$	number of clusters
$N_s$	number of subsystems
$N_s^p$	number of subsystems contained in cluster $C^p$ : $N_s^p := \text{card}(C^p)$
$\mathcal{P}^i$	subsystem $i$
$t$	continuous time $t$
$\theta$	Markov state $\theta \in \Theta \subset \mathbb{N}$
$\zeta$	hybrid state of an uncertain system $\mathcal{P}_\theta$ : $\zeta := (x, \theta)$

## Operators

$\text{He}(\mathcal{A})$	Hermitian matrix associated with a matrix $\mathcal{A}$ : $\text{He}(\mathcal{A}) := \frac{1}{2}\mathcal{A} + \frac{1}{2}\mathcal{A}^\top$
$\mathcal{A} \otimes \mathcal{B}$	Kronecker product of matrices $\mathcal{A} \in \mathbb{R}^{m \times n}$ and $\mathcal{B} \in \mathbb{R}^{q \times p}$ : $\mathcal{A} \otimes \mathcal{B} := [\mathcal{A}_{i,j} \mathcal{B}] \in \mathbb{R}^{mq \times np}$
$\varsigma$	forward shift operator: $\varsigma \eta := [\eta_n \ \eta_1 \ \eta_2 \ \dots \ \eta_{n-1}]^\top$
$\text{vec}(\mathcal{A}), \text{vec}_r(\mathcal{A})$	column vector associated with a discrete ordered set, $r$ -th element of a discrete ordered set $\mathcal{A} = \{a_1, a_2, \dots, a_n\}$ : $\text{vec}(\mathcal{A}) := [a_1 \ a_2 \ \dots \ a_n]^\top, \text{vec}_r(\mathcal{A}) = a_r.$

## Scalars and Constants

$M$	scalar or matrix of sufficiently large positive real numbers
-----	--

## Sets

$\{\cdot\}$	a discrete set, e.g. $\{1, 2, 3\}$
$\setminus$	relative complement: $\mathcal{S}_1 \setminus \mathcal{S}_2 := \{y \in \mathcal{S}_1 \mid y \notin \mathcal{S}_2\}$
$\times$	cartesian product of sets: $\mathcal{S}_1 \times \mathcal{S}_2 := \{(y_1; y_2) \mid y_1 \in \mathcal{S}_1, y_2 \in \mathcal{S}_2\}$
$\cap$	intersection of sets: $\mathcal{S}_1 \cap \mathcal{S}_2 := \{y \mid y \in \mathcal{S}_1 \text{ and } y \in \mathcal{S}_2\}$
$\cup$	union of sets: $\mathcal{S}_1 \cup \mathcal{S}_2 := \{y \mid y \in \mathcal{S}_1 \text{ or } y \in \mathcal{S}_2\}$
$\mathbb{B}$	set of binary numbers: $\mathbb{B} := \{0, 1\}$

$\mathbb{H}^N(\mathbb{R}^{m \times n})$	Set of all $N$ -sequences of $\mathbb{R}^{m \times n}$ matrices: $\mathbb{H}^N(\mathbb{R}^{m \times n}) := \{\mathbf{V} = (V[1], \dots, V[N]) \mid V[o] \in \mathbb{R}^{m \times n}, o \in \mathbb{I}_N\}$ .
$\mathbb{N}, \mathbb{N}_0$	set of natural numbers, set of natural numbers including zero
$\mathbb{R}_{>0}, \mathbb{R}_{\geq 0}$	set of positive real numbers, set of non-negative real numbers
$\mathbb{R}^n$	set of real vectors with $n$ elements
$\mathbb{S}^n$	set of symmetric matrices: $\mathbb{S}^n := \{M \in \mathbb{R}^{n \times n} \mid M = M^T\}$
$\mathbb{S}_{>0}^n$	set of symmetric positive definite matrices: $\mathbb{S}_{>0}^n := \{M \in \mathbb{S}^n \mid M \succ 0\}$
$\mathbb{Z}$	set of integers
$\mathcal{B}_r^n(y)$	closed ball of dimension $n \in \mathbb{N}$ , radius $r \in \mathbb{R}_{>0}$ , and with center $y \in \mathbb{R}^n$ : $\mathcal{B}_r^n(y) := \{\bar{y} \in \mathbb{R}^n \mid \ \bar{y} - y\  \leq r\}$
$\text{card}(\mathcal{S})$	cardinality of a set $\mathcal{S}$ , e.g. $\text{card}(\{0, 2, 4\}) = 3$
$\mathbb{C}$	set of complex numbers
$\mathbb{C}_1, \mathbb{C}_{<1}$	unit circle and open unit disc in the complex plane: $\mathbb{C}_1 := \{y \in \mathbb{C} \mid  y  = 1\}$ , $\mathbb{C}_{<1} := \{y \in \mathbb{C} \mid  y  < 1\}$
$\mathbb{I}_n$	ordered index set: $\mathbb{I}_n := \{1, \dots, n\}$
$\mathcal{N}_c$	set of cluster indices: $\mathcal{N}_c := \{1, \dots, N_c\}$
$\mathcal{N}_s$	set of subsystem indices: $\mathcal{N}_s := \{1, \dots, N_s\}$
$\mathcal{N}_s^i$	set of subsystem indices without $i$ : $\mathcal{N}_s^i := \mathcal{N}_s \setminus \{i\}$
$\Phi$	switching sequence of a periodic system: $\Phi := \{\varphi_{N_\varphi-1}, \dots, \varphi_1, \varphi_0\}$
$\mathcal{R}^i$	subset of controller indices $j \in \mathcal{N}_s$ with $\mathcal{C}^i$ receiving information to $\mathcal{C}^j$
$\mathbb{T}$	discrete time domain: $\mathbb{T} := \{t_k \mid t_k = k\Delta t + t_0, \Delta t \in \mathbb{R}_{>0}, t_0 \in \mathbb{R}_{\geq 0}, k \in \mathbb{N}_0\}$
$\mathcal{T}^i$	subset of controller indices $j \in \mathcal{N}_s$ with $\mathcal{C}^i$ transmitting information to $\mathcal{C}^j$
$\Theta$	discrete, ordered set of Markov states: $\Theta := \{1, \dots, N_\theta\}$
$\mathbb{U}$	continuous input space: $\mathbb{U} \subseteq \mathbb{R}^{n_u}$
$\mathbb{W}$	set of disturbances

$\mathbb{X}$  continuous state space:  $\mathbb{X} \subseteq \mathbb{R}^{n_x}$

$\mathcal{X}$  subset of or equal to the set of local state vectors:  
 $\mathcal{X} \subseteq \{x^i \mid i \in \mathcal{N}\}$

## Vectors and Matrices

$0_{m \times n}$  zero matrix  $0_{m \times n} \in \mathbb{R}^{m \times n}$  of dimension  $m \times n$ , with  $0_n := 0_{n \times n}$

$1_{m \times n}$  matrix or vector of ones of dimension  $m \times n$ , with  $1_n := 1_{n \times n}$

$(\cdot)^\top$  transpose of a vector or matrix

$\mathcal{A}, \mathcal{C}$  subset  $\mathcal{C}$  of block-columns of a partitioned matrix  $\mathcal{A} = [\mathcal{A}_{i,j}]$

$\star$  abbreviation of entries in symmetric matrices:  $\begin{bmatrix} \mathcal{A} & \mathcal{B} \\ \star & \mathcal{C} \end{bmatrix} := \begin{bmatrix} \mathcal{A} & \mathcal{B} \\ \mathcal{B}^\top & \mathcal{C} \end{bmatrix}$

$A, B, E$  matrices defining linear dynamics

$\mathbf{A}, \mathbf{B}, \mathbf{E}$   $N$ -sequences of matrices defining linear hybrid dynamics, with,  
 e.g.,  $\mathbf{A} \in \mathbb{H}^N(\mathbb{R}^{n \times n})$

$\Gamma$  subsystem interconnection structure matrix:  $\Gamma \in \mathbb{R}_{\geq 0}^{N_s \times N_s}$

$I_n$  identity matrix  $I_n \in \mathbb{R}^{n \times n}$  of dimension  $n$

$K$  feedback matrix

$\lambda_{\min}(\cdot), \lambda_{\max}(\cdot)$  smallest and largest eigenvalue of a matrix

$\Lambda(\cdot)$  set of eigenvalues of a quadratic matrix

$\mu_k$  probability distribution of the Markov state  $\theta_k$  at time  $k$ :  
 $\mu_{k,m} := \Pr(\theta_k = m)$

$\|\cdot\|$  Euclidean norm of a matrix or vector

$\|\cdot\|_\infty$  infinity norm of a matrix or vector

$\|\cdot\|_{1,\infty}$  induced 1,  $\infty$ -norm of a matrix:  $\|\mathcal{A}\|_{1,\infty} = \max_{i,j} |\mathcal{A}_{i,j}|$

$P$  transition probability matrix of the Markov chain  $\mathcal{M}$ :  
 $P = [p_{m,n}], p_{m,n} := \Pr(\theta_{k+1} = n \mid \theta_k = m)$

$\Phi_A[\varphi_{k_1}, \varphi_{k_0}]$  state-transition matrix associated with a periodic system  $\mathcal{P}_p$ ,  
 see p.81 for a definition

$\Psi_A[\varphi_k]$  monodromy matrix associated with a periodic system  $\mathcal{P}_p$ , see  
 p.81 for a definition

$\ \cdot\ _Q$	weighted norm with weight $Q$ , e.g.: $\ x\ _Q^2 := x^\top Qx$
$\Sigma$	adjacency matrix associated with the communication graph $\mathcal{G}$
$T_\bullet$	transformation or permutation matrix, e.g. $T_x$
$u_k$	input of the overall system $\mathcal{P}$ at time $k$
$u_k^i$	input of subsystem $\mathcal{P}^i$ at time $k$
$w_k$	disturbance acting on the dynamic system $\mathcal{P}$ at time $k$
$w_k$	disturbance acting on subsystem $\mathcal{P}^i$ at time $k$
$x_k$	state of the overall system $\mathcal{P}$ at time $k$
$x_k^i$	state of subsystem $\mathcal{P}^i$ at time $k$
$z_k$	controlled variable of the overall system $\mathcal{P}$ at time $k$
$z_k^i$	controlled variable of subsystem $\mathcal{P}^i$ at time $k$

# List of Abbreviations

ADMM	alternating direction method of multipliers
AGC	area generation control
ARE	algebraic Riccati equation
BIBO	bounded-input/bounded-output
BMI	bilinear matrix inequality
BnB	branch-and-bound
CALE	coupled algebraic Lyapunov equation
CARE	coupled algebraic Riccati equation
DES	discrete-event system
DM	Dulmage-Mendelsohn
DSF	dynamical structure function
IQC	integral-quadratic constraint
JMS	jump Markov system
JMLS	jump Markov linear system
JSMS	jump semi-Markov system
LBT	lower block-triangular
LTI	linear time-invariant
LMI	linear matrix inequality
LP	linear program
LPV	linear parameter-varying
LQ	linear quadratic
LQR	linear quadratic regulator
LSS	large-scale system
MAS	multi-agent system
MIMO	multi-input/multi-output
MIP	mixed-integer program
MISDP	mixed-integer semidefinite program
MPC	model predictive control
MSS	mean-square stability

NCS	networked control system
PDE	partial differential equation
QP	quadratic program
RGA	relative gain array
SCT design	simultaneous control and network topology design
SDP	semidefinite program
TCP	transmission control protocol
UBT	upper block-triangular
w.r.t.	with respect to

# References

- [1] A. Aghdam and E. Davison, “Decentralized switching control for hierarchical systems,” *Automatica*, vol. 43, pp. 1092 – 1100, 2007.
- [2] H. Amann and J. Escher, *Analysis III*. Springer, 2009.
- [3] B. Anderson and J. Moore, *Optimal Control - Linear Quadratic Methods*. Dover Publications, Inc., 2007.
- [4] B. Anderson and J. Moore, *Optimal Filtering*. Dover Publications, Inc., 1979.
- [5] J. Anderson, A. Teixeira, H. Sandberg, and A. Papachristodoulou, “Dynamical system decomposition using dissipation inequalities,” in *Conference on Decision and Control*, 2011, pp. 211 – 216.
- [6] J. Anderson and A. Papachristodoulou, “Dynamical system decomposition for efficient, sparse analysis,” in *Conference on Decision and Control*, 2010, pp. 6565 – 6570.
- [7] G. Antonelli, “Interconnected dynamic systems - an overview on distributed control,” *IEEE Control Systems*, vol. 33, no. 1, pp. 76 – 88, 2013.
- [8] A. Antoulas, *Approximation of Large-Scale Dynamical Systems*. Society for Industrial and Applied Mathematics, 2005.
- [9] P. Antsaklis and A. Michel, *Linear Systems*, 2nd ed. Boston: Birkhäuser, 2006.
- [10] V. Armentano and M. Singh, “A procedure to eliminate decentralized fixed modes with reduced information exchange,” *IEEE Transactions on Automatic Control*, vol. 95, no. 1, pp. 9 – 28, 1982.
- [11] D. Arzelier, D. Peaucelle, C. Farges, and J. Daafouz, “Robust analysis and synthesis of linear polytopic discrete-time periodic systems via LMIs,” in *Conference on Decision and Control*, 2005, pp. 5734 – 5739.
- [12] J. Baillieul and P. Antsaklis, “Control and communication challenges in networked real-time systems,” *Proceedings of the IEEE*, vol. 95, no. 1, pp. 9–28, 2007.



- [13] L. Bakule, “Decentralized control: An overview.” in *11th IFAC Symposium on Large Scale Complex Systems: Theory and Applications*, 2007, pp. 39 – 48.
- [14] L. Bakule, “Decentralized control: Status and outlook,” *Annual Reviews in Control*, vol. 38, pp. 71 – 80, 2014.
- [15] B. Bamieh, M. Jovanović, P. Mitra, and S. Patterson, “Coherence in large-scale networks: Dimension-dependent limitations of local feedback,” *IEEE Transactions on Automatic Control*, vol. 57, no. 9, pp. 2235 – 2249, 2012.
- [16] B. Bamieh, F. Paganini, and M. Dahleh, “Distributed control of spatially invariant systems,” *IEEE Transactions on Automatic Control*, vol. 47, no. 7, pp. 1091 – 1107, 2002.
- [17] D. Barcelli, A. Bemporad, and G. Ripaccioli, “Decentralized hierarchical multi-rate control of constrained linear systems,” in *18th IFAC World Congress*, 2011, pp. 277 – 283.
- [18] N. Bauer, M. Donkers, N. van de Wouw, and W. Heemels, “Decentralized observer-based control via networked communication,” *Automatica*, vol. 49, pp. 2074 – 2086, 2013.
- [19] P. Benner, V. Mehrmann, and D. Sorensen, Eds., *Dimension Reduction of Large-Scale Systems*. Springer, 2005.
- [20] S. Bittanti and P. Colaneri, “Invariant representations of discrete-time periodic systems,” *Automatica*, vol. 36, pp. 1777 – 1793, 2000.
- [21] S. Bittanti and P. Colaneri, *Periodic Systems: Filtering and Control*. Springer, 2009.
- [22] R. Bobiti, R. Gielen, and M. Lazar, “Non-conservative and tractable stability tests for general linear interconnected systems with an application to power systems,” in *4th IFAC Workshop on Distributed Estimation and Control in Networked Systems*, 2013, pp. 152 – 158.
- [23] P. Bolzern, P. Colaneri, and G. De Nicolao, “Markov jump linear systems with switching transition rates: mean square stability with dwell-time.” *Automatica*, vol. 46, no. 6, pp. 1081 – 1088, 2010.
- [24] F. Borrelli and T. Keviczky, “Distributed LQR design for identical dynamically decoupled systems,” *IEEE Transactions on Automatic Control*, vol. 53, no. 8, pp. 1901 – 1912, 2008.
- [25] S. Boyd, L. El Ghaoui, E. Feron, and V. Balakrishnan, *Linear Matrix Inequalities in System and Control Theory*. Society for Industrial and Applied Mathematics, 1994.

- 
- [26] S. Boyd and L. Vandenberghe, *Convex Optimization*. Cambridge University Press, 2009.
- [27] E. Bristol, “On a new measure of interaction for multivariable process control,” *IEEE Transactions on Automatic Control*, vol. 11, no. 1, pp. 133 – 134, 1966.
- [28] I. Bronshtein, K. Semendyayev, G. Musiol, and H. Muehlig, *Handbook of Mathematics*, 4th ed. Springer, 2004.
- [29] N. Campos and A. Sanchez, “Towards the formal implementation of hierarchical discrete-event controllers in automated manufacturing systems,” in *14th IFAC Symposium on Information Control Problems in Manufacturing*, 2012, pp. 224 – 229.
- [30] A. Conley and M. Salgado, “Gramian based interaction measure,” in *Conference on Decision and Control*, 2000, pp. 5020 – 5022.
- [31] O. Costa, M. Fragoso, and R. Marques, *Discrete-Time Markov Jump Linear Systems*. London: Springer, 2005.
- [32] E. Davison and T. Chang, “Decentralized stabilization and pole assignment for general proper systems,” *IEEE Transactions on Automatic Control*, vol. 35, no. 6, pp. 652 – 664, 1990.
- [33] M. De Oliveira, J. Geromel, and J. Bernussou, “Extended  $\mathcal{H}_2$  and  $\mathcal{H}_\infty$  norm characterizations and controller parametrizations for discrete-time systems,” *Int. Journal of Control*, vol. 75, no. 9, pp. 666 – 679, 2002.
- [34] C. De Souza and A. Trofino, “An LMI approach to stabilization of linear discrete-time periodic systems,” *Int. Journal of Control*, vol. 73, no. 8, pp. 696 – 703, 2000.
- [35] O. Demir and J. Lunze, “A decomposition approach to decentralized and distributed control of spatially interconnected systems,” in *18th IFAC World Congress*, 2011, pp. 9109 – 9114.
- [36] Z. Di, “Control with structural constraints: Theory and implementation,” Ph.D. Thesis, University of Illinois at Urbana-Champaign, 2007.
- [37] J. do Val, J. Geromel, and A. Gonçalves, “The  $\mathcal{H}_2$ -control for jump linear systems: cluster observation of the Markov state,” *Automatica*, vol. 38, pp. 343 – 349, 2002.
- [38] P. Dorato and A. Levis, “Optimal linear regulators: The discrete-time case,” *IEEE Transactions on Automatic Control*, vol. 16, no. 6, pp. 613 – 620, 1971.
- [39] G.-R. Duan and H.-H. Yu, *LMIs in Control Systems - Analysis, Design and Applications*. CRC Press, 2013.

- [40] G. Dullerud and F. Paganini, *A Course on Robust Control Theory*. Springer, 2000.
- [41] Y. Ebihara, D. Peaucelle, and D. Arzelier, “Periodically time-varying memory state-feedback controller synthesis for discrete-time linear systems,” *Automatica*, vol. 47, pp. 14 – 25, 2011.
- [42] J. Eilbrecht, “Distributed control of interconnected systems using hierarchical dynamic output feedback,” Master Thesis, Technische Universität Braunschweig, Institut für Verkehrssicherheit und Automatisierungstechnik, 2016.
- [43] J. Eilbrecht, M. Jilg, and O. Stursberg, “Distributed  $\mathcal{H}_2$ -optimized output feedback controller design using the ADMM,” in *20th IFAC World Congress*, 2017, pp. 10 389 – 10 394.
- [44] V. Fambrini and C. Ocampo-Martinez, “Modelling and decentralized model predictive control of drinking water networks - the barcelona case study,” Institut de Robòtica i Informàtica Industrial, Tech. Rep. IRI-TR-09-04, 2009.
- [45] M. Fardad, F. Lin, and M. Jovanović, “Design of optimal sparse interconnection graphs for synchronization of oscillator networks,” *IEEE Transactions on Automatic Control*, vol. 59, no. 9, pp. 2457 – 2462, 2014.
- [46] C. Farges, D. Peaucelle, D. Arzelier, and J. Daafouz, “Robust  $\mathcal{H}_2$  performance analysis and synthesis of linear polytopic discrete-time periodic systems via LMIs,” *Systems and Control Letters*, vol. 56, pp. 159 – 166, 2007.
- [47] F. Fele, J. Maestre, E. Camacho, and F. Muros, “Coalitional control: an irrigation canal case study,” in *10th IEEE International Conference on Networking, Sensing and Control*, 2013.
- [48] I. Gradshteyn and I. Ryzhik, *Table of Integrals, Series, and Products*, A. Jeffrey, Ed. Academic Press, 1980.
- [49] J. Grainger and W. Stevenson, *Power system analysis*. McGraw-Hill, 2003.
- [50] D. Groß and O. Stursberg, “Distributed control and network topology design for interconnected systems.” in *Conference on Decision and Control*, 2011, pp. 8112–8117.
- [51] D. Groß, “Distributed model predictive control with event-based communication,” Ph.D. Thesis, Universität Kassel, Faculty of Electrical Engineering and Computer Sciences. Kassel University Press, 2014.
- [52] D. Groß, M. Jilg, and O. Stursberg, “Design of distributed controllers and communication topologies considering link failures,” in *European Control Conference*, 2013, pp. 3288 – 3294.

- 
- [53] R. Hermans, “Distributed control of deregulated electrical power networks,” Ph.D. Thesis, Eindhoven University of Technology, 2012.
- [54] C. Hoffmann, A. Eichler, and H. Werner, “Distributed control of linear parameter-varying decomposable systems,” in *American Control Conference*, 2013, pp. 2380 – 2385.
- [55] C. Hoffmann, A. Eichler, and H. Werner, “Control of heterogeneous groups of systems interconnected through directed and switching topologies,” *IEEE Transactions on Automatic Control*, vol. 60, no. 7, pp. 1904 – 1909, 2015.
- [56] J. Huang and Y. Shi, “Stochastic stability and robust stabilization of semi-Markov jump linear systems,” *International Journal of Robust and Nonlinear Control*, vol. 23, pp. 2028 – 2043, 2013.
- [57] M. Jamshidi, Ed., *System of Systems Engineering: Innovations for the 21st Century*. Wiley, 2009.
- [58] M. Jilg and O. Stursberg, “Hierarchical distributed control for interconnected systems,” in *13th IFAC Symposium on Large Scale Complex Systems: Theory and Applications*, 2013, pp. 419 – 425.
- [59] M. Jilg and O. Stursberg, “Optimized distributed control and topology design for hierarchically interconnected systems,” in *European Control Conference*, 2013, pp. 4340 – 4346.
- [60] M. Jilg and O. Stursberg, “On the computation of local quadratic performance indices for hierarchically interconnected systems,” in *European Control Conference*, 2014, pp. 1574 – 1581.
- [61] M. Jilg and O. Stursberg, “Hierarchical distributed control of a class of interconnected jump semi-Markov systems,” in *European Control Conference*, 2016, pp. 236 – 242.
- [62] M. Jilg, J. Tonne, and O. Stursberg, “Design of distributed  $\mathcal{H}_2$ -optimized controllers considering stochastic communication link failures,” in *American Control Conference*, 2015, pp. 3540 – 3545.
- [63] P. Koltai and O. Junge, “Optimal value functions for weakly coupled systems: a posteriori estimates,” *Journal of Applied Mathematics and Mechanics*, vol. 94, no. 4, pp. 345 – 355, 2014.
- [64] I. Kondratiev, R. Dougal, G. Veselov, and A. Kolesnikov, “Hierarchical control for electromechanical systems based on synergetic control theory,” in *IEEE Multi-conference on Systems and Control*, 2009, pp. 495 – 500.

- [65] H. Kwakernaak and R. Sivan, *Linear Optimal Control Systems*. Wiley-Interscience, 1972.
- [66] B. Labibi, B. Lohmann, A. Sedigh, and P. Maralani, “Decentralized stabilization of large-scale systems via state-feedback and using descriptor systems,” *IEEE Transactions on Systems, Man, and Cybernetics*, vol. 33, no. 6, pp. 771 – 776, 2003.
- [67] C. Langbort, R. Chandra, and R. D’Andrea, “Distributed control design for systems interconnected over an arbitrary graph,” *IEEE Transactions on Automatic Control*, vol. 49, no. 9, pp. 1502 – 1519, 2004.
- [68] A. Langville and W. Stewart, “The kronecker product and stochastic automata networks,” *Journal of Computational and Applied Mathematics*, vol. 167, pp. 429 – 447, 2004.
- [69] J. Lavaei and A. Aghdam, “Decentralized control design for interconnected systems based on a centralized reference controller,” in *Conference on Decision and Control*, 2006.
- [70] J. Lavaei, A. Momeni, and A. Aghdam, “A near-optimal decentralized servomechanism controller for hierarchical interconnected systems,” in *Conference on Decision and Control*, 2007.
- [71] R. Leduc, “Hierarchical interface-based supervisory control,” Ph.D. Thesis, Graduate Department of Electrical and Computer Engineering, University of Toronto, 2003.
- [72] E. Lee, “Computing foundations and practice for cyber-physical systems: A preliminary report,” Technical Report, Department of Electrical Engineering and Computer Sciences, University of California at Berkeley, 2007.
- [73] D. Li, “Hierarchical control for large-scale systems with general multiple linear-quadratic structure,” *Automatica*, vol. 29, no. 6, pp. 1451 – 1461, 1993.
- [74] L. Li and F. Paganini, “LMI relaxation to Riccati equation in structured control,” *International Journal of Control*, vol. 80, no. 4, pp. 527 – 539, 2007.
- [75] L. Li, V. Ugrinovskii, and R. Orsi, “Decentralized robust control of uncertain Markov jump parameter systems via output feedback,” *Automatica*, vol. 43, pp. 1932 – 1944, 2007.
- [76] F. Lin, M. Fardad, and M. Jovanović, “Sparse feedback synthesis via the alternating direction method of multipliers,” in *American Control Conference*, 2012, pp. 4765 – 4770.

- 
- [77] F. Lin, M. Fardad, and M. Jovanović, “Augmented Lagrangian approach to design of structured optimal state feedback gains,” *IEEE Transactions on Automatic Control*, vol. 56, no. 12, pp. 2923 – 2929, 2011.
- [78] F. Lin, M. Fardad, and M. Jovanović, “Design of optimal sparse feedback gains via the alternating direction method of multipliers,” *IEEE Transactions on Automatic Control*, vol. 58, no. 9, pp. 2426 – 2431, 2013.
- [79] J. Löfberg, “YALMIP : A toolbox for modeling and optimization in MATLAB,” in *13th IEEE International Symposium on Computer Aided Control System Design*, Taipei, Taiwan, 2004, pp. 284 – 289.
- [80] J. Lunze, Ed., *Control Theory of Digitally Networked Dynamic Systems*. Springer, 2014.
- [81] J. Lygeros, “Hierarchical, hybrid control of large scale systems,” Ph.D. Thesis, University of California, Berkeley, 1996.
- [82] S. Ma, J. Xiong, V. Ugrinovskii, and I. Petersen, “Robust decentralized stabilization of markovian jump large-scale systems: A neighboring mode dependent approach,” *Automatica*, vol. 49, pp. 3105 – 3111, 2013.
- [83] K. Mårtensson, “Gradient methods for large-scale and distributed linear quadratic control,” Ph.D. Thesis, Department of Automatic Control, Lund University, 2012.
- [84] J. Maestre, D. Muñoz de la Peña, A. Jiménez Losada, E. Algaba, and E. Camacho, “A coalitional control scheme with applications to cooperative game theory,” *Optimal Control Applications and Methods*, vol. 35, pp. 592 – 608, 2014.
- [85] M. Mahmoud, *Decentralized Systems with Design Constraints*. Springer London, 2011.
- [86] M. Mahmoud, M. Hassan, and M. Darwish, *Large-Scale Control Systems - Theories and Techniques*. Marcel Dekker, 1985.
- [87] M. Mahmoud and M. Singh, *Discrete Systems*. Springer, 1984.
- [88] L. Marinovici, J. Lian, K. Kalsi, P. Du, and M. Elizondo, “Distributed hierarchical control architecture for transient dynamics improvement in power systems,” *IEEE Transactions on Power Systems*, vol. 28, no. 3, pp. 3065 – 3074, 2012.
- [89] J. Markovski, A. Sokolova, N. Trča, and E. de Vink, “Compositionality for Markov reward chains with fast transitions,” in *Formal Methods and Stochastic Models for Performance Evaluation*, ser. Springer Lecture Notes in Computer Science, K. Wolter, Ed., 2007, pp. 18 – 32.

- [90] P. Massioni, “Distributed control for alpha-heterogeneous dynamically coupled systems,” *Systems and Control Letters*, vol. 72, pp. 30 – 35, 2014.
- [91] P. Massioni and M. Verhaegen, “Distributed control for identical dynamically coupled systems: A decomposition approach,” *IEEE Transactions on Automatic Control*, vol. 54, no. 1, pp. 124 – 135, 2009.
- [92] M. Mesarović, D. Macko, and Y. Takahara, *Theory of Hierarchical, Multilevel, Systems*. Academic Press, 1970.
- [93] J. Mohammadpour and K. Grigoriadis, Eds., *Efficient Modeling and Control of Large-Scale Systems*. Springer, 2010.
- [94] T. Moor, J. Raisch, and J. Davoren, “Admissibility criteria for a hierarchical design of hybrid control systems,” in *Conference on Analysis and Design of Hybrid Systems*, 2003, pp. 389 – 394.
- [95] MOSEK ApS, *The MOSEK optimization software. Version 7.1.0.41.2015*, 2015. [Online]. Available: <http://docs.mosek.com/7.1/capi.pdf>
- [96] N. Motee and A. Jadbabaie, “Optimal control of spatially distributed systems,” *IEEE Transactions on Automatic Control*, vol. 53, no. 7, pp. 1616 – 1629, 2008.
- [97] N. Motee, A. Jadbabaie, and B. Bamieh, “On decentralized optimal control and information structures,” in *American Control Conference*, 2008, pp. 4985 – 4990.
- [98] A. Otto, J. Hall, A. Hickford, R. Nicholls, D. Alderson, S. Barr, and M. Tran, “A quantified system-of-systems modeling framework for robust national infrastructure planning,” *IEEE Systems Journal*, vol. 10, no. 2, pp. 385 – 396, 2016.
- [99] A. Ouammi, H. Dagdougui, and R. Sacile, “Optimal control of power flows and energy local storages in a network of microgrids modeled as a system of systems,” *IEEE Transactions on Automatic Control*, vol. 23, no. 1, pp. 128 – 138, 2015.
- [100] M. Pai, *Power System Stability: Analysis by the Direct Method of Lyapunov*. North-Holland Publishing Company, 1981.
- [101] B. Park and W. Kwon, “Robust one-step receding horizon control of discrete-time markovian jump uncertain systems,” *Automatica*, vol. 38, no. 7, pp. 1229 – 1235, 2002.
- [102] A. Pothén and C. Fan, “Computing the block triangular form of a sparse matrix,” *ACM Transactions on Mathematical Software*, vol. 16, no. 4, pp. 303 – 324, December 1990.

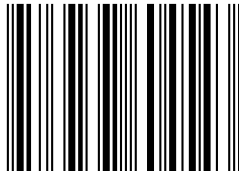
- 
- [103] M. Rafiee and A. Bayen, “Optimal network topology design in multi-agent systems for efficient average consensus,” in *Conference on Decision and Control*, 2010, pp. 3877 – 3883.
- [104] A. Rai and S. Warnick, “A technique for designing stabilizing distributed controllers with arbitrary signal structure constraints,” in *European Control Conference*, 2013, pp. 3282 – 3287.
- [105] A. Rantzer, “Dynamic dual decomposition for distributed control,” in *American Control Conference*, 2009, pp. 884 – 888.
- [106] M. Rotkowitz, “Parametrization of all stabilizing controllers subject to any structural constraint,” in *Conference of Decision and Control*, 2010, pp. 108 – 113.
- [107] M. Rotkowitz and S. Lall, “A characterization of convex problems in decentralized control,” *IEEE Transactions on Automatic Control*, vol. 51, no. 2, pp. 274 – 286, 2006.
- [108] N. Sandell, Jr., P. Varaiya, M. Athans, and M. Safonov, “Survey of decentralized control methods for large scale systems,” *IEEE Transactions on Automatic Control*, vol. 23, no. 2, pp. 108 – 128, 1978.
- [109] C. Scherer, “Structured  $\mathcal{H}_\infty$ -optimal control for nested interconnections: A state-space solution,” *Systems & Control Letters*, vol. 62, pp. 1105 – 1113, 2013.
- [110] C. W. Scherer, P. Gahinet, and M. Chilali, “Multiobjective output-feedback control via lmi optimization,” *IEEE Transactions on Automatic Control*, vol. 42, no. 7, pp. 896 – 911, 1997.
- [111] S. Schuler, P. Li, J. Lam, and F. Allgöwer, “Design of structured dynamic output-feedback controllers for interconnected systems,” *International Journal of Control*, vol. 84, no. 12, pp. 2081 – 2091, 2011.
- [112] C. Schwartz and A. Haddad, “Control of jump linear systems having semi-Markov sojourn times,” in *Conference on Decision and Control*, 2003.
- [113] G. Seber and A. Lee, *Linear Regression Analysis*, 2nd ed. John Wiley and Sons, 2003.
- [114] P. Shah and P. Parrilo, “ $\mathcal{H}_2$ -optimal decentralized control over posets: A state-space solution for state-feedback,” *IEEE Transactions on Automatic Control*, vol. 58, no. 12, pp. 3084 – 3096, 2013.
- [115] J. Shamma, Ed., *Cooperative Control of Distributed Multi-Agent Systems*. Wiley, 2007.



- [116] J. Shamma and G. Arslan, “A decomposition approach to distributed control of spatially invariant systems,” *IEEE Transactions on Automatic Control*, vol. 51, no. 4, pp. 701 – 707, 2006.
- [117] P. Shi and F. Li, “A survey on markovian jump systems: Modeling and design,” *Int. Journal of Control, Automation and Systems*, vol. 13, no. 1, pp. 73 – 92, 2015.
- [118] E. Simon, “Optimal static output feedback design through direct search,” in *Conference on Decision and Control and European Control Conference*, 2011, pp. 296 – 301.
- [119] M. Singh, *Dynamical hierarchical control*. North-Holland, 1977.
- [120] H. Soliman, M. Darwish, and J. Fantin, “Stabilization of a large-scale power system via a multilevel technique,” *International Journal of Systems Science*, vol. 9, no. 10, pp. 1091 – 1111, 1978.
- [121] Y. Song, S. Liu, and G. Wei, “Constrained robust distributed model predictive control for uncertain discrete-time markovian jump linear system,” *Journal of The Franklin Institute*, vol. 352, pp. 73 – 92, 2015.
- [122] B. Stewart, J. Rawlings, and S. Wright, “Hierarchical cooperative distributed model predictive control,” in *American Control Conference*, 2010, pp. 3963 – 3968.
- [123] J. Sturm, “Using SeDuMi 1.02, a Matlab toolbox for optimization over symmetric cones,” *Opt. Methods and Software*, vol. 11, pp. 625–653, 1999.
- [124] O. Stursberg, “Hierarchical and distributed discrete event control of manufacturing processes,” in *17th Conference on Emerging Technologies and Factory Automation*, 2012, pp. 1 – 8.
- [125] J. Swigart and S. Lall, “Optimal controller synthesis for decentralized systems over graphs via spectral factorization,” *IEEE Transactions on Automatic Control*, vol. 59, no. 9, pp. 2311 – 2323, 2014.
- [126] P. Tabuada, S. Caliskan, M. Rungger, and R. Majumdar, “Towards robustness for cyber-physical systems,” *IEEE Transactions on Automatic Control*, vol. 59, no. 12, pp. 3151 – 3163, 2014.
- [127] D. Tarraf, Ed., *Control of Cyber-Physical Systems*. Springer, 2013.
- [128] J. Tonne, “Verteilte Regelung verkoppelter linearer sprungfähiger Markov-Systeme,” Master Thesis, University of Kassel, Department of Electrical Engineering and Computer Science, supervised by: Martin Jilg and Olaf Stursberg, 2014.

- 
- [129] J. Tréguët, D. Peaucelle, D. Arzelier, and Y. Ebihara, “Periodic memory state-feedback controller: New formulation, analysis, and design results,” *IEEE Transactions on Automatic Control*, vol. 58, no. 8, pp. 1986 – 2000, 2013.
- [130] A. Varga, “An overview of recent developments in computational methods for periodic systems,” in *IFAC Workshop on Periodic Control Systems*, 2007.
- [131] D. Šiljak, *Large-Scale Dynamic Systems - Stability and Structure*, A. P. Sage, Ed. North-Holland, 1978.
- [132] D. Šiljak, *Decentralized Control of Complex Systems*. Academic Press, Inc., 1991.
- [133] B. Wang and J. Zhang, “Distributed output feedback control of Markov jump multi-agent systems,” *Automatica*, vol. 49, no. 5, pp. 1397 – 1402, 2013.
- [134] B.-C. Wang, “Mean field team decision problems for markov jump multiagent systems,” in *Chinese Control Conference*, 2015, pp. 1845 – 1850.
- [135] S.-H. Wang and E. Davison, “On the stabilization of decentralized control systems,” *IEEE Transactions on Automatic Control*, vol. AC-18, no. 5, pp. 473 – 478, 1973.
- [136] H. Williams, *Model Building in Mathematical Programming*, 4th ed. Wiley, 1999.
- [137] R. Wiśniewski and J. Stoustrup, “Generalized  $\mathcal{H}_2$  control synthesis for periodic systems,” in *American Control Conference*, 2001, pp. 2600 – 2605.
- [138] B. Wittenmark and M. Salgado, “Hankel-norm based interaction measure for input-output pairing,” in *15th IFAC World Congress*, 2002.
- [139] J. Xiong, V. Ugrinovskii, and I. Petersen, “Local mode dependent decentralized stabilization of uncertain markovian jump large-scale systems,” *IEEE Trans. on Automatic Control*, 2009.
- [140] A. Zečević and D. Šiljak, *Control of Complex Systems - Structural Constraints and Uncertainty*. Springer, 2010.
- [141] L. Zhang, Y. Leng, and P. Colaneri, “Stability and stabilization of discrete-time semi-Markov jump linear systems via semi-Markov kernel approach,” *IEEE Transactions on Automatic Control*, vol. 61, no. 2, pp. 503 – 508, 2016.
- [142] K. Zhou, J. Doyle, and K. Glover, *Robust and Optimal Control*. Prentice Hall, 1996.

ISBN 978-3-7376-0454-3



9 783737 604543 >